ABSTRACT

STUDY OF RADIATION AND MECHANICAL ATTRIBUTES OF DIAGNOSTIC X-RAY INSTALLATIONS IN MIZORAM

JONATHAN LALRINMAWIA

DEPARTMENT OF PHYSICS

MIZORAM UNIVERSITY

STUDY OF RADIATION AND MECHANICAL ATTRIBUTES OF DIAGNOSTIC X-RAY INSTALLATIONS IN MIZORAM

By

Jonathan Lalrinmawia

Physics Department

Submitted

in partial fulfillment of the requirement of the Degree of Doctor of Philosophy

in Physics of Mizoram University, Aizawl.

MIZORAM UNIVERSITY
DEPARTMENT OF PHYSICS
Aizawl - 796004, MIZORAM, India
(A Central University Established by an Act of Parliament of India)

Prof. R. C. Tiwari
Supervisor & Head
Ph:+91-389-2330522(O) +91-9862300514 (M) & Fax: +91-389-2330435
Email: ramesh_mzu@rediffmail.com

Date:

CERTIFICATE

This is to certify that the thesis entitled "**Study of radiation and mechanical attributes of diagnostic X-ray installations in Mizoram**" submitted by Jonathan Lalrinmawia (Registration No. MZU/Ph.D/917 of 21.04.2016), for the degree of Doctor of Philosophy in Physics, of the Mizoram University: Aizawl, India, embodies the record of original investigations carried out by him under my supervision. He has been duly registered and the thesis presented is worthy of being considered for the award of Ph.D. degree. This research work has not been submitted for any degree of any other university.

(PROF. RAMESH CHANDRA TIWARI)
Supervisor
Department of Physics
School of Physical Science

(DR. KHAM SUAN PAU)
Joint Supervisor
Department of Radiation Oncology
Mizoram State Cancer Institute
And
Head, Radiation Safety Agency
Directorate of Hospital and Medical Education

This Thesis is dedicated to

my Grandmothers

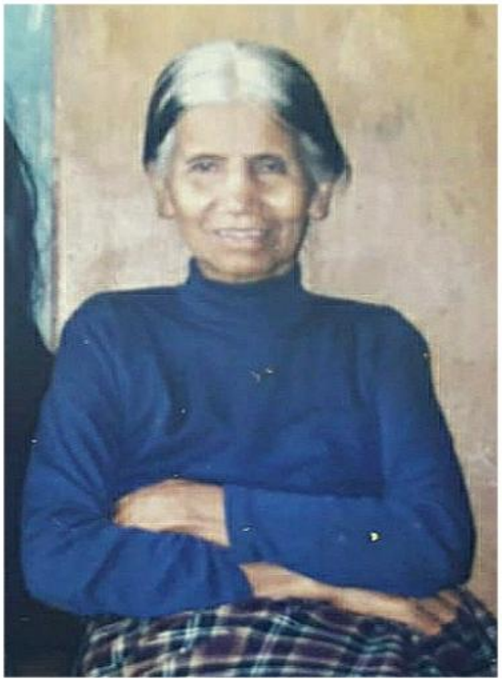

and all the X-ray pioneers

DECLARATION

Mizoram University

December, 2019

I Jonathan Lalrinmawia, hereby declare that the subject matter of this thesis is the record of work done by me, that the contents of this thesis did not form basis of the award of any previous degree to me or to do the best of my knowledge to anybody else, and that the thesis has not been submitted by me for any research degree in any other University/Institute.

This is being submitted to the Mizoram University for the degree of Doctor of Philosophy in Physics.

Dated: (JONATHAN LALRINMAWIA)

Candidate

(HEAD)

Department of Physics

School of Physical Science

(PROF. RAMESH CHANDRA TIWARI)

Supervisor

ACKNOWLEDGEMENT

First and foremost, I thank God for giving me good health and his guidance and protection throughout the completion of my research.

I would like to express my gratitude to my supervisor, Prof. Ramesh Chandra Tiwari, Head, Department of Physics, School of Physical Sciences, for his supervision, advice and encouragement during the entire period of the study.

I am also very grateful to my joint supervisor, Dr. Kham Suan Pau, Medical Physicist, Department of Oncology, Mizoram State Cancer Institute (MSCI) for his endless support and encouragement throughout my Ph. D.

I am also thankful to Atomic Energy Regulatory Board, Government of India for the financial grants they provided through major research project (No. AERB/CSRP/Proj.No. 58/02/2014). I am grateful to MSCI, Zemabawk, Aizawl for allowing me to use such instruments for the entire research work. And thank you to all the MSCI doctors for helping me and motivating me while working in the Institute.

I want to say thank you to all the X-ray machine owners and the technicians across the states of Mizoram who are involved in this study. They cooperated with me in operating X-ray machine and in collection of data. And also to all the teaching and non-teaching staff of Physics Department, MZU for all the help they provided during my research. I am thankful to all my colleagues, other research scholar for the help they provided. Thank you for all the good time we spent together.

I am grateful to all my colleagues in Mizoram Board of School Education for their support and advice regarding my research. In a very special way, I would like to thank my friend, Dr. Zothanpuia Hnamte, Assistant Professor, Department of Biotechnology, Pachhunga University College for always helping me and giving me advice whenever I needed.

As a final thought, I can never give enough thanks to my parents and all my family for the support and endless prayers throughout my research.

Date: (JONATHAN LALRINMAWIA)

TABLE OF CONTENTS

Contents		Page No.
Title of the Thesis		i
Dedication		ii
Certificate		iii
Declaration		iv
Acknowledgement		v
Table of Contents		vii
Abbreviations and Symbols		xiii
List of Figures		xxi
List of Tables		xxvi
Chapter 1	: Introduction	1
1.1	: Discovery of X-rays	2
1.2	: X-ray production	3
1.2.1	: Characteristics interactions	4
1.2.2	: Bremsstrahlung interactions	8
1.3	: Properties of X-ray beam	10
1.3.1	: Beam quantity	10
1.3.2	: Beam quality	12
1.4	: Emission spectrum	13
1.5	: Interaction of X-rays with matter	20
1.5.1	: Photoelectric effect	20

1.5.2 : Compton scattering 23

1.5.3 : Thomson scattering 27

1.5.4 : Pair production 29

1.6 : Attenuation of X-rays 30

1.6.1 : Linear attenuation coefficient and Exponential attenuation 31

1.6.2 : Mass, Electronic and Atomic attenuation coefficients 35

1.6.3 : Factors affecting attenuation 35

1.6.4 : Total attenuation coefficient 36

1.6.5 : Total energy transfer and Absorption coefficients 38

1.6.6 : The Relative important of different types of interactions 39

1.7 : Biological effects of X-rays 40

1.7.1 : Direct and indirect effect 41

1.7.2 : Effects of radiation on cells 42

1.7.3 : Effects of radiation on organs and body 43

1.7.4 : Deterministic radiation effects 43

1.7.5 : Stochastic radiation effects 44

1.8 : Fundamental principles of radiation protection 45

1.9 : Radiation safety regulations (National Safety Code) 46

1.9.1 : Safety specifications for medical diagnostic X-ray equipment (general purpose radiographic equipment) and protective devices 47

1.9.2 : Radiation protection and work practice 49

1.9.3 : Personnel requirements and responsibilities 49

1.9.4 : Regulatory controls 50

1.9.5 : Dose limits 50

1.10 : Background and the scope of the study 51

Chapter 2 : Review of Literature 54

Chapter 3 : Materials and Methods 79

3.1 : Radiographic equipment 80

3.1.1 : Fixed X-ray, mobile-fixed X-ray and mobile X-ray machine 80

3.1.2 : Diagnostic X-ray tube 83

3.1.3 : Anode 86

3.1.4 : Cathode 87

3.1.5 : Tube housing 88

3.1.6 : Collimator 89

3.2 : Measurement tools 90

3.2.1 : Dosimeter (model 06-526) 90

3.2.2 : kVp meter (Model 07-494) 91

3.2.3 : Survey meter (model 451P) 94

3.2.4 : Collimator/beam alignment test tool (07-661-7662) 96

3.2.5 : Thermo-luminescent dosimeter (TLD badge) 97

3.3 : An enumeration survey of conventional diagnostic X-ray generators and essential safety parameters in Mizoram, India 98

3.3.1 : Output linearity of time 100

3.3.2 : Output linearity of current 102

3.3.3 : Output reproducibility 102

3.3.4 : Tube output (70 kV at FDD=100cm) 103

` 3.3.5 : kVp accuracy 103

3.3.6 : Other safety parameters 104

3.4 : Qualitative study of mechanical parameters of conventional diagnostic X-ray machines in Mizoram, India 105

3.4.1 : Half value layer 105

3.4.2 : Radiation beam and optical field congruency 108

3.2.3 : Perpendicularity between central beam and image receptor 111

3.5 : Evaluation of radiation doses at diagnostic X-ray CPs and outside PEDs in Mizoram, India 113

3.6 : Study on the intensity of radiation attenuated by protective barriers in diagnostic X-ray installations 117

3.7 : Investigation of conventional diagnostic X-ray tube housing leakage radiation using ion chamber survey meter in Mizoram, India 119

Chapter 4 : Results and Discussion 121

4.1 : An enumeration survey of conventional diagnostic X-ray generators and essential safety parameters in Mizoram, India 123

4.1.1 : Linearity of time 123

4.1.2 : Linearity of current 124

4.1.3 : Output reproducibility 125

4.1.4 : Tube output (70 kV at FDD=100cm) 126

4.1.5 : kVp accuracy 128

4.1.6 : Essential safety parameters 129

4.2 : Qualitative study of mechanical parameters of conventional diagnostic X-ray machines in Mizoram, India 133
4.2.1 : Half value layer 133
4.2.2 : Congruency between optical field and radiation beam 138
4.2.3 : Perpendicularity of the central beam and image receptor 143
4.3 : Evaluation of radiation doses at diagnostic X-ray CPs and outside PEDs in Mizoram, India 146
4.3.1 : Exposure rates at CP for both couch and chest missions 146
4.3.2 : Comparison between different utilization of CP barriers 148
4.3.3 : Exposure rates outside the PED for both chest and couch missions 151
4.3.4 : Comparison between lead-line PEDs and other typical PEDs 153
4.3.5 : Workloads for chest and couch examinations 155
4.3.6 : Public and occupational dose levels 158
4.4 : Study on the intensity of radiation attenuated by protective barriers in diagnostic X-ray installations 163
4.4.1 : Attenuation of PEDs 164
4.4.2 : Attenuation of CP Barriers 168
4.5 : Investigation of conventional diagnostic X-ray tube housing leakage radiation using ion chamber survey meter in Mizoram, India 171
Chapter 5 : Summary and Conclusion 178
Appendices : Appendix I: Formulae 188
Appendix II: List of diagnostic X-ray facilities 191

Appendix III: Workload across the present study area 203

References : 228

Brief Bio-Data of the candidate 247

Particulars of the candidate 256

Reprints of research papers

ABBREVIATIONS AND SYMBOLS

1φ	single phase X-ray machine
3φ	three phase X-ray machine
%	percentage
±	plus or minus
°C	degree Celsius, Centigrade/Celsius scale
e	base of natural logarithms with values 2.718
°F	degree Fahrenheit, Fahrenheit scale
ρ	density of the material
μ	linear attenuation coefficient
μ/ρ	mass attenuation coefficient
μ_{e}	electronic attenuation coefficient
μ_{a}	atomic attenuation coefficient
μ_{total}	total attenuation coefficient
μ_{tr}	energy transfer coefficient
τ	photoelectric interaction
τ_{tr}	energy transfer coefficient for photoelectric absorption

$\boldsymbol{\sigma_{coh}}$	Thomson scattering
$\boldsymbol{\sigma_{incoh}}$	Compton scattering
$\boldsymbol{\sigma_{\mathrm{tr}}}$	energy transfer coefficient for Compton scattering
$\boldsymbol{\kappa}$	pair production interaction
$\boldsymbol{\kappa_{\mathrm{tr}}}$	energy transfer coefficient for pair production
μGy	micro-gray
$\boldsymbol{\mu R\ h^{-1}}$	micro-roentgen per hour
μSv	micro-sievert
$\boldsymbol{\mu Sv\ h^{-1}}$	micro-sievert per hour
AAPM	American Association for Physics in Medicine
AC	alternating current
AERB	Atomic Energy Regulatory Board
AEOI	Atomic Energy Organization of Iran
Al	aluminum
ALARA	as low as reasonably achievable
B	Binding energy of electron in the atomic shell: Build-up factors
BARC	Bhaba Atomic Research Center

BSS	International Basic Safety Standards
c	speed of light/photon
CaSO4	Calcium Sulfate
CEC	Commission of European Communities
CL	coefficient of linearity
cm	centimeter
CMOS	complementary metal oxide semiconductor
CNS	central nervous system
CP	control panel of X-ray machine
Cu	Copper
CV	coefficient of variation
d	distance
DNA	Deoxyribonucleic acid
FAO	Food and Agriculture Organization
FDD	focus to detector distance
g	gram
GI	gastrointestinal

H	Hydrogen
H_2O_2	Hydrogen peroxide
HF	high frequency
Hg	mercury
hv	photon energy
hv/c	photon momentum
HVL	half value layer
I	Intensity of X-ray/radiation
IAEA	International Atomic Energy Agency
ICRP	International Commission on Radiological Protection
IEC	International Electro technical Commission
ILO	International Labor Organization
in	inch
IPEM	Institute of Physics and Engineering in Medicine
kg	kilogram
keV	kilo-electron volt ‘1,000 times the base unit of energy, the electron-volt’

kV	kilo-voltage
kVp	peak kilo-voltage ‘the peak voltage applied to the X-ray tube, equal to 1,000 times the voltage; voltage varies with time with X-ray generator-produced waveforms’
lbs	pound
LCD	liquid crystal display
m	mass of photon: meter
mA	input-tube current
mAs	tube loading
MeV	mega-electron volt
mGy	milli-gray
mGy h^{-1}	milli-gray per hour
mm	millimeter
mm Al	aluminum equivalent
mm of Hg	millimeter of mercury
mm Pb	lead equivalent
Mo	Molybdenum
mR	milliroentgen

mR h^{-1}	milliroentgen per hour
msec	milli-second
mSv	millisievert
mSv h^{-1}	millisievert per hour
mSv/y	millisievert per year
NCDRH	National Center for Devices and Radiological Health
Ne	Number of electron per gram
NEXT	Nationwide Evaluation of X-ray Trends
NIST	National Institute of Standard and Technology
NOC	no objection certificate
NRPB	National Radiological Protection Board
NS	Not-significant
OECD	Organization for Economic Cooperation and Development
OH	Hydroxyl
PAHO	Pan American Health Organization
PED	patient entrance door of X-ray room
PMD	Personnel monitoring device

PMS	personnel monitoring service
R/hr	roentgen per hour
Re	Rhenium
RSO	radiation safety officer
S	Significant
SD	standard deviation
SEM	standard error mean
SID	source-to-image distance
SSDL	Secondary Standard Dosimetry Laboratory
T	Kinetic energy of photoelectron: Kinetic energy of struck electron
Th	Thorium
TLD	Thermo luminescent dosimeter
UNSCEAR	United Nations Scientific Committee on the Effects of Atomic Radiation
USA	United States of America
W	tungsten
WHO	World Health Organization

Z	atomic number

LIST OF FIGURES

Fig. Nos.	Figure Captions	Page No.
1.2.1	A characteristic interaction event (Re-drawn from Johnston & Fauber, Essentials of radiographic physics and imaging, Published by Elsevier Mosby, 2012)	5
1.2.2	A bremsstrahlung (brems) interaction event (Re-drawn from Johnston & Fauber, Essentials of radiographic physics and imaging, Published by Elsevier Mosby, 2012)	9
1.4(a)	X-ray emission spectrum (From Johnston & Fauber, Essentials of radiographic physics and imaging, Published by Elsevier Mosby, 2012)	14
1.4(b)	Fig. 1.4 (b): Discrete emission spectrum (From Johnston & Fauber, Essentials of radiographic physics and imaging, Published by Elsevier Mosby, 2012)	15
1.4(c)	Change in milliampererage change the appearance of the X-ray emission spectrum	16
1.4(d)	Change in kilo-voltage peak change the appearance of the X-ray emission spectrum	17
1.4(e)	Additional tube Filtration change the appearance of the X-ray emission spectrum	18
1.4(f)	Change in generator type change the appearance of the X-ray emission spectrum	19
1.5.1	Photoelectric Interaction (Re-drawn from Johnston & Fauber, Essentials of radiographic physics and imaging, Published by Elsevier Mosby, 2012)	22
1.5.2	A Compton scattering event (From Johnston & Fauber, Essentials of radiographic physics and imaging, Published by Elsevier Mosby, 2012)	23
1.5.3	A classical scattering event (Re-drawn from Johnston &	28

	Fauber, Essentials of radiographic physics and imaging, Published by Elsevier Mosby, 2012)	
1.5.4	A Pair production event (Re-drawn from Johnston & Fauber, Essentials of radiographic physics and imaging, Published by Elsevier Mosby, 2012)	30
1.6.1	Graph shows a comparison of the curves for polychromatic and monochromatic radiation (From McKetty, The AAPM/RSNA Physics Tutorial for Residents-X-ray Attenuation, Washington, Radiographics, 1998)	34
1.6.4	Relative importance of photoelectric effect, Compton scattering and pair production at different *hυ* in elements of different Z. Lines show the locus of points at which σ = τ and σ = κ. (From Robley D. Evans, The Atomic Nucleus, copyright 1955, Published by McGraw-Hill)	37
1.7.1(a)	Damage from direct effect	42
1.7.1(b)	Damage from free radicals	42
3.1.1(a)	Mobile X-ray machine	81
3.1.1(b)	Fixed X-ray machine	81
3.1.1(c)	Mobile fixed X-ray machine	82
3.1.2(a)	Schematic diagram of conventional X-ray tube head assembly	85
3.1.2(b)	Realistic picture of conventional X-ray tube	85
3.2.1	A battery operated portable dosimeter (model 06-526)	91
3.2.2(a)	Wide-range digital kVp meter (model 07-494)	92
3.2.2(b)	mAs vs kVp, minimum requirements (Typical single phase X-ray unit)	93
3.2.3	Ion chamber survey meter (model 451P)	95
3.2.4(a)	Beam alignment test tool (07-661-7662)	97
3.2.4(b)	Collimator test tool (07-661-7662)	97
3.2.5	Thermo-luminescent dosimeter used to measure radiation	98

	dose of the investigator	
3.3	Location of 135 X-ray machines, installed in 82 different institution	101
3.4.1	Attenuation curve showing the half value thickness	107
3.4.2(a)	Experimental set up for congruency and perpendicularity test(Re-drawn from Sungita *et al*., 2006)	109
3.4.2(b)	Good field alignment, beam alignment approximately 2° from perpendicular	110
3.4.2(c)	X-ray field alignment error, greater than 3 cm and unacceptable at 40" SID	111
3.4.3	Interpretation of the image of the steel balls in the beam alignment test tool	112
3.5(a)	Layout of the X-ray installation room	114
3.5(b)	A water-phantom setting to measure stray radiation for vertical exposure (couch mission)	115
4.1	Year of installations of diagnostic X-ray machines in the present study area	123
4.1.1	Tube output linearity of time (sec) for 98 conventional diagnostic X-ray machines (standard norm <0.1 or 10%)	124
4.1.2	Tube output linearity of current (mA) for 69 conventional diagnostic X-ray machines (standard norm <0.1 or 10%)	125
4.1.3	Tube output reproducibility for 97 conventional diagnostic X-ray machines (accepted at <0.05 or ±5%)	126
4.1.4	Tube output/table dose (kV=70) for 97 conventional diagnostic X-ray machines (to be in the range 43−52 μGy/mAs)	127
4.1.5	Voltage accuracy for 97 conventional diagnostic X-ray machines (to be within ±0.05 or ±5%)	128
4.2.1(a)	Attenuation curves of 97 diagnostic X-ray machines; an Al filter as attenuator at input tube voltage 70 kVp	136

4.2.1(b)	Total filtration of 97 X-ray machines; measurement were done at 70 kVp	137
4.2.2(a)	Misalignment between the optical light and the X-ray beam of 47 X-ray units	141
4.2.2(b)	Misalignment between the radiation beam and the optical field from the present study	142
4.2.2(c)	Relationship between the year of installation and congruency misalignment	143
4.2.3	Relationship between the year of installation and the perpendicularity of the central beam	144
4.3.1(a)	Exposure rates measured at CPs for chest missions	147
4.3.1(b)	Exposure rates measured at CPs for couch missions	147
4.3.2(a)	Exposure rates measured at CPs for chest missions (comparing different barrier utilizations)	149
4.3.2(b)	Exposure rates measured at CPs for couch missions (comparing different barrier utilizations)	150
4.3.3(a)	Exposure rates measured at the PEDs for chest missions	151
4.3.3(b)	Exposure rates measured at the PEDs for couch missions	152
4.3.4(a)	Exposure rates measured at the PEDs for chest missions (comparing different barrier utilizations)	154
4.3.4(b)	Exposure rates measured at the PEDs for couch missions (comparing different barrier utilizations)	154
4.3.5	Workload of different institutions for both chest and couch examinations	157
4.3.6(a)	Doses at the CPs (occupational dose) caused by stray radiation ([a]AERB dose limit for radiation workers)	161
4.3.6(b)	Doses at the PEDs (public dose) owing to stray radiation ([a]AERB dose limit for members of the public)	163
4.4.1(a)	Exposure rates measured outside PEDs with door open and close in chest and couch missions	165

4.4.1(b)	Percentage of attenuation; attenuated by solid wood, plywood, lead and plywood-plane sheet-lined door	167
4.4.2(a)	Exposure rates measured at CPs with and without barriers in chest and couch missions	169
4.4.2(b)	Percentage of attenuation; attenuated by lead, concrete, plywood and plywood-plan sheet-lined barriers	170
4.5.1	Maximum tube housing leakage radiation in 93 X-ray machines [[a]AERB and other regulatory body safety limit 115 mR in one hour; [b]maximum leakage 58 mR in one hour]	175

LIST OF TABLES

Table Nos.	Captions	Page No.
1.2.1(a)	Critical X ray Absorption Energies (keV) (From Storm and Israel, 1970)	7
1.2.1(b)	Principal Emission Lines in keV for Tungsten and Molybdenum (From Storm and Israel, 1970)	8
1.6.3	Physical properties of selected materials (From McKetty, 1998)	36
1.6.6	Types of Photon Interactions in Water	40
3.1.1(a)	Working and out of order diagnostic X-ray machines distribution across Mizoram in June 2016	82
3.1.1(b)	Condemn diagnostic X-ray machines distribution across Mizoram in June 2016	83
3.2.2	FDD Settings	94
3.3	X-ray facilities and their respective workloads in Mizoram during June 2015 –June 2016	100
3.4.1	X-ray machines with a defect that made determination of a given parameter impossible	106
3.6	Input parameters settings for stray radiation rate measurement	118
4.1.6	16 important safety parameters in diagnostic X-ray installations	130
4.2.1(a)	Output consistency (coefficient of variation) of 97 X-ray units	135
4.2.1(b)	Total filtration of 97 X-ray units	135
4.2.2	Congruency between the radiation beam and the optical field of 47 X-ray machines	140
4.2.3(a)	Angle between the central X-ray beam and image receptor of 53 X-ray units	145
4.2.3(b)	Status of the congruency and perpendicularity of different manufacturers of diagnostic X-ray units	145

4.3.1	Exposure rates measured at CPs behind different arrangements of protective barriers at different installations	148
4.3.3	Exposure rates measured at different types of PEDs in different installations	152
4.3.5	Workload of diagnostic X-ray facilities in the present study area	156
4.3.6(a)	Exposure rates and workload for the three highest public and occupational doses	159
4.3.6(b)	Exposure rates and workload for low occupational and public doses	160
4.4.1(a)	Difference between exposure rates measured with and without PEDs in chest and couch missions	165
4.4.1(b)	Attenuation (percentage) of different types of PED	167
4.2.2(a)	Difference between exposure rates measured with and without CP barriers in chest and couch missions	169
4.2.2(b)	Attenuation (percentage) of different types of CP barrier	170
4.5.1	Tube housing leakage exposure rates measured at left, right, front, back, and top direction of the X-ray tube	173
4.5.2	Comparison of radiation leakage between left, right, front, back and top direction of X-ray tube	174
4.5.3	Comparison between maximum leakage radiation in AERB type approval units and unknown type approval units	176
4.5.4	Comparison between maximum leakage radiation in fixed and mobile X-ray machines	177
5.1	Comparison of Work done by authors with the similar work done by other researchers from Middle East, Asia, Africa and Europe	184

CHAPTER I

INTRODUCTION

1.1 Discovery of X-rays

Dr. Wilhelm Conrad Roentgen produced and detected X-rays on November 8, 1895, while experimenting with a Crookes's cathode ray tube. His investigation was so rigorous that he discovered practically every property of X-rays we know today. During Dr. Roentgen's investigation of X-rays, in a series of experiments he observed that the bones of his hand were visible on a barium platinocyanide screen. To capture such an image, he experimented with exposing photographic plates to X-rays and found that they did indeed expose the plate, creating a photograph. As part of his initial communications and presentation, he included the famous photograph (now properly referred to as a radiograph) of his wife Bertha's hand. The publication of this radiograph led to an almost immediate recognition of the medical significance of X-rays. Other researchers around the world began experimenting with the radiography of different parts of the body. Physicians readily embraced this new technology and immediately put it to use to find bullets, kidney stones, gallbladder stones and broken bones (Johnston and Fauber, 2012).

The accidental discovery of X-rays marked the introduction to mankind of a totally new and unexpected phenomenon in nature i.e. ionizing radiation. The original findings were followed rapidly by the discovery of radioactivity and sources of ionizing radiation with properties different from those of X-rays (Stannard, 1988). Radioactivity did not at first excite the investigative minds of the time; only about a dozen of papers on radioactivity were published in the first year after its discovery compared with more than a thousand on X-rays (Brodsky and Kathren, 1989). The huge potential for medical applications of X-rays was evident from the first investigations. As experience was gained in the early days, it became more and more evident that ionizing radiation can harm biological systems. However, today, many unique and significant benefits to human life are realized through the utilization of radiation and its various sources (Turner, 2005; Smith and Doll, 1981).

1.2 X-ray production

The production of X-rays involves the bombardment of a thick target with energetic electrons. These electrons undergo a complex sequence of collisions and scattering processes during the slowing down process, which results in the production of bremsstrahlung and characteristic radiation (IAEA, 2014; Sprawls, 2017).

An X-ray tube consists of two electrodes namely a negative glow cathode which works on thermionic emission of electrons and a positive electrode known as anode. The electrodes are incapsuled in a vacuum (Carlsson and Carlsson, 1996; Johns and Cunningham, 1983). Exposure factors have been selected from the control panel of X-ray machine; by applying electricity to the cathode, anode and filament. Electrons have been boiled off of the filament and are accelerated towards the anode at tremendous speeds (Johnston and Fauber, 2012). The electrons gain kinetic energy which is the product of their charge and the potential difference between the cathode and the anode. If the potential difference is 100 kilo-volts (*kV*), each electron will gain a kinetic energy of 100 kilo-electron volts (*keV*) (Carlsson and Carlsson, 1996). The filament electrons enter the face of the tungsten (*W*) target to a depth of approximately 0.5 mm interacting with the tungsten atoms in their path. To produce

X-rays, filament electrons interact with target atoms in two ways: *characteristics interactions* and *bremsstrahlung (brems) interactions*. It should be noted that most of the interactions (approximately 99%) do not result in X-rays but produce only heat (Johnston and Fauber, 2012; Johns and Cunningham, 1983).

1.2.1 Characteristics Interactions

It involves the filament electron and an orbital electron of a target atom. In general, a filament electron enters a target atom, strikes an orbital electron and gets removed from the orbit if its energy is greater than the binding energy of the orbital electron. The orbital shells fill from the shell nearest to the nucleus outward and a vacancy in a shell makes the atom unstable. To correct this condition, outer-shell electrons drop to fill inner-shell vacancies. As such the outer-shell electron must give up some of its potential energy. This energy is given off as a characteristic X-ray photon as shown in Fig. 1.2.1. This process of outer-shell electrons filling inner-shell vacancies continues down the line, creating a cascading effect called a *characteristic cascade*. Each time an orbital electron moves to a lower orbit, a characteristic photon is produced. This process is not necessarily orderly. If a filament electron removes a K-shell electron from an atom, the most likely electron to fill the vacancy is an L shell because of proximity. But any outer-shell electron can fill the K-shell vacancy; it is just not as likely to do so (Johnston and Fauber, 2012).

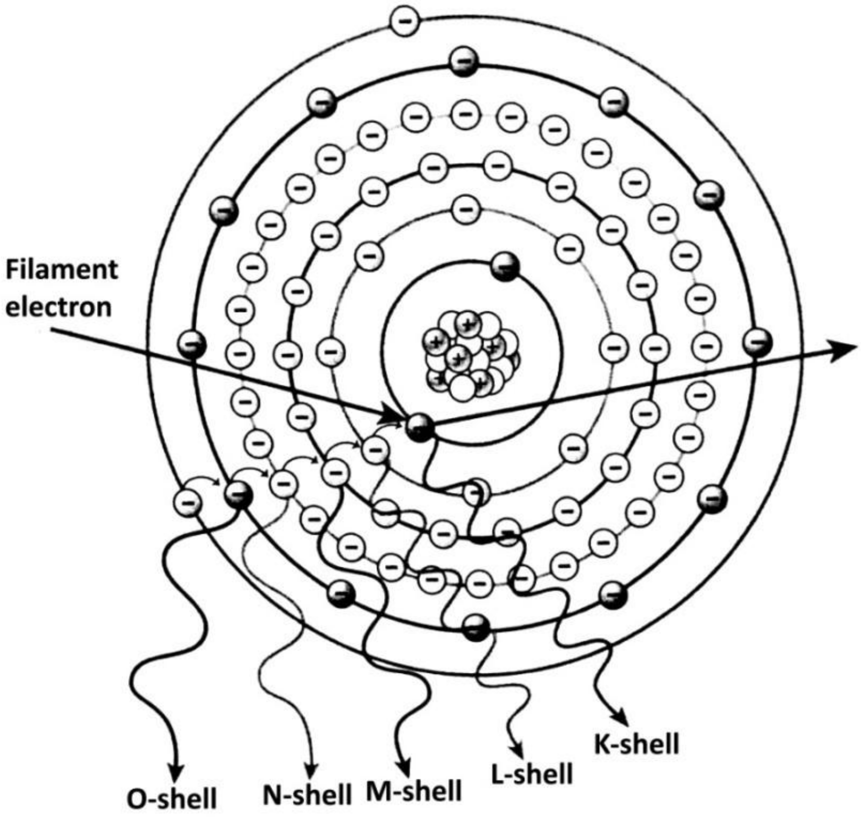

Fig. 1.2.1: A characteristic interaction event (Re-drawn from Johnston and Fauber, Essentials of radiographic physics and imaging, Published by Elsevier Mosby, 2012)

Characteristic radiations are so called because their energy is characteristic or dependent on the difference in binding energy between the two shells involved. The electron shells of each element have specific binding energies. A tungsten atom has 74 electrons orbiting around its nucleus in six different shells. The filament electron may interact with any of them, but medical imaging generally focuses on K-shell (innermost shell) interactions because they are the highest energy and the most useful for imaging purposes. K-shell electrons in tungsten have the strongest binding energy at 69.5 keV. For a filament electron to knock out this orbital electron, it must acquire energy equal to or greater than 69.5 keV. For all practical purposes using a general purpose X-ray machine, if a radiographer selects a peak kilo-voltage (*kVp*) less than 70 on the control panel, no photons will be produced from K-shell interactions (Carlsson and Carlsson, 1996; Johnston and Fauber, 2012; IAEA, 2014). For example, if a filament electron has 50 keV of kinetic energy and strikes a tungsten K-shell electron (binding energy=69.5 keV), it does not have the energy to remove it. The result of this type of interaction is heat production and this happens most of the time as noted earlier. In such cases the filament electron, having lost all of its kinetic energy, then drifts away to fill a vacancy in another atom or become part of the current through the tube. However, if that same filament electron had 100 keV of energy, it would easily remove the K-shell orbital electron and be deflected in a new direction. It would still have 30 keV of energy left, with which it can interact with another atom (Johnston and Fauber, 2012).

If an outer-shell electron is filling a K-shell, regardless of where that filling electron is coming from, the photon produced is called K characteristic (Johnston and Fauber, 2012). Careful investigations have shown that the L shell is really made up of three sub-shells (L_I, L_{II} and L_{III}), the M shell of 5 sub-shells (I to V) and the N shell of 7 sub-shells. The energies of these shells have been measured with great precision by Storm and Israel (1970), few of the data are given in Table 1.2.1 (a). The entries in the table are in keV and thus give the voltages in kilovolts required to excite the particular level. For example, in tungsten 69.525 kV is required on the tube to eject the K electron from the atom. If this voltage is supplied, all the K lines will appear. Further, when an electron moves from the L_{III} to the K shell, energy is radiated and the amount is the difference between the corresponding energy levels of Table 1.2.1 (a), i.e. 69.525 - 10.204 = 59.321 keV. It is referred as a K-L_{III} transition. The photon emitted is called the $K\alpha_1$ line, a notation that comes from the early days of X-ray spectroscopy (Johns and Cunningham, 1983).

Table 1.2.1 (a): Critical X ray Absorption Energies (keV) (From Storm and Israel, 1970)

Shell	Oxygen Z=8	Calcium Z=20	Copper Z=29	Molybdenum Z=42	Tin Z=50	Tungsten Z=74	Lead Z=82
K	0.533	4.037	8.981	20.000	29.200	69.525	88.004
L_I	0.024	1.438	1.096	2.867	4.465	12.098	15.861
L_{II}	0.009	0.350	0.953	2.625	4.156	11.541	15.200
L_{III}	0.009	0.346	0.933	2.521	3.929	10.204	13.035
M_I	-	0.044	0.122	0.505	0.884	2.820	3.851
M_{II}	Not	0.025	0.074	0.410	0.756	2.575	3.554
M_{II}	filled	0.025	0.074	0.392	0.714	2.281	3.066
M_{IV}	-	-	0.007	0.230	0.493	1.871	2.586
M_V	-	-	0.007	0.228	0.485	1.809	2.484

One might expect a K line for a transition from all of the L, M and N shells to the K shell. Quantum mechanical reasoning shows, however, that many of the transitions are forbidden and only those that follow certain selection rules are allowed. A few of the important emission lines from tungsten and molybdenum (*Mo*) are given in Table 1.2.1 (b). In addition, the relative numbers emitted are also given.

Table 1.2.1 (b): Principal emission lines in keV for Tungsten and Molybdenum (From Storm and Israel, 1970)

K Lines Tungsten				L Lines Tungsten			
Transition	Symbol	Energy (keV)	Relative No.	Transition	Symbol	Energy (keV)	Relative No.
K-N$_{II}$N$_{III}$	Kβ_2	69.081	7	L$_I$-N$_{III}$	Lγ_5	11.674	10
K-M$_{III}$	Kβ_{21}	67.244	21	L$_I$-N$_{III}$	Lγ_1	11.285	24
K-M$_{II}$	Kβ_3	66.950	11	L$_{III}$-N$_V$	Lβ_2	9.962	18
K-L$_{III}$	Kα_1	59.321	100	L$_I$-M$_{III}$	Lβ_3	9.817	37
K-L$_{II}$	Kα_2	57.984	58	L$_{II}$-M$_{IV}$	Lβ_1	9.670	127
Molybdenum				L$_I$-M$_{II}$	Lβ_4	9.523	29
K-M$_{II}$M$_{III}$	Kβ_{31}	19.602	24	L$_{III}$-M$_V$	Lα_1	8.395	100
K-L$_{III}$	Kα_1	17.479	100	L$_{III}$-M$_{IV}$	Lα_2	8.333	11
K-L$_{II}$	Kα_2	17.375	52				

1.2.2 Bremsstrahlung interactions

In bremsstrahlung interactions, the filament electron misses all of the orbital electrons and interacts with the nucleus of the target atom. The electron is negatively charged and the nucleus is positively charged and there will be Coulomb forces of interaction between the two. The strength of this attraction depends on how close the filament electron passes to the target nucleus. The attraction causes the filament electron to slow down and change direction and in doing so the filament electron will lose kinetic energy. This energy is released as brems photon, the closer the filament electron passes, the stronger the Coulomb force of attraction (Fig. 1.2.2). The stronger this attraction, the more energy the filament electron loses and the stronger the resultant brems photon. Because of this, the brems photon can vary from the maximum kVp selected to near zero (Johnston and Fauber, 2012). Brems photons constitute the main part of the X-rays being used in X-ray diagnostic imaging and the relative amount of bremsstrahlung emitted increases with increasing electron kinectic energy and with increasing atomic number, Z, of the anode material (Carlsson and Carlsson, 1996; IAEA, 2014). The brems photon energy can be calculated by subtracting the energy that the filament electron leaves the atom with from the energy it had upon entering. The average energy of a brems photon is one third of the kVp selected at the control panel (CP) (Johnston and Fauber, 2012). The probability of bremsstrahlung emission is proportional to the value of Z^2 and is higher for higher atomic number materials such as tungsten (Z = 74). However, even for this material, the efficiency of bremsstrahlung production is less than 1% for 100 keV electrons (IAEA, 2014).

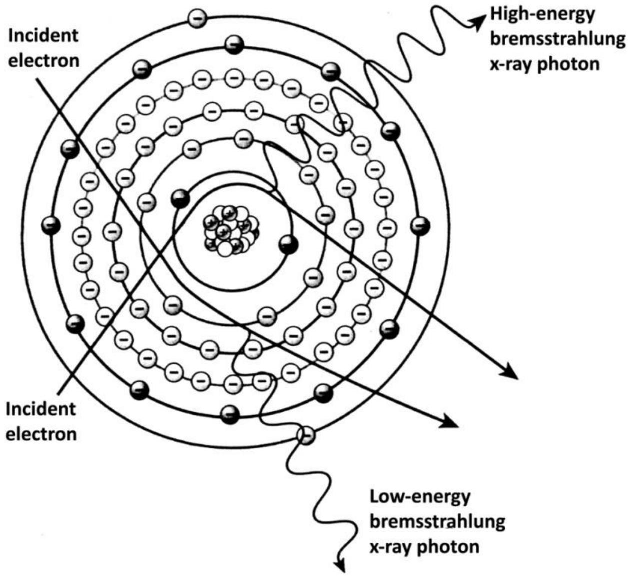
Incident electron
High-energy bremsstrahlung x-ray photon
Incident electron
Low-energy bremsstrahlung x-ray photon

Fig. 1.2.2: A bremsstrahlung (brems) interaction event (Re-drawn from Johnston and Fauber, Essentials of radiographic physics and imaging, Published by Elsevier Mosby, 2012)

In a tungsten target most of the photons are brems for two reasons. First, with characteristics interactions, only those involving the K shell are of sufficient energy to be useful. All others are too weak to contribute to the radiographic image and are typically filtered out of the beam by the 2.5 mm of total filtration that is built into the tube head assembly. Because tungsten has a K-shell binding energy of 69.5 keV, only those kilo-voltage peak setting of 70 kVp or greater produce K-characteristic photons. All lower settings result in a beam made up entirely of brems. Second, the filament electron is more likely to miss the orbital electrons of the target atom because they are in constant motion and the atom is mostly empty space (Johnston and Fauber, 2012).

The X-ray beam that originated from the X-ray machine collimator which exposed the patient is name as primary beam. Where, the X-ray beam that continues to exist after interaction with the patient and is exiting the patient to expose the image receptor is called remnant beam. The remnant beam is composed of transmitted photons and scattered photons (Johnston and Fauber, 2012).

1.3 Properties of X-ray beam

1.3.1 Beam Quantity

Beam quantity is the total number of X-ray photons in a beam and it depends on kVp, tube loading (mAs), filtration and distance. Beam quantity should be associated with radiation dose which means all other factors remaining constant, an increase in quantity increases the radiation dose. Among different factors, beam quantity mainly depends on mAs because mAs controls the number of electrons boiled off of the filament and available to produce X-rays. That is why mAs is considered as the primary factor controlling the quantity of the beam. Doubling the mAs doubles the X-ray output. When adjustments in quantity are desired, mAs is the factor adjusted (Johnston and Fauber, 2012).

At the same time, beam quantity varies as the square of the ratio of the change in kVp. Therefore, if the kVp is doubled, the quantity increases by a factor of four. However, because kVp controls both the number and energy of X-rays in the beam, a small change in kVp exerts a large effect on exposure to the image receptor. A 15% increase in kVp is equivalent to doubling the mAs. It is less advantageous to use kVp to change beam quantity because it influences many other factors (e.g., penetrability and scatter production) related to image production and is less predictable in its imaging effect where quantity is concerned (Johnston and Fauber, 2012).

Beam quantity or the intensity of the X-ray beam varies inversely as the square of the distance-*inverse square law*. The inverse square law is expressed as $I_1/I_2 = d^2{}_2/d^2{}_1$. That is, the intensity (I) quadruples if the distance (d) is reduced to one half of the original value. X-ray photons diverge as they travel away from the source and if the distance is shorter they do not have the opportunity to diverge as much and are then concentrated on a small area (Johnston and Fauber, 2012).

The use of *filtration* decreases X-ray quantity to an extent that it depends on the thickness and type of filtration material. Filtration absorbs low-energy photons that do not contribute to the image. Added filtration placed at the collimator serves to reduce patient dose by removing such photons.

1.3.2 Beam Quality

Beam quality simply refers to the penetrating ability of the X-ray beam. Penetration refers to those X-ray photons which are having the ability to transmit through the body and reach the image receptor. X-ray photons that reach the image receptor create the dark shades of the image and areas where no photons reach result in the light areas of the image. As such, it is desirable for some of the X-ray photons to go through the anatomic area of interest or no diagnostic image would result. Both are needed to create the diagnostic image. Beam quality is mainly affected by kVp and filtration and is controlled by adjusting kVp. As the kVp increases, the beam's ability to penetrate matter also increases and vice versa. X-ray beams with high energy (from high input kVp settings) are said to be hard beam or high-quality. X-ray beams with low energy (from low input kVp settings) are said to be soft beam or low-quality (Johnston and Fauber, 2012).

Filtration serves to remove the lower-energy photons to make the average energy higher (Johnston and Fauber, 2012). X-rays generated in the anode pass various attenuating materials before leaving the tube housing. These materials include the anode, tube envelope exit port, insulating oil and the window of the tube housing. This *inherent filtration* is measured in aluminum equivalents (mm Al). Measurement of the aluminum equivalent is usually made at 80 kVp. Typically, the inherent filtration ranges from 0.5 to 1 mm Al. Since filtration effectively reduces the low energy component in the X-ray spectrum, a minimum total filtration of at least 2.5 mm Al is required to reduce unnecessary patient dose. Additional filter material is positioned between the tube window and collimation assembly as required. The effect of added filtration on the X-ray output is an increase in the mean photon energy and half value layer of the beam (IAEA, 2014).

Half-value layer (HVL) is used to measure the penetrating ability or beam quality of an X-ray beam. It is defined as the thickness of absorbing material i.e., aluminium (Al) or aluminum equivalent filtration, necessary to reduce the energy of the beam to one-half its original intensity. Normal HVL of general diagnostic beams is 3 to 5 mm Al (Johnston and Fauber, 2012). Further, uses of added filtration reduces the intensity of the X-ray beam, increases the HVL, decreases patient exposure and improves images quality for a given radiation dose (McKetty, 1998).

1.4 Emission Spectrum

The emission spectrum graphically illustrates the X-ray beam as shown in Fig. 1.4 (a). Characteristics photons have a discrete emission spectrum whereas brems photons have a continuous emission spectrum. X-ray emission spectrum is formed by combining the essential parts of these two spectrums. The y-axis represents the number of X-rays and the x-axis represents the X-ray energy. Because brems photons are the result of the filament electrons’ attraction to the nucleus, their energy depends on the strength of this attraction. Their energy can range from just above zero to the maximum kVp selected on the control panel. A graph of brems photons creates a bell-shaped continuum (Johnston and Fauber, 2012).

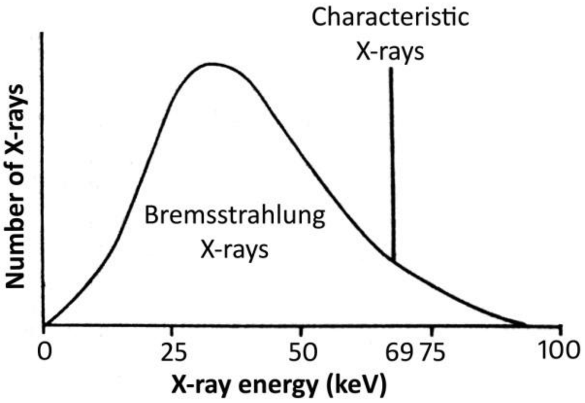

Fig. 1.4 (a): X-ray emission spectrum (From Johnston and Fauber, Essentials of radiographic physics and imaging, Published by Elsevier Mosby, 2012)

The *discrete emission spectrum* illustrates characteristic X-ray production.

With tungsten targets, K-characteristic X-rays are of the greatest importance because they contribute to the radiographic image. Beginning on the right side of the graph, K-characteristic photons have an energy range of approximately 57 keV (if an L electron fills the K-shell vacancy) to 69 keV (if the O or P shell fills the K-shell vacancy). Then moving down the x-axis, L-characteristic X-ray energies are plotted. They have an energy range of approximately 9 keV (if M shell electron fills the L-shell vacancy) to 12 keV (if an O or P shell electron fills the L-shell vacancy). Beyond L-characteristic there is really no point in plotting the energies because they are so low that X-ray machine filtered out of the beam and are of no consequence as illustrated in the Fig. 1.4 (b) (Johnston and Fauber, 2012).

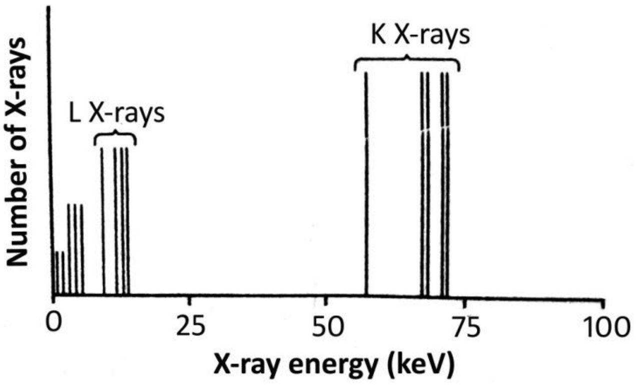

Fig. 1.4 (b): Discrete emission spectrum (From Johnston and Fauber, Essentials of radiographic physics and imaging, Published by Elsevier Mosby, 2012)

Five factors change the appearance of the X-ray emission spectrum: *input tube current (mA), kVp, tube filtration, generator type and target material*. Changes in *mA* affect beam quantity. All other factors remaining constant, an increase in *mA* increases the amplitude of both the continuous and discrete portions of the spectrum. When *mA* is increased on the control panel, more electrons are boiled off of the filament and are available for X-ray production. This increases the quantity of X-rays produced. Because the *kVp* setting controls energy, the spectrum does not move along the x-axis with changes in *mA*, nor does the discrete line move because it is related specially to the target material as shown in Fig. 1.4 (c) (Johnston and Fauber, 2012).

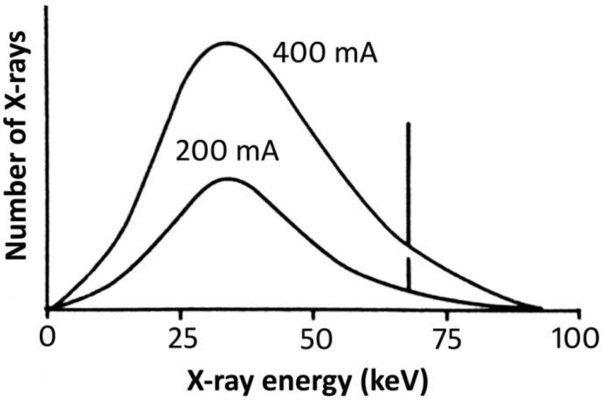

Fig. 1.4 (c): Change in milliampererage change the appearance of the X-ray emission spectrum

All other factors remaining constant, an increase in *kVp* increases the amplitude of both continuous and discrete portions of the spectrum and shifts the right side of the curve along the x-axis. When the input kVp is increased it gives filament electrons more kinetic energy to produce X-rays and increasing the kinetic energy overall. The result is more photons (quantity), which increases the amplitude of the spectrum and higher-energy photons (quality), which shifts the right side of the curve farther to the right. The discrete line does not move because it is related specifically to the target material as shown in Fig. 1.4 (d) (Johnston and Fauber, 2012).

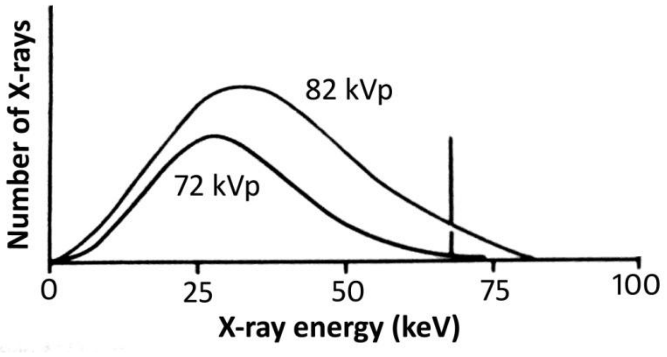

Fig. 1.4 (d): Change in kilo-voltage peak change the appearance of the X-ray emission spectrum

The addition of tube filtration or introducing a more efficient filtration material into the tube head assembly removes photons from the beam. All other factors remaining constant, an increase in tube filtration causes a decrease in quantity and an increase in quality. The removal of photons causes a decrease in quantity reflected by a decrease in amplitude of both the continuous and discrete portions of the curve. Because it removes more low-energy photons than high-energy photons, there is a greater decrease on the left side of the continuous portion and there is a shift in the peak of the curve to the right. The low energy photons removed, the average energy is higher. Again, the discrete line does not move because it is related specially to the target material as depicted in Fig. 1.4 (e) (Johnston and Fauber, 2012).

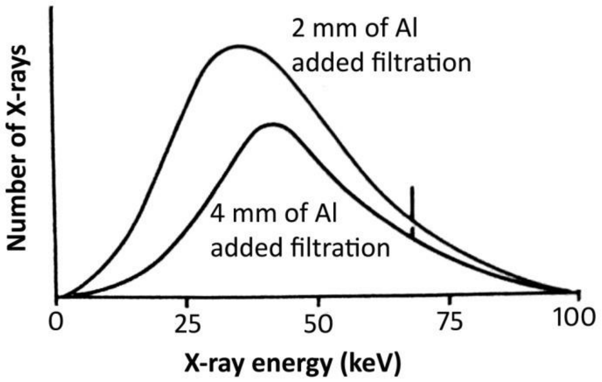

Fig. 1.4 (e): Additional tube filtration change the appearance of the X-ray emission spectrum

Changes in the X-ray generator type changes the X-ray production efficiency of the machine. High-frequency X-ray units are much more efficient in producing X-rays than single-phase units. This means that with the same amount of electricity, a high-frequency unit produces more X-rays. This is represented in the X-ray emission spectrum with increase in amplitude and average energy. If a generator operates more efficiently, more filament electrons have the energy to produce X-rays, increasing quantity (amplitude). There are also a greater number of higher-energy photons, increasing the average energy and shifting the peak to the right as shown in Fig. 1.4 (f).

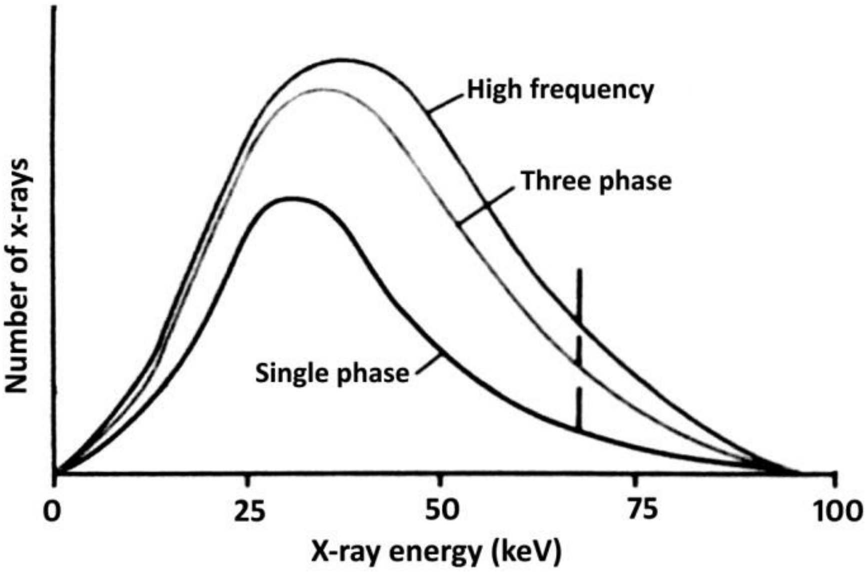

Fig. 1.4 (f): Change in generator type change the appearance of the X-ray emission spectrum

The general radiographer does not have the ability to select the target material used, except in mammography diagnostic X-ray machine. Although virtually, all radiographic X-ray tubes employ tungsten targets, it is instructive to consider how altering the target material might affect the emission spectrum. As the atomic number of the target material goes up, so does the average energy, quantity of photons and the position of the discrete line of the spectrum. With increase in atomic number, each atom is more complex, representing a bigger "target" for filament electrons to interact with. This increases the likelihood of interaction, the number of photons produced and the number of higher-energy photons as well as the average energy.

1.5 Interaction of X-rays with matter

An understanding of the basic mechanisms by which photons and charged particles interact with atoms, nuclei and molecules is fundamental to dosimetry, shielding and the interpretation of all manner of physical and biological effects produced by radiation (Turner, 2005). At the same time, to understand the relationship between attenuation and energy, one must be familiar with three of the basic interactions of X-rays photons with matter: *photoelectric*, *Compton* and *pair production interactions* (McKetty, 1998). In most health physics applications that involve X-rays, at least one of the three principle interaction mechanisms with atoms plays an important role (Turner, 2005). It is important to minimize the physical effects of X-ray photons on the patient that result in radiation dose and biological harm. It allows the radiographer to better manipulate how the particular anatomic area of interest appears radio-graphically (Johnston and Fauber, 2012).

1.5.1 Photoelectric Effect

In the photoelectric process, an incident photon with energy $h\nu$ is absorbed by an atom. The photon disappears and an electron is ejected from the atom as shown in Fig. 1.5.1. The electron emerges with kinetic energy $T = h\nu - B$, where B is the binding energy of the electron in one of the states of the atomic shell, K, L, M or N, from which it came (Turner, 2005). The atom is left in the excited state and emits characteristics radiation and Auger electrons as it returns to the ground state (Johns and Cunningham, 1983). The more closely bound the electron, the higher is its binding energy; consequently, the energy of the ejected electron is lower (McKetty, 1998). The probability of photoelectric interaction depends on the energy of the incident photons and the atomic number of the tissue atoms with which they interact. For photoelectric interactions to occur, the incident X-ray photon energy must be greater than or equal to the inner-shell binding energy of the tissue atoms involved. As the energy of incident photon begins to exceed the inner-shell binding energy of the tissue atom, the chances of photoelectric interaction begin to decline and the chances increase that it will penetrate the tissue. This function is a cubic relationship. That is, the probability of a photoelectric event is inversely proportional to the cube of the X-ray energy and directly proportional to the third power of the atomic number of the absorber. What this means to the radiographer is that if a kVp range is too high for the anatomic part of interest, then less absorption takes place and some absorption is necessary for image formation (McKetty, 1998; Johnston and Fauber, 2012).

Photoelectric absorption is the dominant mode of attenuation for low-energy photons in the range of several tens or hundreds of keV, depending of the atomic number of the absorbing atoms. At the lowest energies, ejection of an outer-shell electron might be the only event energetically possible. With increasing energy, the photoelectric attenuation coefficient for an element shows abrupt rises at the energies where ejection of an electron from an inner shell or sub shell becomes energetically possible (Turner, 2005). Photoelectric absorption contributes significantly to patient dose occurred with each diagnostic image. Eventhough some absorption is necessary to produce an X-ray image, it is the radiographer's responsibility to select input factors that strike a balance between image quality and patient dose. In photoelectric interactions, as with Compton interactions, the tissue atom is ionized. In the case of photoelectric interactions, the inner-shell vacancy makes the atom unstable and to regain stability a characteristic cascade occurs, producing secondary X-ray photons. This cascade is the same phenomenon that occurs with Compton interactions that produces secondary photons. Again, these secondary photons are of low energy and are absorbed by the body in other photoelectric events. Note that the absorption of these secondary photons also contributes to patient dose (Johnston and Fauber, 2012).

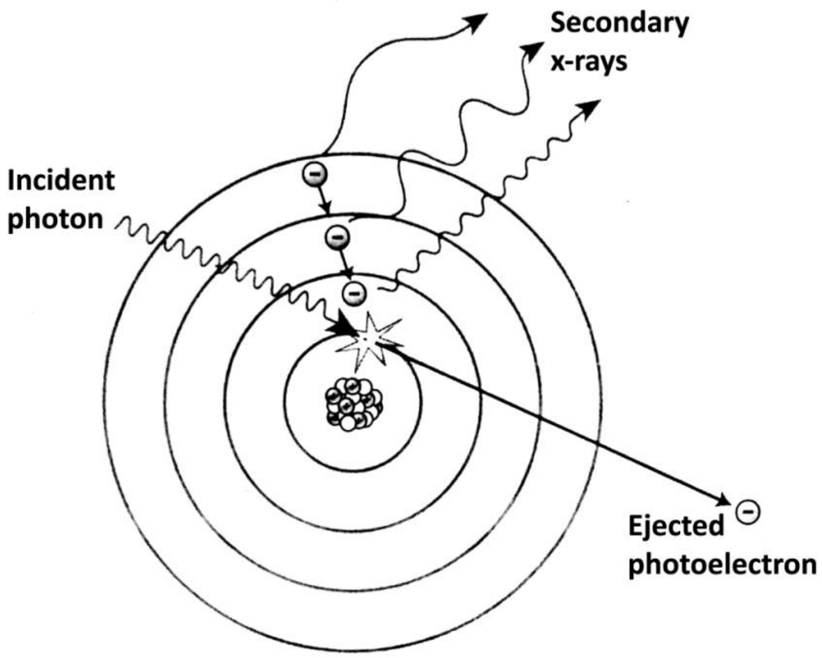

Fig.1.5.1: Photoelectric Interaction (Re-drawn from Johnston and Fauber, Essentials of radiographic physics and imaging, Published by Elsevier Mosby, 2012)

1.5.2 Compton scattering

In this interaction, an incident X-ray photon enters a tissue atom, interacts with an orbital electron and removes it from its shell. In doing so, the incident X-ray photon loses up to one third of its energy and is usually deflected in a new direction (Johnston and Fauber, 2012).

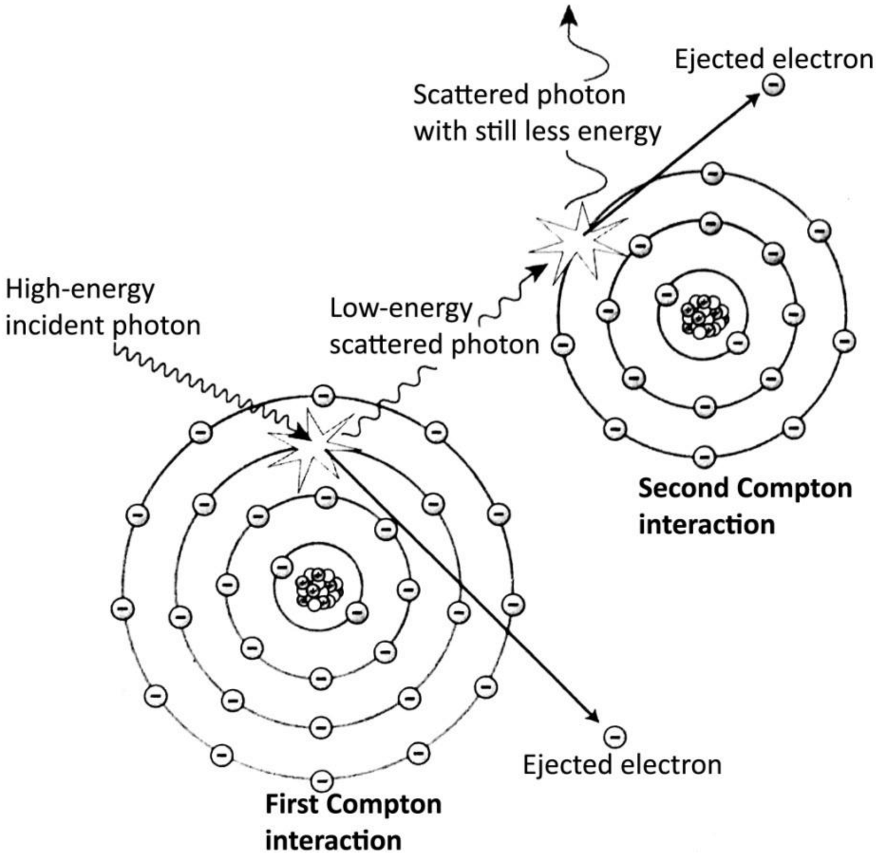
Ejected electron
Scattered photon
with still less energy
High-energy
incident photon
Low-energy
scattered photon
Second Compton
interaction
Ejected electron
First Compton
interaction

Fig. 1.5.2: A Compton scattering event (From Johnston and Fauber, Essentials of radiographic physics and imaging, Published by Elsevier Mosby, 2012)

Compton interaction does three things; namely first, it ionizes the atom, making it unstable. Ionization in the body is significant because the atom is changed and may bond differently to other atoms, potentially causing biological damage. If one of the middle orbital shells is involved, then a characteristic cascade (outer-shell electrons filling inner-shell vacancies and emitting X-ray photons) also results, creating characteristic photons just as in the tube target. But here they are called secondary photons (X-ray photons) but of a rather low-energy range. Such photons generally contribute only to patient dose. Second, the ejected electron, called a Compton electron or secondary electron, leaves the atom with enough energy to go through interactions of its own in adjacent atoms. The type of interaction that the Compton electron will undergoes mainly depends on its energy and the type of atom it interacts with. Third, the incident photon is deflected in a new direction and is now a Compton scatter photon as shown in Fig. 1.5.2. It too, has enough energy to go through other interactions in the tissues or exit the patient and interact with the image receptor. The problem with Compton scatter interacting with the image receptor is that it is not following its original path through the body and strikes the image receptor in the wrong area. In doing so, it contributes no useful information to the image and only results in image fog. Because most scattered photons are still directed toward the image receptor and result in image fog, it is desirable to minimize Compton scattering as much as possible (Johnston and Fauber, 2012).

Compton scattering is one of the most common interactions between X-ray photons and the human body in general diagnostic imaging and is responsible for most of the scatter that fogs the image. The probability of Compton scattering does not depend on the atomic number of atoms involved. Compton scattering may occur in both bone and soft tissue. The probability of Compton scattering is related to the energy of the photon. As photon energy increases, the probability of penetrating a given tissue without interaction increases. However, with this increase in photon energy, the likelihood of Compton interactions relative to photoelectric interactions also increases (Johnston and Fauber, 2012).

In a simplified treatment, a photon with energy *hν* and momentum *hν/c* collides with an atomic electron. The photon is scattered at an angle θ with respect to its original direction of travel and the struck electron recoils with kinetic energy T at another angle. As a result of the collision, the photon has less energy and momentum than before, the difference being transferred to the electron. Independently of the details of the mechanism of Compton scattering, the conservation of total energy and momentum provides useful relationships between the partners after the interaction. The kinetic energy of the struck electron is given by

$$T = h\nu \frac{1-\cos\theta}{\frac{mc^2}{h\nu}+1-\cos\theta} \qquad \text{------------ (1)}$$

Compton scatter photons may travel in any direction from their point of scattering. A deflection of zero degrees means no energy is transferred (Johnston and Fauber, 2012). The electron receives the maximum energy when the photon is scattered in the backward direction. With $\theta = 180°$, this energy is

$$T_{\max} = \frac{2h\nu}{2+\frac{mc^2}{h\nu}} \qquad \text{------------- (2)}$$

In principle, these and other relationships derived from the conservation laws need corrections due to the binding of the atomic electron, which was assumed to be free. In practice, however, at low energies where the corrections might be appreciable, photoelectric absorption is typically a much more important interaction. The energy of the scattered photon is

$$h\nu' = \frac{h\nu}{1+\frac{h\nu}{mc^2}(1-\cos\theta)} \qquad \text{------------ (3)}$$

At increasingly high energies, the energy of the back-scattered photon thus approaches the value $h\nu' = mc^2/2 = 0.256$ mega-electron volt (*MeV*). A remarkable feature of the scattering observed by Compton is that the shift in wavelength between the incident and scattered photons seen at any given angle is independent of the incident-photon energy. The conservation laws show that

$$\Delta\lambda = \frac{h}{mc}(1-\cos\theta) \qquad \text{------------ (4)}$$

for all incident energies. The constant, $h/mc = 2.426 \text{ X } 10^{-12}$ m, is called the Compton wavelength. It is the wavelength of a photon with energy equal to the rest energy mc^2 = 0.5110 MeV of the electron (Turner, 2005).

It is very important to keep in mind that the scattered photon still retains about two thirds of its energy. This is one reason that the radiographer should never stand near the patient during X-ray examination. Some Compton scatter photons exit the patient and would expose the radiographer. This is why shielding (lead aprons, lead gloves, etc.) is necessary during fluoroscopy or any procedure in which the radiographer or other health care worker may be near the patient and X-ray tube during exposure. It is important for the radiographer to remember that Compton scattering is the major source of occupational exposure (Johnston and Fauber, 2012). The angular distribution for the scattered photons is given by the Klein-Nishina formula (Klein and Nishina, 1929).

Whereas the photoelectric effect accounts for most of the attenuation of low-energy photons, its influence falls rapidly with increasing energy. At the same time, the probability for Compton scattering of a photon increases. Compton scattering is the dominant mode of attenuation from intermediate energies to beyond the threshold (1.022 MeV) for pair production. Photoelectric and Compton interactions produce attenuation in the diagnostic energy range. Again, photoelectric interactions are important for a low-energy range (up to 50 keV) and materials with a large atomic number. Compton interaction is predominant in the intermediate energy range (60 keV-2 MeV) for all materials, regardless of atomic number (Turner, 2005; McKetty, 1998).

1.5.3 Thomson scattering

In this scattering event, the incident X-ray photon interacts with an orbital electron of a tissue atom and change direction. In this classical interaction the incident X-ray photon is having low energy, generally less than 10 keV. When such low-energy incident photons interact with tissue atoms, they are not likely to remove orbital electrons from their shell. However, they absorb the X-ray photon energy, causing excitation of the atom and then immediately release the energy in a new direction. As the energy is re-emitted in a whole new direction, it is now called as scattered photon. The scattered photon has equal energy to the incident photon but travels in a new direction (Fig. 1.5.3). Due to its low energy, most classical scatter photons are absorbed in the body through other interactions mechanism and do not contribute significantly to the image, but do add slightly to patient dose (Johnston and Fauber, 2012).

With increasing photon energy, the probability for coherent scattering decreases while increases with increasing atomic number. However, at higher atomic numbers, the relative fraction tends to decreases as the strong increase of photoelectric absorption with increasing atomic number. For Al, the relative probability for coherent scattering is 13% at 50 keV (Johnston and Fauber, 2012).

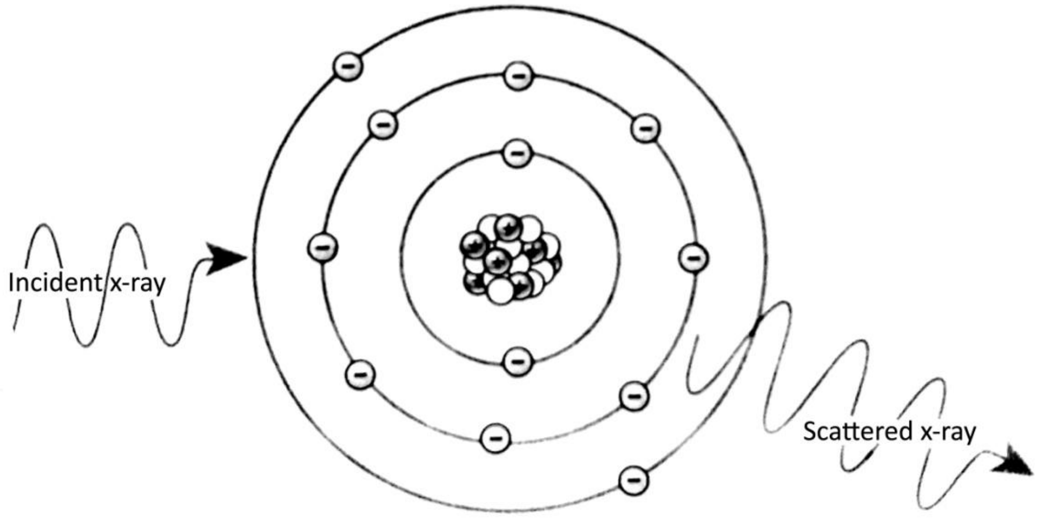

Fig. 1.5.3: A classical scattering event (Re-drawn from Johnston and Fauber, Essentials of radiographic physics and imaging, Published by Elsevier Mosby, 2012)

1.5.4 Pair Production

Absorption of a photon by an electron in a negative-energy state is called pair production. A photon with energy $hv \geq 2\ mc^2 = 1.022$ MeV disappears and an electron-positron pair appears with particle kinetic energies T_- and T_+. The photon energy is converted into the total energy of the pair: $hv = 2\ mc^2 + T_- + T_+$ (Turner, 2005). Pair production can occur only if the energy of the incident photon is greater than 1.02 MeV. Therefore, this interaction does not occur in the energy range of X-ray beams used for diagnostic radiology (McKetty, 1998). In this interaction, two particles are produced; a positron (positively charged electron) and an electron (Fig. 1.5.4). For these particles to exist, they must each have energy of 0.51 MeV (the energy equivalent of an electron). The photon energy 1.02 MeV is shared between the two as kinetic energy (Johnston and Fauber, 2012). Both particles travel out of the atom. Before coming to rest in another atom the electron undergoes many interactions. The positron is an unnatural particle and as such travels until it strikes an electron, causing an annihilation event. In this annihilation event, the positron and the electron interacts with are destroyed and their energy is converted into two X-ray photons that radiate out of the atom (Johnston and Fauber, 2012).

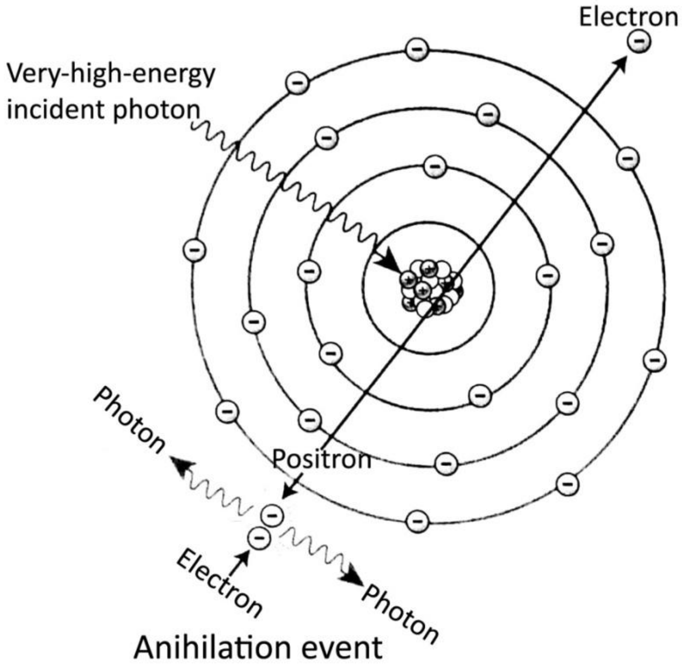
Electron
Very-high-energy
incident photon
Photon
Positron
Electron
Photon
Anihilation event

Fig. 1.5.4: A Pair production event (Re-drawn from Johnston and Fauber, Essentials of radiographic physics and imaging, Published by Elsevier Mosby, 2012)

1.6 Attenuation of X-rays

In conventional radiography, an X-ray beam is passed through the body section and projects an image onto a receptor. The beam that emerges from the body varies in intensity. The variation in intensity is caused by X-ray attenuation in the body, which depends on the penetration characteristics of the beam and the physical characteristics of the tissues. The reduction may be caused by absorption or by deflection of photons from the beam and can be affected by different factors such as beam energy, thickness and atomic number of the absorber (McKetty, 1998).

1.6.1 Linear Attenuation coefficient and Exponential Attenuation

An attenuation coefficient is a measure of the quantity of radiation attenuated by a given thickness of an absorbing material. The linear attenuation coefficient (μ) is the fractional change in X-ray intensity per the thickness of the attenuating material. The linear attenuation coefficient is measured in units of per unit length, which is most commonly expressed in terms of centimeters (cm) or mm. Attenuation rate can also be expressed in terms of the mass of the material encountered by photons (McKetty, 1998). Following equation gives the number of interactions in a slab of thickness Δx bombarded by N_o photons.

$$n = \mu \, N_o \, \Delta x \qquad \text{-------------------} \; (5)$$

where, n - no. of photons interact with attenuator and be removed from the beam.

μ - constant of proportionality called *linear attenuation coefficient* (m^{-1}).

N_o - no. of photons in the beam from the source

Δx - slab material which attenuate radiation.

As the thickness of the attenuating material increases, the equation is no longer correct and the relationship becomes nonlinear. Equation 5 can be written as,

$$\Delta N = - \, \mu \, N_o \, \Delta x \qquad \text{-------------------} \; (6)$$

‘This equation describes how N_o changes as we pass through the attenuator’

where, ΔN - change in number of photons in the beam passing through Δx.

ΔN - $-n$ because N is reduced by one for each interaction.

Equation (7) may be used to calculate the attenuation by any thickness of material when the incident and transmitted photon intensity is measured, whereas the equation (5) and (6) is only applicable when the fractional reduction by a layer of material is very small.

$$N = N_o e^{-\mu x} \qquad \text{------------------- (7)}$$

where, N - no. of transmitted photons by any thickness x

N_o - the no. of incident photons

e - base of natural logarithms with values 2.718 (Johns and Cunningham, 1983; McKetty, 1998)

In diagnostic radiology, photon intensity is the quantity that is most often measured (McKetty, 1998). According to equation (7), there is always a finite probability that some incident photons will get through a shield of any thickness without having an interaction. At the same time equation (7) is valid only if the attenuation coefficient is actually constant and this is only true if the photons in the incident beam all have the same energy (a mono-energetic beam) and if the beam is narrow (Turner, 2005). Polychromatic beams contain a spectrum of photon energies. With an X-ray beam, the maximum photon energy is determined by the peak kilo-voltage used to generate the beam. Mainly because of the spectrum of photon energies, the transmission of polychromatic beam through an absorber does not strictly follow equation (7).

The transmission of electromagnetic radiation through shields under conditions of 'poor' geometry can be formulated approximately in terms of a buildup factor, *B*. *B* is never less than unity. Buildup factors have been determined for a number of different materials, different source and shield geometries and different photon energies. They also depend on the specific quantity under consideration, such as intensity, exposure or absorb dose.

$$N = N_o\, e^{-\mu x} B\, (x,\, h\nu,\, A,\, L) \qquad \text{----------------}\ (8)$$

where, B - rather a complicated factor, sometimes called a photon buildup factor, that takes account of the photons scattered by the attenuator.
x - thickness of attenuator
$h\nu$ - energy of photon
A- area and
L - length of attenuator.

When a polychromatic beam passes through an absorber, photons of low energy are attenuated more rapidly than the higher energy photons; therefore, both the number of transmitted photons and the quality of the beam change with increasing amounts of an absorber. A semi-logarithmic plot of the number of photons in a polychromatic beam as a function of the thickness of the attenuating materials will be curve. The initial slope of the curve is steep because the low-energy photons are attenuated, but, as the beam becomes more monochromatic, the slope decreases. A comparison of the curves for polychromatic and monochromatic is shown in Fig.1.6.1.

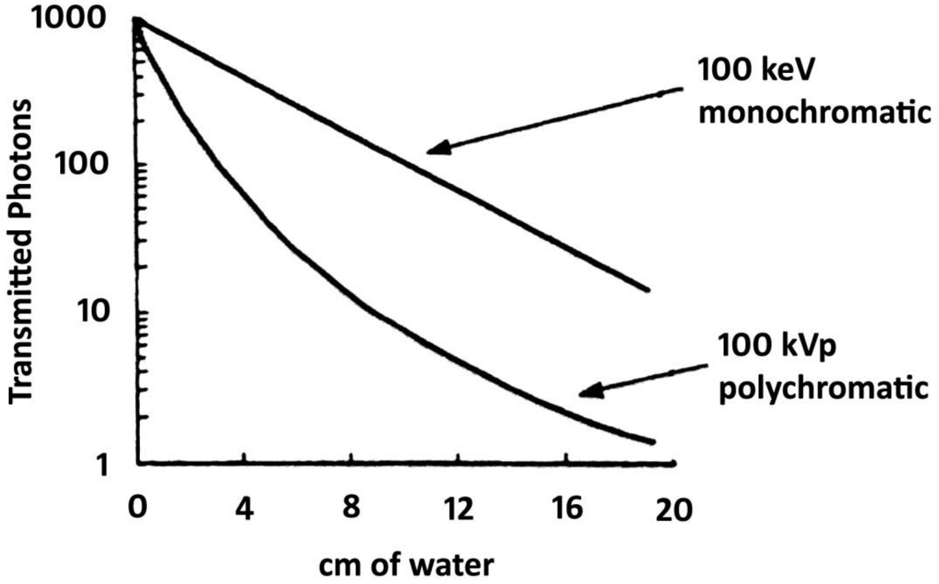

Fig. 1.6.1: Graph shows a comparison of the curves for polychromatic and monochromatic radiation (From McKetty, The AAPM/RSNA Physics Tutorial for Residents-X-ray Attenuation, Washington, *Radiographics*, 1998)

An important point here is the comparison between kilo-electron volt and peak kilo-voltage. A mono-energetic X-ray photon beam at 100 keV(effective energy, 100 keV) is substantially more penetrating than a comparable X-ray photon beam produced at 100 kVp (effective energy, 40 keV, depending on filtration of the beam). Most of the X-ray photons in a bremsstrahlung spectrum are composed of substantially lower energies than the peak energy, thus resulting in a significant increase in attenuation, which is nonlinear on the semi-logarithmic graph illustrated (Curry TS, 1990).

1.6.2 Mass, Electronic and Atomic Attenuation Coefficients

Mass attenuation coefficient (μ/ρ) is the more fundamental attenuation coefficient, which is obtained by dividing the linear attenuation coefficient (μ) by the density of the material through which the photons pass (ρ). Mass attenuation coefficient is the rate of photon interactions per unit area mass and is independent of the physical state of the material. The unit of the mass attenuation coefficient is m^2/Kg. The range of energies used in X-ray imaging is chosen to optimize the diagnostic X-ray information and to minimize the radiation absorbed by the patient. Both these factors depend on the mass attenuation coefficients of various materials and tissues (McKetty, 1998). *Electronic attenuation coefficient* (μ_e) is the attenuation coefficient which is obtained by dividing mass coefficient (μ/ρ) by number of electron per gram (N_e), m^2/el is the derived unit. The *atomic attenuation coefficient* (μ_a) is the fraction of an incident X-ray beam that is attenuated by a single atom i.e. the probability that an X-ray absorber atom will interact with one of the photons in the X-ray beam. Atomic attenuation coefficient is obtained by dividing mass attenuation coefficient (μ/ρ) by number of atoms per gram (N_e), m^2/at is the derived unit. (Johns and Cunningham, 1983; McKetty, 1998)

1.6.3 Factors affecting attenuation

Several factors affect attenuation, some are related to the X-ray beam and the others to properties of the matter through which the radiation is passing. The factors include beam energy, the number of photons traversing the attenuating medium or absorber and the atomic number of the absorber. As noted, the greater the thickness of the attenuating material, the greater is the attenuation. Similarly, as the atomic number or density of the material increases, the attenuation produced by a given thickness increases. Thus, different material such as water, fat, bone and air have different linear attenuation coefficients as do the different physical states or densities of a material table 1.6.3 (Johns and Cunningham, 1983; McKetty, 1998).

Table 1.6.3: Physical properties of selected materials (From McKetty, 1998)

Sl/ No	Material	Effective Atomic Number (Z)	Density (g/cm^3)	50 keV Linear Attenuation Coefficient (cm^{-1})
1	Water	7.4	1.0	0.214
2	Fat	5.92	0.91	0.193
3	Compact bone	13.8	1.85	0.573
4	Air	7.64	0.00129	0.00029

1.6.4 Total Attenuation Coefficient

When single photon interacts with matter, any of the four processes may occur. In any one interaction only one process can take place, but in many interactions all of them may occur. The total attenuation coefficient, μ_{total}, is thus the sum of the four components:

$$\mu_{total} = \tau + \sigma_{coh} + \sigma_{incoh} + \kappa \qquad \text{------------------ (9)}$$

where, τ - photoelectric interaction

σ_{coh} - Thomson (coherent) scattering

σ_{incoh} - Compton (incoherent) interaction

κ - pair production interaction

In low *Z* materials, σ_{coh} is usually negligible except very low energies (<10 kev) and is often omitted from the sum (Johns and Cunningham, 1983). The same relationship holds between the mass attenuation coefficients for the different mechanisms. Figure 1.6.4 shows the relative importance of the three interactions at different energies in different elements. The lines are drawn at the values of *Z* and *hν* for which the probabilities for the two adjacent effects are equal. As already mentioned, the photoelectric effect is the most important for low energies and high *Z*. At intermediate energies the Compton effects is the dominant mode of attenuation for all *Z*. Pair production dominates at high energies and large *Z*. For compounds and mixtures of materials, the attenuation coefficients are assumed to be the sum of the individual, independent atomic contributions (Turner, 2005).

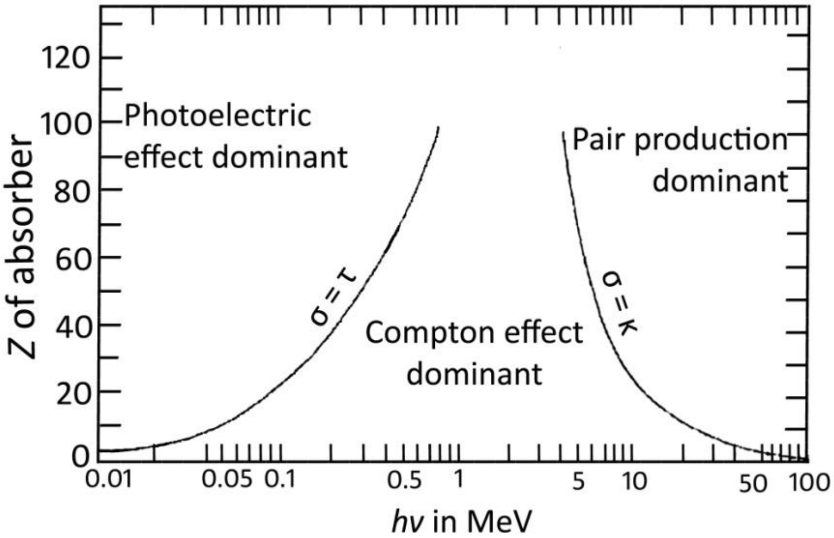

Fig. 1.6.4: Relative importance of photoelectric effect, Compton scattering and pair production at different *hν* in elements of different Z. Lines show the locus of points at which σ = τ and σ = κ. (From Robley D. Evans, The Atomic Nucleus, copyright 1955, Published by McGraw-Hill)

1.6.5 Total Energy Transfer and Absorption Coefficients

For dosimetry, one often needs to assess the energy transferred or energy absorbed in a material exposed to photons. The energy transfer coefficient, μ_{tr}, is defined as the product of the attenuation coefficient and the average fraction of the energy of the removed photon that is transferred as initial kinetic energy to secondary charged particles. This coefficient is defined next for each of the three principal photon-interaction mechanisms (Turner, 2005).

The energy transfer coefficient for photoelectric absorption is, therefore,

$$\tau_{tr} = \tau(1-\frac{\delta}{h\nu}) \qquad \text{--------------------- (10)}$$

where, δ represents the average energy released as fluorescence radiation per photoelectric event, then the fraction $\delta/h\nu$ of the incident photon's energy is not imparted to secondary electrons. For Compton scattering, the energy transfer coefficient is given by

$$\sigma_{tr} = \sigma\frac{T_{avg}}{h\nu} \qquad \text{---------------------- (11)}$$

where, $T_{avg}/h\nu$ is the average fraction of the photon energy that is transferred to the Compton electron. When pair production takes place in a nuclear field, an electron-positron pair is created with initial kinetic energy $h\nu$ - 2 mc^2, according to eqn ($h\nu = 2\ mc^2 + T_- + T_+$). The energy-transfer coefficient is then

$$\kappa_{tr} = \kappa(1-\frac{2mc^2}{h\nu}) \qquad \text{---------------------- (12)}$$

This relationship neglects the small contribution from energy transfer by triplet production. Also, positrons that annihilate in flight lead to a slight decrease in the value implied by the above equation. The total linear energy-transfer coefficient μ_{tr} for photons of energy $h\nu$ in a uniform absorber is the sum of equations (10), (11) and (12):

$$\mu_{tr} = \tau(1-\frac{\delta}{h\nu}) + \sigma\frac{T_{avg}}{h\nu} + \kappa(1-\frac{2mc^2}{h\nu}) \qquad \text{---- (13)}$$

To a good approximation this quantity determines the conversion of incident-photon energy into kinetic energy of secondary electrons and positrons in an absorber. Also included is the average energy of Auger electrons following photoelectric absorption (Turner, 2005).

1.6.6 The Relative Important of Different Types of Interactions

The percentage of the interactions that are photoelectric is;

$$100\ \tau/(\tau + \sigma_{coh} + \sigma_{inc} + \kappa) = 100\ \tau/\mu \qquad \text{----- (14)}$$

The percentage of energy transfer to photoelectrons is;

$$100\ \tau_{tr}/(\tau_{tr} + \sigma tr + \kappa_{tr}) \qquad \text{----------------------- (15)}$$

Similar expressions for the other processes, the percentage of energy transfer radiated from the system by bremsstrahlung is calculated by

$$= 100\ (1 - E_{ab}/E_{tr}) \qquad \text{---------------------- (16)}$$

(This fraction becomes important only above 10 MeV; Up to 50 keV - Photoelectric absorption is important; 60 to 90 keV - Photoelectric and Compton are both important; 200 keV to 2 MeV - Compton absorption alone is there; 5 to 10 MeV - Pair production begins to be important; 50 to 1000 MeV - Pair production is most important)

Table 1.6.6: Types of Photon Interactions in Water

h*ν* (keV)	% Interactions by Each Process				% Energy Transferred			% Energy Lost to Bremsstrahlung (h)
	Coh	Compton	Photo	Pair	Compton	Photo	Pair	
10.0	4.5	3.1	92.4	0.0	0.1	99.9	0.0	0.0
15.0	8.5	10.8	80.7	0.0	0.4	99.6	0.0	0.0
20.0	11.6	23.3	65.1	0.0	1.3	98.7	0.0	0.0
30.0	13.0	50.7	36.3	0.0	6.8	93.2	0.0	0.0
40.0	11.0	69.6	19.4	0.0	19.3	80.7	0.0	0.0
50.0	8.6	80.4	11.0	0.0	37.2	62.8	0.0	0.0
60.0	6.8	86.6	6.6	0.0	55.0	45.0	0.0	0.0
80.0	4.5	92.6	2.9	0.0	78.8	21.2	0.0	0.0
100.0	3.1	95.3	1.5	0.0	89.6	10.4	0.0	0.0
150.0	1.6	97.9	0.5	0.0	97.4	2.6	0.0	0.0

1.7 Biological effects of X-rays

X-rays are ionizing radiation and have potential to disrupt the structure of organic molecules in cells. Generally, biological effects of radiation begin with the ionization of atoms. Ionizing radiation like X-rays has enough energy to remove electrons from the atoms that make up molecules of the tissue. The affected tissues further affect organs and hence, the whole human body.

1.7.1 Direct and indirect effect

Chromosomes are considered to be the most important target to X-rays since they contain the genetic information and instructions required for the cell to perform its function and to make copies of itself for reproduction purposes. A chromosome is an organized package of Deoxyribonucleic acid (DNA) or a thread-like structure found in the nucleus of the cell. Direct effect includes the direct ionization of the DNA molecule as shown in Fig. 1.7.1 (a), which may result in genetic damage. This kind of damage can disturb the reproduction and survival of the cells (USNRC, 2014). However, DNA counts for a very small portion of a cell. The human body mostly consists of water molecules. Upon exposure of ionizing radiation there are more chances that radiation will interact with water molecules. This interaction might result in formation of free radicals as described in Fig. 1.7.1 (b) and toxic substances which attacks the DNA. This indirect effect of radiation on DNA is more probable than direct action.

When pure water is irradiated, the interaction of radiation with water causes the breakdown of water into hydrogen (H) and hydroxyls (OH). Hydrogen and hydroxyls may recombine or interact with other ions resulting in the formation of harmful compounds, for example hydrogen peroxide (H_2O_2). Hydrogen peroxide is a very powerful oxidizing agent and hence it has adverse effects on cells or molecules (USNRC, 2014).

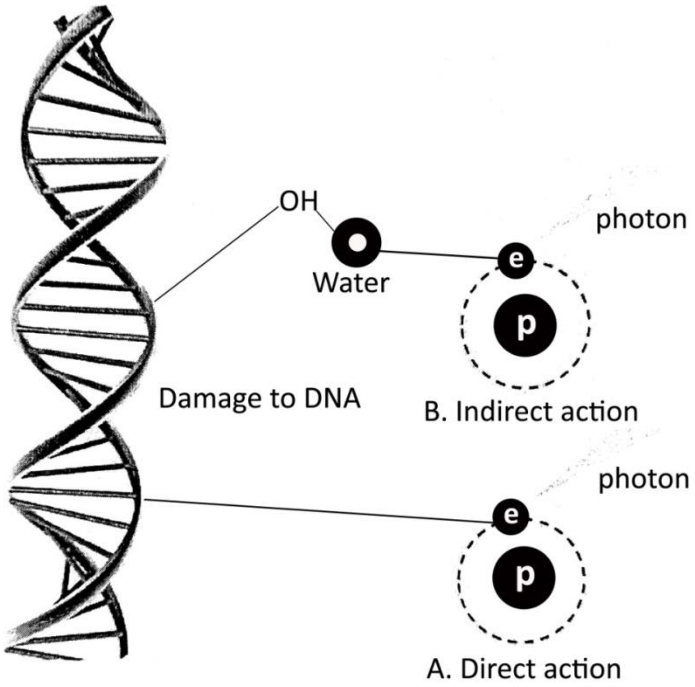

Fig. 1.7.1: (a) Damage from direct effect (b) Damage from free radicals

1.7.2 Effects of radiation on cells

The sensitivity of human body's organs is directly related to the sensitivity of cells. However, all cells are not exactly identical and hence they are not equally sensitive to radiation. For example, germline cells are particularly sensitive to radiation while mature differentiated cells are less sensitive. Living cells can be classified upon their reproduction rate and the relative sensitivity towards radiation (USNRC, 2014). Lymphocytes known also as white blood cells are most sensitive to radiation as they regenerate constantly. Reproductive and gastrointestinal cells are not regenerating as quickly as lymphocytes and therefore they are less sensitive. Nerve and muscle cells regenerate very slowly and hence they are least sensitive cells to radiation.

1.7.3 Effects of radiation on organs and body

The human body is made up of many organs and each organ of the body is made up of specialized cells. Hence, the sensitivity of the various organs of the human body is associated with the relative sensitivity of the cells. For example, the blood forming cells are one of the most sensitive cells due to their rapid regeneration rate, the blood forming organs are one of the most sensitive organs to radiation. Nerve cells and muscle are relatively insensitive to radiation and therefore, so are the brain and muscles. The factors that affect the whole body from exposure of radiation depend on the total dose being received by a person, type of cells being exposed to radiation, type of radiation, age of an individual being exposed, part of body exposed as some parts are more sensitive than others, general state of health of an individual and time interval over which dose is received (USNRC, 2014).

1.7.4 Deterministic radiation effects

Deterministic effects, also known as non-stochastic effects, are those responses which increase in severity with increased radiation dose. Deterministic effects occur when human body receives high radiation dose over relatively short amount of time. This effects results in lots of dead cells. Deterministic effect is characterized by a threshold below which the effect is not seen. This threshold varies from person to person as well as from tissue to tissue (Herman and Thomas, 2009). High-level exposure within a short period of time sometimes referred to as 'acute' exposure. Acute radiation syndromes are classified as; the hemopoietic syndrome, the gastrointestinal (GI) syndrome and the central nervous system (CNS) syndrome.

The hemopoietic syndrome is associated with the blood forming tissues. People with the hemopoietic syndrome have shown changes in blood count. The GI syndrome occurs when body receives a total dose of about 10 Gy or more and results in complete destruction of bone marrow as well destruction of the intestinal epithelium. The GI syndromes usually results in death within several weeks after exposure. The CNS syndrome occurs when body is exposed to a dose of about 20 Gy.

In case of low-energy X-rays, skin is the main target of exposure. The radiation exposure on skin may result in erythema or changes of pigmentation, epilation, blistering, necrosis and ulceration. Other than skin, eyes sensitive target for high-dose radiation among occupational workers using analytical X-rays. Irradiation on eye lens might cause damage in the epithelial cells of the lens capsule. Radiation exposure to the lens of eye might result in blindness as abnormal lens fibers would prevent light to reach retina.

1.7.5 Stochastic radiation effects

Stochastic effects are effects which show up years after exposure. Unlike deterministic effects stochastic effects can occur from single cell damage. For stochastic effects there is no threshold and under certain exposure conditions stochastic effects may or may not occur. Stochastic effects may result in the genetic effects, somatic effects or in-utero effects (Herman and Thomas, 2009).

Genetic effects are abnormalities that may take place in the future generations of exposed individuals. These effects involve the mutation of very specific cells, specifically the sperm or egg cells. Mutations of these reproductive cells are passed to the offspring of the individual exposed. However, it is very hard to determine whether occurrence of genetic effect is due to ionizing radiation as there is lack of studies and evidences. Somatic effects are the most significant effects from an occupational risk perspective. In somatic effects the consequences are suffered by the individual exposed, usually the radiation worker. Cancer is one of the greatest concerns in somatic effects for radiation workers who receive low doses over a long period of time. Unlike genetic effects, many studies have been completed which directly link the induction of cancer and exposure to radiation. In-utero effects involves the production of deformities in developing embryos. The effects from in-utero exposure can be considered part of somatic effects. The malformation of embryos produced does not indicate a genetic effect since it is the embryo that is exposed not the reproductive cells of the parents.

1.8 Fundamental principles of radiation protection

Almost all international and national standards and regulations in radiation protection are based on the recommendations of International Commission on Radiological Protection (ICRP). The most important fundamental principles for radiation protection are known as the principle of justification, the principle of optimization of protection and the principle of application of dose limits (ICRP, 2007).

The principle of justification simply refers that any decision that alters the radiation exposure situation should do more good than harm. This principle roughly means that, the benefits of using radiation should be more than the drawbacks of its use. For example, no source of exposure should be introduced unless its advantages outweigh its risks.

The principle of optimization of protection means that the likelihood of incurring exposures, the number of people exposed and the amount of their individual doses should all be kept as low as reasonably achievable, taking into account societal as well as economic factors. This principle is also known as 'as low as reasonably achievable' (ALARA).

The principle of application of dose limits means that the entire dose to any individual from regulated sources in planned exposure situations other than medical exposure of patients should not exceed the appropriate dose limits recommended by the various Commissions. The current dose limits in India are discussed in radiation safety regulation –national safety code.

1.9 Radiation Safety Regulations (National Safety Code)

To ensure radiation safety for users, members of the public and the environment the government of India constituted Atomic Energy Regulatory Board (AERB) under the Atomic Energy Act, 1962. Further, the government of India entrusted AERB with the responsibility of developing and implementing appropriate regulatory measures. Accordingly, AERB issued the first 'Safety code for medical diagnostic X-ray equipment and installations, AERB/SC/MED-2' in December 1986 (AERB, 1986). However, to consider changes in the recommendations of ICRP and to incorporate the latest regulatory requirements relevant to medical diagnostic X-ray practice, the first safety code has been revised. The revised code 'Medical diagnostic

X-ray equipment and installations, AERB/SC/MED-2 (Rev. 1)' approved by the AERB on 5th October, 2001, which replaced the previous safety code. In order to ensure that radiation workers and members of the public are not exposed to radiation in excess of limits specified by the competent authority under the Radiation Protection Rules, 1971 and by safety directives issued from time to time the revised code intended to govern radiation safety in design, installation and operation of X-ray generating equipment for medical diagnostic purposes (AERB, 2001).

1.9.1 Safety specifications for medical diagnostic X-ray equipment (general purpose radiographic equipment) and protective devices

Diagnostic X-ray machine shall have facilities for tube positioning, target-to-film distance selection, useful beam centering and angulations, positioning of the patient and the X-ray film for exposure in the preferred way and suitable features to display the same. The protective barrier between control panel-operator and patient-X-ray tube shall be of appropriate size and design to shield the operator adequately against stray radiation. It shall have a minimum lead equivalence of 1.5 mm and a viewing window of approximately 1.5 mm lead equivalence shall be provided on the barrier. Protective aprons and gloves shall have a minimum lead equivalence of 0.25 mm whereas gonad shields shall have a minimum lead equivalence of 0.5 mm. The cassette pass box intended for installation in the X-ray room wall shall have a shielding of 2.0 mm lead equivalence. Suitable overlap of protecting materials shall be provided at the joints so as to ensure minimum prescribed shielding all over the surface of all radiation protection devices. The total filtration shall be specified on the tube housing and total permanent filtration of the tube shall be not less than 1.5 mm Al.

The layout of diagnostic X-ray rooms shall be such that the number of doors for entry to the X-ray rooms shall be kept to the minimum. The unit shall be so located that it shall not be possible to direct the primary X-ray beam towards control panel, dark room, door, windows and areas of high occupancy. Further, the room housing shall be not less than 18 m^2 for general purpose radiography and conventional fluoroscopy equipment. Not more than one unit of any type of equipment shall be installed in the same room and no single dimension of these X-ray rooms shall be less than 4 m. Unshielded openings in an X-ray room for ventilation shall be located above a height of 2 m from the finished floor level outside the X-ray room. The control panel of the X-ray equipment operating up to 125 kVp can be located inside the X-ray room. However, the control panel of diagnostic X-ray equipment operating at 125 kVp or above shall be installed in a separate room but contiguous to the X-ray room and appropriate shielding plus direct viewing and oral communication facilities between the operator and the patient should be available. Further, the distance between X-ray unit-chest stand and control panel shall be not less than 3 m for general purpose fixed X-ray equipment. Patient waiting areas shall make available outside the X-ray room. A suitable warning signal such as red light shall be provided at a conspicuous place outside the X-ray room and kept "ON" when the unit is in use to warn persons from entering the room.

1.9.2 Radiation protection and work practice

Gonad shields shall be used to protect the reproductive organs of the patient unless it would interfere with the information desired. Eve shields shall be provided to protect the eyes of patients undergoing such special examinations as carotid angiography. Thyroid shields shall be used where necessary. All radiation workers shall use suitable personnel monitoring devices (PMD), as instructed by the employer. The field size shall be restricted to the minimum that is consistent with the diagnostic requirement to ensure minimum possible dose to the patient. Especially in paediatric radiology particular attention shall be paid to restricting field size. Gonads, if not required, shall not be exposed to primary X-ray beam.

1.9.3 Personnel requirements and responsibilities

In any diagnostic X-ray installation the ultimate responsibility of ensuring radiation safety, availability of radiation safety officer (RSO) and qualified personnel for handling of X-ray equipment and providing them requisite equipment and facilities shall rest with the employer. The employer shall also be responsible for ensuring that PMDs are made available to the radiation workers. All diagnostic X-ray installations shall have a qualified X-ray technologist to operate the X-ray unit. X-ray technologist and other staff shall ensure appropriate patient protection, public protection and operational safety in handling X-ray equipment.

1.9.4 Regulatory controls

Before marketing the X-ray equipment, the manufacturer shall acquire a type approval certificate from the competent authority for indigenously made machine. For foreign machine, the importing agency shall obtain a no objection certificate (NOC) from the competent authority. X-ray equipment shall be registered with the competent authority by the person acquiring the equipment. Registration shall be done only after the installation is approved from radiation safety perspective.

The diagnostic X-ray installations shall be made available by the employer/owner for inspection at all reasonable times, to the competent authority or its representative to ensure compliance with safety code. Any person who contravenes the provisions of the Radiation Protection Rules,1971, elaborated in the safety code or any other terms or conditions of the license/registration/certification granted to him/her by the competent authority, is punishable under the Atomic Energy Act,1962 sections 24, 25 and 26. The punishment may include fine, imprisonment or both, depending on the severity of the offence.

1.9.5 Dose limits

For workers the cumulative effective dose over five years shall not exceed 100 milli-sievert (*mSv*). Where, the effective dose in any calendar year during a five-year shall not exceed 30 mSv. The equivalent dose in any calendar year to the lens of the eye shall not exceed 150 mSv and the equivalent dose in any calendar year to the hands, skin and feet shall not exceed 500 mSv. In case of a woman worker of reproductive age, once pregnancy has been established, the conceptus shall be protected by applying a supplementary equivalent dose limit to the surface of the woman's abdomen of 2 mSv for the remainder of the pregnancy.

For trainees the effective dose in any calendar year shall not exceed 6 mSv. For public the effective radiation dose in any calendar year shall not exceed 1 msv. In special circumstances, a higher value of effective dose is allowed in a single year, provided that the effective dose averaged over a five year period does not exceed 1 mSv/y.

1.10 Background and the scope of the study

Shortly after the discovery of X-rays the harmful effects of radiation that results from inadequate protection were widely known (Archer, 1995). The recent study reported that the risk for solid cancers increased significantly as cumulative radiation exposure increased (Sun *et al*., 2016). In developed countries, the contribution of diagnostic X-rays to cancer ranged from 0.6−1.8% of the cumulative risk of cancer upto the age of 75 years (Gonzalez and Darby, 2004). In addition to that ionizing radiation originated form medical diagnostic X-rays machines have been reported to be the major contributor of public exposure to man-made ionizing radiation (Bennett, 1991). Approximately 51% of the population dose was estimated to be caused by diagnostic X-ray examinations (Bushong, 2013). Utilization of X-rays, even at low doses typically encountered in diagnostic radiology, is associated with the risk of cancer induction and other stochastic effects (ICRP, 2001)

Twenty seven years ago, Supe *et al*. (1992) reported that “most of the rural areas have very old X-ray machines for which quality assurance tests have never been undertaken" from the study of 'estimation and significance of patient dose from diagnostic X-ray practices in India'. Till today, it seems equally true that no proper quality assurance tests as per AERB guidelines have been performed for the X-ray machines in Mizoram. In the present complete enumeration study, the X-ray generators such as linearity of time (*sec*), linearity of current (*mA*), output reproducibility, peak voltage (*kVp*) accuracy, table dose (*µGy/mAs*) and other 16 important safety parameters were considered. These are the parameters controlled and adjusted by the radiographer for generating a suitable exposure rates. That is why they are very important to achieve one of the basic safety principles called ALARA.

Concerning mechanical parameters of conventional diagnostic X-rays machine the authors considered HVL, congruency between the radiation beam and the optical field plus perpendicularity of the central beam to the image receptor. HVL thickness is measured to observe the permanently installed filter on the X-ray tube is maintained to minimize patient exposure. Many times fault in congruency and misalignment in central beam results unnecessary radiation dose through repeated exposure. Using calculated workload and exposure rates, doses at control panel and outside patient entrance door (PED) were calculated and compared to the safety standards. In addition to that, assessments of the safety status of different kind of shielding materials were performed through evaluating and comparing the amount of intensity of radiation attenuated by different types of PEDs as well as CP barriers. With the international standard test procedure tube housing leakage of all working conventional diagnostic X-ray machines were studied. To the best of authors' knowledge, no such studies had been performed or reported in the present study area in the past. The results were compared with the standard safety limits recommended by various regulatory bodies. Further, such results were also compared with the previous studies as well.

The main objectives of the present investigation are:

- To investigate mechanical properties of X-ray units; such as optical and radiation field congruence, central radiation beam alignment perpendicularity.
- To investigate input/output characteristics of X-ray units; such as accelerating potential, tube current, exposure time, output consistency, radiation filter.
- To investigate radiation characteristics of X-ray installations; such as leakage and scattered radiations from diagnostic X-ray units,
- Comparison of the data generated with National and International standard and recommendations for improvement.

CHAPTER 2

REVIEW OF LITERATURE

Diagnostic X-ray imaging is one of the basic and fastest ways for physicians to view the internal organs and structures of the human body, which has no proper substitute till today (Asadinezhad *et al*., 2017). In spite of the technological advances in other modern imaging techniques the use of X-rays in medical radiography has continued to increase. In many countries, particularly in developing countries, conventional radiography is still a leading diagnostic tool in comparison with other imaging techniques such as digital radiography, computed tomography, magnetic resonance imaging etc. (Muhogora *et al*., 2008). The frequency of radiographic examinations over the past five years had roughly doubled and in some countries even tripled (report of the United Nations Scientific Committee on the Effects of Atomic Radiation, UNSCEAR). The population exposure due to medical radiation is likely to be increasing worldwide, particularly in the countries where medical services are in the earlier stages of development (UNSCEAR, 2000). These rapid increases in demand of medical X-ray have led to unnecessary radiation exposure (Rasuli *et al*., 2015).

After few weeks of the discovery of X-rays by Roentgen in November of 1895, articles describing the problematic effects of these mysterious rays on patients and radiation workers began to appear in journals. However, there was no consensus on what individuals needed to be protected from harm or how this protection was to be achieved (Archer, 1995; Maree, 1995). Thompson (1896) thought that the injury was caused by the X-rays or by something that constantly accompanies them. He himself was skeptical as to the traumatism and exposed his own hand at a distance of a few inches to a Crookes tube, an experiment which resulted in severe dermatitis. It was not until 1900 that Thompson’s theory was proven correct. However radiation protection efforts did not begin immediately. Only after weeks of the announcement of the discovery of X-rays, radioactivity was discovered by Henri Becquerel. Radioactivity did not at first excite the investigative minds of the time; only about a dozen papers on radioactivity were published in the first year after its discovery compared with more than a thousand on X-rays (Brodsky and Kathren, 1989).

In the early days, the cathode ray tubes and X-ray generators used for exposures were inefficient and the X-ray output varied considerably in quantity and quality. Exposure times were commonly in the 20−30 minute range and some exposures took up to two hours, because of this, the early ventures into medical imaging came at a price. Many operators and patients suffered from acute radio-dermatitis (radiation burns). There were even cases of electrocution of the operator in setting up the equipment for exposure because the equipment was not enclosed and shielded as it is today (Johnston and Fauber, 2012).

Taylor (1979) has defined several periods in the early history of protection from X-ray. Period one (1895−1913), while there was an awareness of the need for radiation protection during this time, there is no evidence of concerted actions designed to reach an agreement on radiation protection standards. Period two (1913−1922), the first rudimentary outlines of radiation protection recommendations were developed by the British X-ray and Radium Protection Committee and various committees in the United States (US) and Germany. None of these bodies agreed on physical measurements during this period. Period three (1922−1928), the first

International Congress of Radiology met in 1925 and recognized the need for action on radiation protection but no significant work was done until the Congress met again in 1928. During this period there were great strides made in the measurements of radiation and proposals made to house X-ray tubes in shielded containers. However many unshielded tubes were still in use. Period four (1928−1934), the ICRP was formed in 1928 and soon issued the first set of international radiation protection recommendations. The Roentgen was defined and quantitative shielding data became available. After 1934, various organizations from many nations began to develop standards for the protection of workers and the general public.

Today, the radiation doses received by the patients in radiographic examinations are generally considered to be small in comparison with a huge benefits derived from these examinations (Mettler, 2001). Consequently, the generic justification for radiographic examinations is widely accepted. However, two concerns remain from the radiation protection point of view. The first one is poor image quality produced in radiographic examinations. It is increasingly recognized that there is a tremendous amount of waste of resources, particularly in developing countries, because images of poor quality have been reported in earlier studies to be as much as 15%−40% of all images (Rehani, 1995; Rehani *et al*., 1995; Rehani *et al*., 1992). Poor-quality images result in unnecessary radiation exposure to patients through repeated radiographic examinations, loss of diagnostic information and increased social costs in addition to the economic costs of health care. The second concern is the significant variation in dose levels to patients of similar size undergoing the same type of radiographic examination. In 1982, ICRP stated that the dose to patients from a given type of examination may vary between hospitals by a factor of 2−10 (ICRP, 1982). Experience from various national surveys has shown even larger variation in patient doses for the same examinations to a factor of 20 or more in different hospitals or even in different rooms in the same hospital (Hart *et al*., 2002; Havukainen and Pirinen, 1993; Gray *et al*., 2005). In this regard, the standards require the establishment of diagnostic reference levels or guidance levels for medical exposure by appropriate professional bodies in consultation with national health and regulatory authorities (ICRP, 1991; Spelic *et al*., 2004; Shrimpton, 1986; European commission, 1996; Archer, 2005).

The International Basic Safety Standards (BSS) was developed by the International Atomic Energy Agency (IAEA) with co-sponsorship of the Food and Agriculture Organization of the United Nations (FAO), the International Labor Organization (ILO), the Nuclear Energy Agency of the Organization for Economic Cooperation and Development (OECD/NEA), the Pan American Health Organization (PAHO) and the World Health Organization (WHO) require attention to image quality by considering corrective actions if such exposures do not provide useful diagnostic information and do not provide medical benefits to patients (IAEA, 1996). Similar recommendations were provided by other international and national bodies such as the ICRP, the United States' Nationwide Evaluation of X-ray Trends (NEXT) program, the United Kingdom's National Radiological Protection Board (NRPB) and the Commission of European Communities (CEC) (ICRP, 1991; Spelic *et al*., 2004; Shrimpton, 1986; European commission, 1996). In India, the AERB is the national regulatory body (AERB, 2006). The AERB sets the national standards and safety codes that specify the safe use of radiation sources, including diagnostic X-ray machines (AERB, 1983; Grover *et al*., 2002).

Muhogora *et al*. (2008) identified from the multinational study that high frequency of poor-quality radiographs across the participated hospitals from Africa, Asia and Eastern Europe had been found. The observed high percentage of poor image quality is likely due to an absent or in effective quality assurance program at hospitals that participated in this survey. Information on image quality and patient dose is better known in some developed countries where quality assurance programs have already been set up and a number of national surveys performed. However, similar information is grossly lacking in the majority of the developing countries, where efforts to establish quality assurance programs were initiated by the IAEA. The primary goal of a radiology quality assurance program is to ensure adequate clinical diagnostic information together with low possible radiation exposure for patient (ALARA principle). This can be achieved by optimum operating parameters such as kVp, collimator alignment, linearity of mA, time of exposure and the filtration **(**Al-Kinani and Mohsen, 2014**)**.

During the last decades, radiation protection and dosimetry in medical X-ray imaging practice has been extensively studied (Vlachos *et al*., 2015). For X-ray machines, without appropriate quality control and preventative maintenance service the benefits of reduced dose to the patient and early diagnosis may not be realized. Quality control and preventive maintenance also make it possible to unify X-ray imaging practices (Sungita *et al*., 2006). Medical diagnostic X-rays have been reported to be the major contributor of public exposure to man-made ionizing radiation (Bennett, 1991). About 51% of the population dose was estimated to be caused by radiographic X-ray examinations (Bushong, 2013). Therefore, suitable equipment and safe practice are essential for good quality images with optimal doses. Through quality control program in diagnostic radiology it is feasible to get information on quality of radiology equipment used for diagnosis and minimizing the doses received by medical personnel, public and patients (Kharita *et al*., 2017).

The main objective of radiation protection is to ensure that the doses received by workers and members of the public are kept below permissible levels (Binks, 1955). On the other hand, provision of high-quality healthcare services is the main purpose of using medical devices (Jomehzadeh *et al*., 2016). In addition, medical exposures are the most considerable source of ionizing radiation not only to the patients and radiation workers but also to the general public. So, X-ray diagnosis is the most important field, exposures resulting from these examinations have to be reasonably controlled to decrease health risk (Jankowski and Staniszewska, 2000). It is well-known that the essential requirement in the practical approach to radiation protection is measurement of the hazard (Simkin and Dixon, 1998; Cunha *et al*., 1992).

In 1995 a study was performed by Gori *et al.* on quality control in the radiological departments of the Florence general hospital, Italy. They mentioned that all the radiological facilities, in total exceeding one hundred, have been monitored for a quality control programme since 1991. For monitoring purposes, total beam filtration, radiation leakage, exposure time, focal spot size, kVp, accuracy of beam limiting devices, radiation output and spatial resolution of II-TV systems were measured. The digital meter NERO 6000 by Victoreen was used to measure linearity of radiation output, accuracy of X-ray tube potential, exposure time and total beam filtration (through HVL). The results obtained were compared with the tolerance limits established by International Electrotechnical Commission (IEC). In most cases poor agreement of the equipment performance with the selected tolerance limits appeared. Exposure time accuracy turned out to be the worse parameter because of the old age of the equipment. However, the authors mentioned that the investigation become effective to some extent in improving the compliance with the tolerance limits in those departments where a cooperative contact with the radiographers and the maintenance staff was established**.** It was reported by Rehani *et al*. in 1995 that large amount of data on radiation doses in diagnostic radiology exists while there is absolute lack of information at user's level. They estimated that 1 cm increase in field size results in irradiation of 600−900 cubic-centimeter of extra volume of patient which may contain sensitive tissue, 5 kVp increase results in exposure of 35−65 mR, with more effect in case of lumbar spine and abdomen X-ray and lesser for chest and D-spine, 5 mAs error results in 4−25 mR.

In 1998 Schandorf and Tetteh analyzed the status of X-ray diagnosis in Ghana. They reported that there is one Physician for about 4200 people in Ghana. The annual frequency of X-ray examinations during the period 1990−1996 ranged from six to 11 per thousand populations. Among different examinations, chest X-ray account for 46.5% of the annual frequencies. The survey revealed that there is an absence of established acceptance testing procedures for newly installed X-ray machines. Neither routine checks at regular intervals to ensure self-consistency of equipment performance nor institutional level performance checks followed by major repairs of faulty equipment were conducted. The results of repeated exposures undertaken indicated a need for quality assurance programmes. Quality assurance programme must be taken seriously to avert considerable cost and high patient doses. The authors recommended that radiation workers may attend adequate training in the selection of procedures so as to ensure that patient doses as low as reasonably practicable in order to achieve the desired diagnostic objective.

Zoetelief performed a study in 1998 regarding quality control in diagnostic radiology in the Netherlands and reported that the existing legislation in the Netherlands includes only a few criteria for equipment used in diagnostic radiology. In addition to that the criteria are not all operational and measurement methods are lacking. As such, upon the initiative of the Dutch Ministry of Health, Welfare and Sports, the relevant professional societies, in collaboration with the former TNO Centre for Radiological Protection and Dosimetry, eleven guidelines for quality control of equipment used in diagnostic radiology, including test procedures, test frequencies and limiting values were formulated.

The physical parameters of 14 X-ray machines located at 14 different hospitals in Egypt were investigated by Hamed *et al*. in 1999. The diagnostic X-ray parameters such as tube current, tube voltage, filtration, exposure time and exposure to the patient were studied. The electronic X-ray test device model 4000M+, Victoreen was used to measure average tube voltage, exposure (mR) and exposure time. They reported that 77% units had a voltage deviation ±10%; 75% machines showed time difference of ±10%. Regarding half value thickness 85.71% units were having Al filter thickness less than recommended value. The authors mentioned the possibility of over-exposing every patient mainly because of the quantity of radiation necessary for each exam is determined by the technologist.

Jankowski and Staniszewska, (2000) analyzed the methodology for set-up of a quality control system of diagnostic X-ray units in Poland. They mentioned that a national system of patient dose reduction is not yet operative whereas relatively high number of examinations (715 per 1000 inhabitants in 1995) took place in Poland. Besides that some investigations were needed to be analyzed for the current situation before the introduction of such a system. The results of measurements of a number or physical parameters for different types of X-ray units were presented together with a collection of data concerning the entrance dose to adult patients in conventional examinations i.e. radiographs of the chest, spine and abdomen. The results and conclusions obtained were compared with the recommendations of the IAEA reference levels. On this basis, the proposal concerning the details of the Polish quality control system (foreseen in the coming years) and local intervention levels were presented.

The potential for patient dose reduction in diagnostic radiology was investigated in five major Tanzanian hospitals by Muhogora and Nyanda (2001). The results showed that dose reductions in chest X-ray examinations ranged from

15%−50%. For abdomen and pelvis X-ray examinations, the dose reductions ranged from 24%−73% and from 25%−72%, respectively. The respective dose reductions for lumbar spine and LAT projections ranged from 4%−58% and from 16%−77%. They concluded that significant dose reductions can be achieved in the country without loss of diagnostic information that will reduce radiation risk to patients.

Wang *et al*. (2002) studied cancer incidence among Chinese radiation workers (1950 –1995), in which 27,011 diagnostic X-ray workers were compared with 25,782 other medical specialists employed between 1950 and 1980 in order to identify human malignant tumors produced by protracted and fractionated exposure to ionizing radiation and to assess resultant cancer risk. Significant cancer risk was observed among medical diagnostic X-ray workers. For leukemia and cancers of skin, female breast, lung, liver, bladder and esophagus significantly elevated risks were found. The patterns of risk suggest that the excesses of skin cancer, leukemia and female breast cancer and possibly thyroid cancer were related to occupational exposure to X-rays. The average cumulative dose for the later cohort (employed from 1970 to 1980) was 82 mGy and the earlier cohort (employed before 1970) was 551 mGy. They concluded that in a long term exposure to ionizing radiation (cumulative dose reaches a certain level) a significant cancer risk can be induced.

During the quality control procedure of a new mobile X-ray unit, Tsalafoutas (2006) revealed that the leakage radiation was well in excess of the current safety limit of 1 mSv h^{-1}. As a result, the X-ray unit was returned to the vendor company and it was replaced by a new unit of the same brand and model. Leakage measurements revealed that the second X-ray unit also showed the same problem. After consulting the vendor company and the tube manufacturer, the author discovered that the excessive leakage identified in those two X-ray units was not due to a defective construction, but due to the methodology with which the maximum permissible leakage was derived and therefore the tube shielding had been determined beyond the safety limit.

Sungita *et al.* in 2006 investigated the status of diagnostic X-ray machines in Tanzania with the purpose to produce the data needed to formulate quality control and preventive maintenance policies and strategies. The main motive of such work was the rapid increase in the numbers of X-ray machines in Tanzania but with limited technical support to maintain and operate them, which possibly increase radiation risk to patients and lower diagnostic accuracy. Further, these policies and strategies were needed to ensure that patients receive the lowest possible radiation risk and maximum health benefits from diagnostic X-ray examinations. Four quality control tests were performed on a total of 196 diagnostic X-ray units. The timer accuracy was tested on 120 units, accurate beam alignment and collimation were tested on 80 units and a radiation leakage test was performed on 47 units plus preventative maintenance tests were performed on all 196 X-ray machines. The result indicated that the units tested for quality control, 57% failed the timer accuracy test, 59% failed the kilovoltage (kVp) test, 60% failed the beam alignment test and 20% failed the radiation leakage test. Only 13% of the units passed the preventive maintenance test, 53% of the units were defective and 34% were out of order. As a result of these findings, the Tanzanian government had introduced a rehabilitation project to service X-ray units and replaced non operational X-ray unit with new machines having good support service from the suppliers. X-ray maintenance retraining programs were also introduced by the government.

Kharita *et al*., (2008) evaluated the national quality assurance program for X-ray diagnostic radiology in Syrian government hospitals. In this study, two periods were covered, the first period was from 1986−1998 (149 X-ray machines in 52 hospitals were considered) and the second period from 1999−2005 (95 X-ray machines in 41 hospitals were considered). They reported that most of the X-ray machines studied were within the acceptable performance, except few machines needed recalibration for some parameters. In the second period considerable improvement of about 50% was observed. The authors concluded that those improvements could be attributed to the establishment of an effective National Regulatory Authority in Syria in 1998 that introduced and gradually enforced the quality assurance necessity for X-ray equipment as part of the licensing process and to the relatively newer X-ray machines covered in the second period.

Quality control survey of diagnostics imaging equipment in Bosnia and Herzegovina (Republic of Srpska) has been systematically carried out since the year 2001. Bosnjak *et al*., (2008) conducted a study on implementation of quality assurance in diagnostic radiology mainly focused on X-ray tubes and generators for diagnostic radiology units in 92 radiology departments. In addition to that workplace monitoring and usage of personal protective devices for staff and patients were also covered. Ionizing chamber X-ray Gamma Dosimeter 27091 was used to measure the rate of air kerma in controlled and supervised area. For measuring exposure time, radiation output and X-ray tube voltage the multimeter NERO 8000 mAx (Victoreen, USA) was used. In 2001, tube voltage accuracy, exposure time accuracy, radiation output reproducibility, radiation output level and linearity of the radiation output with kV^2p were good criteria in 32%, 61%, 81%, 54% and 90% X-ray units. Whereas in 2005 X-ray machine quality improved to 71%, 75%, 94%, 65% and 81% in those parameters. Regarding beam alignment between light and radiation fields, 40% units were in unsatisfactory level in 2001 while in 2005 it reduces to 18%. As such the authors observed improvements in the implementation of the quality control programme within the period of 2001−2005. Further during 2001 to 2005, more attention was given to appropriate maintenance of imaging equipment, which was one of the main problems in the past.

Muhogora *et al*., in 2008 conducted a multinational study by surveying the image quality and the entrance surface air kerma for patients in radiographic examinations and performed comparisons with diagnostic reference levels. Survey was carried out in 12 countries from Africa, Asia and Eastern Europe, covering 45 hospitals. The rate of poor images and image quality grade were noted and causes for unsatisfactory image quality were investigated. On the basis of X-ray tube output measurements and X-ray exposure parameters, the entrance surface doses for adult patients were determined in terms of the entrance surface air kerma. Comparison of radiation dose levels with diagnostic reference levels was carried out. The fraction of diagnostic images which was rated as poor was as high as 53%. The image quality was improved up to 16% points in Africa, 13% in Asia and 22% in Eastern Europe after implementation of a quality control program. The majority of doses were below diagnostic reference levels, although patient doses varied by a factor of up to 88. The mean entrance surface air kerma values in mGy were 0.33 (chest, posteroanterior), 4.07 (lumbar spine, anteroposterior), 8.53 (lumbar spine, lateral), 3.64 (abdomen, anteroposterior), 3.68 (pelvis, anteroposterior) and 2.41(skull, anteroposterior). Patient doses were found to be similar to doses in developed countries and patient dose reductions ranging from 1.4%−85% were achieved. Poor image quality constituted a major source of unnecessary exposure to patients in developing countries. Comparison with other surveys indicates that patient dose levels in these countries are not higher than those in developed countries.

A study on radiological safety and quality assurance audit of 118 medical X-ray diagnostic machines installed in 45 major hospitals in India was carried out by Sonawane *et al.* in 2010. The main objective of the audit was to verify compliance with the regulatory requirements stipulated by the national regulatory body. The assessment mainly covered congruence of radiation and optical field, accuracy check of accelerating potential (kVp), total filtration and linearity of tube current (mA station) and timer; in addition, they also reviewed medical X-ray diagnostic installations with reference to room layout of X-ray machines and conduct of radiological protection survey. A quality assurance instruments such as, dose Test-O-Meter (ToM) (Model 6001), a kVp Test-O-Meter (ToM) (Model RAD/FLU-9001), ionization chamber-based radiation survey meter model Gun Monitor and other standard accessories were used for the required measurements. The important areas where there was noncompliance with the national safety code were inaccuracy of kVp calibration (23%), lack of congruence of radiation and optical field (23%), nonlinearity of mA station (16%) and timer (9%), improper collimator/diaphragm (19.6%), faulty adjustor knob for alignment of field size(4%), non-availability of warning light (red light) at the entrance of the X-ray room (29%) and use of protective barriers (mobile) without lead glass viewing window (14%). They concluded that the present study may be a reasonably good representation of the situation in the country as a whole. It contributed significantly to the development of radiological safety by the way of the steps already taken and by providing a vital feed back to the national regulatory body.

A radiological safety survey was carried out on 100 medical diagnostic X-ray machines installed in public and private medical facilities throughout Malaysia by Amin *et al*. in 2012. The authors verified the safety status of the machines based on Malaysian Standard MS 838, 1985 (Code of Radiation Protection-Medical X-ray Diagnosis). The measurements on machine performance consisted of operating voltage (kVp) and exposure (time, reproducibility and linearity). The X-ray beam properties such as collimation, filtration and leakage (including scattered radiation outside the operating room) are also measured. Image quality such as resolution, contrast and focal spot size are determined as required by MS 838. Out of 100 machines surveyed, 98% have satisfied the requirement of kVp accuracy of which maximum deviation did not exceed 5% or 5 kV (whichever is greater). In terms of radiation output, more than 50% of the machines have a deviation of less than 5% and the rest has the deviation of 6%−10%. The allowed deviation is 10%. All the machines complied with the leakage and scattered radiation requirements where MS

838 stipulated the value of 100 mR/h and 10 mR/week respectively. Other safety practice such as the availability of red light at the entrance door was 100% complied with.

Hassan *et al*., (2012) studied the factors affecting the beam quality, such as the exposure time (mSec), kilo-volt peak (kVp), tube current (mAs) and the absorbed dose in (μGy) for different examinations. They reported that maximum absorbed dose measured per mAs was 594±239 and 12.5±3.7 μGy for the abdomen and the chest, respectively, while the absorbed dose at the elbow was 18±6 μGy, which was the lowest dose recorded. The compound and expanded uncertainties accompanying these measurements were 4±0.35% and 8±0.7%, respectively. The measurements were done as per quality control tests acceptance procedures.

In 2012, 33 different hospitals/institutions from Kathmandu and sub-regional/zonal hospitals from different parts of Nepal were monitored by Adhikari *et al.* They observed that around 70% of the radiation workers are aware of radiation safety issue. Surveyed 44 diagnostic X-ray machines and 10 computed tomography units were safe. The result showed that around 65% of radiation workers are not monitored towards ionizing radiation. There was no quality assurance program in diagnostic radiology but has a maintenance contract with the company at few centers. They suggested that a regular quality control program on the X-ray equipment by following international codes of practice and regular quality control program for the X-ray equipment at regular intervals (Adhikari *et al*., 2012).

Faraj *et al*., (2013) conducted a measurement on the dose rates at radiographer's place, patient entrance door of X-ray room, waiting area during X-ray imaging and quality control test for radiographic facility with visual inspection at 4 hospitals in Sulaimania city, Kurdistan region, Iraq. The calibrated nuclear radiation meter palm RAD 907 was used which measures the rates of Alpha, Beta, X and Gamma radiations. The results showed that the facilities for safety did not exist in all hospitals. High dose rates were recorded for X-ray and fluoroscopy in most of the hospitals.

Khoshbin *et al*., (2013) performed quality control test on all radiography units operating in Golestan province of Iran. Based on general accepted programs for quality control the authors examined forty-four diagnostic X-ray units. Further, eight important safety parameters such as mA-time reciprocity, kVp accuracy, kVp reproducibility, exposure linearity, exposure reproducibility, timer accuracy, beam alignment and filtration were measured and calculated by a Baracuda X-ray beam analyzer. They found that variance of kVp reproducibility was acceptable in 100% of equipments whereas kVp accuracy was found to be beyond acceptable limit in 29.5% of equipments. Variance of mA-time reciprocity was measured to be within the standard limits. Thirty-nine percent of radiography equipments showed non-linear exposure attitude while 16.7% of them exhibited unacceptable reproducibility of exposure. Moreover, beam misalignment was observed in 29.5% of the X-ray machines. In 43.2% of radiography equipments, timer accuracy was out of permissible range. Among all the parameters timer inaccuracy seems to be a general problem for X-ray machines.

Younis *et al*. (2014) evaluated the radiation protective measures in different diagnostic radiological departments in Erbil hospitals. The palm RAD 907 nuclear radiation meter and Contamination Monitor CoMo 170 were used to measure radiation leakage. Questionnaire was developed to elicit information from the most senior personnel of the hospital. The results showed that the radiation safety facilities were inadequate and the dose rates of 16.4 µSv/hr and 20 µSv/hr were recorded at paramedic's place and technician room respectively. Ionizing radiation dose rates in the reception was 20µSv/hr and in front of the monitor room window was 113 µSv/ hr indicating higher health risk to the paramedic, visitors and personnel at the hospital. They concluded that the radiation protection facilities were in generally poor, indicating high health risk to the paramedics, guests and personnel at the hospitals. Gholamhosseinian *et al*., (2014) utilized Unfors Mult-O-Meter model 303 for surveying accuracy of time and kVp, linearity of exposure with mAs and reproducibility of exposure in radiology centers of hospitals associated with Mashhad University of medical sciences. They identified that 27% of apparatuses in accuracy of kVp, 45% in accuracy of timer and 30% in accuracy of reproducibility were out of accepted range according to recommendations of American Association of Physics in Medicine (AAPM, 2002) and ICRP 103. The authors recommended that some devices should not be used in the mentioned regions and repair, substitution or omissions of some devices were also suggested.

Six conventional medical X-ray machines at Baghdad from different origins and different manufacturing time were studied by Al-Kinani and Mohsen in 2014. The voltage stability of the machine was tested for three units and it was found that the percentage of voltage ripple to two units were 3.79 and 4.856 respectively and for one unit 11.4. From the assessment of current and exposure time it was found that the relationship is linear for two units. HVL of aluminum were 2.6, 2.8 for unit B and C and it is within the accepted value of IAEA, but HVL for unit A was 0.5 which is less than the recommended value**.** Rasuli *et al*., (2015) carried out a study on quality control assessment of conventional diagnostic radiology devices in regularly visited radiology centers of Khuzestan province, Iran. In this study fifteen conventional diagnostic X-ray machines were examined based on the procedure proposed by the Institute of Physics and Engineering in Medicine (IPEM) Report No.77. Ten standard quality control tests, including tube output linearity (time and milliampere), exposure time accuracy and reproducibility, voltage accuracy and reproducibility, filtration (HVL), tube output reproducibility and beam alignment were performed and assessed using Barracuda multi-purpose detector. They observed that the output linearity, exposure time and dose output, as well as, reproducibility of voltage met the standard criteria in all devices. However, the results of the beam alignment test were poor in 60% of the units. They identified that the devices met the standard criteria eventhough radiological devices in Khuzestan province are relatively old with high workload. The reason cited was that may be due to proper after-sale services which are provided by the companies. Although these after-services may be expensive for the institutions, the costs may be significantly reduced if quality control is defined as a routine procedure performed by radiation safety officers or qualified medical physicists.

Vlachos *et al*. measured scatter radiation in diagnostic X-rays for radiation protection purposes by using ionization chamber survey meter (451P-Fluke Biomedical). To identify the dependence of radiographic exposure parameters such as X-ray tube voltage, tube current and distance on secondary radiation, measurement was carried out in conventional radiographic room. They reported that with some exceptions, the results indicated that the scattered radiation was uniform in the space around the water cylindrical phantom. The results also showed that the dose rate due to scattered radiation was affected by the input tube voltage and X-ray filtration. Further, for every half meter away from the phantom the dose rate in air is decrease by approximately 40%.

Gholami *et al*., (2015) carried out a study on evaluation of conventional X-ray exposure parameters such as tube voltage and exposure time in private and governmental hospitals of Lorestan Province, Iran. The measurements were obtained using a factory-calibrated Barracuda dosimeter (model SE-43137). The authors observed that the highest output obtained was ranging from 107×10^{-3} to 147×10^{-3} mGy/mAs. The evaluation of tube voltage accuracy showed a deviation from the standard value, highest ranged varied between 0.30% and 27.52%. Exposure time accuracy evaluation showed that three hospitals exceeded the permitted limit whereas four hospitals complied with the safety requirements (allowing a deviation of ±5%). The authors concluded that old X-ray machines with poor or no maintenance were possibly the main sources of reducing radiographic image quality and increasing patient radiation dose. Quality control according to the standards and features of radiology machines in the teaching hospitals of Hormozgan Province was investigated by Haghparast *et al*., (2015). Among quality control parameters voltage accuracy, voltage reproducibility, exposure time reproducibility, output linearity with mA and adaptation of optical field with radiation field parameters were considered. They reported that quality control of radiology devices in health centers reduces patients' absorbed dose during various radiographies, increases their efficiency and longevity and improves the quality of radiographic images and the disease diagnosis by physician.

Jomehzadeh *et al*., (2016) performed quality control tests on stationary radiographic X-ray machines, installed in 14 governmental hospitals of Kerman province, Iran. Measurements were performed on 28 conventional X-ray machines based on the criteria and protocols recommended by the Atomic Energy Organization of Iran (AEOI) by using a calibrated Gammex quality control kit. The authors found that HVL, kVp reproducibility, kVp accuracy, timer reproducibility, timer accuracy, exposure reproducibility and mA/timer linearity were not within the acceptable limits in 7%, 4%, 25%, 18%, 29%, 11% and 12% of the evaluated units. The authors recommended that AEOI may modify the current policies by changing the frequency of quality control test implementation to at least once a year because radiographic X-ray equipments in the study area were relatively old with a high workload.

In Syria Kharita *et al*., (2017) performed a quality control audit for radiography and fluoroscopy devices (2005−2013) owned by private sector. The main purpose was to verify compliance of performance of X-ray machines with the regulatory requirements stipulated by the national regulatory body. 487 X-ray diagnostic machines (363 radiography and 124 fluoroscopy devices), installed in 306 medical diagnostic radiology centers in 14 provinces in Syria were considered. A measurement tool, NERO (Victoreen model 8000) which was calibrated at the National Secondary Standard Dosimetry Laboratory (SSDL) and traceable to Network of Secondary Standard Dosimetry Laboratories (IAEA) was employed. Standard quality control tool kits were used to evaluate tube and generator of the X-ray machines, which constituted timer accuracy, potential (kVp), tube filtration, radiation output consistency, small and large X-ray beam collimation and alignment, focal spot sizes as well as high-and low-resolution. They reported that most of the assessed operating parameters were in compliance with the standards stipulated by the National Regulatory Authority. Non-compliance for the assessed parameters, maximum value (28.77%) pertained to accuracy of kVp calibration for radiography units. The findings of this quality control program, illustrated that most of the considered diagnostic X-ray devices had acceptable performance and few of them need to be recalibrated for some parameters.

Quality control tests on randomly selected radiology devices installed in diagnostic imaging departments of Iran was conducted by Asadinezhad *et al.* in 2017. In total, quality control tests were conducted on 51 conventional diagnostic X-ray machines installed in 20 cities of lran. The investigators employed a calibrated Mult-O-Meter to evaluate the exposure time, accuracy of peak kilovoltage (kVp), reproducibility of exposure, exposure linearity and reciprocity, and half-value layer (HVL). They reported that 38.6% of devices had intolerable variance of kVp accuracy. In exposure time accuracy test 34.5% of devices were out of the acceptable limits. Further, in exposure linearity and exposure reciprocity, 46.7% and 53.1% of devices variance was greater than the acceptable range. Concerning reproducibility of exposure test, the reproducibility variance and percentage of tube output variations in 19.4% of devices exceeded the limits. Moreover, 14.7% of the devices showed thickness of HVL lower than the acceptable limit. According to the results of this study, there were wide variations in quality control test results, perhaps mainly due to the fact that it is not an obligation to implement quality control programs in Iran. The most important problems were kVp and timer inaccuracy, non-reciprocity of exposure, nonlinearity of exposure with milliampere-second (mAs).

Hashemi *et al*., (2019) investigated the condition of randomly selected conventional radiographic X-ray devices installed in radiology centers of Great Khorasan Province, Iran. The authors intended to produce the data which is needed to formulate quality control policies, because these are necessary to guarantee the accuracy of the diagnosis while minimizing the radiation dose. This study was performed using Piranha Multi-purpose detector (MPD, M654, RTI Electronics, Sweden) to measure quality control parameters in order to unify X-ray imaging practices using international procedure. Under quality control parameters exposure time accuracy, tube output linearity with time and milliampere (mA), voltage accuracy, exposure time reproducibility, voltage reproducibility and tube output reproducibility were considered. They found that in a kVp range 55−70, 67.6% of an alternating current (AC) generator and 93.5% of High Frequency (HF) generator units were within the acceptable limit. In timer accuracy test, 2.4% of an AC generator and 4.1% of HF generator units did not complied with the safety requirement. In output linearity (mA), 96.7% of an AC generator and 98.4% of HF generator machines were within acceptable limit. Regarding tube output linearity (sec) 5.1% below 100 msec and 1.2% above 100 msec of an AC generator machine were out of acceptable limit. The authors reported that the implementation of high-frequency X-ray generators were more beneficial compared to alternative current generators (single phase machine), due to their better accuracy, efficient, linearity and reproducibility. The quality control program was not conducted at regular intervals in some of the investigated radiology centers, mostly because of inadequate enforcement by national regulatory authorities for implementation of quality control program.

CHAPTER 3

MATERIALS AND METHODS

3.1 Radiographic equipment

3.1.1 Fixed X-ray, mobile-fixed X-ray and mobile X-ray machine

Generally, conventional diagnostic X-ray equipment may be classified as mobile and permanently installed machine. Mobile X-ray, as its name implies, is a unit on wheels that can be taken to the patient’s bedside, the emergency department, surgery or wherever it may be needed as shown in Fig. 3.1.1 (a). Fixed or permanently installed machine refers to units that are fixed in place in a particular room specifically designed for the purpose and are not intended to be mobile is shown in Fig. 3.1.1 (b). Permanently installed does not mean that it can never be removed, of course, just that it cannot be wheeled to another location. Fixed X-ray consists of the tube, collimator, table, control console, tube stand and wall unit (Johnston and Fauber, 2012). In the present study area large number of mobile X-ray were installed in a particular X-ray room and used exactly same as permanently installed X-ray machine as depicted in Fig. 3.1.1 (c). This type of X-ray is simply called as mobile-fixed X-ray. In total, there were 195 X-ray facilities at 118 different institutions across the state of Mizoram as shown in Table 3.1.1 (a) and (b). Out of which 26 X-ray machines were condemned because these machines were beyond repair (Table 3.1.1 (b)). So, the total numbers of working and out of order diagnostic X-ray machines recorded in Mizoram were 169 in 116 different institutions until June 2016 (Table 3.1.1 (a)). Among these, 109 (64.50%) were AERB-type approved units and 60(35.50%) machines had unknown approval statuses because of missing information.

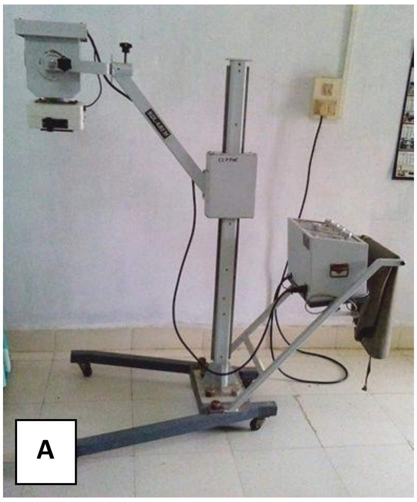

Fig. 3.1.1 (a): Mobile X-ray machine

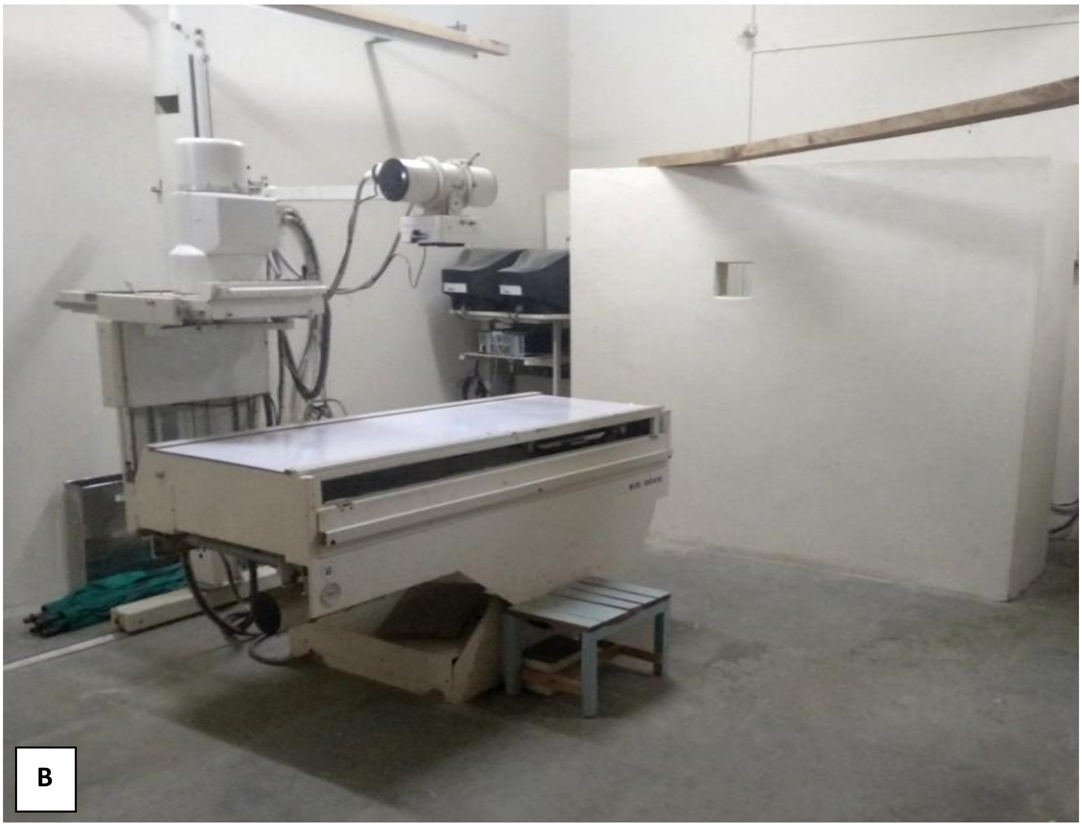

Fig. 3.1.1 (b): Fixed X-ray machine

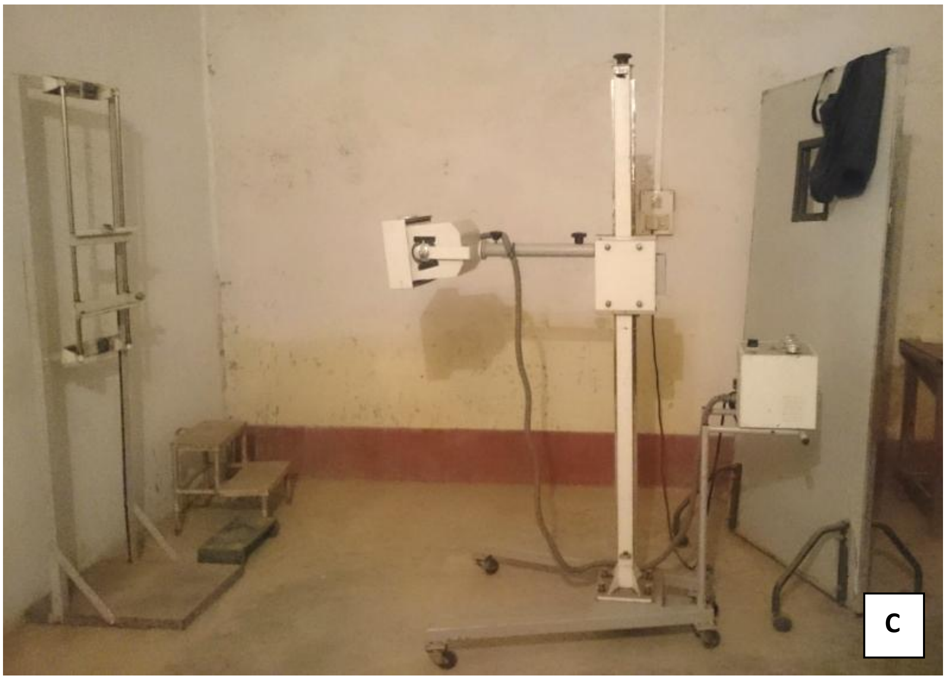

Fig. 3.1.1 (c): Mobile-fixed X-ray machine

Table 3.1.1 (a): Working and out of order diagnostic X-ray machines distribution across Mizoram in June 2016

X-ray facilities	Aizawl	Cham-phai	Kol-asib	Mamit	Siaha	Lawng-tlai	Lun-glei	Ser-chhip	Total
No of Ins.	72	11	6	3	3	4	12	5	116
Cath-Lab	1	0	0	0	0	0	0	0	1
CT-Scan	4	0	0	0	0	0	0	0	4
Fluoroscopy	8	0	0	0	0	0	0	0	8
Fixed X-ray	24	4	4	1	2	5	7	2	49
Mobile-fixed	19	8	4	3	2	3	9	5	53
Mobile	6	0	0	1	0	0	2	0	9
Mammo-graphy	2	0	0	0	0	0	0	0	2
Dental	41	0	1	0	1	0	0	0	43
Total	105	12	9	5	5	8	18	7	169

Percentage	62.1%	7.1%	5.3%	3%	3%	4.7%	10.7%	4.1%	100%

Table 3.1.1 (b): Condemn diagnostic X-ray machines distribution across Mizoram in June 2016

X-ray facilities	Aizawl	Cham-phai	Kolasib	Mamit	Siaha	Lawng-tlai	Lun-glei	Ser-chhip	Total
Fixed X-ray	1	0	0	0	0	1	0	0	2
Mobile-fixed	8	2	3	1	1	2	2	3	22
Dental	2	0	0	0	0	0	0	0	2
Total	11	2	3	1	1	3	2	3	26

3.1.2 Diagnostic X-ray Tube

The diagnostic X-ray tube head assembly consists of the X-ray tube, collimator and tube stand. The X-ray tube is located in a protective housing that provides solid stable mechanical support. The X-ray tube is a special diode (two electrodes) tube that converts electrical energy into X-rays and produces heat as by-product (Johnston and Fauber, 2012). The principal components of an X-ray tube are an electron source from heated tungsten filament, with a focusing cup serving as the tube cathode, an anode or target and a tube envelope to maintain an interior vacuum (IAEA, 2014). The X-ray tube is oriented so that generally the cathode is over the foot and the anode is over the head of the table. When facing the X-ray tube assembly, the anode is on the radiographer's left and the cathode is on the right as shown in Fig. 3.1.2 (a) and (b) (Johnston and Fauber, 2012). The filament is heated by a current that controls the thermionic emission of electrons, which, in turn, determines the electronic current flowing from the cathode to anode. The accelerating potential difference applied between the cathode and anode controls both X-ray energy and yield. Thus, the two main circuits operate within the X-ray tube are; the filament circuit and the tube voltage circuit. Typical anode currents, depending on the examination mode, are 100 mA − >1000 mA in single exposures. The typical range of tube voltages is 40−150 kV for general diagnostic radiology (IAEA, 2014).

Diagnostic X-ray tubes are designed to produce a sharp shadow picture of a part of the patient. Even if the patient is completely immobilized, some physiological motion is always present due to respiration and heart motion. In order to ensure that the picture be sharp, the X-rays must come from a ‘point source’ and exposure must be short enough to freeze the motion. A ‘point source’ and ‘very short exposure’ are, however, incompatible since they imply an infinite electron flux concentrated on zero area of the target, which would destroy it. X-ray tube manufacturers have found a number of ways to spread the electrons over a large area of the target and yet make the X-rays appear to come from a much smaller one (John and Cunningham, 1983).

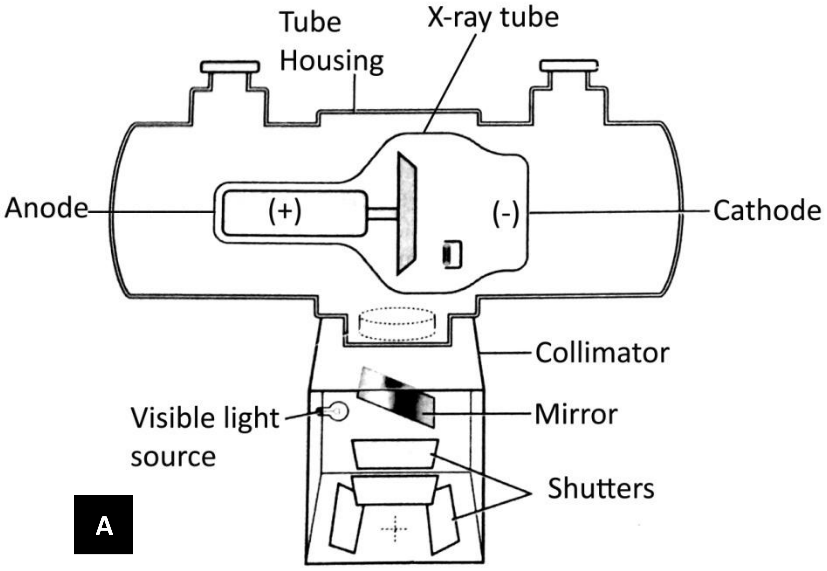
Tube Housing
X-ray tube
Anode
(+)
(-)
Cathode
Collimator
Visible light source
Mirror
Shutters
A

Fig. 3.1.2 (a): Schematic diagram of conventional X-ray tube head assembly

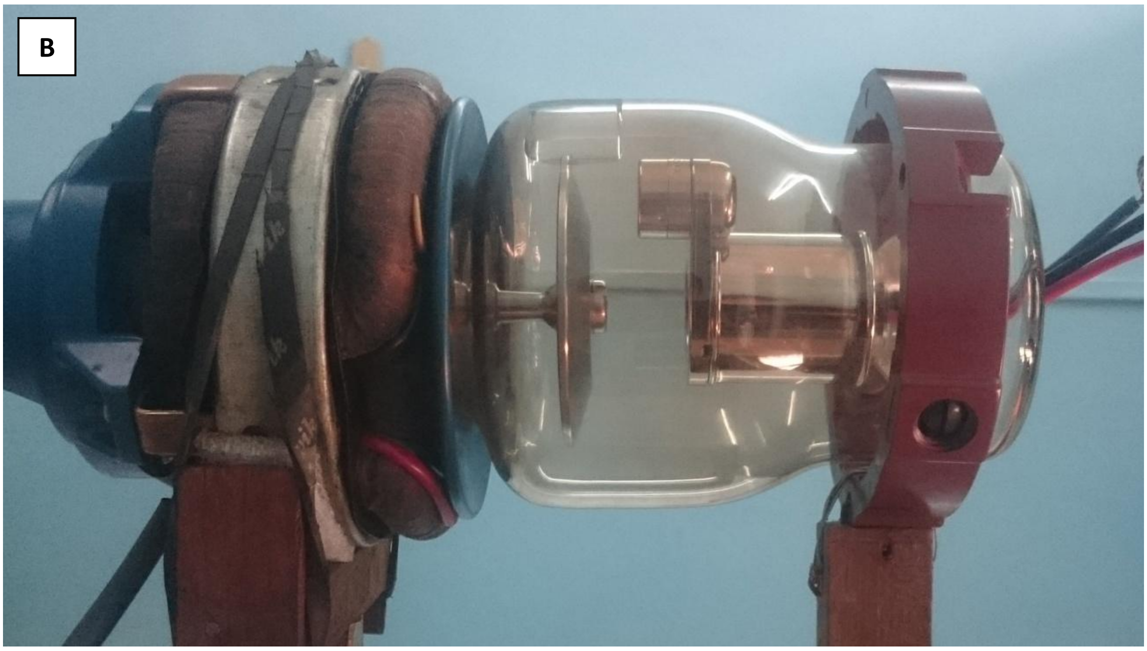

Fig. 3.1.2 (b): Realistic picture of conventional X-ray tube

3.1.3 Anode

The anode is the positive end of the tube as shown in Fig. 3.1.2 (a). It provides the target for electron interaction to produce X-rays and is an electrical and thermal conductor (Johnston and Fauber, 2012). Since the major part of the energy of the electrons is converted into heat in the anode, the anode materials should have a high melting point and good heat conduction ability. To get a high relative amount of X-ray energy, the anode material should be of high atomic number. Tungsten is the dominating anode material and is in modern X-ray tubes often mixed with rhenium (Z_W=74; Z_{Re}=75) (Carlsson and Carlsson, 1996). There are two designs for the anode, one is the *stationary anode*, which is basically a tungsten button fixed in a copper rod. It is called stationary because the target does not move; stationary anodes were used in old tube designs and may still be found in dental X-ray units or those requiring very small exposure techniques. The primary disadvantage of stationary anode is that the electrons always hit the same small target area of the anode; therefore, heat builds up rapidly and can damage the tube. This problem limits the exposure technique factors that can be used and this limitation spurred the development of rotating-anode designs. Another design the *rotating-anode* is mainly used in general-purpose tubes today. As a core material rotating anode consists of a molybdenum disc which is coated with tungsten and mounted on a copper (Cu) shaft with a core made of molybdenum. Copper is used as part of the shaft because it has excellent electrical and thermal conductive properties. Molybdenum is used as the disc base and core because it has a low thermal conductivity, which slows down migration of heat into the rotor bearings (minimizing heat damage) and it is a strong but light alloy, making it easier to rotate the anode.

The purpose of rotating the anode is to spread the tremendous heat produced during X-ray production over a larger surface area. Instead of electrons always striking the same small surface area (as with stationary anodes), the electrons strike only a small part of the total anode surface area at any one time and that area changes. The focal ‘spot’ becomes a focal ‘track,’ with the rotating anode and the heat build-up spread over the focal track circumference rather than on one spot. This greatly increases the heat-load capacity and the exposure techniques that can be utilized for generating photons. The target material (coating) made of tungsten has very high melting point (3400° C or 6152° F) and it has excellent thermal conductivity. Further, it has a high atomic number, improving the efficiency of X-ray production (Johnston and Fauber, 2012). The addition of rhenium to the tungsten makes the target tougher and less likely to crack under the severe stresses caused by heating (John and Cunningham, 1983).

3.1.4 Cathode

The cathode is the negative end of the tube and provides the source of electrons needed for X-ray production as shown in Fig. 3.1.2 (a). Most conventional X-ray tubes have two filaments and are known as dual-focus tubes. The large and small focal-spot options on the operating console represent the two filaments. These two filaments is a coil of wire generally 7−15 mm long and 1−2 mm wide. They are usually made of tungsten with 1%−2% thorium added. Tungsten does not vaporize easily because it has a very high melting point. Thorium is a radioactive metallic element that is added to increase thermionic emission (boiling off of electrons) and extend filament life (Johnston and Fauber, 2012). Several factors can shorten the life of an X-ray tube or damage it. Most have to do with the thermal characteristics of X-ray production and are within the radiographer's control. In particular, the regular use of very high (maximum) exposure, lower but very long exposure factors and overloading the filament are the major causes of tube failure (Johnston and Fauber, 2012).

3.1.5 Tube Housing

Because both heat and X-rays are produced, the tube is covered in special tube housing. Tube housing is made of metal and has a special mounting bracket for the X-ray tube and high-voltage receptacles to deliver electricity to the X-ray tube as shown in Fig. 3.1.2 (a). It is also filled with oil that surrounds the X-ray tube to help dissipate the heat produced. Cooling fans are also built into the housing to help dissipate heat. This housing is a lead-lined metal structure that also serves as an electrical insulator and thermal cushion for the tube itself as depicted in Fig. 3.1.2 (a). X-rays are produced in all directions and another role of the housing is to absorb most of the photons travelling in directions other than toward the patient. This is called *leakage radiation* and the housing design reduces this radiation to less than 100 mR/hr, as required by regulation (Johnston and Fauber, 2012).

3.1.6 Collimator

The collimator is a box-shaped device attached to the bottom of the tube housing Fig. 3.1.2 (a). The collimator serves to restrict the X-ray beam to the area of the body of interest and to help localize the beam to that area. To restrict the beam, the collimator is fitted with two pairs of lead shutters. Two buttons on the face of the collimator adjust these shutters. One button controls the shutters that adjust the width of the beam and the other button controls the shutters that adjust the length of the beam. The collimator also contains a light source, a mirror and a clear plastic covering over the bottom with cross-hairs imprinted on it. The plane mirror reflects the optical light through the plastic and casts a shadow of the cross-hairs onto the patient. The shutters adjust the size of the light field, which represents the radiation field that will be produced. The light field and the crosshairs show the radiographer the dimensions of the X-ray field and where it will enter the patient’s body. Periodically, a quality-control test, called a radiation field/light congruence test, is conducted to check this mirror (Johnston and Fauber, 2012). The benefits of collimating the beam are reduction in patient dose and improvement of image contrast due to a reduction in scattered radiation (IAEA, 2014).

Just under the table top is a Bucky assembly. This device has a tray and locks to hold the image receptor in place and a grid positioned between the patient and image receptor to clean up the remnant beam (X-ray beam exiting the patient) before it exposes to the receptor. The CP provides the radiographer with control of all the parameters necessary to produce a diagnostic image. The radiographer uses the CP to select the kVp and mAs that is applied to the X-ray tube to produce X-rays (Johnston and Fauber, 2012).

3.2 Measurement tools

3.2.1 Dosimeter (model 06-526)

For measuring the output radiation of diagnostic X-ray equipment a battery operated portable dosimeter (RAD-CHECK PLUS model 06-526, Fluke Biomedical-Cleveland, Ohio, USA) was used (Fig. 3.2.1). The exposure which was detected by an internal ionization chamber is displayed on a 3 ½ digital liquid crystal display (LCD) as either:

- *exposure, in Roentgens 0.001 − 1.999 R or SI units of milligrays 0.01 − 19.99 mGy.*
- *rate, in Roentgens per minute 0.01 − 1.999 R/min or SI units of milligrays per minute 0.1 − 199.9 mGy/min.*

The calibration measurements were traceable to the National Institute of Standard and Technology (NIST, Gaithersburg, MD, USA). The *dimensions* of the dosimeter is 6 in (w)×6.3 in (d)×2.5 in (h) (154×160×64 mm) with 1.1 lbs (500 g) having measurement effective area of 18.3 cm^2. The *standard calibration* is 5% at 75 kVp with 4 mm Al-filtration at 22° C (72° F) and one atmosphere -760 mm of Hg. The *operating condition* is 10°−40° C (50°−104° F) (Operator manual dosimeter, 2006).

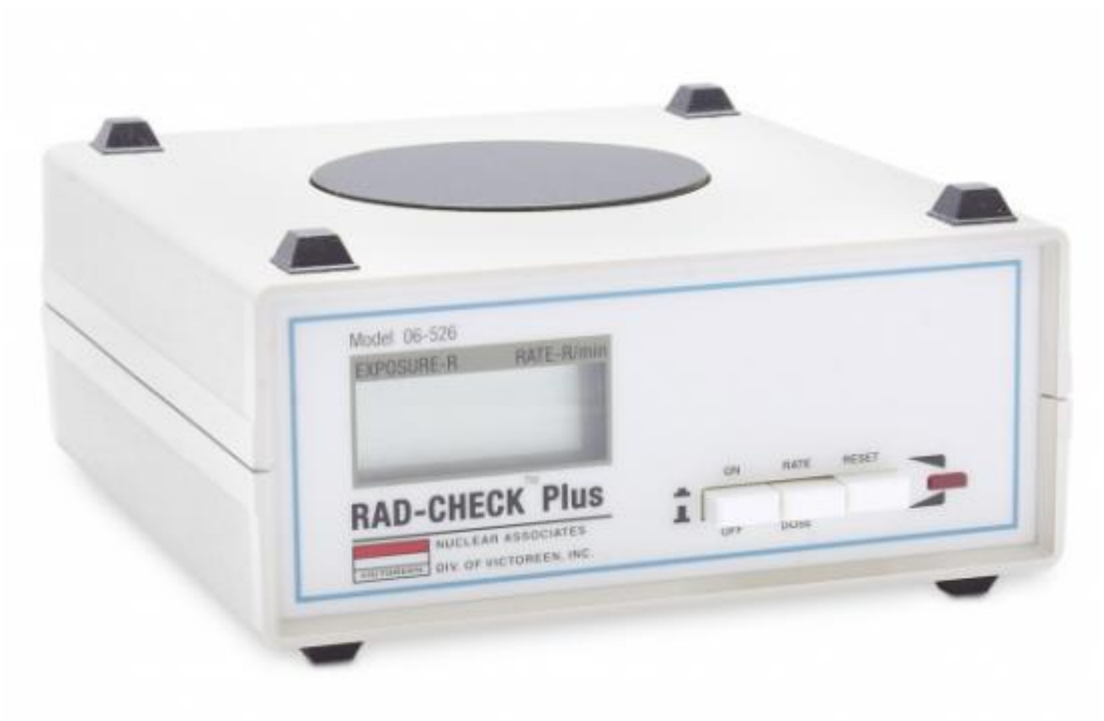
Model 06-526
EXPOSURE-R
RATE-R/min
RAD-CHECK Plus
NUCLEAR ASSOCIATES
DIV. OF VICTOREEN, INC.
VICTOREEN
ON
RATE
RESET
OFF
DOSE

Fig. 3.2.1: A battery operated portable dosimeter (model 06-526)

3.2.2 kVp meter (Model 07-494)

The wide-range digital kVp meter (model 07-494, Fluke Biomedical, Cleveland, Ohio, USA) is a portable, battery operated unit which non-invasively measures the effective peak potential applied to tungsten target of diagnostic X-ray tube as shown in Fig. 3.2.2 (a). It uses two differentially filtered X-ray detectors whose ratio of integrated outputs is calibrated over the ranges of 50−90 kVp and 80−150 kVp. The desired range is selected using the range selector on the top of the unit. The digital kVp meter has an auto reset feature. lt senses when a new exposure takes place, resets the display for a new reading and turns on the auto reset LED for 0.5 seconds or the duration of the exposure, whichever is greater. The calibration measurements were traceable to the National Institute of Standard and Technology (NIST, Gaithersburg, MD, USA) (Operator manual kVp meter, 2006).

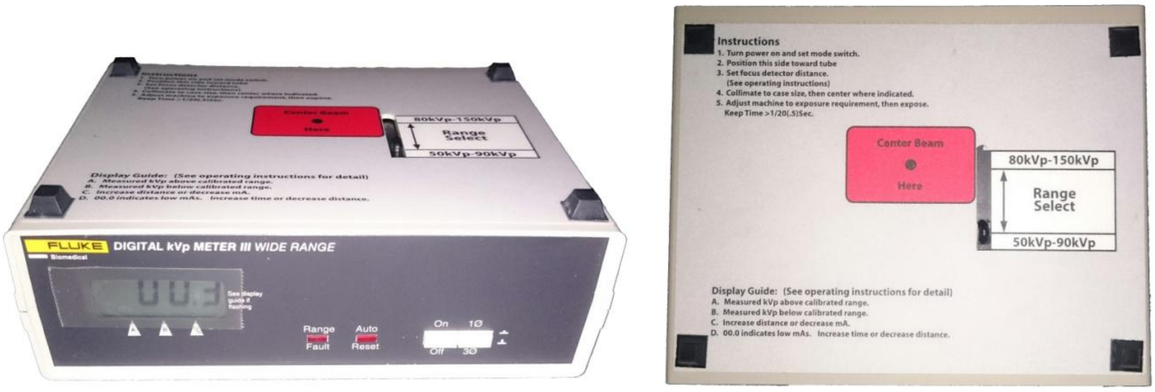
FLUKE
Biomedical
DIGITAL kVp METER III WIDE RANGE
Range Fault
Auto Reset
On 1Ø
Off 3Ø
Instructions
1. Turn power on and set mode switch.
2. Position this side toward tube
3. Set focus detector distance.
(See operating instructions)
4. Collimate to case size, then center where indicated.
5. Adjust machine to exposure requirement, then expose.
Keep Time >1/20(.5)Sec.
Center Beam
Here
80kVp-150kVp
Range Select
50kVp-90kVp
Display Guide: (See operating instructions for detail)
A. Measured kVp above calibrated range.
B. Measured kVp below calibrated range.
C. Increase distance or decrease mA.
D. 00.0 indicates low mAs. Increase time or decrease distance.

Fig. 3.2.2 (a): Wide-range digital kVp meter (model 07-494)

The kVp meter has two *measurement ranges*; low: 50 kVp–90 kVp and high: 80 kVp–150 kVp with *resolution* of 0.1 kVp. It has *accuracy* ± 3% or 3 kV, whichever is greater (tungsten target X-ray tube with 4.5 mm Al-total filtration) and *reproducibility* of ±1 kV or 1%, whichever is greater. The *dimensions* of the kVp meter is 2.5 in×8 in×6 in, (6.4 cm×20.3 cm×15.2 cm) (h×w×d) with 2.4 lbs. (1.1 kg). The mAs requirements can be set based on the following graph shown in Fig. 3.2.2 (b). The curves provided as guidelines for selecting the mAs required for a particular kVp measurement. Any mAs beyond the required amount is not used in the measurement. However, the curves are derived from single-phase measurements. Three phase machines generally require 70% of the mAs determined from the curves. Specific mAs requirements depend on the factors namely detector sensitivity, tube filtration, radiation waveform, focus to detector distance (FDD) and mAs errors in the X-ray machine (Operator manual kVp meter, 2006)

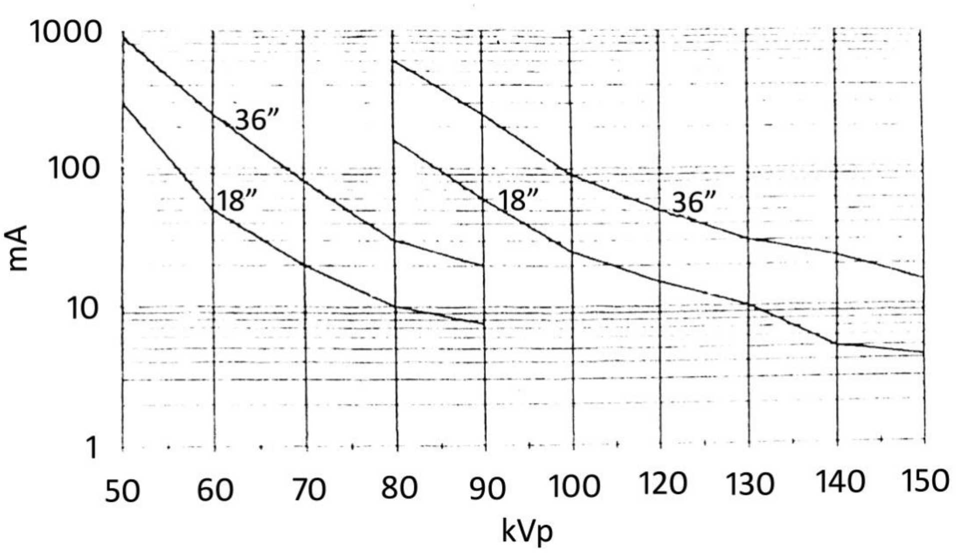

Fig. 3.2.2 (b): mAs vs kVp, minimum requirements (Typical single phase X-ray unit)

Theory and Applications

The kVp measurement is computed from a measurement of the linear absorption coefficient (μ) of the hardened X-ray beam. As we already discussed, an X-ray beam is composed primarily of two parts- the bremsstrahlung radiation and the characteristic radiation. Bremsstrahlung radiation predominates below 70 kV. When the beam potential crosses the 70 kV threshold, an apparent beam hardening takes place due to the sudden increase in the emission of higher energy X-rays. Until approximately 90 kV the linear absorption coefficient, μ, increases at continually faster rates. Above 90 kV, the characteristic radiation contributes less hardening to the beam and becomes less important. The bremsstrahlung radiation again dominates and μ increases at a slower rate. Use of dual range filters above 90 kVp helps minimize this effect. Beam spectrum changes also occur with different waveforms. Single-phase waveforms display different readings compared to three phase waveforms, depending on the position of the range selector switch. Correction for waveform effect is made by selecting the appropriate position (i.e., single phase or three phase) using the front panel phase selection switch. Table 3.2.2 lists FDD settings generally used to keep the mAs requirement between 20 and 100. However, the FDD does not affect the accuracy of the kV results.

Table 3.2.2: FDD Settings

Selected Range kVp	kVP	FDD
50 - 90 kVp	50 to 70	18 in (45 cm)
	70 to 90	36 in (30 cm)
80 - 150 kVp	80 to 100	18 in (45 cm)
	100 to 150	36 in (30 cm)

3.2.3 Survey meter (model 451P)

The ion chamber survey meter (model 451P, Fluke Biomedical, Everett, WA, USA) is a battery operated, hand-held, pressurized unit designed to measure X-ray and gamma ray above 25 keV and beta radiation above 1 MeV, using the latest complementary metal oxide semiconductor (CMOS) and LCD technology (Fig. 3.2.3). The survey meter readout consists of a 2-1/2 digit LCD and a 100 segment analog bar graph. The unit of measurement is auto-ranging and auto-zeroing and has an auto ON backlight. When the ambient light conditions fall below twilight levels the backlight automatically comes on. If the rate exceeds 5 R/hr an internal factory set alarm will blink the display. 200 hours of continuous operation is provided by two 9-volt batteries, located in the rear of the instrument (Fig. 3.2.3). The calibration measurements are traceable to the National Institute of Standards and Technology (NIST, Gaithersburg, MD, USA) (Operator manual survey meter, 2013).

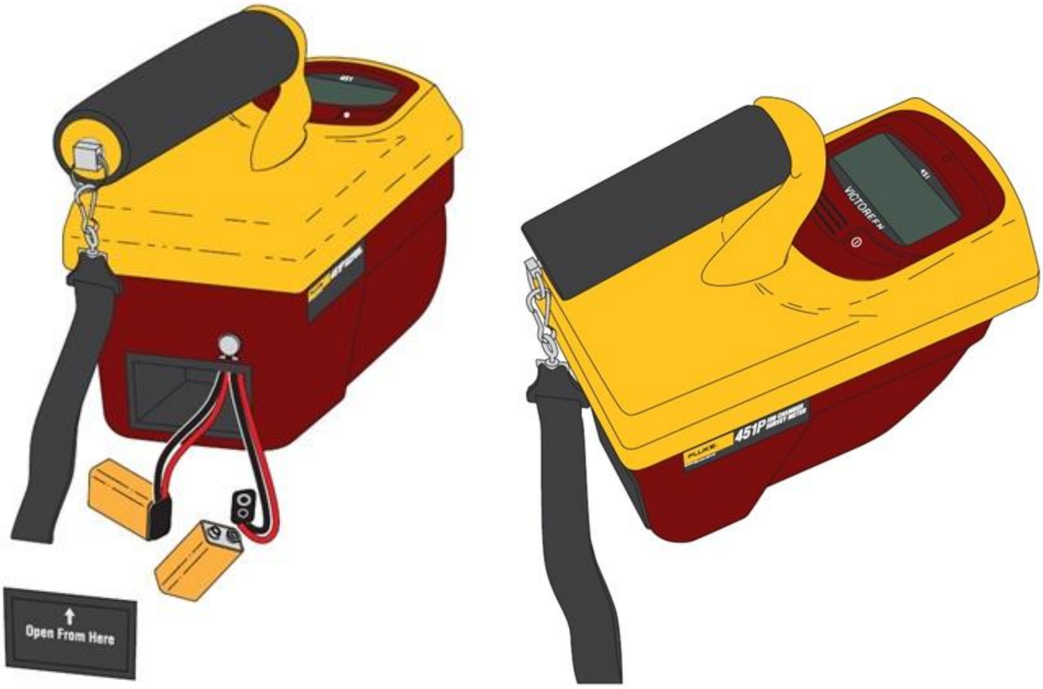

Fig. 3.2.3: Ion chamber survey meter (model 451P)

The *response time* of the survey meter was 5 s for 0 μR h^{-1} to 500 μR h^{-1} (0 μSv h^{-1} to 5 μSv h^{-1}); 2 s for 0 mR h^{-1} to 5 mR h^{-1} (0 μSv h^{-1} to 50 μSv h^{-1}); 1.8 s for 0 mR h^{-1} to 500 mR h^{-1} (0 mSv h^{-1} to 5 mSv h^{-1}). The survey meter has *accuracy* of ± 10% reading between 10% and 100% of full-scale indication on any range with precision within 5% reading. It had a *detector* of 230-cc active volume air ionization chamber, pressurized to 8 atmospheres plastic chamber wall 200 mg/cm2 thick. The *dimensions* of the survey meter is 8.5 (l)×4.5 (w)×8.6 in (h) (21×11.4 ×21.3 cm) with approximately 2.6 lb (1.2 kg).

Theory of Operation

The survey meter is calibrated in exposure rate units of roentgens/hour (or sieverts/hour) for gamma and X-radiation in the energy range of 20 keV to 2 MeV. It is lightweight electronic equipment that requires the computational capabilities of a microprocessor to make it operate. It functions in a multiplex mode called quadriplex which uses four (4) back-planes to accommodate the 128 elements of the display. The microprocessor performs data collection, averaging and multiplication by stored calibration factors, range changing and battery check functions, in addition to driving the LCD. Between computational periods, it ‘sleeps’ in a low power mode to conserve battery power. The digital LCD display updates at one second intervals to nearest the current bar display update. The bar graph and digits display do not always show the same reading because the bar graph is faster than the digital update. It is more convenient to watch the bar graph when the reading is changing quickly and to read the value of a slowly changing or static reading by looking at the digital display.

3.2.4 Collimator/beam alignment test tool (07-661-7662)

The collimator test tool is considered to assess the light X-ray alignment according to National Center for Devices and Radiological Health (NCDRH) specifications. The beam alignment test tool, when used with the collimator test tool, provides a simple test for beam alignment perpendicularity. The beam alignment test tool is a plastic cylinder, 6 inches tall with a 1/16-inch-diameter steel ball at each end as depicted in Fig. 3.2.4 (a). When the tool sits upright on a level surface, the upper ball is directly above the one in the base. The collimator test tool is a flat plate with a rectangular outline and markings etched on its surface as shown in Fig. 3.2.4 (b).

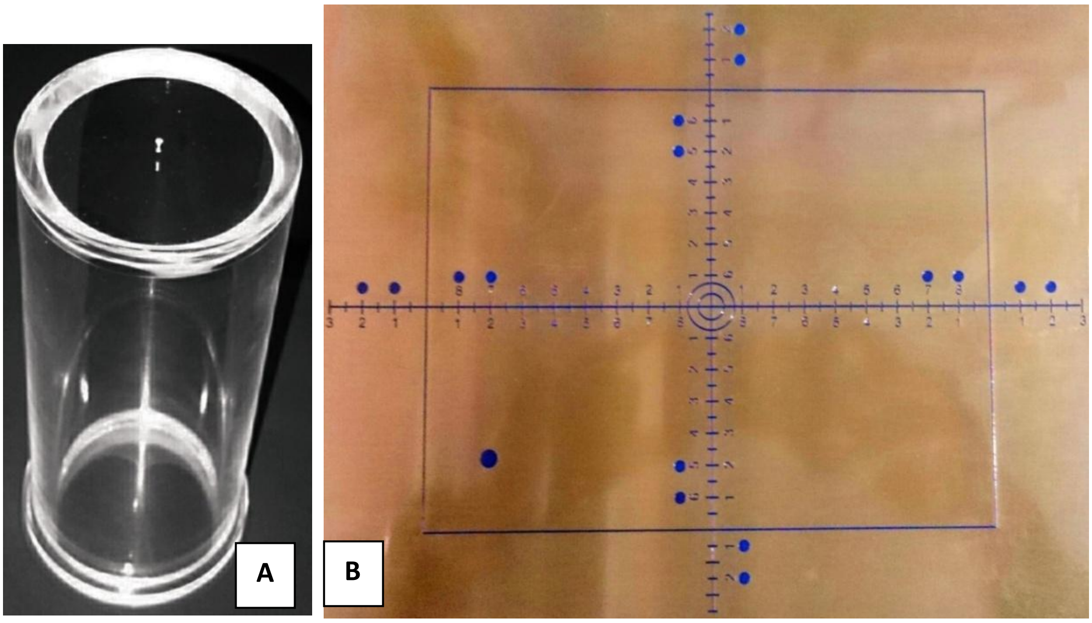

Fig. 3.2.4: (a) Beam alignment test tool; (b) Collimator test tool (07-661-7662)

3.2.5 Thermo Luminescent Dosimeter (TLD Badge)

As personnel monitoring service (PMS) is a part of regulatory requirements stipulated by AERB-GOI, the investigator procure 1 thermo-luminescent dosimeter (TLD) badge. A complete TLD badge consists of a TLD (based on CaSO4) card and a plastic cassette for holding the TLD card as shown in Fig. 3.2.5. The badge was put to the clothing of a person with the help of a crocodile clip attached to the badge. This will enables us to know whether we are working within the safe dose limits prescribe by AERB. TLD card was changed quarterly and return to Utra-Tech laboratory, Chhattisgarh for dose assessment. This laboratory is Bhaba Atomic Research Center (BARC) accredited TLD personnel monitoring laboratory.

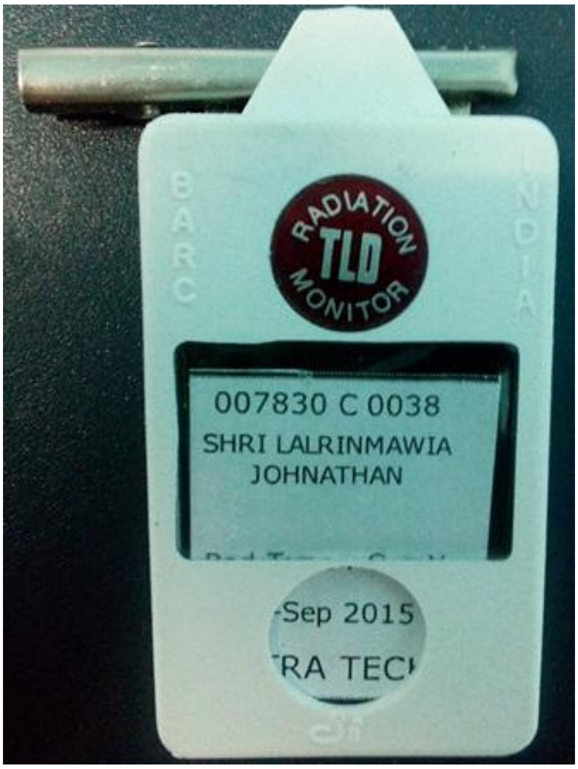
BARC
INDIA
RADIATION
TLD
MONITOR
007830 C 0038
SHRI LALRINMAWIA
JOHNATHAN
-Sep 2015
RA TEC

Fig. 3.2.5: Thermo-luminescent dosimeter used to measure radiation dose of the investigator

3.3 An enumeration survey of conventional diagnostic X-ray generators and essential safety parameters in Mizoram, India

Among different X-ray facilities shown in Table 3.1.1 (a) and (b), 135 (69.2%) were conventional diagnostic X-ray machines and 90.9% of the total workload (5687.21 mA-min/week) had been performed in the conventional X-ray machines (Table 3.3). The locations and details of the 135 conventional diagnostic X-ray machines installed in 82 different institutions are shown in Fig. 3.3. However, the electronic parameters could not be measured from all 135 conventional diagnostic X-ray machines, as 24 machines were condemned; others were out of order; and some of them faced power supply problem.

X-ray machine generators provide the electrical power to the X-ray tube and give option for selection of the technique parameters. Control of X-ray quality and quantity is attained through adjustments of the voltage potential in kilovolts, the X-ray tube current in milliamperes and the exposure time in seconds, which are user-adjusted at the X-ray generator console (Seibert, 2004). Among X-ray generator parameters linearity of time (sec), current (mA) and tube output reproducibility were measured by setting 100 cm FDD. The radiation field size was adjusted to cover only the sensitive area of detector in order to avoid secondary radiation to the detector. To measure output radiation of conventional diagnostic X-ray generators, a battery-operated portable dosimeter (Rad-Check^{TM} Plus model 06-526, Fluke Biomedical-Cleveland, Ohio, USA) was used (Operator manual dosimeter, 2006). A portable wide-range digital kVp meter (model 07-494, Fluke Biomedical-Cleveland, Ohio, USA); battery operated unit was used to measure non-invasively, the effective peak potential applied to a target of X-ray tube (Operator manual kVp meter, 2006). 16 other important survey parameters like X-ray room layout, frequency of quality assurance, patient entrance door (PED), personnel monitoring service (PMS) etc. were considered by observation and interview method.

Table 3.3: X-ray facilities and their respective workloads in Mizoram during June 2015 –June 2016

Type of X-ray facilities	Conventional X-rays	Dental X-rays	Others*	Total
X-ray facilities	135(69.2%)	45(23.1%)	15(07.7%)	195
Condemn X-ray	24(92.3%)	2(7.7%)	Nil	26
Workload (mA-min/week)	5172.16(90.9%)	140.06(2.5%)	374.99(6.6%)	5687.21

* (Cath-Lab, CT-Scan, Fluoroscopy, Mammography and Dental X-ray)

3.3.1 Output Linearity of Time

To measure output linearity of time (sec), input voltage and current were fixed and at least four exposures were performed at different time intervals (e.g. 0.2, 0.4, 0.6 and 0.8 sec). For particular exposure time (i.e. 2 secs) not less than three exposures were performed with the same input parameters to calculate the average value. The *X* parameters which were defined as dose to mAs ratio was calculated for each exposure time setting. Then, coefficient of linearity (*CL*) was calculated by using equation (17) (Wagner *et al*., 1992; Shepard *et al*., 2002; AEOI, 2012; Rasuli *et al*., 2015). Among 135 conventional diagnostic X-ray machines, linearity of time was measured from 98 (72.6%) units.

$$CL_{(\mathrm{sec})} = \frac{\overline{X}_{\max} - \overline{X}_{\min}}{\overline{X}_{\max} + \overline{X}_{\min}} \qquad \text{------------------ (17)}$$

where, $\overline{X} = \dfrac{Avg.Dose}{mAs}$

This *CL* should be <0.1 or 10% (Shepard *et al*., 2002; Papp, 2011; AEOI, 2012).

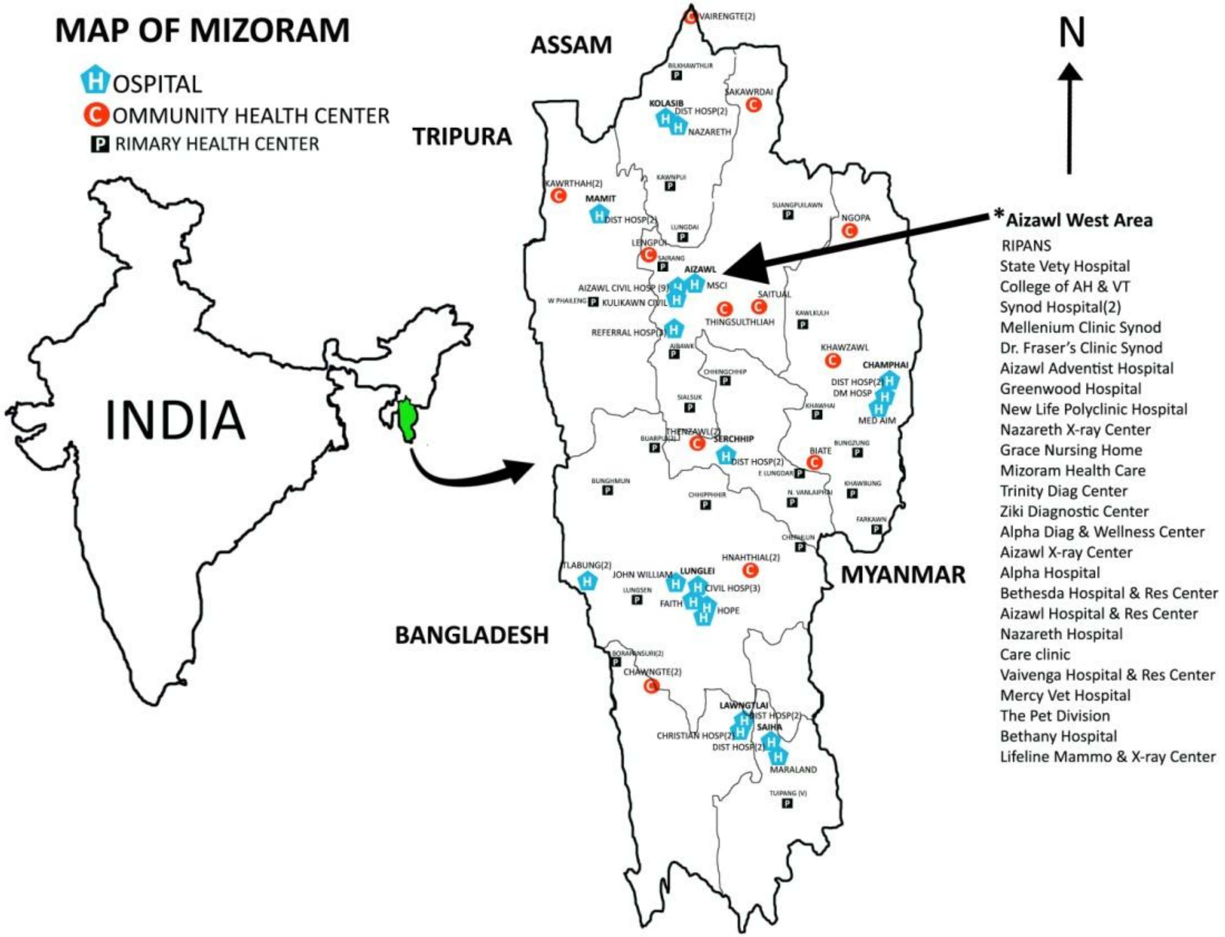
MAP OF MIZORAM
H OSPITAL
C OMMUNITY HEALTH CENTER
P RIMARY HEALTH CENTER
INDIA
ASSAM
TRIPURA
BANGLADESH
MYANMAR
N
VAIRENGTE(2)
BILKHAWTHLIR
SAKAWRDAI
KOLASIB
DIST HOSP(2)
NAZARETH
KAWNPUI
KAWRTHAH(2)
MAMIT
DIST HOSP(2)
LUNGDAI
SUANGPUILAWN
NGOPA
LENGPUI
SAIRANG
AIZAWL
AIZAWL CIVIL HOSP (9)
MSCI
W PHAILENG
KULIKAWN CIVIL
SAITUAL
THINGSULTHLIAH
KAWLKULH
REFERRAL HOSP(3)
AIBAWK
KHAWZAWL
CHAMPHAI
DIST HOSP(2)
DM HOSP
MED AIM
CHHINGCHHIP
SIALSUK
KHAWHAI
THENZAWL(2)
SERCHHIP
BUARPUI(2)
DIST HOSP(2)
BIATE
BUNGZUNG
E LUNGDAR
BUNGHMUN
CHHIPPHIR
N. VANLAIPHAI
KHAWBUNG
FARKAWN
CHERHLUN
HNAHTHIAL(2)
TLABUNG(2)
JOHN WILLIAM
LUNGLEI
CIVIL HOSP(3)
LUNGSEN
FAITH
HOPE
BORAPANSURI(2)
CHAWNGTE(2)
LAWNGTLAI
DIST HOSP(2)
SAIHA
CHRISTIAN HOSP(2)
DIST HOSP(2)
MARALAND
TUIPANG (V)
*Aizawl West Area
RIPANS
State Vety Hospital
College of AH & VT
Synod Hospital(2)
Mellenium Clinic Synod
Dr. Fraser's Clinic Synod
Aizawl Adventist Hospital
Greenwood Hospital
New Life Polyclinic Hospital
Nazareth X-ray Center
Grace Nursing Home
Mizoram Health Care
Trinity Diag Center
Ziki Diagnostic Center
Alpha Diag & Wellness Center
Aizawl X-ray Center
Alpha Hospital
Bethesda Hospital & Res Center
Aizawl Hospital & Res Center
Nazareth Hospital
Care clinic
Vaivenga Hospital & Res Center
Mercy Vet Hospital
The Pet Division
Bethany Hospital
Lifeline Mammo & X-ray Center

Fig. 3.3: Location of 135 X-ray machines, installed in 82 different institutions

3.3.2 Output Linearity of Current

The linearity of a radiation output as a function of current was determined by setting constant tube voltage and exposure time, four successive exposures were performed with different tube current intervals (e.g. 50, 100, 200 and 300 mA). For a particular tube current, at least three exposures were made with the same input parameters for calculating average measurement. The *X* parameters were defined as dose to mAs ratio and were calculated for each tube current setting. The *CL* calculated from equation (18) (Shepard *et al*., 2002; AEOI, 2012) was set for <0.1 or 10% (Wagner *et al*., 1992; Shepard *et al*., 2002; Papp, 2011; IPEM, 1998; AERB format for QA; AEOI, 2012). Linearity of current was measured from 69 (51.1%) conventional diagnostic X-ray machines. Diagnostic X-ray machines which can operate only at a particular fixed current (mA) due to malfunction in mA loading station also exists other than condemned and out of order machines.

$$CL_{(mA)} = \frac{\overline{X}_{\max} - \overline{X}_{\min}}{\overline{X}_{\max} + \overline{X}_{\min}}$$

where, $\overline{X} = \frac{Avg.Dose}{mAs}$ ------------------ (18)

3.3.3 Output Reproducibility

At constant tube voltage and tube loading, not less than five exposures were performed to evaluate X-ray tube output reproducibility. The coefficient of variation '*CV*' obtained from equation (19) was accepted at <0.05 or ±5% (ICRP, 2007; Shepard *et al*., 2002; Papp, 2011; IPEM, 1998; AERB format for QA; AEOI, 2012).

Reproducibility of tube output was considered from 97 (71.9%) conventional diagnostic X-ray machines.

$$CV = \frac{1}{\overline{X}}\sqrt{\frac{\sum_{i=1}^{n}(X_i - \overline{X})^2}{n-1}} \qquad \text{------------------ (19)}$$

3.3.4 Tube Output (70 kV at FDD=100cm)

At tube voltage 70 kVp and a typical tube loading, the X-ray dose was measured at 100 cm FDD. This assessment can be used for evaluating patient's skin dose (Rasuli *et al*., 2015). The table dose obtained from equation (20) was expected to be in the range 43− 52 µGy/mAs (IPEM, 1998). Tube output could be measured from 97 (71.9%) units.

$$X = \frac{Avg.Dose}{mAs} \qquad \text{------------------ (20)}$$

3.3.5 kVp Accuracy

The digital kVp meter (model 07-494, Fluke Biomedical, Cleveland, Ohio, USA) was used to determine kVp accuracy for several stations of the X-ray machine. As a result, a significant cause of poor image quality can be immediately diagnosed without affecting patient throughput. The kVp meter was positioned in the center of the beam. The measurement area of the meter is 2 square inches and is located on the top panel of the unit. Measurements made on other parts of the beam will result in inaccurate readings due to the fact that the beam spectrum is different for different parts of the beam. The *heel effect* is an example of such a beam spectrum change

(Operator manual kVp meter, 2006). To evaluate kVp accuracy, the authors measured from 50 kVp–150 kVp (5 kVp steps) where tube loading and FDD were set as per Fluke manual for different accelerating potentials. The authors set the phase switch to the single-phase (1φ) or three-phase (3φ) position according to the type of machine measured (Operator manual kVp meter, 2006). In some equipments, it was impossible to set kVp higher than 90 kV due to improper and insufficient power supply. However, the authors set the range selector switch (located on the top panel) to the appropriate range for the kV to be measured. Voltage accuracy expected to be within 5% was considered from the equation (21) (ICRP, 2007; Shepard *et al*., 2002; Papp, 2011; IPEM, 1998). From 135 conventional units kVp accuracy could be measured from 97 (71.9%) machines.

$$VoltageAccuracy = \frac{kV(measured) - kV(selected)}{kV(selected)} \quad \text{------------------ (21)}$$

3.3.6 Other Safety Parameters

Other than diagnostic X-ray generator parameters, the investigators took several data from 16 important safety parameters such as frequency of quality assurance, X-ray room layout, availability of PMS, lead apron, gonad shielding, repeated exposure and repetition reason, qualified personnel, collimator bulb, field size knob, PED, protective barrier, waiting area, chest stand, warning light, dark rooms were checked and recorded. This information was collected from radiation workers and/or the heads of institutions through observation and interviews.

3.4 Qualitative study of mechanical parameters of conventional diagnostic X-ray machines in Mizoram, India

The authors considered the mechanical characteristics of conventional diagnostic X-rays such as HVL, congruency between radiation beam and the optical field and perpendicularity of the central beam (Ebiswa *et al.*, 2009).

3.4.1 Half Value Layer

HVL is inversely proportional to the attenuation coefficient and is related as follows:

$$\frac{I}{I_o} = e^{-\mu x}$$

According to the definition of HVL,

$$D_{1/2} = \frac{0.6931}{\mu} \qquad \text{------------------ (22)}$$

where, $D_{1/2}$ is the HVL thickness (John and Cunningham, 1983; Ahmad, 2015; Meredith and Massey, 1992).

A battery-operated portable dosimeter (RAD-CHECK^{TM} PLUS model 06-526, Fluke Biomedical-Cleveland, Ohio, USA) was used to measure primary beam from a conventional X-ray machine (Operator manual dosimeter, 2006). Aluminum sheets with different thicknesses (two sheets 0.5 mm thick; three sheets 1.0mm thick) were used to filter the ionizing radiation using a measuring stand (Rasuli *et al.*, 2016). The HVL could be measured for 97 of 135 conventional X-ray units (71.85%) because 14 units were out of order and 24 had been condemned (Table 3.4.1).

Table 3.4.1: X-ray machines with a defect that made determination of a given parameter impossible

Details of defects	No of X-ray units	Parameters that could not be studied by authors
Circular collimators in mobile X-ray	32	Congruency, Perpendicularity
Optical field not working	4	Congruency, Perpendicularity
Non-adjustable collimator	6	Congruency
Darkroom not functioning	8	Congruency, Perpendicularity
X-ray out of order	14	Congruency, Perpendicularity, HVL
X-ray condemned	24	Congruency, Perpendicularity, HVL

To measure the HVL, the author set the source at a table-top distance of 100 cm and centered the X-ray field by adjusting the dosimeter position through the collimator so the entire chamber would be included in the X-ray field. The HVL was measured at a constant tube voltage setting; 70 kVp was used for conventional X-ray equipment. Keeping the tube voltage and tube loading at a constant, exposure was made without the Al-filter. This was followed by exposures with 0.5, 1.0, 1.5, 2.0, 2.5 and 3.0 mm of Al placed in the X-ray beam on top of the test stand. The test stand was placed in relation with the X-ray beam such that the filter lay at the center between the X-ray source and detector. Throughout this experiment, the input parameter was kept constant and the test stand, X-ray tube and dosimeter were maintained at fixed positions. The transmission percentage was calculated from each data point and a graph was plotted for transmission percentage versus Al-thickness.

The author drew a horizontal line from the point corresponding to one-half of the original exposure and noted the half value thickness in millimeters (mm) (Fig. 3.4.1) (Gray *et al*., 1983). However, the value of a suitable HVL may not be acquired because this measurement of arrangement was not a narrow beam. According to the AERB safety code for 70 to 100 kV, the minimum filtration of a useful beam for a maximum rated operating tube potential should be 2.0 mm of Al (AERB, 2001). However, according to international standards, the total filtration in the useful beam should be equivalent to not less than 2.5 mm of Al (IAEA, 2014; Health Canada, 2008; Euratom radiation protection no. 91).

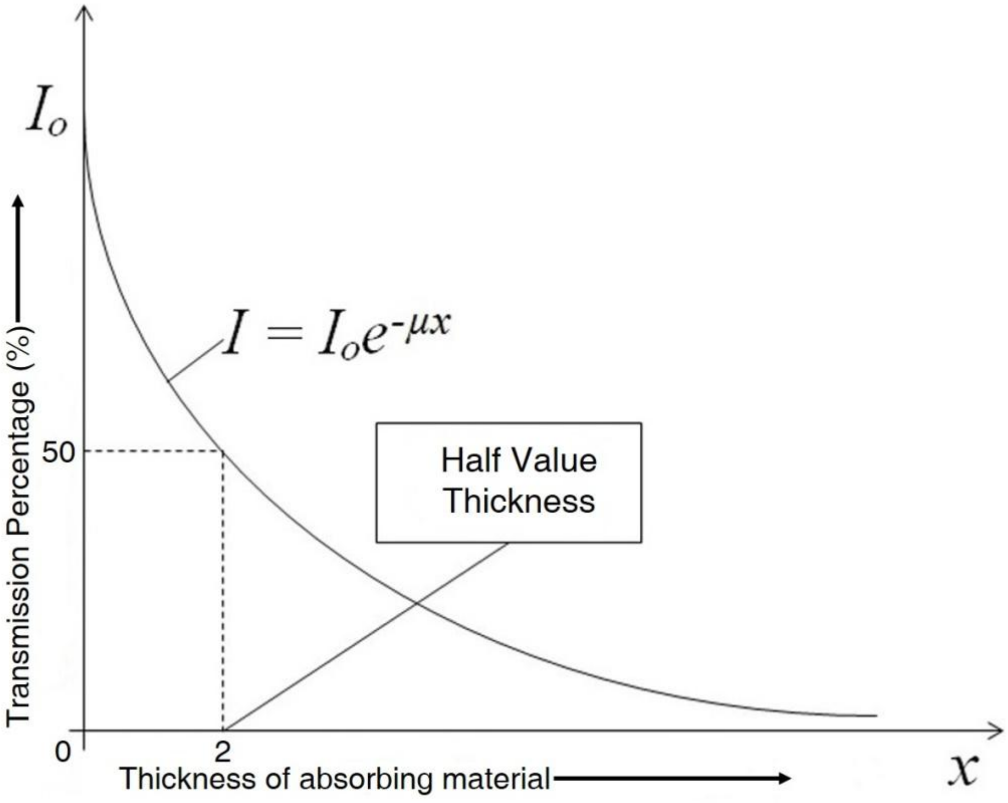

Fig. 3.4.1: Attenuation curve showing the half value thickness

kVp accuracy and tube output consistency were also measured to improve clarification. A wide-range digital kVp meter (model 07-494, Fluke Biomedical, Cleveland, Ohio, USA) was used to measure the output kVp. To evaluate output consistency, a battery-operated RAD-CHECK^{TM} PLUS portable dosimeter (model 06-526, Fluke Biomedical-Cleveland, Ohio, USA) was used. The tube output coefficient of variation was calculated for each unit.

3.4.2 Radiation Beam and Optical Field Congruency

A common problem of X-ray machines is the misalignment of the collimator light field and the X-ray field. To test the congruency of the radiation beam and the optical field, a congruency tool (manual no. 07-661-7662, Fluke Biomedical, Cleveland, Ohio, USA) was used. The congruency test tool is a flat copper plate with a rectangular outline and markings etched on the surface (Operator manual collimator and beam alignment tools, 2005). The congruencies of the diagnostic X-ray units with adjustable collimators and working collimator bulbs were studied. For several reasons, the congruency between the radiation and the light field could only be measured in 47(34.81%) units (Table 3.4.1). To measure the congruency, we leveled the table and adjusted the X-ray tube so that the beam was perpendicular to the X-ray machine table. The tube was centered on the table at a distance of 100 cm from the focal spot to the table top. The collimator shutters were adjusted so that the edges of the light field coincided with the rectangular outline of the collimator tool (Operator manual collimator and beam alignment tools, 2005). The collimator tool was oriented such that the dot in the lower left corner corresponded to the position of a supine patient's right shoulder. This allowed the direction of the collimator fault to be determined at a later time. Cassettes of 8 × 10 inches (20×25 cm) were placed on the center top of the table and they were aligned to the X-ray tube and exposed at 60±10 kVp and 10±3 mAs (Fig. 3.4.2 (a)).

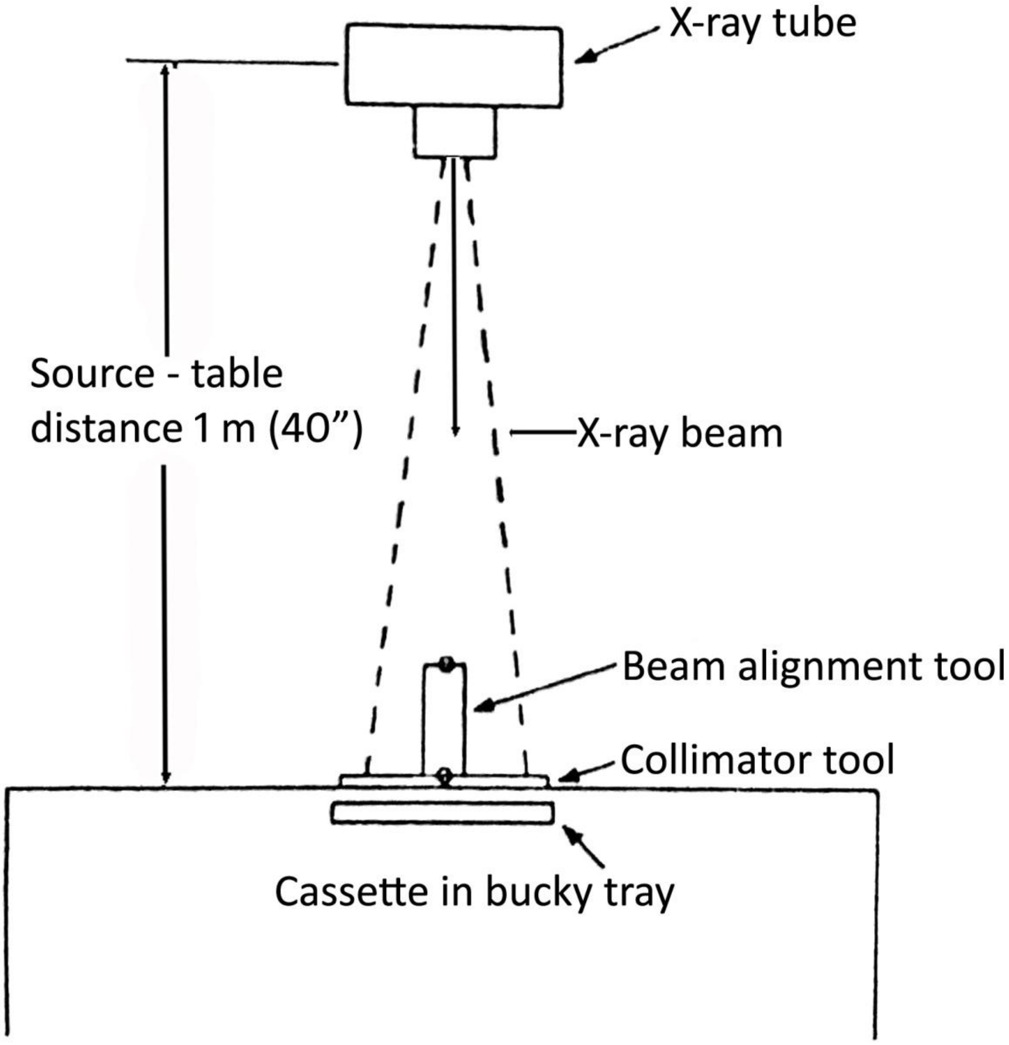
X-ray tube
Source - table distance 1 m (40")
X-ray beam
Beam alignment tool
Collimator tool
Cassette in bucky tray

Fig. 3.4.2 (a): Experimental set up for congruency and perpendicularity test (Re-drawn from Sungita *et al.*, 2006)

The maximum allowed misalignment in congruency between the radiation beam and the optical field is 2% of the source-to-image distance (SID) (Papp, 2015; Euratom radiation protection no. 91). If the X-ray was just within the image of the rectangular frame of the optical field, it indicated good congruency between the light and the X-ray field (Fig. 3.4.2 (b)). However, if an edge of the X-ray field was on the first spot of the rectangular frame, ± 1 cm to either side of the line, then the edges of the X-ray and light fields were misaligned by 1% of the distance between the X-ray source and the table top. Similarly, the edge of the X-ray falling on to the second spot, by ± 2 cm, indicated an error of 2% at 40 inches (100cm). If the congruency misalignment between X-ray field and visible light is larger than ±3 cm then it is rejected at 1 m (40") SID (Fig. 3.4.2 (c)) (Operator manual collimator and beam alignment tools, 2005).

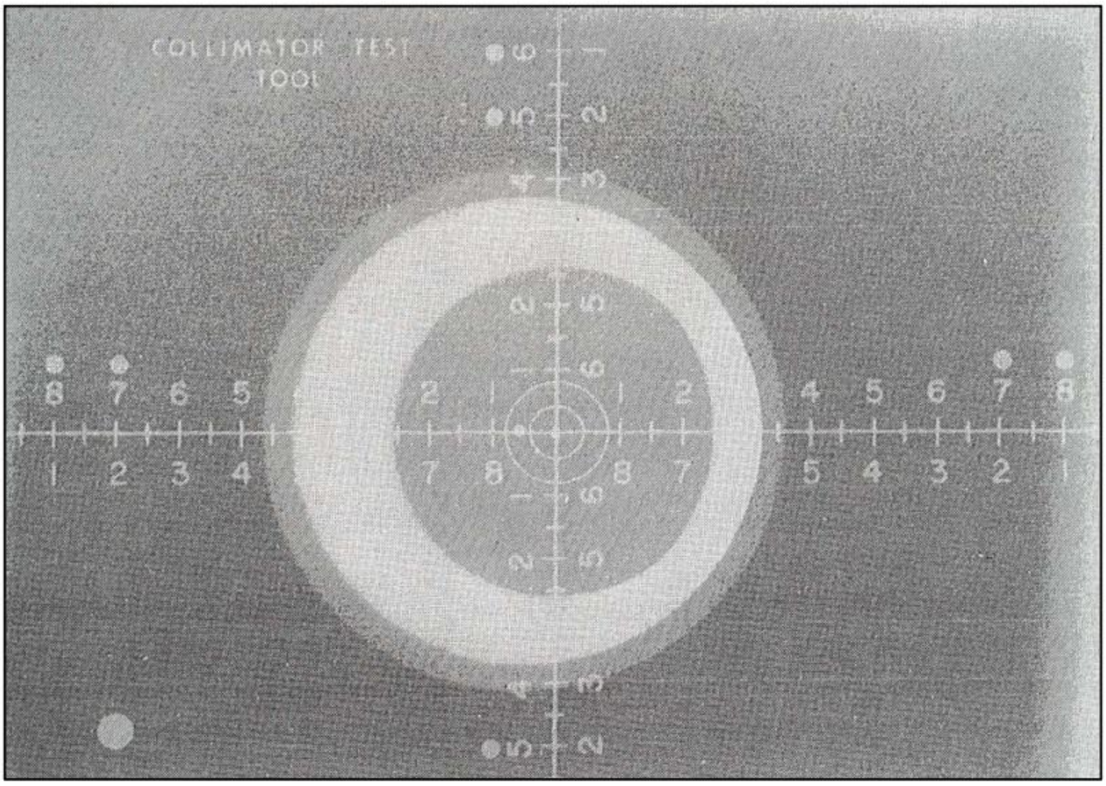

Fig. 3.4.2 (b): Good field alignment, beam alignment approximately 2° from perpendicular

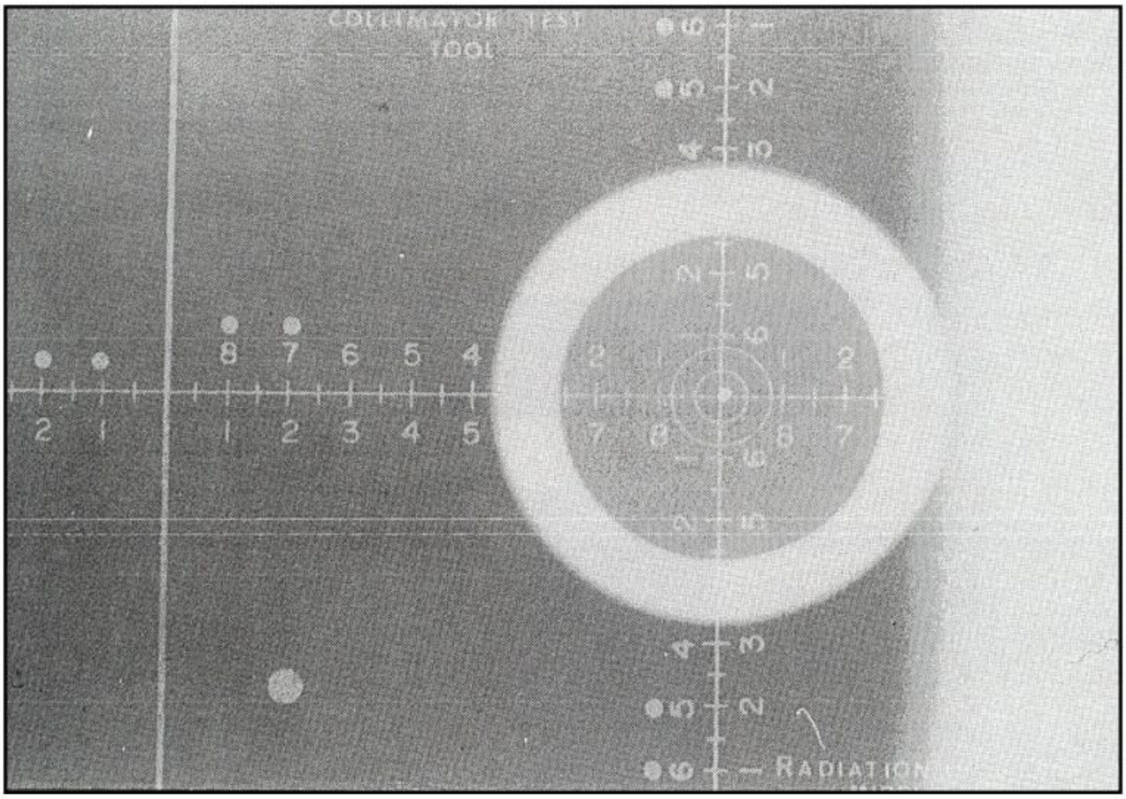

Fig. 3.4.2 (c): X-ray field alignment error, greater than 3 cm and unacceptable at 40” SID

3.2.3 Perpendicularity between the Central Beam and Image Receptor

Similarly, an alignment tool (manual no. 07-661-7662, Fluke Biomedical, Cleveland, Ohio, USA) was used to test central beam alignment perpendicularity. The beam alignment test tool is a plastic cylinder, 6 inches tall with a 1/16-inch-diameter steel ball at each end (Operator manual collimator and beam alignment tools, 2005). The perpendicularity of the diagnostic beam of 53(39.25%) working diagnostic X-ray units was studied (Table 3.4.1). The test used the same experimental set-up as the congruency test; in which we placed the beam alignment test tool in the center of the collimator tool and evaluated them simultaneously (Operator manual collimator and beam alignment tools, 2005).

According to the specifications of the NCDRH, the X-ray beam should be perpendicular to the plane of the image receptor. The following principle was applied for a source-to-table distance of 40 inches. If the images of the two steel balls overlapped, the central beam was perpendicular to the image receptor, within 0.5 degrees (Fig. 3.4.3 A). If the image of the top ball intercepted the first circle, then the beam was approximately 1.5 degrees from perpendicular (Fig. 3.4.3 B). If the image of the top ball intercepted the second circle, the misalignment was approximately 3 degrees (Fig. 3.4.3 C) (Operator manual collimator and beam alignment tools, 2005). As per specifications, the angle between the central beam of X-ray and the plane of the image receptor should not differ by more than 1.5 degrees from the perpendicular (Euratom radiation protection no. 91; Sungita *et al.*, 2006).

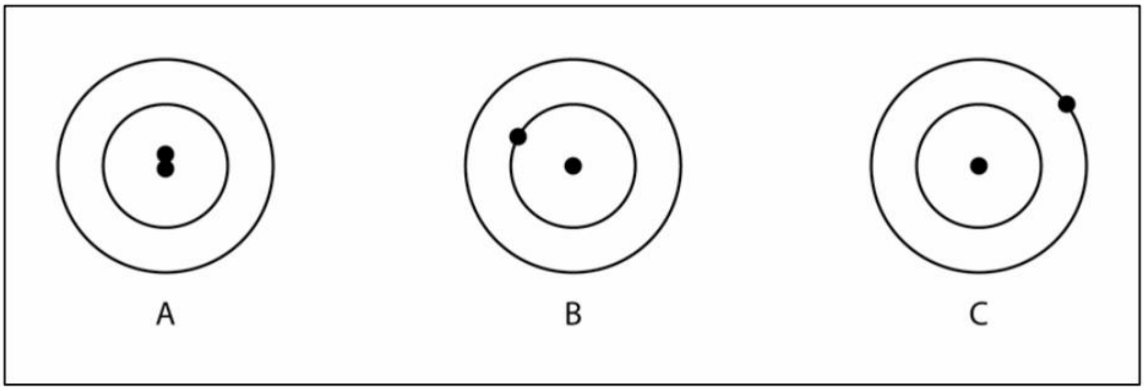

Fig. 3.4.3: Interpretation of the image of the steel balls in the beam alignment test tool

3.5 Evaluation of radiation doses at diagnostic X-ray CPs and outside PEDs in Mizoram, India

In the present study, some of the CPs were properly covered by protective barriers, whereas others were partly covered by a barrier or had no barrier at all. Only a few PEDs had lead-lined doors, whereas others employed typical wooden doors, plywood lined doors or Al-plane sheet-lined doors. The nature, type and thickness of CP barriers and PEDs were measured and recorded. The authors also examined product manuals for accurate information. The protective barriers used by the X-ray users were lead-lined, 6-feet high, 2.5–3-feet wide, with a lead thickness equivalent to 1.5–1.7 mm. The lead-lined doors were 1.5 mm lead-thickness equivalent.

Sketches were made for all X-ray installations indicating X-ray source, couch, chest stand, protective barrier, CP, PED. Distances from the CP to the couch and chest stand and from the couch and chest stand to the PED were measured and recorded as shown in Fig. 3.5 (a). A water phantom, 10-L fresh water in a plastic container, was used as a source of scattered radiation. The plastic container was a perfect cube structure where all the sides (i.e., length, width and height) were equivalent (i.e., 31 cm each). The thickness of this container was 1 cm and it was uniform throughout the body (Fig. 3.5 (b)). It was positioned on the couch for vertical exposure (*couch mission*) and at a chest stand for horizontal exposure (*chest mission*). Field sizes were adjusted to the maximum and focused on the water phantom. Exposure rates were measured at the CP and outside the PED separately for both chest and couch missions. For measuring exposure rates, a pressurized ion-chamber survey meter (Model 451 P, Fluke Biomedical, Everett, WA, USA) was used. All measurements were performed in freeze mode because it provides a constant reference of the highest exposure rate obtained from the time the freeze function is initialized. The highest reading will become visible as a single bar on the bar graph. The freeze bar will shift to the higher measurement point if a measurement obtained exceeds the freeze bar reading. During the freeze mode the operating range of the 451P remains locked on the highest range attained so that the scale and the multiplier remain the same (Operator manual survey meter, 2013).

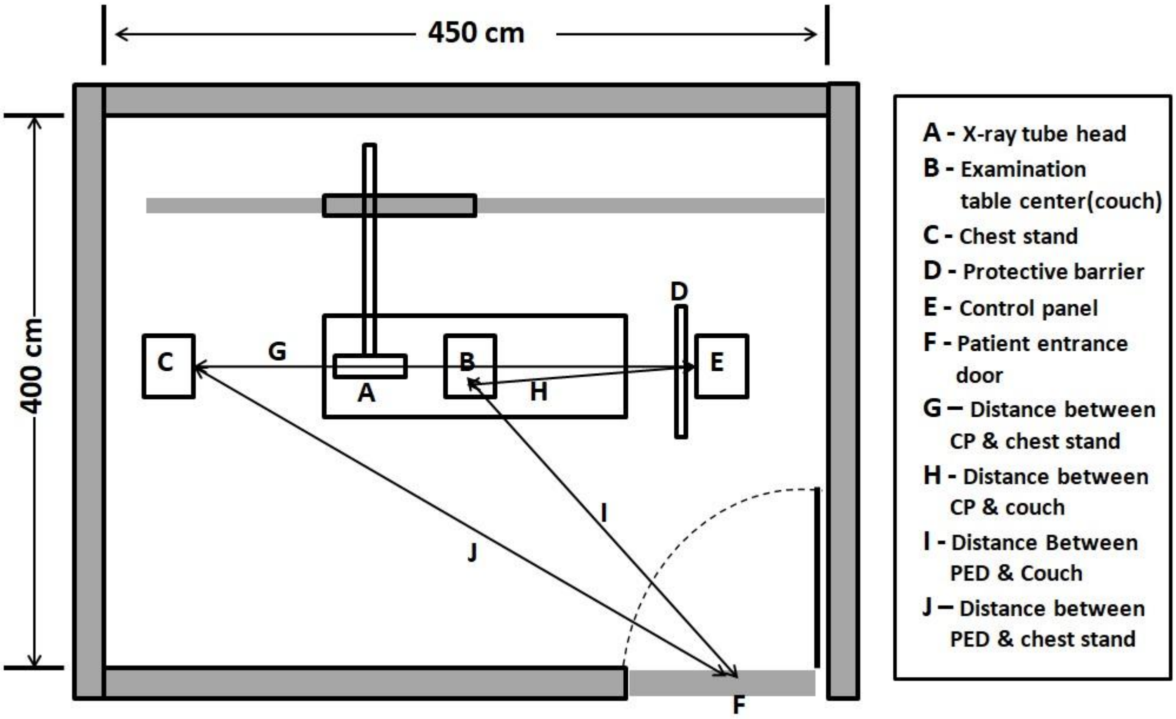
450 cm
400 cm
A
B
C
D
E
F
G
H
I
J
A - X-ray tube head
B - Examination table center(couch)
C - Chest stand
D - Protective barrier
E - Control panel
F - Patient entrance door
G – Distance between CP & chest stand
H - Distance between CP & couch
I - Distance Between PED & Couch
J – Distance between PED & chest stand

Fig. 3.5 (a): Layout of the X-ray installation room

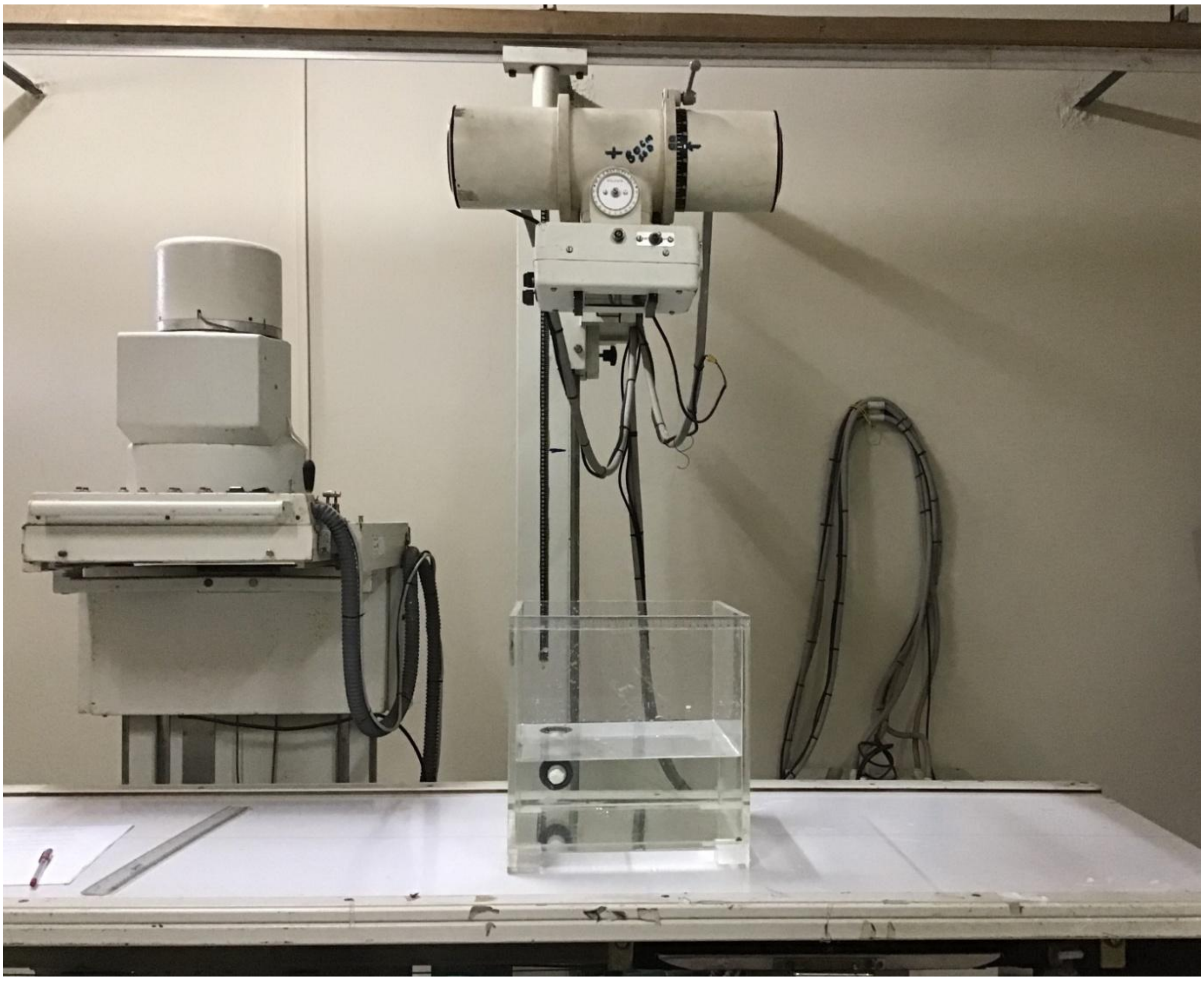

Fig. 3.5 (b): A water-phantom setting to measure stray radiation for vertical exposure (couch mission)

The stray radiation levels at the CP and outside the PED were measured using the maximum accelerating potential setting (i.e., 85–120 kVp) and minimum input tube current (i.e., 25–50 mA) with fixed exposure time of 1 s (Sonawane *et al.*, 2010). The survey meter was placed at a height in relation to the water phantom base with its measuring surface towards the water phantom (Vlachos *et al*., 2015). In this configuration, the survey meter could measure stray radiation scattered from the phantom, the walls, the floor and the ceiling, including leakage from the X-ray tube

(Tsalafoutas, 2006). The workload for each piece of equipment was calculated in mA-min/week using Eq. (23). These workloads were calculated from several parameters such as; patients per day, films per patient, mAs per film and days per week by using formula given by NCRP (NCRP, 2004). Patients per day were calculated based on patient records kept by the institutions. The total number of patient exams throughout a year was divided by the total number of working days during that period.

$$W = \frac{patients}{day} \times \frac{films}{patient} \times \frac{mAs}{film} \times \frac{days}{week} \times \frac{1\min}{60\,\mathrm{s}} \qquad \text{----------------}\ (23)$$

Then, the radiation dose in units of mR/week was calculated from the workload and stray radiation rates using Eq. (24) (AERB format for QA):

$$Dose\left(\frac{mR}{Week}\right) = Workload\left(\frac{mA-min}{Week}\right) \times\ ExposureRate\left(\frac{mR}{h}\right) \times \left(\frac{1}{60}\right) \times \left(\frac{1}{mAused}\right), \qquad \text{---------------}\ (24)$$

where, *mA* is the input-tube current from the survey. The authors measured tube voltage for each machine to improve clarification using a wide-range digital kVp meter (model 07-494, Fluke Biomedical, Cleveland, Ohio, USA). For evaluating kVp accuracy, the authors considered the tube voltage between 50–150 kVp with 5 kVp steps and the tube loading and FDD were set as per the Fluke manual (Operator manual kVp meter, 2006).

In a study of occupational exposure in Brazil by Cunha *et al.* (1992) and a national survey of occupational exposure among diagnostic technologists in South

Korea by Lee *et al.* (2015), radiation workers were monitored. However, in this study, none of the workers or the public were properly monitored using personal monitoring devices, which is the reason the authors followed the method described above.

3.6 Study on the intensity of radiation attenuated by protective barriers in diagnostic X-ray installations

After surveying all the conventional diagnostic X-ray installations in Aizawl, the authors selected ten X-ray machines installed in ten different institutions. Diagnostic X-ray equipment were selected based on the following criteria: fixed and mobile-fixed X-ray machines; presently used for both couch and chest X-ray examinations; AERB type approved unit having PED (lead-lined, wooden, plywood etc.) and CP protective barrier (lead, concrete, plywood etc.); maximum rating of the X-ray machine generator (current, potential and exposure time); accuracy of focus to table top distance; accuracy of tube orientation indication; collimator adjustment.

The survey instrument used to measure stray radiation is a pressurized ion chamber-based survey meter - model 451 P (Fluke Biomedical, 6920 Seaway Blvd., Everett, WA, USA) (Operator manual survey meter, 2013). Sketches were made for every X-ray installations indicating X-ray source, couch, chest stand, protective barrier, CP and PED. Distances of CPs from couch and chest stands along with PEDs from couch and chest stands were measured (in cm) and recorded as it was done in evaluation of radiation dose at CPs and outside PEDs (Fig. 3.5 (a)). In the present study, the protective barriers at CPs were lead-lined, concrete, plywood and plywood plane sheet-lined. At the same time PEDs were lead-lined, solid wood, plywood and plywood plane sheet-lined. A water phantom, ten litres of fresh water in a plastic container was used as source of scattered radiation, which was positioned on a couch for vertical exposure (couch mission) and at chest stand for horizontal exposure (chest mission). The plastic container is a perfect cube where all the sides; length, width and height are equivalent i.e. 31 cm each respectively. The thickness of this container is 1 cm and it is uniform throughout the body (Fig. 3.5 (b)). Field sizes were adjusted to maximum and focused at the water phantom. Exposure rates were measured at the CP with and without barrier; at the PED with door open and close.

The intensity of radiation (with and without door/barrier) at CP and outside PED were measured by setting maximum accelerating potential and minimum current with fixed exposure time as shown in Table 3.6 (Sonawane *et al*., 2010). The survey meter was placed at a height with respect to the phantom base with its measuring surface in the direction of the phantom (Vlachos *et al*., 2015). In this set up, the survey meter could measure radiations scattered from the phantom, the walls, the floor and the ceiling as well as leakage radiation from the tube housing (Tsalafoutas, 2006; Dixon, 1994). All the measurements were performed in freeze mode.

Table 3.6: Input parameters settings for stray radiation rate measurement

Parameters	Set value	As per reference
Accelerating Potential	80 to 120kV	Maximum kV
Current	20 to 80mA	Minimum mA
Time	1s	Fixed

3.7 Investigation of conventional diagnostic X-ray tube housing leakage radiation using ion chamber survey meter in Mizoram, India

For measuring leakage radiation, pressurized ion chamber survey meter (model 451 P, Fluke Biomedical, Everett, WA, USA) was used (Fig. 3.2.3) (Operator manual survey meter, 2013). All the measurements were carried out in freeze mode (Vlachos *et al*., 2015). To measure leakage radiation from X-ray tube, the collimator diaphragms were closed completely and the tube was projected vertically downward. So, the tube is oriented in such a way that the anode is over the head of the table and the cathode is over the foot. When facing the X-ray tube assembly, the anode is on the radiographer's left and the cathode is on the right. The tube leakage measurements were done at a 1 m FDD by putting detector at five different positions viz. left, right, front, back and top of the X-ray tube. The exposure parameters for the present study were maximum accelerating potential (kVp), maximum mA and fixed exposure time (sec) (Ammann and Kutschera, 1997; Tsalafoutas, 2006; Sungita *et al*., 2006; Hassan *et al*., 2012; Johnston and Fauber, 2012).

According to the AERB safety code 2001 for 'medical diagnostic X-ray equipment and installations' it is mentioned that 'every tube housing for medical diagnostic X-ray equipment shall be so constructed that the leakage radiation through the protective tube housing in any direction, averaged over an area not larger than 100 cm^2 with no linear dimension greater than 20 cm, shall not exceed an air kerma of 115 mR (1 mGy) in one hour at a distance of 1 m from the X-ray target when the tube is operating at the maximum rated kVp and for maximum rate current at that kVp' (AERB, 2001). Again, it was reported that the leakage radiation from the tube housing measured at a distance of 1 m from the focus should not exceed 1 mGy (115 mR) in one hour (Euratom radiation protection no. 91). In addition to that, in the NCRP report No. 147, it was given that the manufacturers were required by regulation to limit the leakage radiation to 0.876 mGy h^{-1} (100 mR h^{-1}) at 1m (NCRP, 2004). Compliance with this requirement should be evaluated using the maximum X-ray tube potential and the maximum beam current at that potential for continuous tube operation.

Data presented as *mean, range, coefficient of variation*, *standard deviation* (SD), *standard error mean* (SEM) and *correlation* were analyzed by using SPSS statistics for windows version 17.0. (SPSS, Inc., Chicago, IL, USA). *T-test* was also conducted to check the existence of significant difference between the amount of leakage radiation measured at different position with respect to the X-ray tube as well as to check the significant difference between radiation level measured with and without CP barriers as well as PEDs in chest and couch missions.

CHAPTER 4

RESULTS AND DISCUSSION

The extensive clinical use of diagnostic X-ray equipment has led to the increased radiation exposure to radiation workers and patients (Hashemi *et al*., 2019). X-radiation constitutes a major part of man's exposure to artificial resources of ionizing radiation (UNSCEAR, 2000). Therefore, in radiation protection, radiation exposure to the population due to diagnostic X-ray machines is a very important point of concern (Zoetlief, 1998). It is well-known that radiological protection is generally based on the three basic major principles namely dose limitation, optimization and justification (ICRP, 1991). Optimization in diagnostic radiology indicates that the ionizing radiation dose to the patient should be as low as possible but compatible with the radiological information (image quality) of the images necessary for obtaining an adequate diagnosis or to guide the treatment (Zoetlief, 1998). Or we can simply say that the radiation exposure should be maintained ALARA (Pernicka and McLean, 2007).

In order to achieve ALARA principle, quality assurance programs have been implemented in the diagnostic radiology (NCRP, 1990; ICRP, 2007). The WHO has increasingly highlighted the importance of quality assurance programs in order to reduce radiation exposure, decrease the imposed medical costs and improve the available diagnostic information (WHO, 1982). Furthermore, the aim of quality assurance is to have best X-ray image with minimum dose delivered to the patient and to minimize the production of rejectable poor images. From economic point of view, other advantages are derivable from applying such quality assurance. This includes the extension of the life span of the X-ray machine and the minimization of number of X-ray films rejected (Kharita *et al*., 2008).

4.1 An enumeration survey of conventional diagnostic X-ray generators and essential safety parameters in Mizoram, India

Among 111 diagnostic X-ray machines, the oldest X-ray machine was installed in the year 1972. During the year 1972−2000, 13 X-ray machines were installed, 45 X-ray machines were installed between the year 2001−2010 and 53 X-ray units were installed during the year 2011−2016 (Fig. 4.1). The average age of these X-ray machines was mean±SD of 7.20±6.69 years.

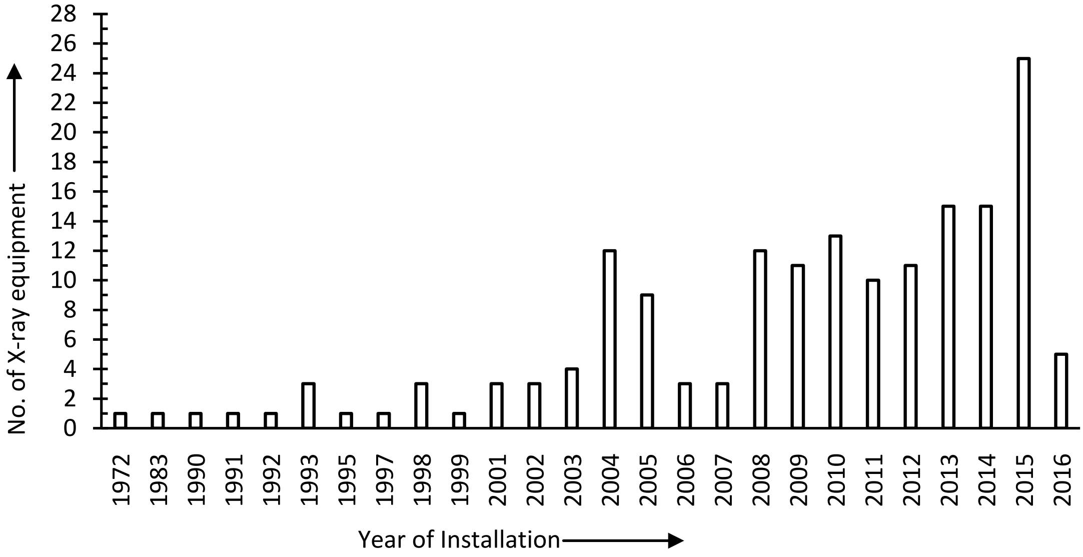

Fig. 4.1 Year of installations of diagnostic X-ray machines in the present study area.

4.1.1 Linearity of Time

Of the 98 X-ray machines tested for linearity of time (sec), 58 (59.2%) units had coefficient of linearity above 0.1 or 10% (Fig. 4.1.1) while, only 40 (40.8%) were within acceptable limits. The highest value for coefficient of linearity of time was 0.93 which is 93%; while the mean±SD value was 0.20±0.19. In the previous studies, output linearity of time for 8.9%−12% machines was found to be beyond acceptance limit (Sonawane *et al.*, 2010; Jomehzadeh *et al.*, 2016). Rasuli *et al.* in 2015 found that all the devices measured were in line with the standard norms in selected hospitals of Khuzestan province, Iran. However, X-ray generators may vary in performance from place to place and even in the same place from machine to machine.

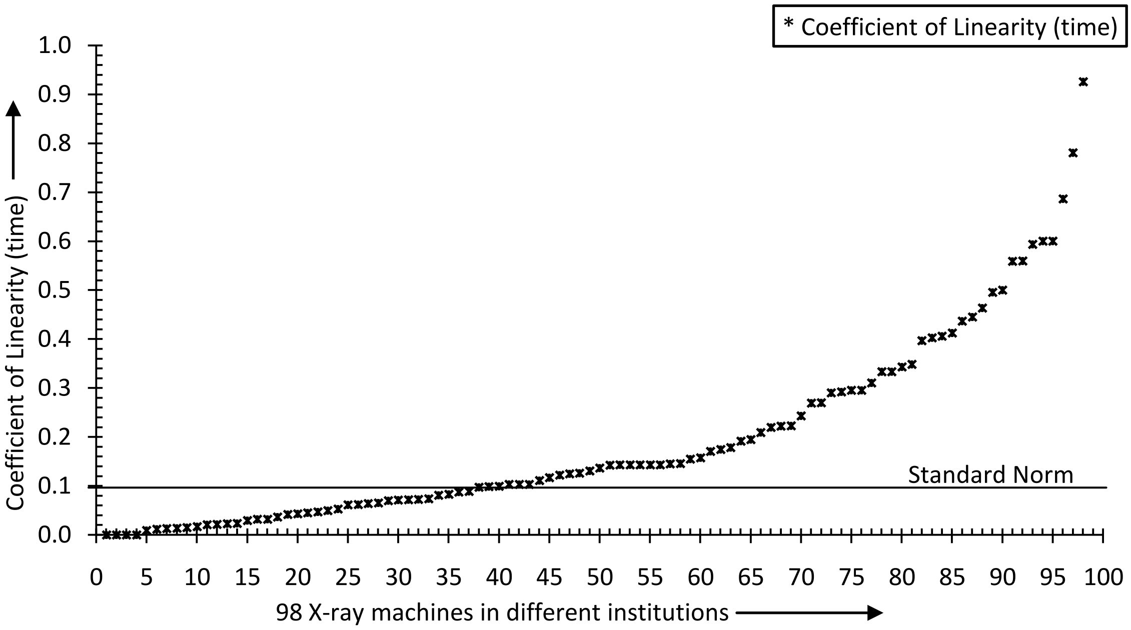

Fig. 4.1.1: Tube output linearity of time (sec) for 98 conventional diagnostic X-ray machines (standard norm <0.1 or 10%)

4.1.2 Linearity of Current

Out of the 69 X-ray machines tested for linearity in terms of mA, 57 (82.6%) units had coefficient of linearity above 0.1 or 10% (Fig. 4.1.2). Only 12 (17.4%) of the units tested were within norms. The highest value for coefficient of linearity of current was 0.97 which is 97%; and the mean±SD value was 0.25±0.18. Regarding output linearity of current, 12%−55% out of acceptable limit were observed in previous studies in different parts of the world (Rasuli *et al.*, 2015; Sonawane *et al.*, 2010; Jomehzadeh *et al.*, 2016; Khoshbin *et al.*, 2013; Asadinezhad *et al.*, 2017; Neofotistou *et al.*, 1995; Saghatchi *et al.*, 2006; Gholamhosseinian *et al.*, 2014; Esmaeili, 2006).

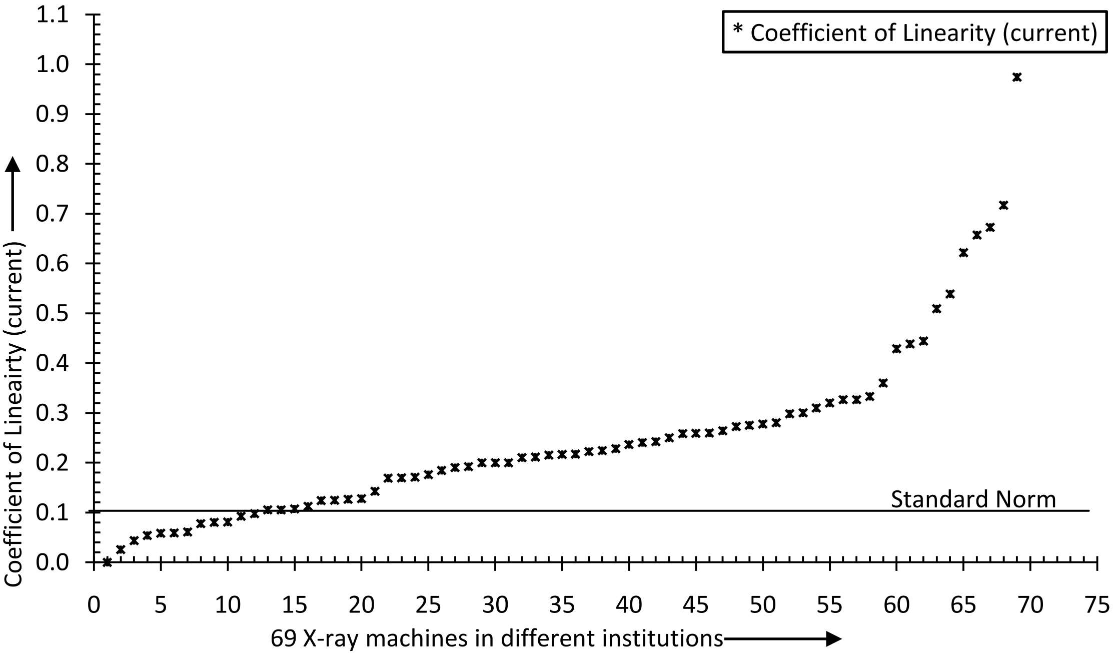

Fig. 4.1.2: Tube output linearity of current (mA) for 69 conventional diagnostic X-ray machines (standard norm <0.1 or 10%)

4.1.3 Output Reproducibility

Out of the 97 X-ray machines tested for output reproducibility, 34 (35.1%) units tested above 0.05 or ±5% (Fig. 4.1.3). The remaining 63 (64.9%) X-ray machines were within acceptable limits. The calculated mean±SD value was

0.08±0.12 and the highest value of tube output coefficient of variation was 0.72 which is 72%. In the previous studies from different regions, it was found that 5%−30% devices were out of acceptable limit (Jomehzadeh *et al*., 2016; Khoshbin *et al*., 2013; Asadinezhad *et al*., 2017; Neofotistou *et al*., 1995; Gholamhosseinian *et al*., 2014; Esmaeili, 2006). Whereas, Rasuli *et al*. (2015) studied conventional radiology devices in selected hospitals of Khuzestan province, Iran and observed that all the devices measured were in line with the acceptable limit.

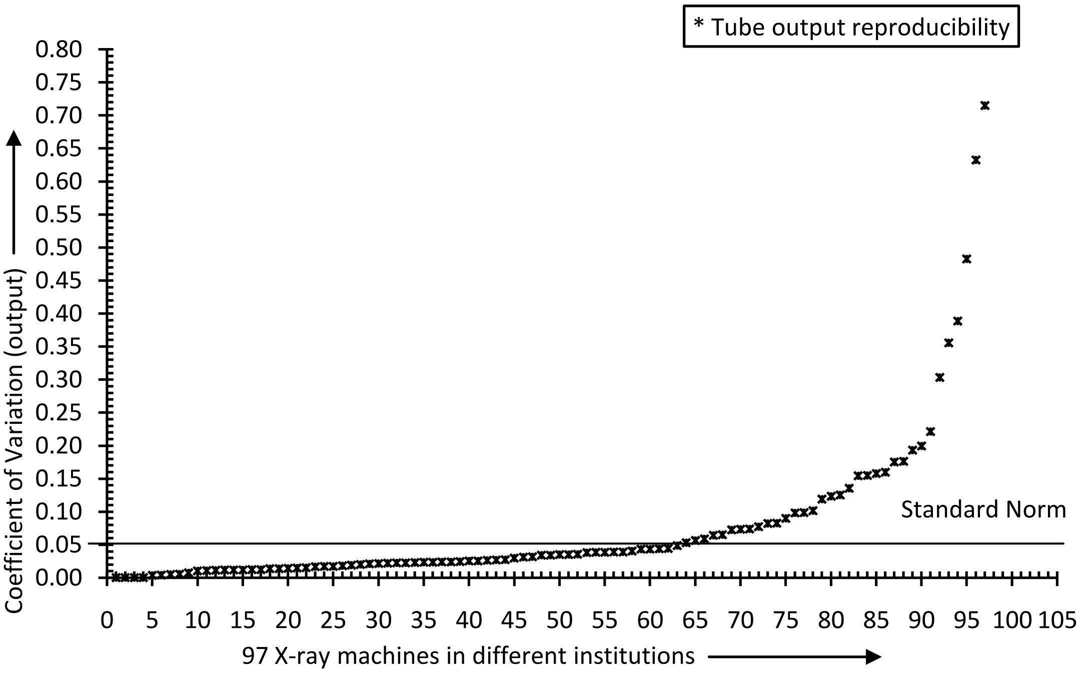

Fig. 4.1.3: Tube output reproducibility for 97 conventional diagnostic X-ray machines (accepted at <0.05 or ±5%)

4.1.4 Tube Output (70 kV at FDD=100cm)

The tube output at 70 kVp (table dose) was measured from 97 conventional diagnostic X-ray machines, 90 (92.8%) units had table doses beyond 43 µGy/mAs–

52 µGy/mAs (Fig. 4.1.4). Only 7 (7.2%) machines were within acceptable limits. It was observed that some of the machines had table doses as high as 236.8 µGy/mAs. This may increase patient dose as well as workers dose through primary and scattered radiation. The X-ray generator that produced only 1.57 µGy/mAs table doses was also observed. In this situation, repeated exposure due to under exposure may occur. To compensate this, radiation worker required increase in the input parameters, which may increase stray radiation. Further, repeated exposure is time consuming and expensive for the patient and workers. Simultaneously, 92.8% X-ray machines table dose were out of the standard limit whereas in the previous study of conventional radiology devices in selected hospitals of Khuzestan province, Iran by Rasuli *et al.* (2015) 46.7% were out of the acceptable limit.

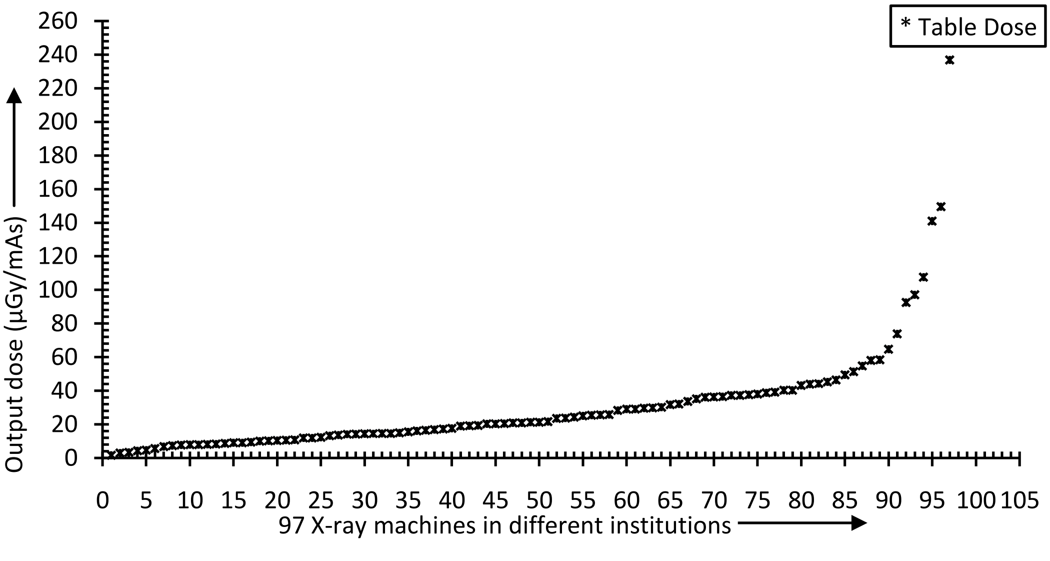

Fig. 4.1.4: Tube output/table dose (kV=70) for 97 conventional diagnostic X-ray machines (to be in the range 43−52 µGy/mAs)

4.1.5 kVp Accuracy

Voltage accuracy measured from 97 conventional diagnostic X-ray machines showed 87 (89.7%) units having coefficient of variation beyond ±0.05 or 5% (Fig. 4.1.5), with only 10 (10.3%) units recording variation within acceptable limits. However, in the previous study 11%−59% intolerance were found in different regions of the world (Kharita *et al*., 2008; Rasuli *et al*., 2015; Sonawane *et al*., 2010; Jomehzadeh *et al*., 2016; Khoshbin *et al*., 2013; Asadinezhad *et al*., 2017; Neofotistou *et al*., 1995; Saghatchi *et al*., 2006; Gholamhosseinian *et al*., 2014; Esmaeili, 2006; Bosnjak *et al*., 2008; Sungita *et al*., 2006). High variations in the incoming line voltage of the generator could be caused by fault in high voltage cables and problems with the auto-transformer circuit (Hasemi *et al*., 2019). It may be important to note that peak kilo-voltage accuracy as well as its measurement can be affected by tube filtration and mAs errors of the X-ray machine (Operator manual kVp meter, 2006).

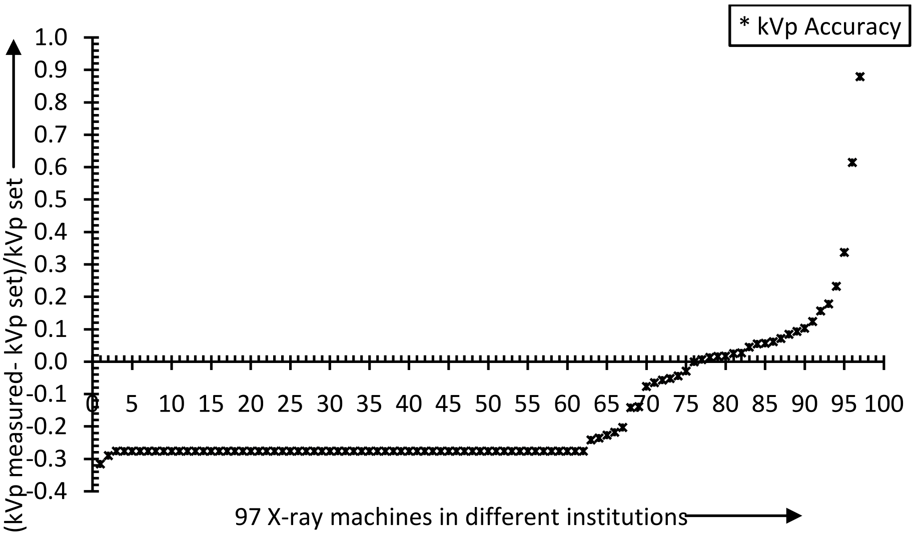

Fig. 4.1.5: Voltage accuracy for 97 conventional diagnostic X-ray machines (to be within ±0.05 or ±5%)

It is observed that the present study appears to have more problems regarding X-ray generators than previous studies. These faults may be due to several reasons; firstly, due to lack of regular quality assurance tests in the past years. For most of the X-ray machines, this survey was the first quality assurance test as per AERB guidelines. Secondly, some of the X-ray machines were old and used without proper maintenance (records) for long periods of time. At least, 28% were installed more than ten years ago. Thirdly, in peak hour, the X-ray machines do not receive its required power supply and in some areas, the power supply voltages were found to be less than 150 V instead of 220 V, in the present study area. Faults in linearity of time, linearity of current, output reproducibility, kVp reproducibility can cause repeated exposure which in turn increases the radiation dose, cost of imaging and duration of imaging. Hassan *et al*. (2012) reported from the 'study of quality assurance of diagnostic X-ray machines and assessment of the absorbed dose to patients' that the total absorbed dose delivered to different organs depends mainly on the X-ray generators.

4.1.6 Essential Safety Parameters

Sixteen important safety parameters assessed by observation and interview, revealed that none of the facilities had performed a regular quality assurance test since installation. In addition to that, 98.7% X-ray machines did not receive proper quality assurance test as recommended by the regulatory body i.e., Atomic Energy Regulatory Board (AERB) in India (AERB format for QA). Concerning PED, only 1.9% installations employed lead-lined PED and the rest used typical wooden door, plywood-lining door, plane-sheet lining door. Of 154 X-ray machines, 46.8% were operated without any protective barrier. In addition, 61.7% installations were equipped with lead aprons.

Regarding PMS, only 11.7% maintained and used PMS properly while 83.1% machines were operated without PMS. Only 15.6% had working warning lights outside the X-ray rooms or patient waiting areas. Also, 92.2% of the facilities recorded repeated examination due to over/under exposures, spoiled films and patient movement. Results obtained for some other important parameters which affect both the quality of the image and safety of the population, are presented in the following table 4.1.6.

Table 4.1.6: 16 important safety parameters in diagnostic X-ray installations

Sl/ No.	Parameters	Variables	No of Units	PCT (%)
1.	Types of X-ray (155 X-ray machines)	1. Fixed X-ray	046	29.7
		2. Mobile-Fixed X-ray	102	65.8
		3. Mobile X-ray	007	04.5
2.	Frequency of QA (155 X-ray machines)	1. Regular	000	0
		2. Once	002	01.3
		3. Never	153	98.7
3.	PED (155 X-ray machines)	1. Lead lining	003	01.9
		2. No lead lining	145	93.6
		3. No door	007	04.5
4.	Protective barrier (154 X-ray machines)	1. With lead glass	057	37.0
		2. Without lead glass	025	16.2
		3. No barrier	072	46.8
5.	Waiting area	1. Away from PED	131	85.1

	(154 X-ray machines)	2. Near PED	020	13.0
		3. Inside	003	01.9
6.	Chest stands (154 X-ray machines)	1. Away from PED & window	132	85.7
		2. Near PED	012	07.8
		3. Near window	010	06.5
7.	Warning lights (154 X-ray machines)	1. Available & working	024	15.6
		2. Available but not working	002	01.3
		3. Not available	128	83.1
8.	PMS (154 X-ray machines)	1. Available & used	018	11.7
		2. Available but not used	008	05.2
		3. Not available	128	83.1
9.	Lead apron (154 X-ray machines)	1. Available & used	081	52.6
		2. Available but not used	014	09.1
		3. Not available	059	38.3
10.	Gonad shielding (154 X-ray machines)	1. Available & used	007	04.6
		2. Available but not used	000	0
		3. Not available	147	95.4
11.	Dark room (154 X-ray machines)	1. Computed radiography	035	22.7
		2. Completely dark	111	72.1
		3. Partial dark	008	05.2
12.	Repeated exposure (154 X-ray machines)	1. Mostly	002	01.3
		2. Sometimes	142	92.2
		3. Never	010	06.5
13.	Repetition reason (155 X-ray machines)[a]	1. Over/under exposed	080	34.9
		2. Film spoil	033	14.4
		3. Patient movement	116	50.7
14.	Collimator bulb (152 X-ray machines)	1. Available & working	129	84.9
		2. Available but not working	011	07.2
		3. Not available	012	07.9

15.	Field size knob (154 X-ray machines)	1. Available & working	141	91.6
		2. Available but not working	004	02.6
		3. Not available	009	05.8
16.	Personnel (154 X-ray machines)	1. Qualified	143	92.9
		2. Not qualified	001	00.6
		3. Not available	010	06.5

[a] percentage was calculated from 229 because some installations were found to have one or more problem simultaneously

From the records of 16 essential safety parameters, it is very clear that majority of the institutions in the present area are not following the installation guidelines laid down by several regulatory bodies. Improper quality control programs in the past years may be another reason behind such poor results. This situation increases the risk of radiation effects to the patients, public and radiation workers as these parameters directly or indirectly concerned with radiation protection. Further, the negative impact may be under utilization of expensive equipment and less cost-effective of health care services. The authors recommend that proper quality control must be implemented immediately by monitoring each and every diagnostic X-ray installation frequently throughout every year. Hashemi *et al*. (2019) reported that implementation of quality control program on a regular basis in medical diagnostic radiology is essential to reduce X-ray machine malfunctioning and produce high quality diagnostic images with the lowest radiation dose to the patient.

There are few limitations which are to be noted from the present study; first, some of the equipment cannot be operated due to insufficient power supply and few machines were operated at low input power which may affect the X-ray machine output. Second, due to fixed control console switches, few machines cannot be studied at certain input parameters. Third, from the present study, the authors could not clarify all the possible reasons for such defects and were unable to repair those machines as well.

4.2 Qualitative study of mechanical parameters of conventional diagnostic X-ray machines in Mizoram, India

4.2.1 Half Value Layer

Among the mechanical characteristics of X-rays, the HVL is one of the most important parameters that affect both the quantity and quality of the X-ray output (Gray, 1983). HVL is the amount of Al required to reduce the intensity of radiation to one-half of its original value, at a fixed kVp and mAs (Papp, 2015). HVL thickness is measured to guarantee that the permanently installed filter on the X-ray tube is maintained to minimize patient exposure (Gray, 1983). This is the best way to determine if adequate filtration exists, as it is otherwise difficult to measure. At the same time, the addition of a filter for a fixed input parameter has a very small effect on high energy X-rays but removes soft X-rays from the beam. The softer X-ray components are almost completely removed by heavy filtration and the radiation transmitted approaches monochromy (Johns and Cunningham, 1983). Most of the softer X-rays are not transmitted through the patient to form an image, but are absorbed by the patient. Increasing the HVL decreases the patient dose (Papp, 2015). However, the extra filtration eliminates suitable beams and a higher tube load is necessary to reach the desired output; this increases the stray radiation rate (Asadinezhad, 2017).

A graph between the transmission percentage of the X-rays and the thickness of the added Al filter was plotted for each unit as shown in Fig. 4.2.1 (a). The curves were found to be non-linear, as the X-ray beam originating from the diagnostic X-ray unit was not mono-energetic. Each layer of the attenuator (Al) acts as a successive filter and gradually changes the quality and the quantity of the beam. However, under heavy filtration, the softer component of the X-ray beam was almost completely removed due to absorption and scattering by the Al-atoms. The transmitted X-rays were nearly monochromatic and the attenuation curve tended to approach a straight line (Johns and Cunningham, 1983). Most of the attenuation curves displayed exponential behavior and there is a finite chance that some incident photons pass through a filter of any thickness with no interaction (Turner, 2005). The authors observed some irregular exponential curves as shown in Fig. 4.2.1 (a); there were several reasons for the sharp corners. The primary reason was the output inconsistency of different X-ray machines as depicted in Fig. 4.1.3, 35.05% units showed an output coefficient of variation > 0.05. 20.62% units had an output coefficient of variation higher than 0.1 and it was as high as 0.72 as shown in Table 4.2.1 (a), the mean of coefficient of variation for output was 0.08±0.12 SD. Moreover, a few institutions installed X-ray facilities in small rooms where scattered radiation could not be avoided by any experimental set-up and may affect the HVL measurement (Johns and Cunningham, 1983).

Table 4.2.1 (a): Output consistency (coefficient of variation) of 97 X-ray units

Parameter	N	Range	Minimum	Maximum	Mean	S.D.
Output consistency	97	0.72	0.00	0.72	0.08	0.12

Table 4.2.1 (b): Total filtration of 97 X-ray units

Parameters	N	Range	Minimum	Maximum	Mean	S.D.
Total filtration	97	3 mm Al	0.5 mm Al	3.5 mm Al	1.43 mm Al	0.80 mm Al
Age	97	44 years	<1 year	44 years	8.38 years	7.72 years

The HVL thickness at 70 kV was recorded from each curve. The measured value was supposed to be larger than the actual value, as already mentioned, the arrangement was not a narrow beam. From these HVL values, the total filtration for each equipment was derived using a conversion table (NCRP, 1989). The maximum value of the total filtration was 3.5 mm and the minimum was 0.5 mm as shown in Table 4.2.1 (b). These filters significantly minimized the patient dose by filtering soft X-rays that increase the patient dose but do not contribute to image formation (Papp, 2015; Johns and Cunningham, 1983). The filter not only reduced the primary radiation dose, but also scattered dose considerably (Vlachos *et al*., 2015). Out of 97 conventional X-ray units, 27.83% passed and 72.17% failed the test, as per the AERB safety code (AERB, 2001). However, according to international standards, only 15.46% of the equipment did not require filter correction as depicted in Fig. 4.2.1 (b) (IAEA, 2014; Health Canada, 2008; Euratom radiation protection no. 91).

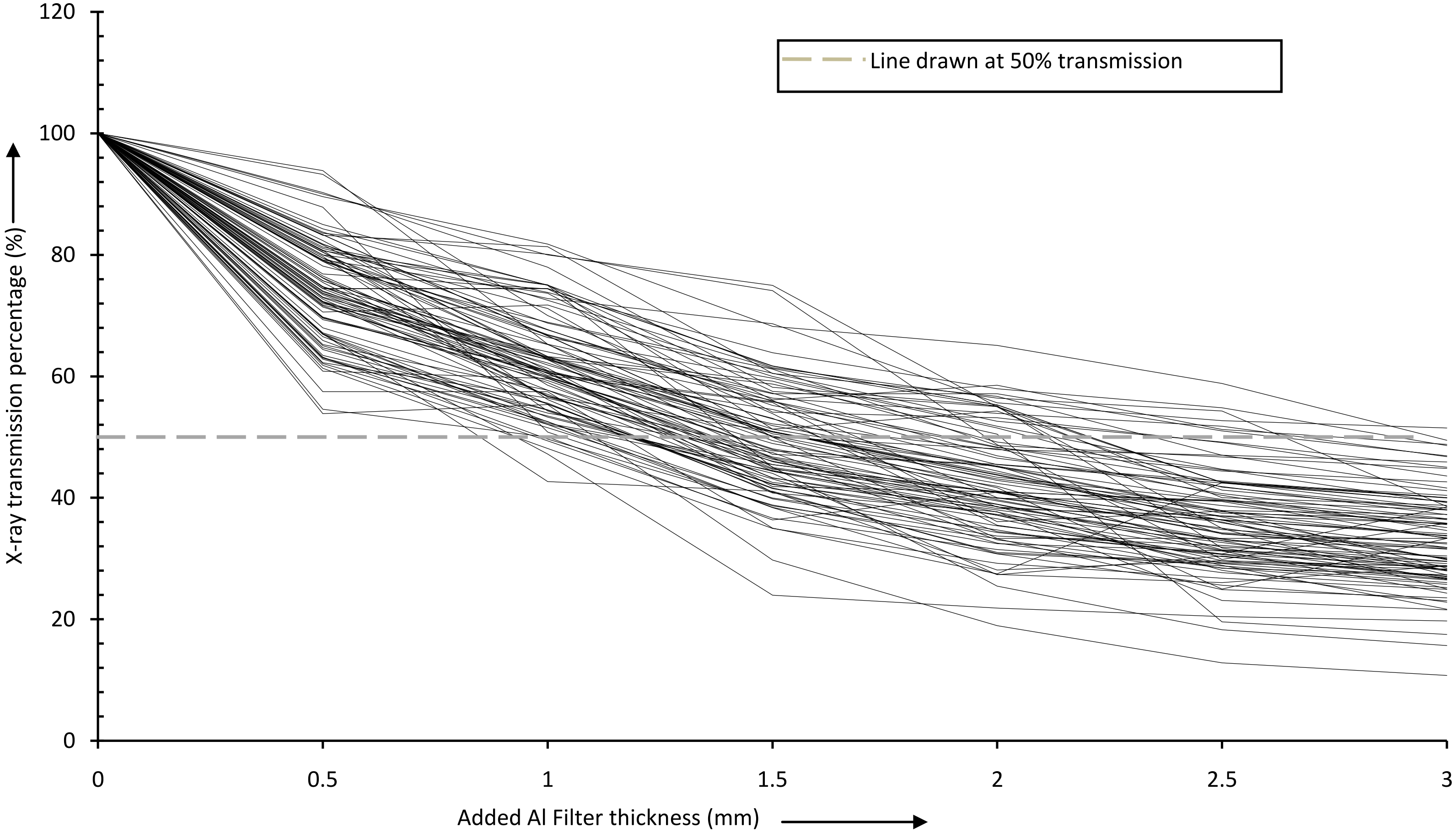

Fig. 4.2.1 (a): Attenuation curves of 97 diagnostic X-ray machines; an Al filter as attenuator at input tube voltage 70 kVp

The calculated mean for the total filtration at the different installations was only 1.43±0.80 SD mm Al, as shown in Table 4.2.1 (b). It appears that most units had insufficient filter, although the mean X-ray tube age was 8.38±7.72 SD years. However, an absence of proper, frequent quality assurance testing seems to be the primary reason for the insufficiency. Furthermore, in a study of the accuracy of output kVp, the authors found that only 23.71% were within ± 10 kV, while others were out of ± 10 kV, as detailed in Fig. 4.1.5. We measured kVp accuracy before studying HVL, but we did not adjust or modify it. As the quality of the X-rays fully depends on the accelerating potential, it can directly affect the HVL thickness and filtration as well (AAPM, 1988).

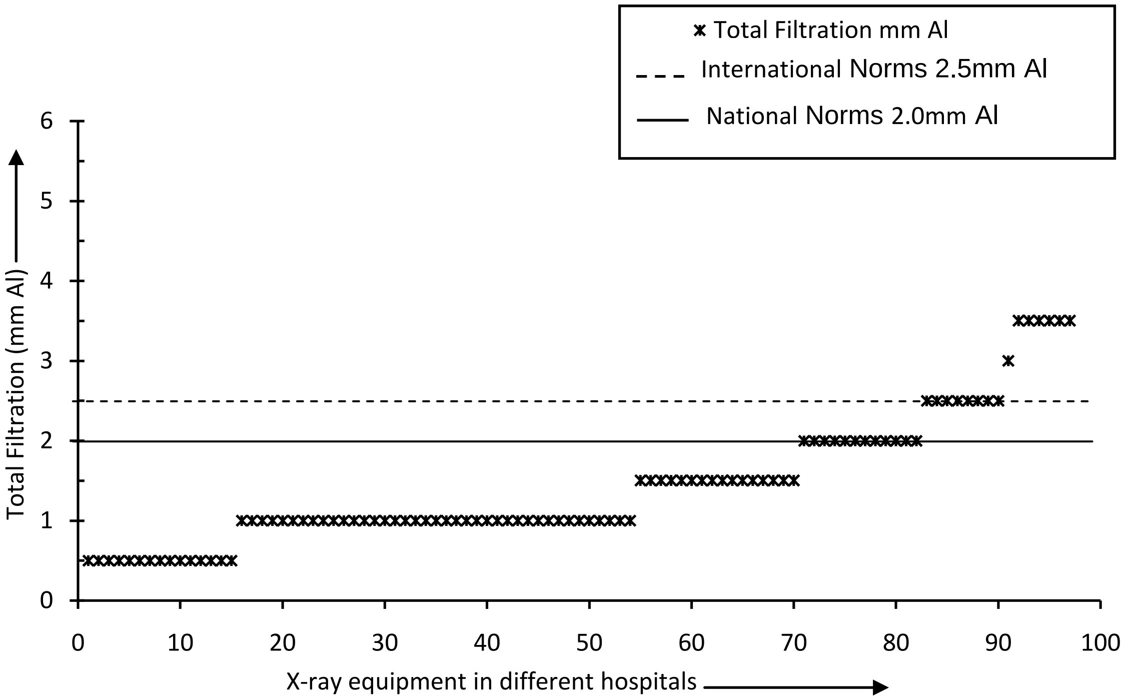

Fig. 4.2.1 (b): Total filtration of 97 X-ray machines; measurement were done at 70 kVp

4.2.2 Congruency between optical field and radiation beam

The purpose of congruency between the X-ray beam and the optical/light field study was to ensure that the light field and X-ray field were properly aligned (Gray *et al.*, 1983). In a clinical environment, it is important to ensure reproducibility from image to image and for the facility to collimate ionizing radiation as much as possible, per the ALARA principle. The radiation produced by diagnostic X-ray machines is invisible to the human eye. Therefore, a collimator-visible light is the only indicator that allows the radiation technician to visualize the location and size of the X-ray field. Visualization of the X-ray field is achieved by a mirror reflecting the light from a light bulb. The bulb position is adjusted so that the reflected light appears to have the same origin as the focal spot of the tube (IAEA, 2014). It is important to assess the congruency between them, as the beam must be aligned to the Bucky tray to avoid anatomy and grid cut-offs.

Among 135 conventional X-ray machines, 32 mobile X-ray machines had circular fixed collimators; the optical light field of 4 X-rays did not work; and 6 types of equipment had non-adjustable collimators. This is because the collimators were being maintained in a permanently fixed position. The authors also found that 8 units were not maintained in a darkroom, 14 units were out of order and 24 units were condemned (Table 2). Due to these constraints, only 47 units were in a ready-to-study condition.

The congruency misalignment of the x-axis varied between 0.50% and 15.30 % of the SID; the congruency of the y-axis varied between 0.50% and 10.90% of

SID (Table 4.2.2). When compared with the safety standards, the x-axes of 32 units were found to be beyond the acceptable limit, whereas only 15 were within the acceptable limit. For y-axis, only 11 of 47 units were within the safety limit as depicted in Fig. 4.2.2 (a) (Gray *et al.*, 1983; Papp, 2015; Euratom radiation protection no. 91). The calculated means for the x and y-axes were 3.78±2.54 SD % and 3.69±2.25 SD % of SID (Table 4.2.2). When considering a whole axis (x and y), 38 of 47 (80.85%) units were outside the acceptable limit. Due to this problem of congruency, radiation workers cannot escape radiation when opening the collimator fully, as previously mentioned. The amount of unwanted primary and secondary radiation increases enormously when opening the collimator fully and the patient and radiation worker dose increases rapidly. In some diagnostic centers with severe misaligned units as shown in Fig. 4.2.2 (b), technicians fully opened the collimator and did not use optical light. Moreover, if the technicians are not mindful of protection issues, the practice may result in an unreasonable increase in the patient dose (Paolicchi *et al.*, 2016).

Table 4.2.2: Congruency between the radiation beam and the optical field of 47 X-ray machines

Congruency	N	Range (% of SID)	Minimum (% of SID)	Maximum (% of SID)	Mean (% of SID)	S.D. (% of SID)
x+x'[a]	47	14.80	0.50	15.30	3.78	2.54
y+y'[b]	47	10.40	0.50	10.90	3.69	2.25
x+x'+y+y'[c]	47	17.90	1.50	19.40	7.47	3.56

[a] total misalignment of both x and x'-axis

[b] total misalignment of both y and y'-axis

[c] total misalignment of all the four axes

Six X-ray units included in the present study were installed in 2015, of which 5 were outside the acceptable limit. This showed that newly installed units also have congruency problems and according to certain bodies, these units require proper, frequent quality checks and maintenance by a service engineer (AERB, 2006) (Fig. 4.2.2 (c)). Out of the 9 units that did not meet the safety standard, 8 were AERB approved. However, of the 38 acceptable units, 28 (73.68%) were AERB approved units and 10 (26.32%) had an unknown approval status due to the lack of information about old machines. Sungita *et al.* (2006) studied 196 diagnostic X-ray units in Tanzania; the accuracy of beam alignment and collimation of 80 units were tested. In their study, 60% of the units passed the tests. In 2010, Sonawane *et al*. reported that 77% of 118 medical diagnostic X-ray machines were within the safety limits from the study of radiological safety status and quality assurance audit of medical X-ray diagnostic installations in India. In comparison to those findings the current situation of the present study area was far behind.

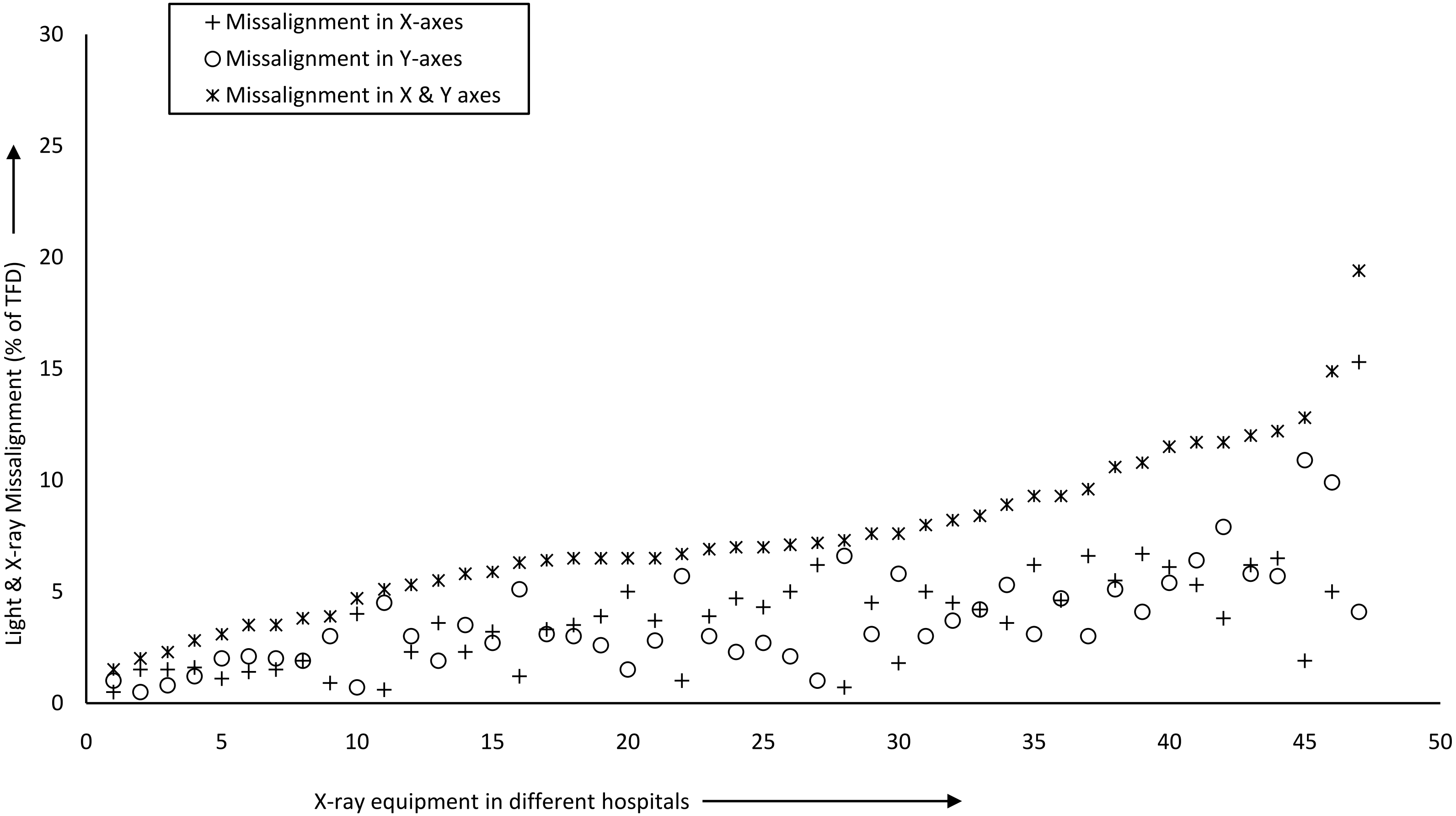

Fig. 4.2.2 (a): Misalignment between the optical light and the X-ray beam of 47 X-ray units

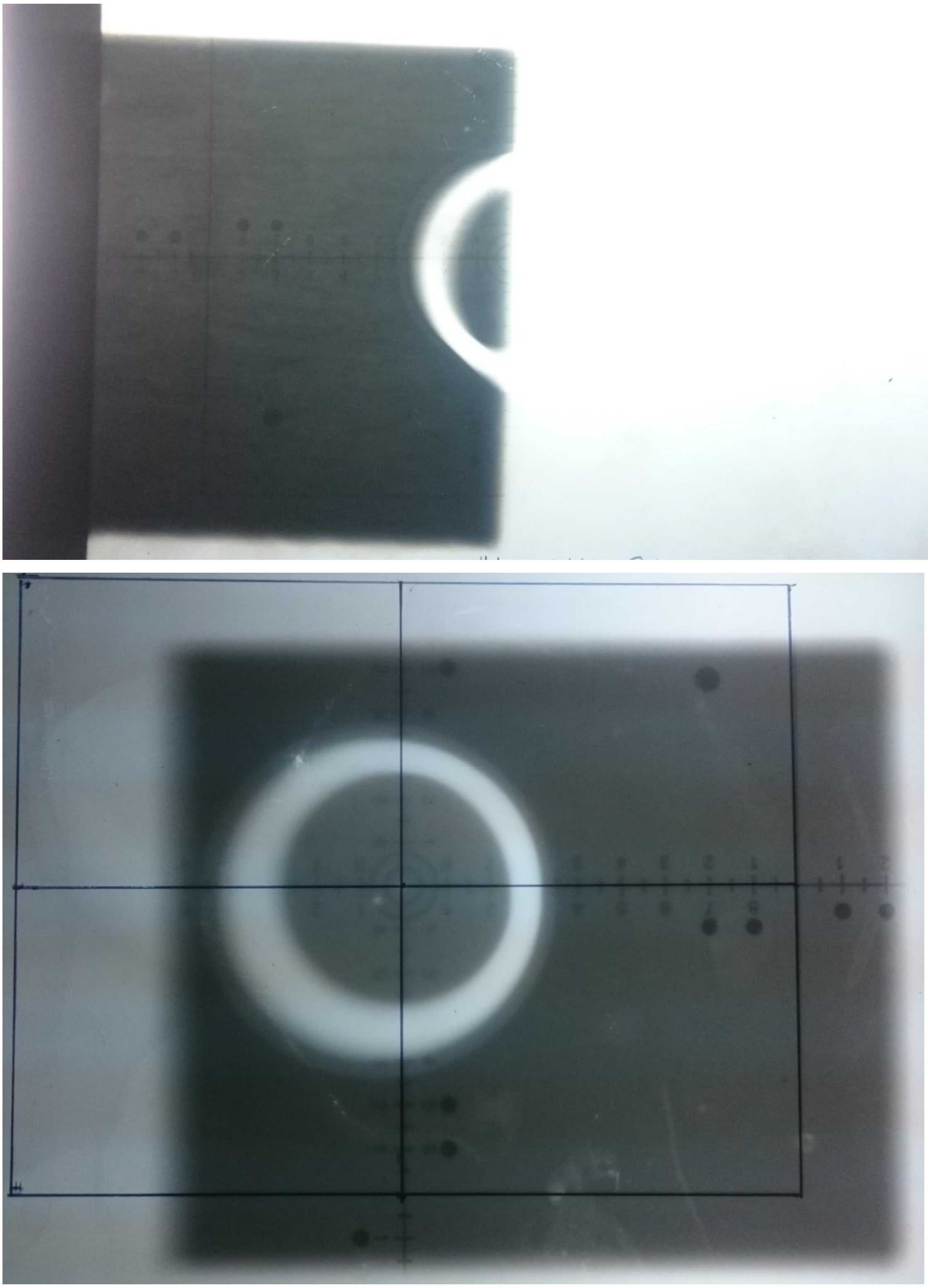

Fig. 4.2.2 (b): Misalignment between the radiation beam and the optical field from the present study

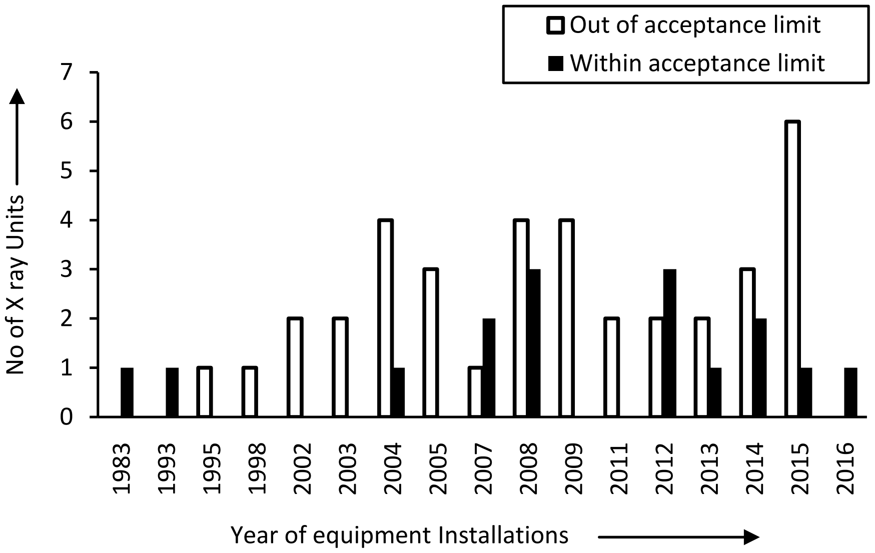

Fig. 4.2.2 (c): Relationship between the year of installation and congruency misalignment

4.2.3 Perpendicularity of the Central Beam and Image Receptor

Assessment of the perpendicularity between the central X-ray beam and the image receptor should be emphasized, as perpendicularity minimizes image distortion, which improves the representation of the anatomy in question. Optical field and X-ray radiation field misalignment may be caused by shifts in the relative positions of the light bulb filament and anode focal spot. Such shifts are caused by differences between light bulbs, changes in the mirror position or shifts in the collimator position on the tube head (AAPM, 1981).

The authors performed perpendicularity measurements on 53 X-ray units; 6 types of equipment with non-adjustable collimators were studied (Table 2). Of the X-ray units with misalignment of less than 1.5 degrees, 30.19% were within the acceptable limit. There were 37 units with misalignment > 1.5 degrees. According to the safety code, 69.81% were outside the acceptable limit as shown in Table 4.2.3 (a)

(Euratom radiation protection no. 91; Sungita *et al.*, 2006). Even for new X-ray units (Fig. 4.2.3), the authors found problems pertaining to congruency between light and radiation, and perpendicularity between the central beam and the image receptor. Of the 7 X-ray units installed in 2015, 6 had problems with beam alignment perpendicularity. Of the 16 units that were within tolerance, 14 were AERB-approved units and 2 were unknown. Of the 37 acceptable units, 27 (72.97%) were AERB approved and 10 (27.03%) were unknown. Owing to problems in perpendicularity, the radiographer often repeats imaging which doubles the dose received. Once again, to minimize the associated radiation risk and maximize the benefit of medical examination, unnecessary radiation exposure should be eliminated (Huda, 2015).

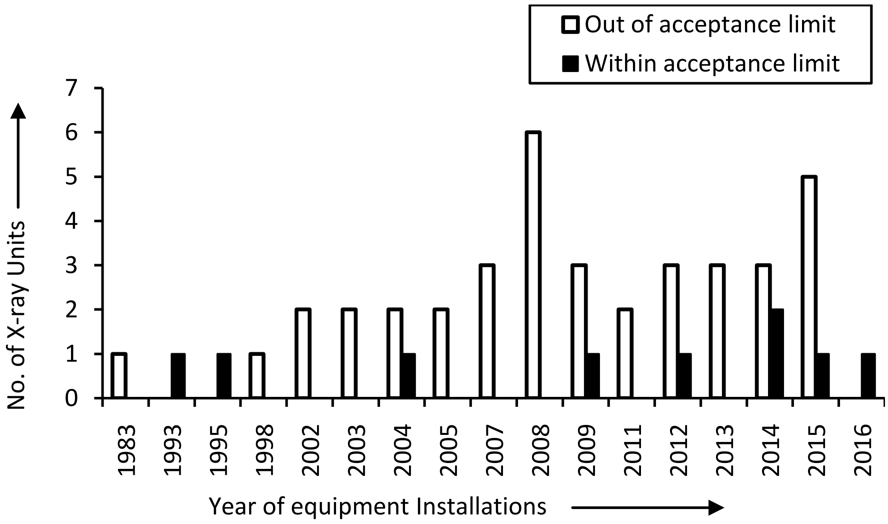

Fig. 4.2.3 Relationship between the year of installation and the perpendicularity of the central beam

Table 4.2.3 (a): Angle between the central X-ray beam and image receptor of 53 X-ray units

Fault in perpendicularity	0.5°	0.5°-1.5°	1.5°-3°	3° above
No. of X-ray units	5	11	17	20

Table 4.2.3 (b) shows different X-ray manufacturers and their congruency and perpendicularity statuses. Among the different manufacturers, ME X-ray Pvt., Ltd. contributes 34.04% in congruency study and 39.62% in the perpendicularity study. At the same time, 87.50% and 61.90% of ME X-rays were outside the acceptable limits of congruency and perpendicularity, respectively.

Table 4.2.3 (b): Status of the congruency and perpendicularity of different manufacturers of diagnostic X-ray units

Manufacturer	Congruency			Perpendicularity		
	Within Tolerance (%)	Out of Tolerance (%)	Total	Within Tolerance (%)	Out of Tolerance (%)	Total
M.E. X-ray(India) Pvt. Ltd.	12.50	87.50	16	38.09	61.90	21
M/s. Siemens Ltd.	16.67	83.33	6	33.33	66.67	6
M/s. Squarem Systems Pvt. Ltd.	20.00	80.00	5	40.00	60.00	5
M/s. Philips Electronics India Ltd.	0.00	100.00	5	0.00	100.00	5
M/s. Wipro GE Healthcare Pvt. Ltd.	75.00	25.00	4	25.00	75.00	4
Allengers Medi Sys	66.67	33.33	3	75.00	25.00	4
Others	0.00	100.00	8	0.00	100.00	8

Total	19.15	80.85	47	30.19	69.81	53

4.3 Evaluation of radiation doses at diagnostic X-ray CPs and outside PEDs in Mizoram, India

4.3.1 Exposure rates at CP for both couch and chest missions

The CP of different X-ray machines were located at different distances from the couch and chest stand. It was observed that 94.29% of CPs were within 300 cm for couch missions and 68.25% were so for chest missions. This is in contrast to the recommended distance, which should be more than 300 cm (AERB, 2001). The stray radiation measured at the CPs was mostly scattered and originated from two main sources: the phantom on the couch and the one on the chest stand. Exposure rates at the CPs in different installations varied from 0.01−360 mR/h in couch missions and 0.03−280 mR/h in chest missions as depicted in Fig. 4.3.1 (a) and (b). For couch missions, 32 CPs were properly protected by barriers, whereas 14 were partly covered by barriers and 24 had none. For chest missions, 29 CPs were properly protected by barriers from stray radiation, whereas 15 were partly covered by barriers and 19 had no barriers at all. For the couch and chest missions where CPs were properly covered by barriers, significantly lower exposure rates were found for different units. By contrast, installations with partial or absent barriers showed very high exposure rates: 50 times more than cases with CPs properly covered with barriers as given in Table 4.3.1.

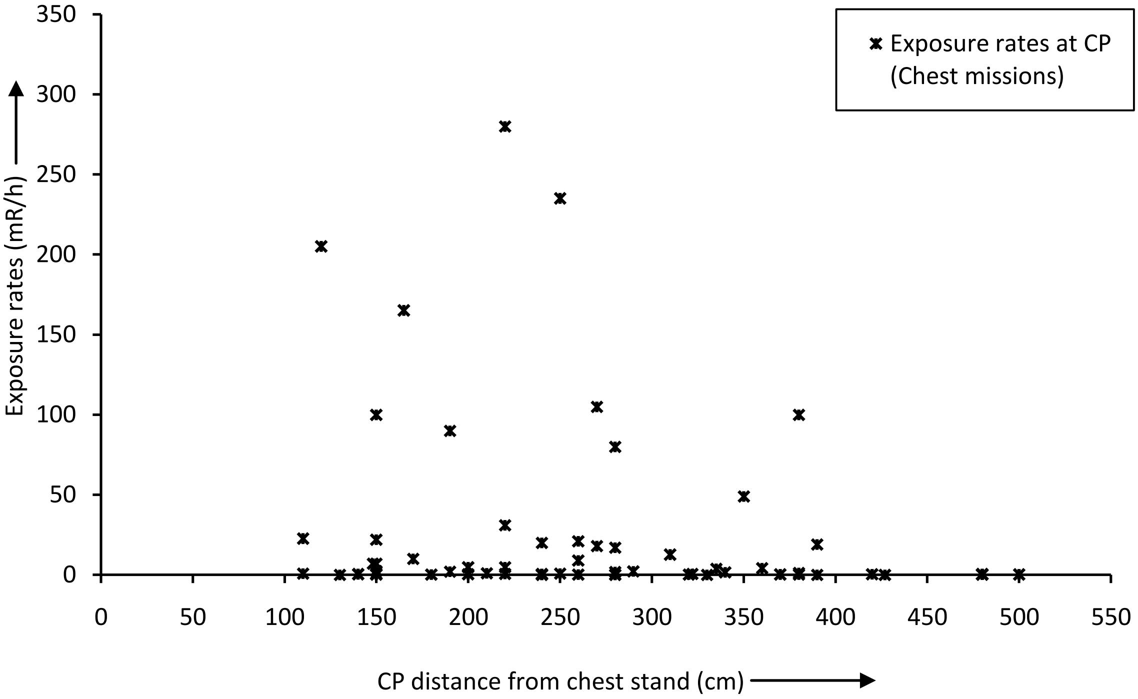

Fig. 4.3.1 (a): Exposure rates measured at CPs for chest missions

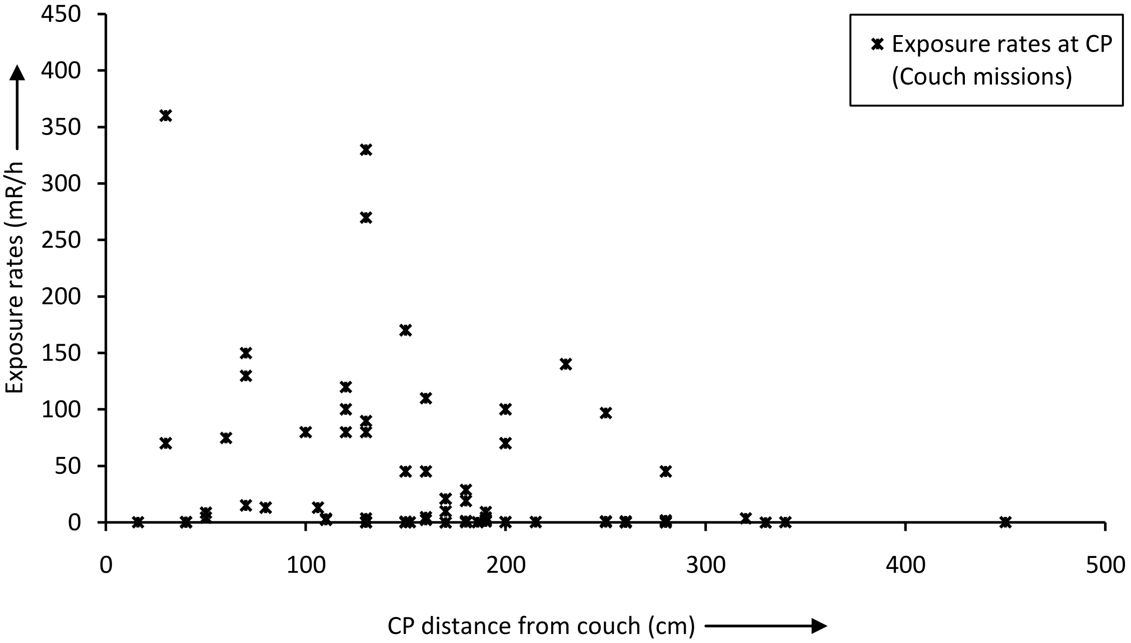

Fig. 4.3.1 (b): Exposure rates measured at CPs for couch missions

Table 4.3.1 Exposure rates measured at CPs behind different arrangements of protective barriers at different installations

Barrier	No. of machines	Min. exposure rates(mR/h)	Max. exposure rates(mR/h)	Range (mR/h)	Mean (mR/h)	S D (mR/h)
Chest Mission						
Covering CP properly	29 (46.03%)	0.03	9	8.97	0.92	1.79
Not covering CP properly	15 (23.81%)	0.05	280	279.96	63.85	81.76
Not available	19 (30.16%)	0.03	235	234.98	35.79	64.95
Couch Mission						
Covering CP properly	32 (45.71%)	0.007	19	18.99	1.74	3.71
Not covering CP properly	14 (20%)	2.4	330	327.6	94.79	97.67
Not available	24 (34.29%)	0.25	360	359.75	65.87	81.45

4.3.2 Comparison between different utilization of CP barriers

The exposure rates for chest missions in installations with CPs properly covered by a protective barrier, CPs with insufficient covers and those with no barriers at all are shown in Fig. 4.3.2 (a). The CPs that were fully covered by protective barriers had relatively negligible exposure rates (i.e., 0.03–9 mR/h with mean±SD of 0.92±1.79 mR/h). Contrastingly, installations in which the CPs were not properly covered had relatively high exposure (0.05–280 mR/h with mean±SD of 63.85±81.76 mR/h). Furthermore, it was found that the exposure rates at CPs where barriers were absent ranged from 0.03–235 mR/h with mean±SD of 35.79±64.95

mR/h (Table 4.3.1). There were institutions that showed low exposure rates, but they had no barriers installed. These types of equipment were mobile-fixed devices with low electronic input parameters and were lower-efficiency units (Fig. 4.3.2 (a)). By comparing the exposure rates at institutions without barriers and with inadequate barriers covering the CPs for chest missions, barriers that did not properly cover CPs had relatively high exposure rates as given in Table 4.3.1. The reason was that, for barriers not covering CPs properly or improperly installed barriers, the operators considered only stray radiation from the couch. For that, they adjusted the barrier. As such, the CPs were fully opened for chest-scattering radiation. In some installations, there were chest stands located adjacent to the CPs. Moreover, for other parameters, such as variation in distance between the chest stand and CP, the generator type may have affected exposure rates.

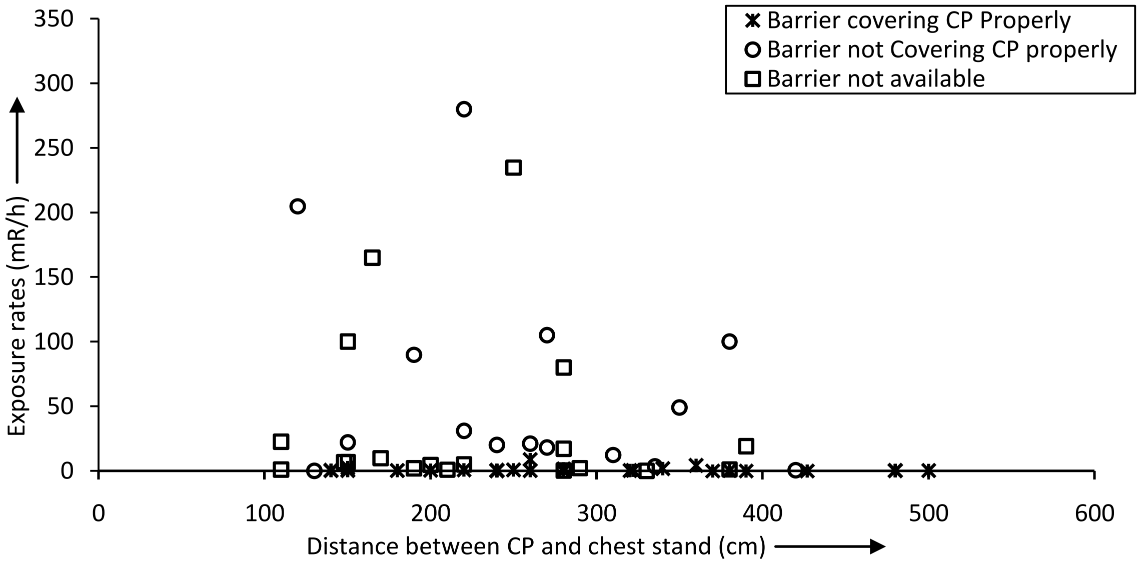

Fig. 4.3.2 (a): Exposure rates measured at CPs for chest missions (comparing different barrier utilizations)

Exposure rates for couch missions in installations covering CPs properly with protective barriers with inadequate CP covers and with no barriers at all are shown in Fig. 4.3.2 (b). For couch missions, the exposure rates for barriers covering the CPs properly varied 0.007–19 mR/h with mean±SD of 1.74±3.71 mR/h. Similar to the chest-mission exposure rates measured at fully covered CPs, these were significantly low. There was not much difference between the exposure rates at CPs with no barriers and those with partial barriers. The former had 0.25–360 mR/h with mean±SD of 65.87±81.45 mR/h, whereas the latter ranged from 2.4–330 mR/h with mean±SD of 94.79±97.67 mR/h (Table 4.3.1). In the present study, the significant effects of distance on the exposure rates were not recognized, even though each piece of equipment was operating with nearly equal parameters. One of the main reasons is that none of the X-ray equipment followed the same installation geometry and even the same models at different institutions showed different efficiencies, such as with kVp reproducibility as shown in Fig. 4.1.5.

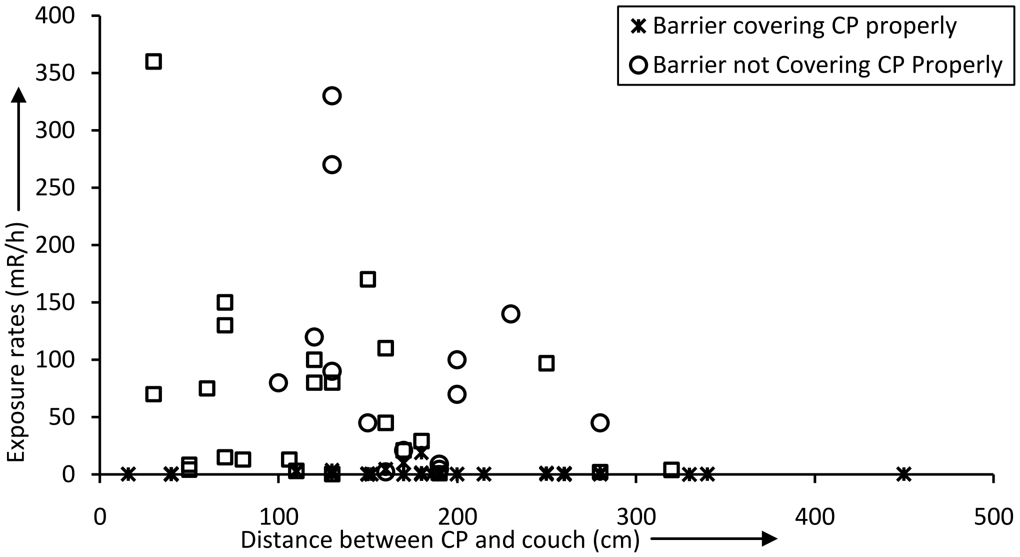

Fig. 4.3.2 (b): Exposure rates measured at CPs for couch missions (comparing different barrier utilizations)

4.3.3 Exposure rates outside the PED for both chest and couch missions

For evaluating public doses, exposure rates outside the PED were measured, where exposure was mainly caused by stray radiation scattered from the phantoms. These were located at different distances from the PED as shown in Fig. 4.3.3 (a) and (b). For chest and couch missions, only two and three installations, respectively, were equipped with lead-lined doors. A large number (>90%) of installations used solid wooden doors, plywood doors, Al plane sheet doors (Table 4.3.3). It was found that all institutions had at least a simple traditional PED. The mean of the exposure rates outside lead-lined PEDs was mean±SD of 0.05±0.04 mR/h and mean±SD of 2.66±2.89 mR/h for chest and couch missions, respectively. Those institutions that did not employ lead-lined doors had a mean exposure rates of mean±SD of 18.16±33.35 mR/h and mean±SD of 24.32±36.94 mR/h for chest and couch missions, respectively. These figures show that lead-lined doors had significantly greater effect on attenuation of the exposure rates compared to the alternatives observed in this study (Table 4.3.3).

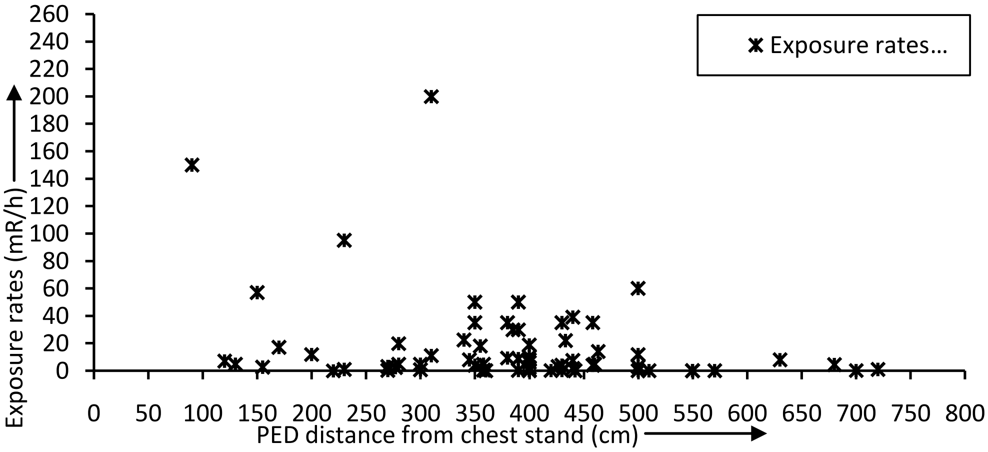

Fig. 4.3.3 (a): Exposure rates measured at the PEDs for chest missions

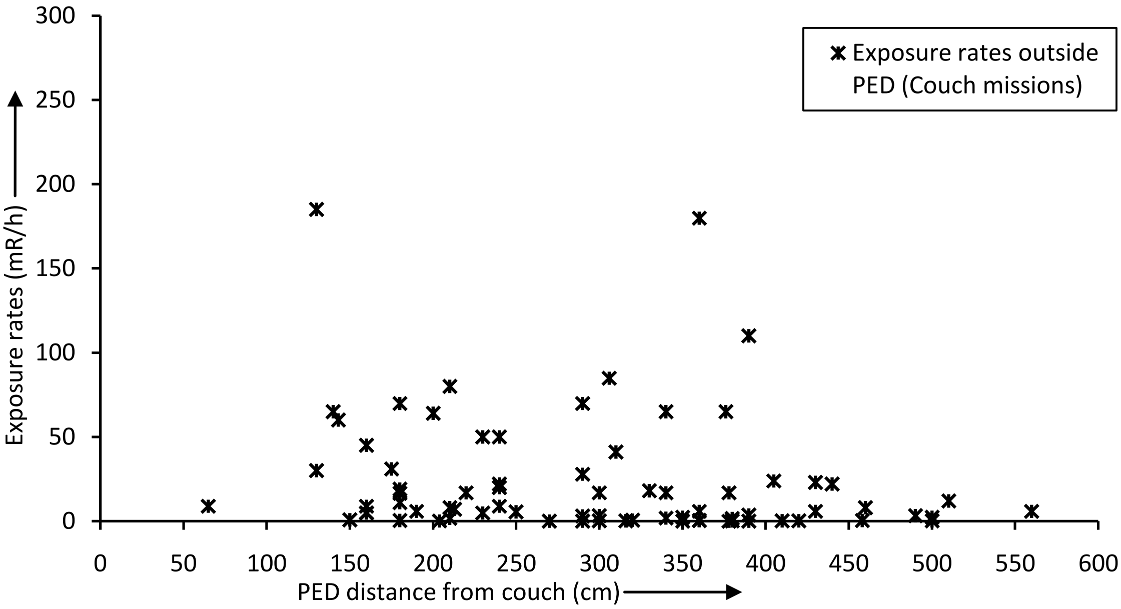

Fig. 4.3.3 (b): Exposure rates measured at the PEDs for couch missions

Table 4.3.3: Exposure rates measured at different types of PEDs in different installations

Type of door	No. of units	Minimum exposure rates (mR/h)	Maximum exposure rates (mR/h)	Range (mR/h)	Mean (mR/h)	S D (mR/h)
Chest Mission						
Lead-lined door	2 (2.9%)	0.03	0.08	0.05	0.05	0.04
No lead-lining	67 (97.1%)	0.001	200	199.99	18.16	33.35
Couch Mission						
Lead-line door	3 (4%)	0.16	5.33	5.17	2.66	2.89
No lead-lining	72 (96%)	0.02	185	184.98	24.32	36.94

4.3.4 Comparison between lead-line PEDs and other typical PEDs

The radiation exposure rates outside PED in installations having lead-lined doors or typical doors for both chest and couch missions are shown in Fig. 4.3.4 (a) and (b). The rates outside the PED for chest missions with lead-lined doors installed were negligibly low (0.08 and 0.03 mR/h). Similarly, for couch missions where lead-lined doors were installed, the rates outside the PEDs ranged from 0.16−5.33 mR/h (Table 4.3.3). These exposure rates show that lead-lined doors are very good shielding materials, which are recommended by a variety of different bodies (AERB, 2001; NCRP, 2004). However, in installations without lead-lining, exposure rates ranged up to 200 mR/h for chest missions to 185 mR/h for couch missions (Table 4.3.3). The high exposure rates in these installations show that alternatives, such as wooden doors, plywood doors and aluminum plane sheets, are not nearly as effective as lead. This was similar to the results for measuring the CP exposure rates. Lower exposure rates were found in few installations where lead-lined doors were not installed. The reason was the same for CP exposure.

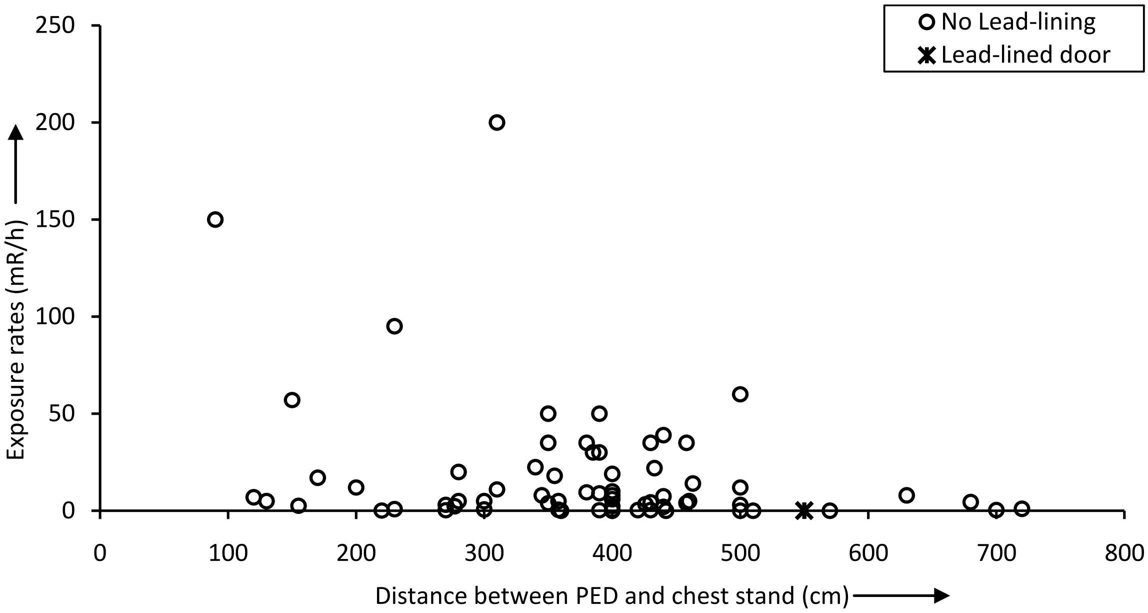

Fig. 4.3.4 (a): Exposure rates measured at the PEDs for chest missions (comparing different barrier utilizations)

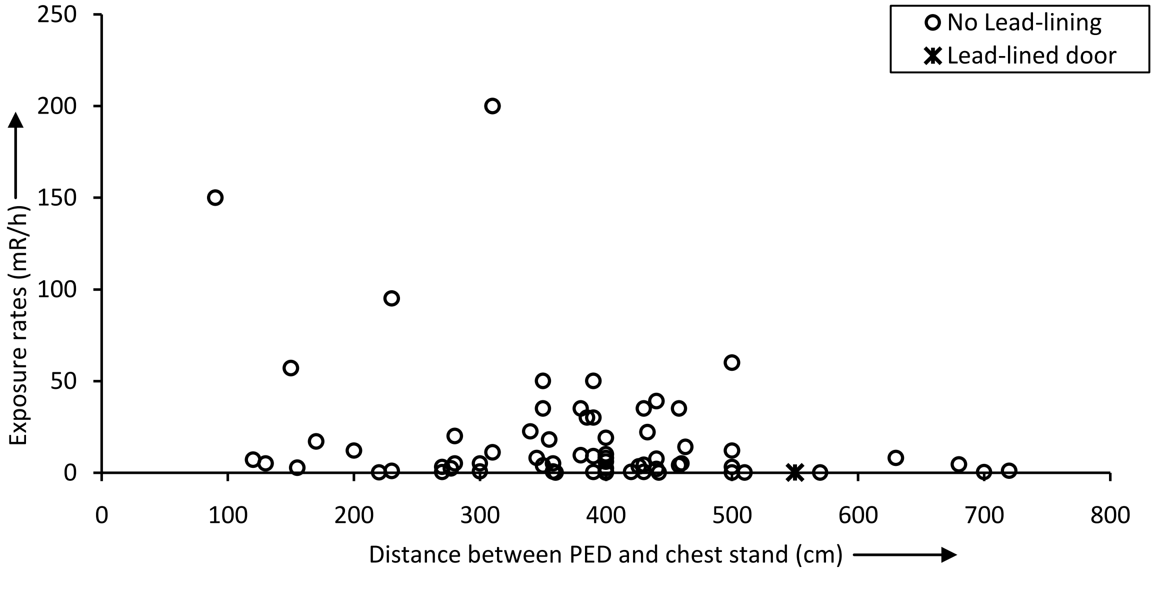

Fig. 4.3.4 (b): Exposure rates measured at the PEDs for couch missions (comparing different barrier utilizations)

4.3.5 Workloads for chest and couch examinations

General diagnostic X-ray examinations are classified as chest, skull, abdomen, pelvic, intravenous pyelogram and extremities. At all institutions, X-ray teams work six days per week. The number of patients examined per day varies amongst institutions. With intravenous pyelograms, 5–6 X-ray films are used, whereas all other examinations use 1 or 2 X-ray film(s). For chest X-ray, the range of 6–50 mAs tube-loading is applied, whereas other examinations use 20–120 mAs, such as when considering table 4.3.5 unit 6, where chest, abdomen, skull and other extremities are examined. For chest X-ray, workload is calculated using Eqn. (25) as follows:

$$W = \frac{1\times1\times25\times6}{60}\text{mA-min/week} \qquad \text{----------------------- (25)}$$

$$= 2.5 \text{ mA-min/week for chest X-ray.}$$

Similarly, other examinations are calculated and summed to get the total workload for a particular installation. The calculated workload shows that the couch workload is greater than that of chest work in almost every institution, because examinations using the chest stands require horizontal projection of the X-ray, whereas all other examinations use vertical projection (Fig. 4.3.5).

Table 4.3.5: Workload of diagnostic X-ray facilities in the present study area

Unit	Patient per day	Film per patient	Tube loading (mAs)	Days per week	Workload (mA-min / week)	Total workload (mA-min/week)	Examinations conducted
5*	1	1	80	6	8	20	Chest
	3	1	40	6	12		Others
6*	1	1	25	6	2.5	20	Chest
	0.2	2	50	6	2		Abdomen
	0.1	1	50	6	0.5		Skull
	3	2	25	6	15		Others
7*	10	1	40	6	40	250	Chest
	5	2	60	6	60		Abdomen
	5	2	45	6	45		Skull
	2	5	60	6	60		IVP
	15	1	30	6	45		Others

*Workload for each piece of equipment was calculated as with units 5, 6 and 7. It can be seen that some diagnostic units examined chest, abdomen, skull, intravenous pyelogram and other extremities, whereas others examined only one, two or more.

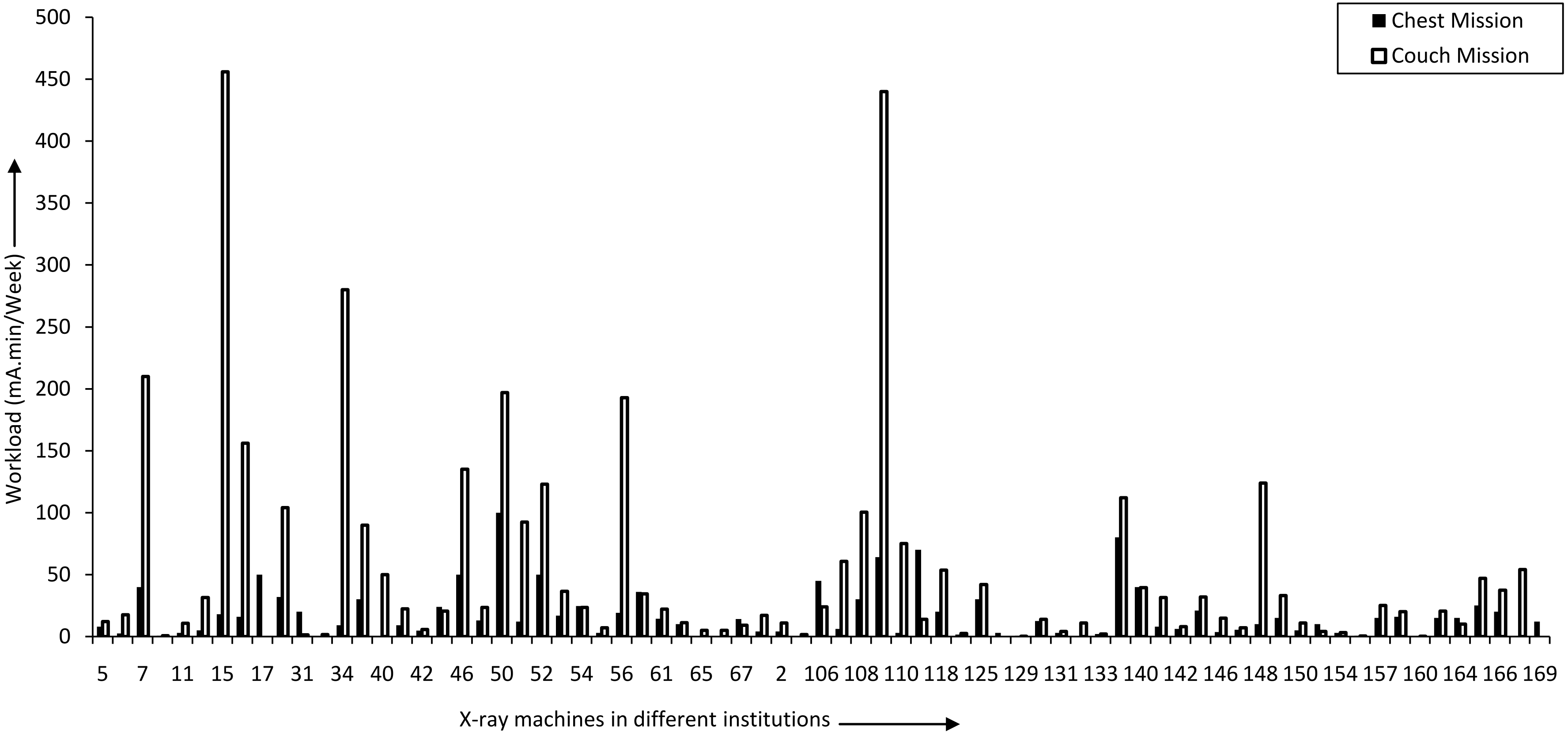

Fig. 4.3.5: Workload of different institutions for both chest and couch examinations

4.3.6 Public and occupational dose levels

Radiation doses calculated as milliroentgen per week at the CPs and outside the PEDs are considered occupational and public doses, respectively. As indicated in Eqn. (24), these doses not only depend on the exposure rates but also on the workload (AERB format for QA). This is why most of the high doses result from high exposure rates and high workloads. However, at a few installations, these two parameters compensated each other. It can be seen from Table 4.3.6 (a) that those installations having high doses had parameters higher than the mean value. Interestingly, some high exposure rates did not always result from high radiation doses, high exposure rates arising from improper barriers, non-protected or unlined doors did not lead to high doses because of low workloads. Some of these were only used for couch missions, whereas others were not used (i.e., there was no workload). Moreover, X-ray units 29, 46 and 52 showed high workloads, but had significantly lower exposure rates because of proper CP covering and lead shielding of the PED. This is why these doses were negligibly low as shown in Table 4.3.6 (b).

Table 4.3.6 (a): Exposure rates and workload for the three highest public and occupational doses

High Public Dose						High Occupational Dose					
Dose (mR/week)		Exposure rates (mR/h)		Workload (mA-min/week)		Dose (mR/week)		Exposure rates (mR/h)		Workload (mA-min/week)	
X-ray Unit[a]	Dose[b]	Chest Mission[c]	Couch Mission[d]	Chest Mission	Couch Mission	X-ray Unit	Dose[e]	Chest Mission	Couch Mission	Chest Mission	Couch Mission
15	3.72	12	24	18	456	34	8.35	100	140	9	280
107	2.52	200	180	6	60.65	56	24.18	4.8	150	19.2	192.84
50	7.11	95	60	100	197	109	18.9	90	90	64	440
Mean	*0.43*	*13.5*	*18.4*	*17.26*	*53.35*	*Mean*	*0.95*	*18.93*	*31.74*	*17.26*	*53.35*

[a] a particular X-ray unit/machine; [b] calculated dose outside PED; [c] chest mission/horizontal exposure [d] couch mission/vertical exposure; [e] calculated dose at CP

*Mean value was calculated from each and every unit

Table 4.3.6 (b): Exposure rates and workload for low occupational and public doses

Public Dose						Occupational Dose					
Dose (mR/week)		Exposure rates (mR/h)		Workload (mA-min/week)		Dose (mR/week)		Exposure rates (mR/h)		Workload (mA-min/week)	
X-ray Unit	Dose	Chest Mission	Couch Mission	Chest Mission	Couch Mission	X-ray Unit	Dose	Chest Mission	Couch Mission	Chest Mission	Couch Mission
10	0	50	80	0	0	11	0.62	0	100	3	10.6
18	0	0	70	0	0	25	0	0	360	0	0
25	0	0	50	0	0	40	1.53	235	0	0.2	50
33	0.02	0	65	0	1.6	49	0	165	0	0	0
63	0.7	57	0	10	11.2	53	1.26	205	0	16.8	36.48
29	0.1	3.1	2	32	104	29	0.02	0.49	0.35	32	104
46	0.52	14	18	50	135	46	0.01	0.34	0.3	50	135
52	0.15	1	3.2	50	123	52	0.02	0.15	0.38	50	123

The occupational doses (which varied from ~0.01–24.18 mR/week) were compared with dose limits for radiation workers prescribed in the AERB Safety Code: 40 mR/week (AERB, 2001; AERB format for QA). All these institutions were well below this dose limit as shown in Fig. 4.3.6 (a). The highest dose found was 24.18 mR/week, which is 60.45% of the dose limit. These doses are still relatively high compared to the others and the reason may be as follows. First, the CP was at a distance of 200 cm from the chest stand and only 70 cm from the couch, which contradicts the recommended distance of 300 cm (AERB, 2001). Second, despite the short distance, the machine was operated without any barrier(s). Third, the workload of 192.84 mA-min/week was high, compared with the mean workload of 53.35 mA-min/week (Table 4.3.6 (a)). Thus, the authors measured high exposure rates at the CP, all of which automatically generated relatively high doses compared with others. Further, the use of properly installed lead protective barriers (1.5–1.7 mmPb) was found to provide adequate protection from stray radiation at CPs. However, less than 50% of the institutions covered their CPs properly.

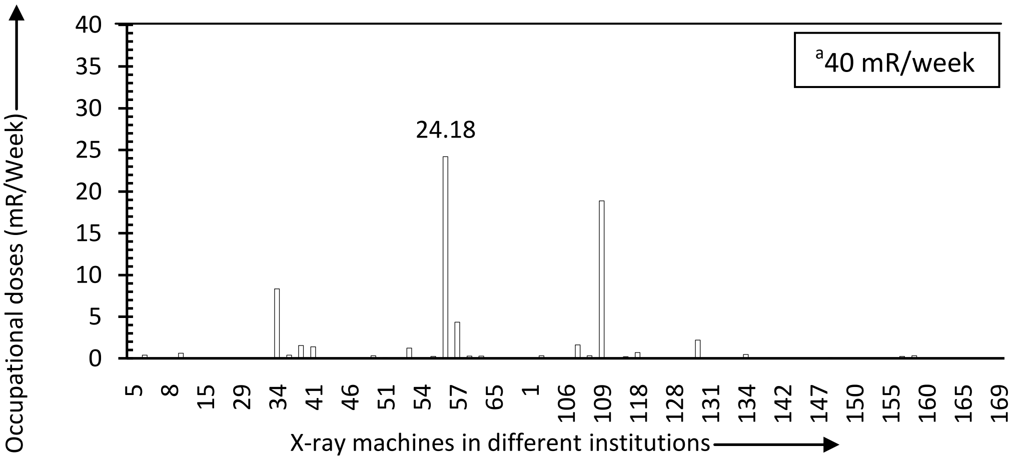

Fig. 4.3.6 (a): Doses at the CPs (occupational dose) caused by stray radiation (^{a}AERB dose limit for radiation workers)

Some marginal doses or overdoses were observed in public spaces outside the PED (Fig. 4.3.6 (b)), relative to the dose limit for the public: 2 mR/week (AERB, 2001). The highest dose found was 7.11 mR/week, which is 3.55 times the public dose limit. High workload is the main reason for such high doses at unit 15 (Fig. 4.3.6 (b)), where the workload of 456 mA-min/week was 8.55 times the mean value. Although the PED was non-lead lined, the distance of the PED from the chest stand (i.e., 500 cm) and from the couch (i.e., 405 cm) results in average exposure rates (Table 4.3.6 (a)). Regarding unit 50, there was inadequate space between the PED and the chest stand (i.e., 230 cm) and the couch (i.e., 143 cm). These high exposure rates were measured outside a plywood PED having a thickness of 0.33 cm. High workloads i.e., 3.69 times the mean value for couch mission and 5.79 times the mean value for chest mission were found. It can be seen that average workload had been performed in unit 107 however high public dose arise from high exposure rates for both chest and couch missions (Table 4.3.6 (a)). These doses could be significantly reduced by following the standard installation layout as well as employing lead-lined doors as recommended by the regulatory bodies (AERB, 2001; NCRP, 2004).

In the present study, radiation doses were found to depend on the input electrical parameters and installation layout. This is why quality assurance tests are mandatory for diagnosing and rectifying machine performance. Because repeated exposures were not included in this study, the doses reported appear underestimated. However, the study used maximum field sizes and longer exposure times than normal X-ray examinations. There was also high kV. Thus, the dose underestimation may have been compensated, falling on the safer side.

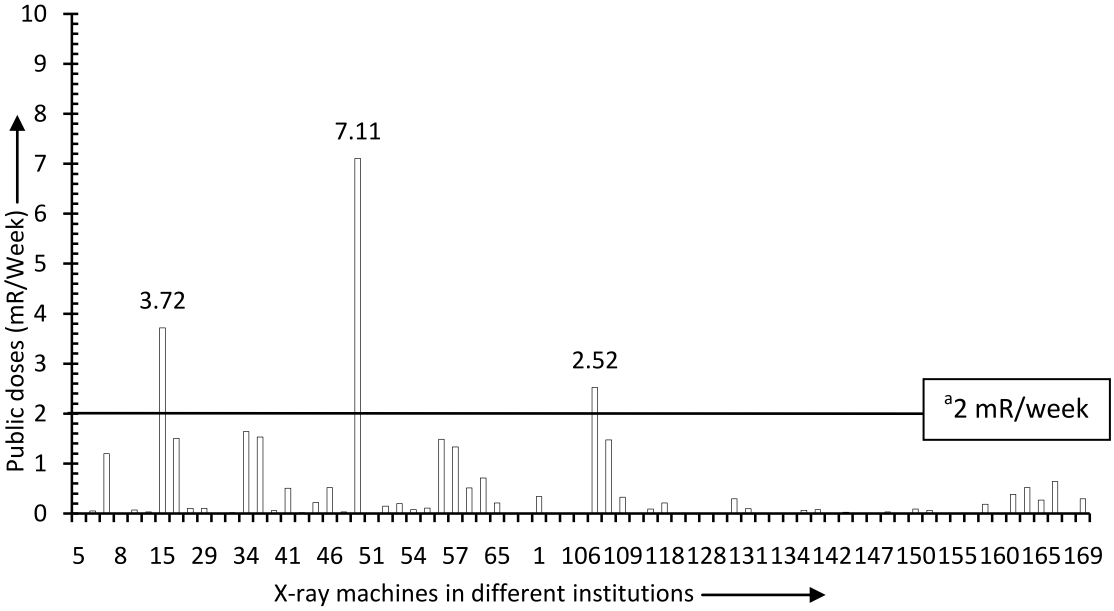

Fig. 4.3.6 (b): Doses at the PEDs (public dose) owing to stray radiation ([a]AERB dose limit for members of the public)

4.4 Study on the intensity of Radiation attenuated by Protective Barriers in diagnostic X-ray installations

It was reported that among radiation workers, the risk of solid cancers increases significantly as cumulative radiation exposure increased (Sun *et al.,* 2016). However, in the previous section it can be seen that proper use of protective barrier at CP and PED significantly reduces radiation dose at CP and outside PED. In the present study area, only 11.2% installations employ lead-lined door and 40.82% employ CP barrier with lead-glass. Others installed solid wood, plywood, Al plane sheet, concrete material for PED barrier as well as CP barrier. Therefore, it is very important to know the safety status of these different kinds of shielding materials and compare with lead material in terms of radiation safety. Archer reported that other materials can be used to complement or replace lead and concrete as an effective barrier against diagnostic energy X-rays (Archer, 1994).

4.4.1 Attenuation of PEDs

The quantity of stray radiation rates outside PED in chest and couch missions are shown in Fig. 4.4.1 (a). These intensities of radiation were measured in closed PED as well as open PED. In chest mission, radiation rates with PEDs ranged from 0.3 µSv/h (0.03 mR/h) to 0.7 mSv/h (70 mR/h) with a mean of 0.19 mSv/h (18.95 mR/h), whereas radiation rates without PEDs varied from 0.02 mSv/h (2.1 mR/h) to 1.2 mSv/h (120 mR/h) with mean 0.55 mSv/h (54.96 mR/h). At the same time, in couch mission, radiation rates measured behind PEDs ranged from 0.3 µSv/h (0.03 mR/h) to 2.2 mSv/h (220 mR/h) with mean 0.43 mSv/h (43.44 mR/h). Similar case is also seen in case of couch mission where radiation rates without PEDs was higher, 0.03 mSv/h (2.8 mR/h) to 2.25 mSv/h (225 mR/h) with mean 0.75 mSv/h (74.73 mR/h). It is comprehensible from Fig. 4.4.1 (a) that all the institutions showed higher radiation rates in the absence of PED. It means that all types of doors attenuated the incident ionizing radiation noticeably by the process of photoelectric effect and Compton scattering. However, the amount of attenuation produced by different types of doors was not similar because interaction process between X-ray and lead-lined door will be different from X-ray and plywood door and so on. In addition to that, in the present study there was a significant difference (0.05 level) between radiation measured with and without PED in chest and couch missions as shown in Table 4.4.1 (a).

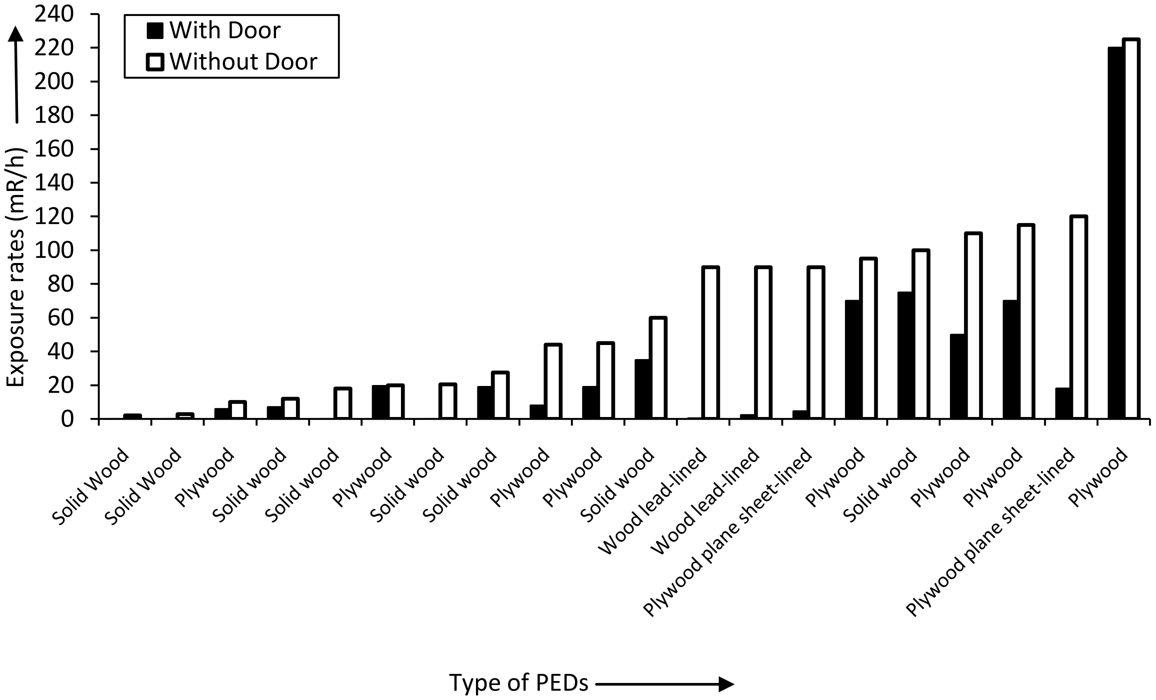

Fig. 4.4.1 (a): Exposure rates measured outside PEDs with door open and close in chest and couch missions

Table 4.4.1 (a): Difference between exposure rates measured with and without PEDs in chest and couch missions

Mission	PED	N	Mean	t-value	*p* value
Chest mission	With PED Without PED	10 10	18.95 54.96	3.09	0.05
Couch mission	With PED Without PED	10 10	43.44 74.73	3.16	0.05

Percentage of attenuation, attenuated by different types of doors i.e. solid wood, plywood, plywood-plane sheet-lined and lead-lined doors with respect to distances are shown in Fig. 4.4.1 (b). The thickness of each type of door as well as their respective attenuation percentage is given in Table 4.4.1 (b). Among different kinds of doors, lead-lined door attenuated radiation in large amount (99.53% in chest mission and 97.44% in couch mission) because they have a greater number of atoms in a unit area (Canada Metal). However, the authors believed that installation layout, distance between source of radiation and shielding plays a very important role because solid wood having almost the same thickness has extensive different amount of attenuation. The solid wooden PED (*[1] Fig 4.4.1 (b)) which showed a good attenuation property was installed behind CP protective barrier for both chest and couch missions. Further, the other wooden door (*[2] Fig 4.4.1 (b)) was installed in a large room, where distance between chest stand and PED in chest mission was 790 cm; 430 cm between couch and PED in couch mission, simultaneously the PED installed almost behind CP barrier. Among the PEDs, even lead-lined door cannot attenuate 100% of the incident radiation. Which is clear from the equation 7 i.e. $N = N_o e^{-\mu x}$ that there will always be a photon which transmit at any thickness without having interaction (Turner, 2005). While plywood doors attenuated about 40% of the incident X-rays, it is almost same as air does in every half meter away from the phantom (Vlachos *et al*., 2015).

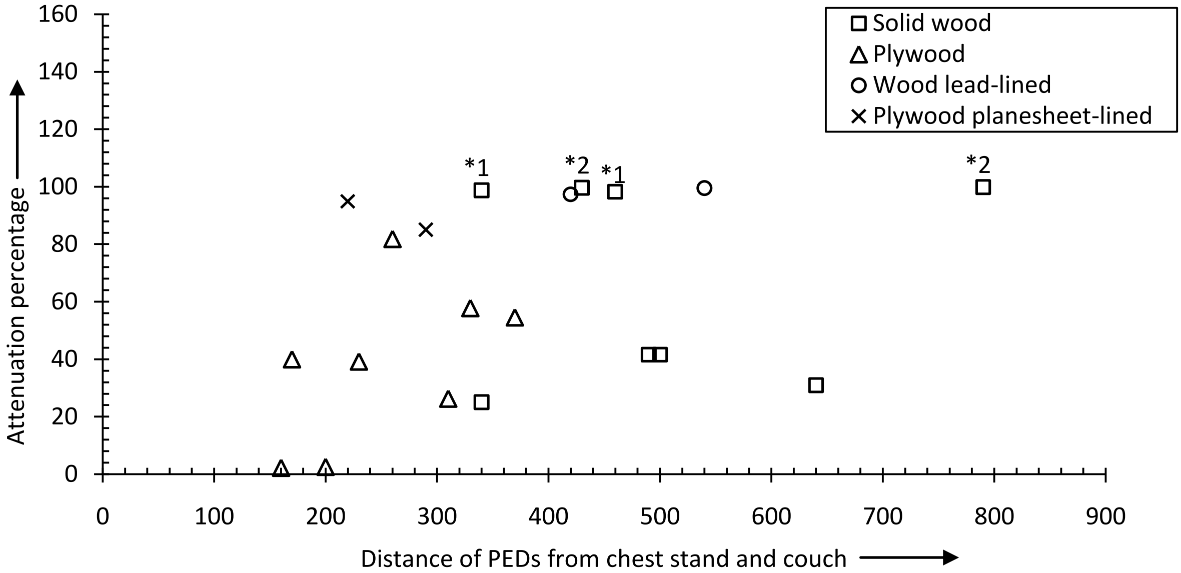

Fig. 4.4.1 (b): Percentage of attenuation; attenuated by solid wood, plywood, lead and plywood-plane sheet-lined door

Table 4.4.1 (b): Attenuation (percentage) of different types of PED

Expt. Unit No.	Types of Door	Thickness (cm)	PCT of Attenuation (Chest Mission)	PCT of Attenuation (Couch Mission)
10	Solid wood	3.2	99.81	99.61
6	Solid wood	3.8	98.33	98.75
1	Solid wood	3.3	41.67	25.00
2	Solid wood	3.5	30.91	41.67
9	Plywood	0.5	40.00	02.50
3	Plywood	0.3	39.13	02.22
8	Plywood	0.3	57.78	81.82
5	Plywood	0.3	54.55	26.32
7	Plywood plane sheet-lined	.1, .3	85.00	95.00
4	Wood lead-lined	4.0	99.53	97.44

4.4.2 Attenuation of CP Barriers

The amount of stray radiation rates behind and in front of CP protective barriers are shown in Fig. 4.2.2 (a). Radiation rates in chest missions with barriers ranged from 2μSv/h (0.2 mR/h) to 0.38 mSv/h (38 mR/h) with mean 0.11 mSv/h (10.56 mR/h), while 0.4 mSv/h (40 mR/h) to 2.35 mSv/h (235 mR/h) with mean 1.13 mSv/h (113.1 mR/h) without barrier. In couch missions, radiation rates measured with barriers varied from 4μSv/h (0.4 mR/h) to 0.6 mSv/h (60 mR/h) with mean 0.17 mSv/h (17.21 mR/h), whereas without barrier it varied from 0.7 mSv/h (70 mR/h) to 5 mSv/h (500 mR/h) with mean 2.66 mSv/h (266.5 mR/h). There exists a significant difference (0.01 level) between radiation measured with and without CP barriers in chest and couch missions (Table 4.2.2 (a)). Except for plywood and plywood plane sheet-lined barriers, all other barriers i.e. lead and concrete were showing a good barrier property, the reason is same as in the case of PED. While all the barriers attenuated radiation, the amount of attenuation was not the same in different barriers mainly due to different scattering mechanism and barrier's physical property. Even though the same input parameters were applied, amount of attenuation for same material was different due to different installation layout, space and tube efficiency.

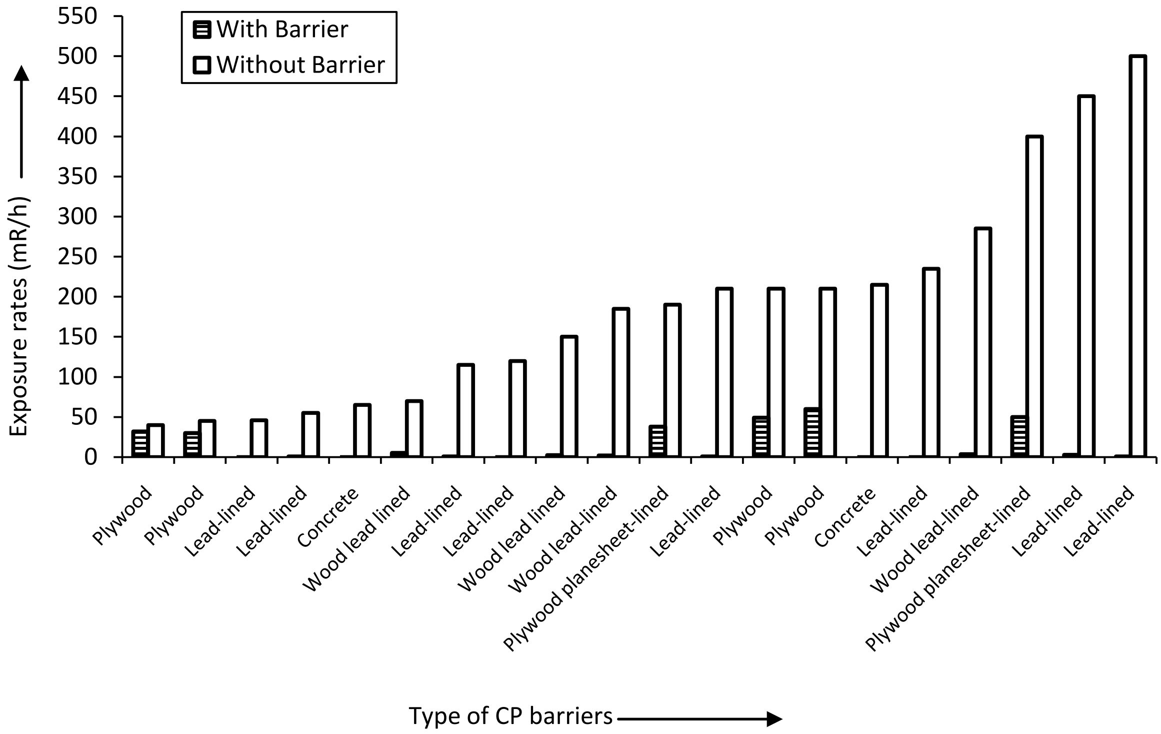

Fig. 4.4.2 (a): Exposure rates measured at CPs with and without barriers in chest and couch missions

Table 4.2.2 (a): Difference between exposure rates measured with and without CP barriers in chest and couch missions

Mission	CP Barrier	N	Mean	t-value	*p* value
Chest Mission	With Barrier	10	10.56	4.25	0.01
	Without Barrier	10	113.1		
Couch Mission	With Barrier	10	17.21	5.49	0.01
	Without Barrier	10	266.5		

Percentages of attenuation, attenuated by different kinds of protective barriers with respect to distance are shown in Fig. 4.4.2 (b). Among different barriers, lead and concrete barriers attenuated more than 90% of incident radiation (Table 4.2.2 (b)). However, plywood and plywood-plane sheet-lined barriers attenuated relatively lesser amount of radiation. As already mentioned, lead and concrete are denser than plywood and thicker in the present study. At the same time the effect of tube efficiency, distance and installation layout could not be controlled as the authors studied the real situation of barrier in different X-ray installations. Even though plywood plane sheet-lined barriers attenuated few portion of incident radiation, it is not recommended because the amounts of stray radiation measured on CPs were considerable and the people behind the barriers are the radiation workers who performed every examination.

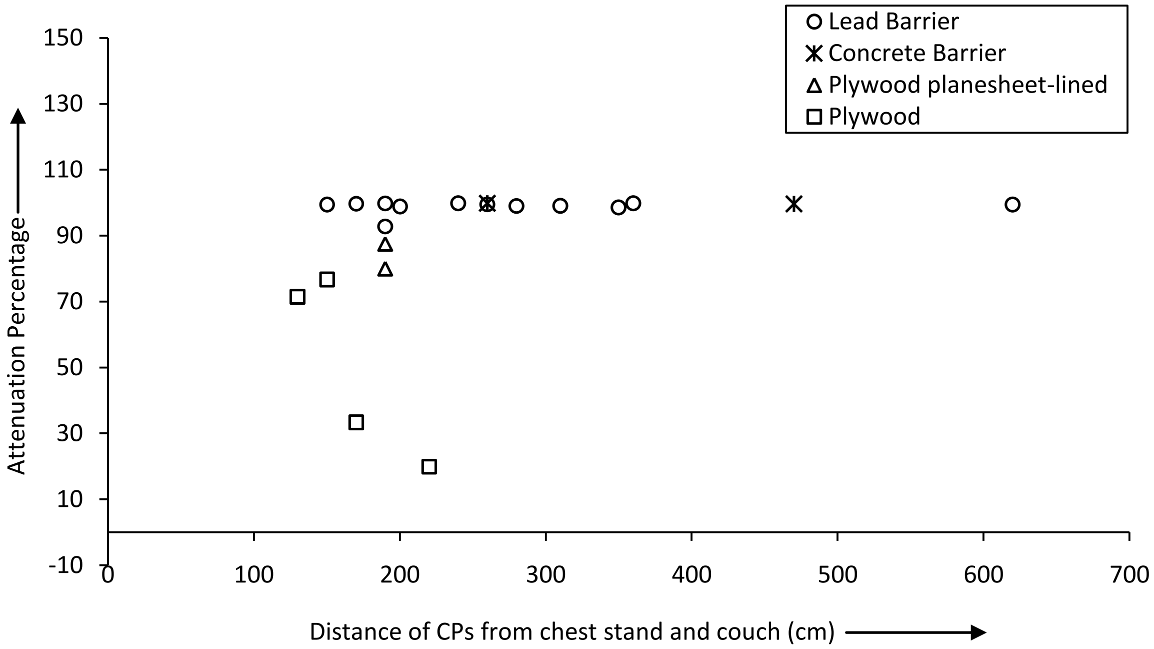

Fig. 4.2.2 (b): Percentage of attenuation; attenuated by lead, concrete, plywood and plywood-plan sheet-lined barriers

Table 4.2.2 (b): Attenuation (percentage) of different types of CP barrier

Expt. Unit No.	Types of Barrier	Thickness (cm)	PCT of Attenuation (Chest Mission)	PCT of Attenuation (Couch Mission)
5	Lead-lined	0.4	99.83	99.42

3	Lead-lined	2.5	99.09	99.77
1	Wood Lead-lined	2	98.53	92.86
4	Lead-lined	0.3	99.83	99.86
6	Wood Lead-lined	0.1, 2.6	99.03	98.81
10	Lead-lined	2	99.43	99.57
9	Plywood	0.3	20.00	76.67
7	Plywood plane sheet-lined	0.1, 0.3	80.00	87.50
2	Concrete	25	99.66	99.81

4.5 Investigation of conventional diagnostic X-ray tube housing leakage radiation using ion chamber survey meter in Mizoram, India

To enhance radiation protection, William H. Rollins, a dental physician in Boston, USA introduced the X-ray tube housing by using lead material in 1899 (Kathren, 1964). In the early days of medical imaging, lead shielding around the X-ray tube was used but before shielding became mandatory, about three decades had passed (Ammann and Kutschera, 1997). In the present day, tube leakage radiation is not emitted through the X-ray tube portal even though it is created inside the X-ray tube. Rather, leakage radiation is transmitted through X-ray tube housing (Simkin and Dixon, 1998). This is why diagnostic X-ray tube housing is lined with thin sheets of lead. This shielding is intended to protect both the patients and personnel from leakage radiation (Seeram and Travis, 1997).

Studies have been performed on tube housing leakage of conventional diagnostic X-ray equipment in different parts of the world. Sungita *et al.* in 2006 performed measurement of tube housing leakage on 47 units in Tanzania and reported ‘Most of the X-ray machines tested for tube leakage gave results that were below 0.5 mSv h^{-1} at 1 m, which complied with safety requirements. Tsalafoutas (2006) performed a study in excessive tube housing leakage due to the methodology used by the manufacturer on two separate mobile X-ray units. Tsalafoutas reported that even at a distance of 3 m from the tube, the leakage radiation exceeded the maximum permissible dose rate. For the second unit, the dose-meter reading at 1 m from the tube was 12.1 µGy; for 1 h with tube current 4 mA, a leakage of 3.5 mGy was derived. The author concluded that after changing the methodology used by the manufacturer, the leakage radiation had been reduced to about 1/8 of its previous value and thus followed the existing leakage radiation limit. In 2012, Hassan *et al.* studied X-ray diagnostic machines used at different medical diagnostic centers in Egypt; they reported that the measured dose of tube housing leakage was in the range of background values 0.15 µSv h^{-1} at 1m.

The tube housing leakage exposure rates measured for 93 diagnostic X-ray machines in each five different positions (i.e., left, right, front, back and top) of the X-ray tube were shown in Table 4.5.1. Exposure rates 0.03 mR h^{-1} was the lowest leakage exposure measured and it was found in back and top positions of the X-ray tube. Leakage exposure rates, 500 mR h^{-1} was the highest leakage radiation rate from all 93 X-ray machines and it was measured in the front direction of the X-ray tube (Table 4.5.1). Comparing radiation exposure rates measured at different positions; rates measured at the front direction of the tube has the highest mean±SEM of 41.61±8.63 mR h^{-1} and rate measured at the top position of the tube has the lowest mean±SEM of 4.57±1.16 mR h^{-1}. Therefore, radiation leakage in the present study was high in the front position of the tube, whereas, it was low at the top position of the X-ray tube. In addition to that, *T*-test was performed between leakages exposure rates measured at these five different positions and the results showed that there was a significant difference (0.01 level) between the top position and the other four directions of the X-ray tube. Further, X-ray tube leakage at the top direction was significantly less than the other four directions. Tsalafoutas (2006) reported that there was an excessive leakage radiation from each position except for one position on the top of the new mobile X-ray tube housing. So, similar case was found in the present study, when compared to the others, the top position showed relatively low leakage radiation rate (Table 4.5.2).

Table 4.5.1: Tube housing leakage exposure rates measured at left, right, front, back and top direction of the X-ray tube

Param-eters	N	Minimum (mR h^{-1})	Maximum (mR h^{-1})	Range (mR h^{-1})	Mean (mR h^{-1})	Std. error of the mean (mR h^{-1})
Left	93	0.09	400	399.91	33.51	6.65
Right	93	0.04	400	399.97	37.32	6.87
Front	93	0.04	500	499.96	41.61	8.63
Back	93	0.03	290	289.97	17.67	4.86
Top	93	0.03	70	69.97	4.57	1.16

Table 4.5.2: Comparison of radiation leakage between left, right, front, back and top direction of X-ray tube

Position of the survey meter w.r.t. X-ray tube	N	t-value	Significant Level
Left and top position	93	**4.29**	S at 0.01
Right and top position		**4.7**	
Front and top position		**4.25**	
Back and top position		**2.62**	

From each five different positions of measurement, the authors selected the highest leakage exposure rates from all the X-ray machines. Then, the maximum leakage radiation level at 1 meter from the tube (mR in one hour) of the X-ray machines were calculated by using the given equation (Fig 4.5.1) (AERB format for QA);

$$\text{Max leakage} = \frac{180\ \text{mA.min in 1 hr} \times \text{Maximum Exposure level}\ (\frac{\text{mR}}{\text{hr}})}{60 \times mA used for\ measurement} \text{-------------} (26)$$

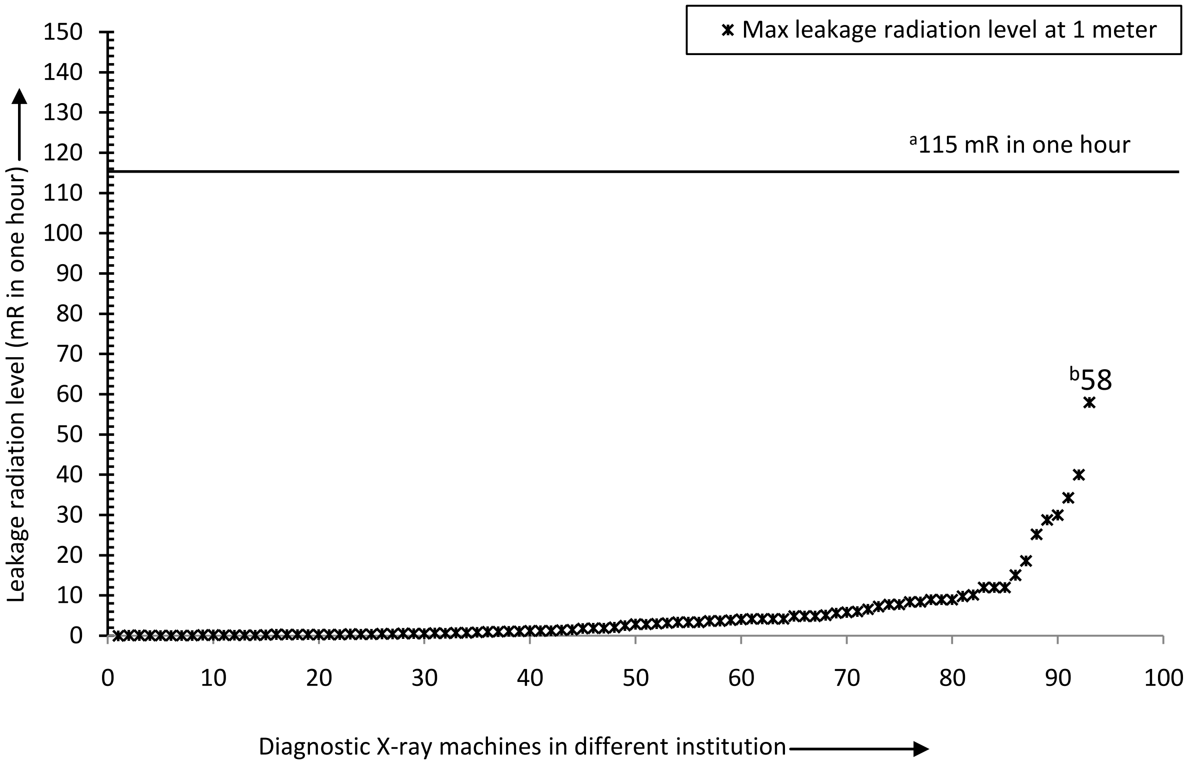

Fig. 4.5.1: Maximum tube housing leakage radiation in 93 X-ray machines [[a]AERB and other regulatory body safety limit 115 mR in one hour; [b]maximum leakage 58 mR in one hour]

The calculated maximum tube housing leakage radiation from 93 X-ray machines ranged between 0.01 mR in one hour to 58 mR in one hour with 5.39±0.97 (mean±SEM) mR in one hour. Leakage radiation levels from 93 X-ray machines were compared to the national and international standard norms; it was found that all the machines complied with the safety standard (AERB, 2001; Euratom radiation protection no. 91). The highest leakage radiation level was 50.43% of the standard limit. The present result is more or less similar to previous studies conducted by Sungita *et al.*, in Tanzania (2006) and Hassan *et al.* in Egypt (2012). However, in the present study, leakage radiations appeared to be relatively higher than the previous studies.

According to AERB type approval machine, 66 machines were AERB type approved units where 27 machines were unknown approval due to lack of information as these machines were so old. The minimum leakage radiation level in AERB type approved units was 0.02 mR in one hour and the maximum was 58 mR in one hour having 6.97±1.31mR (mean±SEM) in one hour. Further, minimum leakage radiation level in not known approval units was 0.01 mR in one hour and the maximum was 8.40 mR in hour with mean±SEM 1.51±0.46 mR in one hour. It appears that the leakage radiation level was higher in AERB type approved machines than the unknown approval type. The *T*-test also showed that the existence of significance difference (0.01 level) between AERB type approved unit and unknown approval status (Table 4.5.3). Besides, as already mentioned, both types of all the machines were within safety standard.

Table 4.5.3: Comparison between maximum leakage radiation in AERB type approval units and unknown type approval units

	N	Mean	t-value	Significant Level
AERB Approved units	66	6.97	**2.63**	S at 0.01
Not known approval units	27	1.52		

Regarding fixed and mobile X-ray machines, 52 machines were mobile X-rays, where, 41 were fixed X-ray machines. Leakage radiation in mobile X-rays ranged between 0.02 mR in one hour to 58 mR in one hour with mean±SEM 6.04±1.53 mR in one hour. In fixed X-rays, leakage radiation ranged from 0.01 mR in one hour to 30 mR in one hour with mean±SEM 4.55±1.04 mR in one hour. It was found that the leakage radiation level is relatively higher in mobile X-ray than fixed X-ray machines even though fixed X-ray can operate at relatively high input parameters. However, there was no significant difference (0.01 level) between fixed and mobile X-ray machines (Table 4.5.4). Further, the correlation between the tube housing leakage and the age of the X-ray machine was only 0.15, therefore, the X-ray tube age is not one of the important reasons for the present tube housing leakage radiation.

Table 4.5.4: Comparison between maximum leakage radiation in fixed and mobile X-ray machines

	N	Mean	t-value	Significant Level
Fixed X-ray machines	41	4.55	**0.76**	NS at 0.01
Mobile X-ray machines	52	6.04		

CHAPTER 5

SUMMARY AND CONCLUSION

Radiation played a very important role in the unparalleled advances in science during the last century. In fact, the huge potential for medical applications of X-rays was evident from the first investigations. Many unique and important benefits to human life are realized through the utilization of radiation and its various sources. Today, diagnostic radiology facilities are widely available in the country as well as the present study area; more than 50% of conventional diagnostic X-ray equipment were installed during the past five years. Large number of people undergoes diagnostic X-ray procedures every year. As experience was gained in the early days, it became increasingly evident that ionizing radiation can damage biological systems. It is therefore very important that adequate attention to safety is paid with regard to this widespread practice. In time, concepts and procedures were developed for protection around radiation sources, and laws were eventually enacted to control exposures of workers and the public to radiation. Knowledge of the image quality as well as dose level and the reasons behind poor quality and higher doses provides a basis for setting corrective actions to optimize the protection of the patient in an effective manner. Work in radiation protection continues today on a large and active scale.

In radiography, radiation dose and image quality are greatly depend on X-ray generator parameters. Among different X-ray generators parameters studied in the present study, 59.2% linearity of time (sec); 82.6% linearity of current (mA); 89.7% peak kilo-voltage (kVp) accuracy; 35.1% output reproducibility; 92.8% table dose (μGy/mAs) were beyond acceptable limits. The reasons for such poor performance were improper quality assurance tests, old machine used without proper maintenance, power supply problems; detailed already discussed in the previous chapter. Hassan *et al*. (2012) reported that the total absorbed dose delivered to different organs depends mainly on the X-ray generators. Therefore, implementation of quality control program on a regular basis is necessary to reduce X-ray machine malfunctioning, to produce high quality diagnostic images with the lowest radiation dose to the patient. It was observed from 16 essential safety parameters that none of the X-ray machines undergone a regular quality assurance test as per the Atomic Energy Regulatory Board (AERB) guidelines, only 1.9% equipment employed lead-line patient entrance door (PED), 46.8% machines were operated without any protective barrier, 83.1% units operated without personnel monitoring services, lead apron were not available in 38.3% machines, 92.2% of the facilities recorded repeated examination due to over/under exposures, spoiled films and patient movement. It can be concluded that due to the absence of proper quality control program in the past, many installations were not following standard installation guidelines which were laid down by several regulatory bodies.

Among the mechanical characteristics of X-rays, half value layer affects both the quantity and quality of the X-rays. It is the amount of aluminum required to reduce the intensity of radiation to one-half of its original value and is measured to guarantee that the permanently installed filter on the X-ray tube is maintained to minimize patient exposure. The calculated total filtrations of conventional X-ray machines at different institutions were compared with national and international standards; 27.83% met the national standard and only 15.46% met the international standard. It appears that most of the equipment in the present study had poor filters.

In congruency between radiation and optical field study, from the 47 units which we could study, 80.85% were found to be beyond the acceptable limit. At the same time, the optical lights of 4 X-ray units did not work; 6 units had fixed their collimators to full, and more than 10 units had misalignments above 10% of the source to image distance. When testing the central beam and image receptor perpendicularity of 53 units, 69.81% of X-ray units were more than 1.5 degrees off perpendicularity and did not pass the test. These faults will result significant increase in patient and radiation worker doses through primary and secondary radiation. In these particular parameters, both new and old X-ray machines had similar problems.

Radiation workers and the general public are mainly exposed to radiation from primary and scattered varieties. However, they receive very small amounts of primary radiation, so that most of the doses result from scattered radiation (Osborn, 1955). Therefore, stray radiation (primary and secondary radiation) rates were measured at control panel (CP) and PED for the assessment of radiation workers and public dose. The authors did not find any excessive doses at the CP, per the safety code. However, the absence of barriers and barriers not effectively covering CPs with respect to couch and chest missions should be rectified to decrease ancillary doses. The highest dose contributed by stray radiation from the couch and chest missions to the CP was 24.18 mR/week, which is 60.45% of the dose limit. There were three installations where the dose outside the PED, a public space, exceeded the safety recommendations of 2 mR/week. The highest dose was found to be 7.11 mR/week, about 3.55 times the dose limit. The most often used materials (i.e., solid wood, plywood-lined, and plane sheet-lined) in the entrance doors attenuated radiation relatively less than did the lead-lined doors. The lead-lined doors appreciably reduced the radiation rate outside the PEDs. Unfortunately, more than 90% of the institutions used traditional doors.

The use of protective shields can significantly reduce radiation exposure of X-ray operators and the general public (Chen *et al*., 1996). At the same time Archer (1994) reported that other materials can be used to complement or replace lead and concrete as an effective barrier against diagnostic energy X-rays. Regarding this a study was performed to measure X-ray intensity attenuated by several protective barriers in CP and PED. It was noticeable from the present study that each type of PED attenuated radiation but in different quantity where lead-lined door attenuated relatively large amount (>90% in chest and couch missions). Installing plywood and plywood-plane sheet-lined door is healthier than no door at all because it attenuated considerable amount of radiation. On the other hand, patient entrance door which can reduce any kinds of stray radiations below a level of 1 mSv y^{-1} is recommended by various regulatory bodies. Again, CP protective barriers attenuated significant amount of incident radiation. Among them, lead and concrete barriers attenuated more than 90% of incident radiation while plywood plane sheet-lined barrier attenuated relatively lesser quantity.

Proper shielding of any X-ray tube, using the standard methodology and leakage limit, is mandatory for the radiation protection of the radiation workers, patients and the public (Tsalafoutas, 2006). In the present investigation of tube housing leakage measurement, the tube housing leakage radiation level among the five different positions was highest in the front direction of the tube and lowest at the top direction of the X-ray tube. Leakage radiation in the direction of the left and right position from the tube was not significantly different. In comparison to national and international safety standard, tube housing leakage of all the X-ray machines were well below the safety limit. Regarding fixed and mobile X-ray machines, there was no significant difference in leakage radiation between them even though fixed X-ray can operate at higher input parameter.

The information obtained from the present investigation will be very useful for establishment of effective quality assurance programs as this kind of information is lacking in the present study area as well as in many developing country. At the same time, comparison of work done by the authors with the similar work done by other researchers from Middle East, Asia, Africa and Europe was carried out and shown in Table 5.1. It may be important to highlight that in the initial stage of the present investigation i.e. 2015, majority of the radiographers and institutional heads were not acquainted with the benefits and significance of X-ray quality assurance test. Furthermore, none of the installations then, had registration with regulatory bodies neither were they licensed under the AERB, India. The main reason was that the present study area is one of the economical backward areas and located in the remote part of Northeast India where there is poor infrastructural base in almost every discipline. However, through Radiation Safety Agency-Government of Mizoram mission, in March 2019, 124 installations (i.e., ≈73%) were having licensed under AERB, India (AERB eLORA).

Table 5.1: Comparison of work done by authors with the similar work done by other researchers from Middle East, Asia, Africa and Europe

Region	Parameters/findings of the previous study (*Within acceptable limit*)	Present study (n=135) (*Within acceptable limit*)
Middle East **Iran**-Asadinezhad *et al.*, 2017 (n=51) **Syria**-Kharita *et al.*, 2017 (n=487) **Iran**-Rasuli *et al.*, 2015 (n=15) **Asia** **India**-Sonawane *et al.*, 2010 (n=118)	**Iran**-Voltage accuracy 61.4%; Tube output linearity (sec) 65.5%; Tube output linearity (mA) 53.3%; Output reproducibility 80.6%; HVL 85.3% **Syria**-Voltage accuracy 43.69%; Tube output linearity (sec) 59.74%; Output reproducibility 96.95%; Total filtration 58.77%; Congruency ≈70%; Perpendicularity 76.77% **Iran**-Voltage accuracy 86.6%; Tube output linearity (sec) 100%; Tube output linearity (mA) 86.7%; Output reproducibility 100%; Tube output (70kV) 53.3%; Total filtration 73.3%; Congruency 93.3% **India**-Voltage accuracy 76.79%; Tube output linearity (sec) 91.07%; Tube output	**Voltage accuracy** 10.3% (±0.05 or 5%) The present study lagged behind all the previous studies. It may be important to note that some studies were conducted more than 20 years ago. Amin *et al.*, (2012) found that 98% were within the acceptance limit. **Tube output linearity (sec)** 40.8% (0.1 or 10%) In this parameter, two studies (Hamed *et al*. & Gori *et al.*) fall behind the present study. However these studies were conducted 20 years back. Rasuli *et al.*, (2015) reported that all the machines were in lined with acceptance limit. **Tube output linearity (mA)** 17.4% (0.1 or 10%) Present study does not keep pace with the other study from different part of the world. **Output reproducibility** 64.9% (0.05 or ±5%) Two studies (Rasuli *et al*. & Sonawane *et al.*) found all the devices were within the acceptable limit. However, a study

Malaysia-Amin *et al.*, 2012 (n=100) **Africa** **Tanzania**-Sungita *et al.*, 2006 (n=196) **Egypt**-Hassan *et al.*, 2012 (n=118) **Egypt**-Hamed *et al.*, 1999 (n=14) **Europe** **Italy**-Gori *et al.*, 1995 **Republic of Srpska**-Bosnjak *et al.*, 2008 (n=230)	linearity (mA) 83.93%; Output reproducibility ≈100%; Total filtration ≈100%; Congruency 76.79% **Malaysia**-Voltage accuracy 98%; Output reproducibility ≈50%; Tube housing leakage 100% **Tanzania**-Voltage accuracy 41%; Tube output linearity (sec) 43%; Beam alignment 40%; Tube housing leakage 80% **Egypt**-CP & PED 100%; Tube housing leakage 100% **Egypt**-Voltage accuracy 23%; Tube output linearity (sec) 25%; HVL 14.29% **Italy**-Voltage accuracy 81%; Tube output linearity (sec) 19%; Output linearity 94%; Total filtration 81%; Congruency 69% **Srpska**-Voltage accuracy 71%; Exposure time accuracy 75%; Radiation output reproducibility 94%; Congruency 82%	performed by Amin *et al*. fall behind the present study. **Tube output** 7.2% (43 µGy/mAs–52 µGy/mAs) The present study lagged behind the previous study. **Total filtration** 15.46% (>2.5 mm Al) One study (Hamed *et al*.) fall behind the present study, while the others performed better than the present study. Sonawane *et al*. observed that all the devices were within the acceptable limit. **Congruency** 19.15% (2% of SID) **Perpendicularity** 30.19% (<1.5°) The present study trail behind the previous studies in congruency and perpendicularity study, Rasuli *et al*. observed 93.3% acceptable units in congruency study. **Occupational dose (CP)** 100% (40 mR/week) Other study also obtained the same result. **Public dose (PED)** 95.83% (2 mR/week) Hassan *et al*. found all the doses measured followed safety limit. **Tube housing leakage** 100% (115 mR in one hour) One study from Africa fall behind the present study, others were showed 100% performance.

Recommendation and Suggestions:

Regular quality control of conventional X-ray equipment and fixing their defects can play an important role in increasing the machine longevity, reducing absorbed dose of patients, and improving the quality of radiographic images. Performing strict quality control on all diagnostic X-ray facilities is one of the radiation protection priorities that should be done periodically. If quality control is defined as a routine procedure, the cost of after sale services may be significantly reduced especially if it is performed by the radiation safety officers or qualified medical physicist. The participation of medical physicists, radiographers and radiologists in the implementation of quality control programs at various stages of development will enhance equipment performance improvement in the present study area.

It may be very important to note that X-ray examinations remain operator-dependent even after employing the best X-ray equipment. Most radiation workers in the developed country have been appropriately trained and educated for the safe use of ionizing radiation regarding medical imaging. Periodic in-service training is necessary to maintain those skills especially in the remote areas of the developing country. It also appears to be very important to provide detailed in-service training when new technology is introduced into the medical imaging process. At last it may be important to highlight that the common assumption of radiation doses to patients in developing countries are always higher than those in developed countries is not correct (Muhogora *et al*., 2008).

Future Scope of the study:

In the present study, the investigators considered conventional diagnostic X-ray machine among different X-ray facilities such as Cath-lab, computed tomography, fluoroscopy, mammography, dental X-ray. This is mainly due to the fact that 90.9% (5172.16 mA-min/week) of all examinations across the state i.e. Mizoram were carried out in this type of X-ray equipment. However, the number of such equipment along with workload will increase in future as it already happens in a developed country. Therefore, such study will be very much interesting because equipment like computed tomography, cath-lab, fluoroscopy produced large amount of ionizing radiation compared to conventional machines.

From the present study the authors observed that some parameters of diagnostic X-ray machines were out of acceptable limit. Therefore, assessment of patient entrance dose with a suitable design dosimeter will reflect the actual dose received by the patient during X-ray examination. Then, these doses can be compared between different hospitals or even in different rooms in the same hospital plus with national and international data.

APPENDICES

Appendix-I: Formulae

The measured data presented as the standard deviation, standard error mean, coefficient of variation, correlation and T-test were analyzed using SPSS Statistics for Windows, Version 17.0 (SPSS, Inc., Chicago, IL, USA). The calculations can also be done manually by using the following formulae.

Standard deviation (SD):

$$SD = \sqrt{\frac{\Sigma\left(x - \bar{x}\right)^2}{N - 1}}$$

Where, *N* is the total number of observations.

Standard error of mean (SEM):

$$SEM = \frac{SD}{\sqrt{N}}$$

***Coefficient of variation (CV)*:**

$$CV = \frac{1}{\bar{X}} \sqrt{\sum_{i=1}^{n} \frac{\left(X_i - \bar{X}\right)^2}{n - 1}}$$

Correlation coefficient **(r)** between the two set of variables '*x*' and '*y*' can be obtained by the following relation:

$$r = \frac{\Sigma\left(\left(x-\bar{x}\right)\left(y-\bar{y}\right)\right)}{\sqrt{\left(\Sigma\left(x-\bar{x}\right)^{2}\Sigma\left(y-\bar{y}\right)^{2}\right)}}$$

Where $\bar{x}$ and $\bar{y}$ are the means of x and y respectively.

T-test **(t)**: T-value can be obtained by dividing the value of each regression coefficient by its respective standard error. A t-test is used to check the existence of significance difference between two variables.

Significance **(p-value)**: The significance of the t-test and F-ratio can be obtained from the t-distribution and F-distribution tables respectively.

Appendix II: Table: All X-ray facilities in the present study area until June 2016

Sl. no. of Institution /hospital	Name of institution/hospital	Sl. no. of Unit	Type of Unit	Name of equipment	Type App. status	kVp	mA	Sec	Year of Instal-lation
Aizawl District									
1	Thingsulthliah Community Health Center	1	MF[1]	Intelix 100mA	Na[2]	100	100	10	2015
2	Sakawrdai Community Health Center	2	MF	ME 5085	A[3]	85	50	5	2011
3	Saitual Sub-District Hospital	3	F[4]	ME 1010	A	100	100	5	2014
4	Suangpuilawn Primary Health Center	4	MF	ME 5085	A	85	50	5	2013
5	Aibawk Primary Health Center	5	MF	ST 20 P	A	85	20	10	1990
6	Sialsuk Primary Health Center	6	MF	ME 5085	A	85	50	5	2014
7	State Referral Hospital, Falkawn (3)	7	F	ME-3010	A	100	300	5	2012
		8	MF	ME-5085	A	85	50	5	2012
		9	M[5]	Cosmos 5	Na	Na	Na	Na	2012

8	Lengpui Primary Health Center	10	MF	ST 20 P	A	85	20	10	2005
9	Sairang Primary Health Center	11	MF	Comet-3	Na	85	50	6	2005
10	Mizoram State Cancer Institute, Zemabawk	12	F	ME 5025	A	125	500	5	2008
		13	CT[6]	Brilliance CT,7875	A	Na	Na	Na	2009
		14	FL[7]	ME X-ray	Na	Na	Na	Na	2008
11	Aizawl Civil Hospital room no 3 (14) Room no. 4 Room no. 2 Orthopedic department Orthopedic department CT-Scan Mammography X-ray dept. from male & paediatric Casualty Intensive care unit Morgue room Dental	15	F	ME-3010	A	100	300	5	1998
		16	F	ME-3010	A	100	300	5	2003
		17	MF	Cosmos-5	Na	Na	Na	Na	2004
		18	MF	ME 5085	A	85	50	5	2004
		19	FL	Multimobil 5 E (C arm)	A	Na	Na	Na	2013
		20	CT	Bright Speed Elite	A	Na	Na	Na	2015
		21	MM[8]	FLAT-III, 1FLHF6/033/C	Na	Na	Na	Na	2013
		22	M	ME 5085	A	85	50	5	2004
		23	M	ME 5085	A	85	50	5	2004
		24	M	ME 5085	A	85	50	5	2004
		25	MF	ME 5085	A	85	50	5	2014

	Dental Neonatal intensive care unit	26	D[9]	Confident C-51A	Na	Na	Na	Na	2001
		27	D	CCX Digital Trophy	Na	Na	Na	Na	2003
		28	M	ME 5085	A	85	50	5	2004
12	Regional Institute of Paramedical and Nursing Sciences (RIPANS), Zemabawk	29	F	ME 5025	A	125	500	5	2013
13	Civil Hospital Cardiology Department	30	CL[10]	ALLATH-80	Na	Na	Na	Na	2014
14	Kulikawn Civil Hospital	31	MF	ME 5085	A	85	50	5	2005
15	State Vety Hospital, Khatla	32	F		Na	Na	Na	Na	2015
16	College of Animal Husbandry & Veterinary Science, Selesih	33	F	Heliophos-D	A	125	500	5	2013
17	Synod Hospital, Durtlang (8)	34	F	Pleophos-D	A	125	300	5	1983
		35	F	Heliophos-D	A	125	500	5	1993
		36	FL	Multimibil-5E	A	Na	Na	Na	2005
		37	FL	Allengers-HF-49 R	A	Na	Na	Na	2004
		38	FL	Multimobil - 5C	A	Na	Na	Na	2005

		39	CT	Bright Speed Elite	A	Na	Na	Na	2008
	Synod Hospital Millenium clinic	40	MF	Multimobil 10	A	125	160	Na	2008
	Dr. Fraser clinic unit of Synod Hospital	41	MF	Genius 60	A	100	60	Na	2012
18	Aizawl Adventist Hospital	42	F	Olympicks 3012D	Na	Na	Na	Na	2012
		43	D	Gomax 10 DRS	A	Na	Na	Na	2009
19	Greenwood Hospital, Bawngkawn	44	F	Diagnox-300	A	125	300	Na	2003
		45	FL	Smart View 3000	Na	Na	Na	Na	2015
20	New Life Polyclinic Hospital, Chanmari	46	F	ME-3010	A	100	300	5	1995
		47	FL	MEX 2000 (Meditronix)	A	Na	Na	Na	2010
21	Nazareth X-ray Center (RIT), NIMAT, Chaltlang	48	F	DXD-300	A	Na	Na	Na	2011
22	Grace Nursing Home, Lower Zarkawt	49	F	Allengers 325 FC	A	125	300	Na	2015
23	Mizoram Health Care, Dawrpui	50	F	ME-3010	A	100	300	5	2008
24	Trinity Diagnostic Centre, Zarkawt	51	F	DX-525	A	125	500		2004
25	Ziki Diagnostic Centre, Dawrpui	52	F	ME-3010	A	100	300	5	2005

26	Alpha Diagnostic & Wellness Center, Dawrpui	53	F	DX-300	A	100	300	Na	2009
27	Aizawl X-ray Center, Dawrpui	54	F	Diagnox-60	A	100	60	Na	2005
28	Alpha Hospital, Kulikawn	55	MF	Sappho Series	Na	Na	Na	Na	2015
29	Bethesda Hospital & Research Center	56	MF	Diagnox-60	A	100	60	Na	2007
30	Aizawl Hospital & Research Center (4)	57	F	DX-300	A	Na	Na	Na	2014
		58	CT	Brivo CT-325	A	Na	Na	Na	2015
		59	FL	Mexsicom-2000	A	Na	Na	Na	2010
		60	D	Gomex 10 DRS	A	Na	Na	Na	2009
31	Nazareth Hospital, Ramhlun (2)	61	MF	Diagnox-60	A	Na	Na	Na	2013
		62	D	Technomac 20	Na	Na	Na	Na	2004
32	Care Clinic	63	F	AMS-100	Na	Na	Na	Na	2008
33	Vaivenga Hospital & Research Center	64	M	ME 5085	A	85	50	5	2009
34	Mercy Veterinary Hospital, Ramhlun	65	MF	Allengers 100 CBM	Na	Na	Na	Na	2015
35	The Pet Division, Kulikawn	66	MF	MDX 100	A	Na	Na	Na	2015

36	Bethany Hospital	67	F	MDX 100	A	Na	Na	Na	2015
37	Faith Dental Clinic	68	D	Technomac 20	Na	Na	Na	Na	2013
38	Aizawl Dental Chamber	69	D	Gomex 10 DRS	A	Na	Na	Na	2009
39	My Dentist, Chanmari	70	D	Ray 68 (W)	A	Na	Na	Na	2015
40	V.L. Dental Clinic, Zarkawt	71	D	Confident (C70E)	A	Na	Na	Na	2015
41	RIDA Dental Clinic, Zarkawt	72	D	AMS 6010 E	A	Na	Na	Na	2016
42	Hope Dental Clinic, Ramhlun Venglai	73	D	C-651 (Confident)	Na	Na	Na	Na	2013
43	Gratia Dental Care, Tuikual South	74	D	Confidental	A	Na	Na	Na	2013
44	J.T.M Dental Clinic, Khatla	75	D	Confident	Na	Na	Na	Na	2006
45	Dental Zone, Bawngkawn	76	D	Technomac	Na	Na	Na	Na	2013
46	Grace Dental Clinic, Lower Zarkawt	77	D	Ray 68 (W)	A	Na	Na	Na	2016
47	Senorita Dental Clinic, Sikulpuikawn	78	D	AVT	Na	Na	Na	Na	2010
48	Perfect Dental Clinic, Bawngkawn	79	D	Technomac	Na	Na	Na	Na	2008
49	Dental Cave, Chanmari	80	D	Technomac	Na	Na	Na	Na	2014
50	Dental Delight, Chaltlang Darkawn	81	D	Confident C-51I	Na	Na	Na	Na	2010
51	Smile Concept, Thangridema	82	D	Gomex 10 DRS	A	Na	Na	Na	2008

	Building, Dawrpui								
52	Dent-O-Plus, V.L.T. Muana Building, Dawrpui	83	D	CCX Digital Trophy	Na	Na	Na	Na	2005
53	Zoram Dental Chamber, RITZ Building, Dawrpui	84	D	Gomex 10 DRS	A				2005
		85	D	Spectro 70X	Na				2006
54	Lifeline Mammography & X-ray Center, Dawrpui	86	MM	Mammography	Na	Na	Na	Na	2016
		87	F	Allengers 325	A	Na	Na	Na	2016
55	Dental Cave, Dawrpui	88	D	Technomac	Na	Na	Na	Na	2015
56	Lexis Dental Clinic, Dawrpui	89	D	AMS 6010 E	A	Na	Na	Na	2012
57	Kevin Dental Care & Kevin Drug Store, Dawrpui	90	D	Biodent-1070-D	Na	Na	Na	Na	2014
58	Cosmic Dental Care, Dawrpui Jail Veng	91	D	Confident C 70 E	A	Na	Na	Na	2015
59	Shalom Dental Care, Dawrpui Veng	92	D	C 50	Na	Na	Na	Na	1997
60	Alpha Dental Care, Dawrpui	93	D	Confident C 70 F	Na	Na	Na	Na	2010
61	P.D. Dental Clinic, Zarkawt	94	D	Evolution X 3000	Na	Na	Na	Na	2014
62	Smile Care Dental Clinic, Chhinga Veng	95	D	IntraOs 70 BlueX	A	Na	Na	Na	2014

63	V.L. Bela's Dental Clinic	96	D	IntraOs 70 BlueX	A	Na	Na	Na	2004
64	Dentogenic Concept Dental Clinic, Lower Zarkawt	97	D	AMS 6010	A	Na	Na	Na	2011
65	ConfiDENTAL, Zarkawt	98	D	Gomex 10 DRS	A	Na	Na	Na	2010
66	Cee Vee Dental Care, Dawrpui	99	D	IntraOs 70 BlueX	A	Na	Na	Na	2010
67	Dental Escort, Zarkawt	100	D	AMS 6010	A	Na	Na	Na	2012
68	Align Orthodontics, Zarkawt	101	D	Gomax DGT 10	A	Na	Na	Na	2015
69	Damdiai Dental Clinic, Vaivakawn	102	D	IntraOs 70 BlueX	A	Na	Na	Na	2016
70	Dental Plaza, Vaivakawn	103	D	C 5	Na	Na	Na	Na	2010
71	Graceland Dental Clinic, Jail Veng Dawrpui	104	D	C 51	Na	Na	Na	Na	2001
72	Dental Point, Dawrpui	105	D	Denfort International	Na	Na	Na	Na	2011
Lunglei District									
73	Christian Hospital, Serkawn (2)	106	F	Siemens	Na	85	30	6	1972
		107	F	Heliophos D	A	125	500	5	2009
74	Faith Hospital & Research Center, Lunglei	108	F	ME 1010	A	100	100	5	2012

75	Hope Hospital, Lunglei	109	MF	Sappho 1010	Na	100	100	5	2015
76	Lunglei Civil Hospital (3)	110	MF	ME 5085	A	85	50	5	2011
		111	MF	ME 5085	A	85	50	5	2011
		112	F	ME 3010	A	100	300	5	1998
77	John Williams Hospital	113	F	Multiphos 15 Single Tube	A	125	200	Na	2015
78	Lungsen Primary Health Center	114	M	ME 5085	A	85	50	5	2013
79	Chhipphir Primary Health Center	115	MF	ME 5085	A	85	50	5	2011
80	Tlabung Sub-District Hospital (2)	116	MF	Comet 3	Na	85	50	6	1993
		117	MF	Intelix 100mA	Na	100	100	10	2015
81	Hnahthial Community Health Center (2)	118	F	ME 1010	A	125	100	5	2014
		119	MF	Medico-P50	A	85	50	6	2013
82	Cherhlun Primary Health Center	120	MF	Intelix 100mA	Na	100	100	10	2015
83	Buarpui Primary Health Center (2)	121	F	ME 1010	A	100	100	5	2014
		122	MF	ME 5085	A	85	50	5	2010
84	Bunghmun Primary Health Center	123	M	Intelix 100mA	Na	100	100	10	2015
Siaha District									
85	Tuipang Primary Health Center	124	MF	Comet 3	Na	85	50	6	2013

86	Maraland Gospel Centenary Hospital	125	F	DXD-3010 D	Na	125	300	5	2008
87	District Hospital, Siaha (3)	126	F	3085-FR	Na	85	30	5	2010
		127	MF	ME 5085	A	85	50	5	2006
		128	D	AMS 6010	Na	60	10	Na	2012
Kolasib District									
88	Nazareth Nursing Home, Kolasib	129	MF	AMS 60	A	100	60	10	2007
89	Kawnpui Primary Health Center	130	MF	Medico-P50	A	85	50	6	2011
90	Bilkhawthlir Primary Health Center	131	F	ME 1010	A	100	100	5	2013
91	Vairengte Community Health Center (2)	132	MF	Comet 3	Na	85	50	6	2009
		133	MF	Stallion 20P	A	85	20	10	1999
92	District Hospital, Kolasib (3)	134	F	ME 3010	A	100	300	5	2002
		135	D	IRIX-70-23	A	70	8	Na	2011
		136	F	Comet 8	Na	100	100	Na	2009
93	Lungdai Primary Health Center	137	F	ME 1010	A	100	100	5	2014
Mamit District									
94	W Phaileng Primary Health Center	138	MF	EP 331	Na	100	100	30	2014
95	District Hospital, Mamit (2)	139	MF	Intelix 100mA	Na	100	100	10	2012

		140	MF	ME 5085	A	85	50	5	2008
96	Kawrthah Community Health Center (2)	141	F	ME 1010	A	100	100	5	2013
		142	M	ME 5085	A	85	50	5	2012
Champhai District									
97	District Hospital, Champhai (2)	143	MF	ME 5085	A	85	50	5	2002
		144	F	ME 3010	A	100	300	5	2004
98	Bungzung Primary Health Center	145	MF	Intelix 100mA	Na	100	100	10	2015
99	DM Hospital, Champhai	146	F	Olympicks 100D	Na	100	100	5	2011
100	MED AIM Hospital, Zotlang	147	F	OMS 1010 D	Na	100	100	5	2009
101	Khawzawl Community Health Center	148	MF	Comet 3	Na	85	50	6	2008
102	Khawhai Primary Health Center	149	MF	ME 5085	A	85	50	5	2003
103	Biate Community Health Center	150	MF	Stallion 20P	A	85	20	10	1998
104	Khawbung Primary Health Center	151	MF	ME 5085	A	85	50	5	2001
105	Farkawn Primary Health Center	152	MF	Intelix 100mA	Na	100	100	10	2015
106	Kawlkulh Primary Health Center	153	MF	Medico-P50	A	85	50	6	2010
107	Ngopa Community Health Center	154	F	ME 1010	A	100	100	5	2009
Serchhip District									

108	Chhingchhip Primary Health Center	155	MF	Comet 3	Na	85	50	6	2008
109	E Lungdar Primary Health Center	156	MF	Medico-P50	A	85	50	6	2010
110	N Vanlaiphai Primary Health Center	157	MF	Medico-P50	A	85	50	6	2010
111	District Hospital, Serchhip (2)	158	F	ME 3010	A	100	300	5	2004
		159	MF	MDX 100	A	Na	Na	Na	2016
112	Thenzawl Community Health Center (2)	160	MF	Comet 3	Na	85	50	6	2007
		161	F	ME 1010	A	100	100	5	2014
Lawngtlai District									
113	Barapansury Primary Health Center	162	F	Vision Medical Equipment 100mA M	A	Na	Na	Na	2015
		163	F	Allengers	Na	Na	Na	Na	2015
114	Chawngte Community Health Center (2)	164	MF	Stallion 20P	A	85	20	10	1991
		165	F	ME 1010	A	100	100	5	2014
115	District Hospital, Lawngtlai	166	F	ME 3010	A	100	300	5	2002
		167	MF	Stallion 20P	A	85	20	10	1993
116	Christian Hospital, Lawngtlai (2)	168	F	Ergophos	Na	125	300	5	2015
		169	MF	Yamato	Na	90	10	5	1992

[1]MF-mobile fixed X- ray; [2]Na-not known due to old and inadequate record keeping; [3]A-approved unit; [4]F-fixed X-ray; [5]M-mobile X-ray; [6]CT-computed tomography; [7]FL-fluoroscopy; [8]MM-mammography; [9]D-dental X-ray; [10]CL-cath-lab

Appendix III: Table: Workload of diagnostic X-ray facilities in Mizoram (data taken between June 2015 and June 2016)

Sl. No. of X-ray Unit	Patient per day	Film per patient	Tube loading (mAs)	Days per week	Workload (mA-min / week)	Type of examination performed or reason for no workload	Total Workload (mA-min/week)
1	2	1	20	6	4	Chest	21.175
	0.15	1	65	6	0.975	Abdomen	
	0.4	1	30	6	1.2	Skull	
	0	0	0	0	0	IVP*	
	3	1	50	6	15	Others	
2	2	1	20	6	4	Chest	15
	0.2	1	30	6	0.6	Abdomen	
	0.4	2	30	6	2.4	Skull	
	0	0	0	0	0	IVP	
	4	1	20	6	8	Others	
3	0	0	0	0	0	No technician	0
4	0.2	1	20	6	0.4	Chest	1.9
	0.2	1	30	6	0.6	Abdomen	
	0.1	2	30	6	0.6	Skull	

	0	0	0	0	0	IVP	
	0.15	1	20	6	0.3	Others	
5	1	1	80	6	8	Chest	20
	0	0	0	6	0	Abdomen	
	0	0	0	6	0	Skull	
	0	0	0	6	0	IVP	
	3	1	40	6	12	Others	
6	1	1	25	6	2.5	Chest	20
	0.2	2	50	6	2	Abdomen	
	0.1	1	50	6	0.5	Skull	
	0	0	0	6	0	IVP	
	3	2	25	6	15	Others	
7	10	1	40	6	40	Chest	250
	5	2	60	6	60	Abdomen	
	5	2	45	6	45	Skull	
	2	5	60	6	60	IVP	
	15	1	30	6	45	Others	
8	0.1	1	60	6	0.6	Chest	1.3

	0	0	0	6	0	Abdomen	
	0.1	1	70	6	0.7	Skull	
	0	0	0	6	0	IVP	
	0	0	0	6	0	Others	
9	0	0	0	0	0	Out of order	0
10	0	0	0	0	0	Not used	0
11	1	1	30	6	3	Chest	13.6
	0.4	1	40	6	1.6	Abdomen	
	1	2	30	6	6	Skull	
	0	0	0	0	0	IVP	
	2	1	15	6	3	Others	
12	1	1	50	6	5	Chest	36.5
	1	2	120	6	24	Abdomen	
	0.5	1	70	6	3.5	Skull	
	0	0	0		0	IVP	
	1	1	40	6	4	Others	
13	7	1	87	6	60.9	CT-Scan	60.69
14	0	0	0	0	0	Out of order	0

15	15	1	12	6	18	Chest	474
	5	2	120	6	120	Abdomen	
	4	2	120	6	96	Skull	
	0	0	0		0	IVP	
	60	1	40	6	240	Others	
16	5	1	32	6	16	Chest	172
	1	1	120	6	12	Abdomen	
	0	0	0		0	Skull	
	2	6	120	6	144	IVP	
	0	0	0	0	0	Others	
17	50	1	10	6	50	Chest	50
18	0	0	0	6	0	Not used	0
19	0	0	0	0	0	Not used	0
20	7	1	101	6	70.7	CT-Scan	70.7
21	7	1	90	6	63	Mammography	63
22	0	0	0	6	0	Not used	0
23	0	0	0	6	0	Not used	0
24	4	1	25	6	10	Others	10

25	0	0	0	6	0	Not used	0
26	3	1	6.4	6	1.92	Dental X-ray	1.92
27	0	0	0	0	0	Not used	0
28	3	1	7	6	2.1	Others	2.1
29	20	1	16	6	32	Chest	136
	15	1	40	6	60	Abdomen	
	5	1	40	6	20	Skull	
	0	0	0		0	IVP	
	20	1	12	6	24	Others	
30	5	1	20	6	10	Not used	10
31	5	1	40	6	20	Chest	21.25
	0	0	0	0	0	Abdomen	
	0	0	0	0	0	Skull	
	0	0	0	0	0	IVP	
	0.5	1	25	6	1.25	Others	
32	0	0	0	0	0	Out of order	0
33	1	1	16	6	1.6	Not used	1.6
34	15	1	6	6	9	Chest	289

	10	1	20	6	20	Abdomen	
	10	2	30	6	60	Skull	
	8	5	40	6	160	IVP	
	20	1	20	6	40	Others	
35	30	1	10	6	30	Chest	120
	5	1	30	6	15	Abdomen	
	5	2	30	6	30	Skull	
	3	3	30	6	27	IVP	
	15	1	12	6	18	Others	
36	5	1	20	6	10	Fluoroscopy	10
37	6	1	20	6	12	Fluoroscopy	12
38	6	1	20	6	12	Fluoroscopy	12
39	6	1	101	6	60.6	CT-Scan	60.6
40	0.1	1	20	6	0.2	Chest	50.2
	0	0	0	0	0	Abdomen	
	0	0	0	0	0	Skull	
	0	0	0	0	0	IVP	
	10	1	50	6	50	Others	

41	5	1	18	6	9	Chest	31.4
	0	0	0	0	0	Abdomen	
	5	1	40	6	20	Skull	
	0	0	0	0	0	IVP	
	3	1	8	6	2.4	Others	
42	3	1	16	6	4.8	Chest	10.5
	1	1	18	6	1.8	Abdomen	
	0	0	0	0	0	Skull	
	0.1	5	18	6	0.9	IVP	
	5	1	6	6	3	Others	
43	4	1	16	6	6.4	Dental X-ray	6.4
44	6	1	40	6	24	Chest	44.4
	1	1	44	6	4.4	Abdomen	
	0	0	0	0	0	Skull	
	0.3	5	40	6	6	IVP	
	5	1	20	6	10	Others	
45	5	1	20	6	10	Fluoroscopy	10
46	10	1	50	6	50	Chest	185

	2	2	80	6	32	Abdomen	
	1	1	70	6	7	Skull	
	2	1	80	6	16	IVP	
	10	1	80	6	80	Others	
47	8	1	20	6	16	Fluoroscopy	16
48	2	1	65	6	13	Chest	36.53
	0.5	1	86	6	4.3	Abdomen	
	0.1	1	89	6	0.89	Skull	
	0.1	6	89	6	5.34	IVP	
	2	1	65	6	13	Others	
49		0	0	0	0	Newly installed	0
50	20	1	50	6	100	Chest	297
	10	1	80	6	80	Abdomen	
	1	1	70	6	7	Skull	
	5	1	70	6	35	IVP	
	15	1	50	6	75	Others	
51	15	1	8	6	12	Chest	104.5
	7	1	30	6	21	Abdomen	

	3	1	30	6	9	Skull	
	5	3	25	6	37.5	IVP	
	10	1	25	6	25	Others	
52	20	1	25	6	50	Chest	173
	5	2	60	6	60	Abdomen	
	5	1	60	6	30	Skull	
	1	5	60	6	30	IVP	
	0.5	1	60	6	3	Others	
53	6	1	28	6	16.8	Chest	53.28
	0.1	1	28	6	0.28	Abdomen	
	3	1	50	6	15	Skull	
	0.5	6	28	6	8.4	IVP	
	8	1	16	6	12.8	Others	
54	7	1	35	6	24.5	Chest	48
	0.5	2	50	6	5	Abdomen	
	1	2	50	6	10	Skull	
	0.1	5	50	6	2.5	IVP	
	3	1	20	6	6	Others	

55	1	1	30	6	3	Chest	10.05
	0	0	0	0	0	Abdomen	
	0.2	1	40	6	0.8	Skull	
	0	0	0	0	0	IVP	
	2.5	1	25	6	6.25	Others	
56	4	1	48	6	19.2	Chest	212.04
	0	0	0	0	0	Abdomen	
	0.07	1	120	6	0.84	Skull	
	0	0	0	0	0	IVP	
	8	2	120	6	192	Others	
57	15	1	24	6	36	Chest	70.4
	5	2	20	6	20	Abdomen	
	0.5	1	32	6	1.6	Skull	
	2	1	24	6	4.8	IVP	
	5	1	16	6	8	Others	
58	6	1	50	6	30	CT Scan	30
59	8	1	20	6	16	Fluoroscopy	16
60	1	1	14.4	6	1.44	Dental X-ray	1.44

61	3	1	48	6	14.4	Chest	36.6
	1	1	30	6	3	Abdomen	
	1	1	48	6	4.8	Skull	
	0	0	0	0	0	IVP	
	3	1	48	6	14.4	Others	
62	2	4	14.4	6	11.52	Dental X-ray	11.52
63	5	1	20	6	10	Chest	21.2
	0	0	0	0	0	Abdomen	
	0.1	6	20	6	1.2	Skull	
	0	0	0	0	0	IVP	
	5	1	20	6	10	Others	
64	0.13	1	30	6	0.39	Others	0.39
65	1	1	50	6	5	Others	5
66	1	1	50	6	5	Others	5
67	5	1	28	6	14	Chest	23.1
	0	0	0	0	0	Abdomen	
	1	1	55	6	5.5	Skull	
	0	0	0	0	0	IVP	

	3	1	12	6	3.6	Others	
68	1	1	9.6	6	0.96	Dental X-ray	0.96
69	0.16	2	24	6	0.768	Dental X-ray	0.768
70	0.24	2	4.2	6	0.2016	Dental X-ray	0.2016
71	3	1	4.2	6	1.26	Dental X-ray	1.26
72	0	0	0	0	0	Not used	0
73	2	3	24	6	14.4	Dental X-ray	14.4
74	3	1	5.46	6	1.638	Dental X-ray	1.638
75	3	1	5.6	6	1.68	Dental X-ray	1.68
76	4	3	7.2	6	8.64	Dental X-ray	8.64
77	2	2	4.2	6	1.68	Dental X-ray	1.68
78	5	3	4.8	6	7.2	Dental X-ray	7.2
79	0.08	1	4.8	6	0.0384	Dental X-ray	0.0384
80	3	1	11.2	6	3.36	Dental X-ray	3.36
81	10	1	3.2	6	3.2	Dental X-ray	3.2
82	7	1	16	6	11.2	Dental X-ray	11.2
83	2	1	10	6	2	Dental X-ray	2
84	10	1	11.2	6	11.2	Dental X-ray	11.2

85	10	2	4	6	8	Dental X-ray	8
86	2	1	20	6	4	Mammography	4
87	5	1	20	6	10	Others	10
88	5	1	8	6	4	Dental X-ray	4
89	3	1	11.2	6	3.36	Dental X-ray	3.36
90	1	1	12.5	6	1.25	Dental X-ray	1.25
91	3	1	4.55	6	1.365	Dental X-ray	1.365
92	0	0	0	0	0	Not used	0
93	3	1	12	6	3.6	Dental X-ray	3.6
94	2	1	5.6	6	1.12	Dental X-ray	1.12
95	0.83	1	8	6	0.664	Dental X-ray	0.664
96	2	1	4.55	6	0.91	Dental X-ray	0.91
97	2	1	5	6	1	Dental X-ray	1
98	5	1	14.4	6	7.2	Dental X-ray	7.2
99	2	1	4.55	6	0.91	Dental X-ray	0.91
100	7	1	7	6	4.9	Dental X-ray	4.9
101	0.5	1	24	6	1.2	Dental X-ray	1.2
102	0.5	1	2.45	6	0.1225	Dental X-ray	0.1225

103	0.4	1	8	6	0.32	Dental X-ray	0.32
104	3	1	8.8	6	2.64	Dental X-ray	2.64
105	3	1	12.64	6	3.792	Dental X-ray	3.792
106	10	1	45	6	45	Chest	69
	2	1	60	6	12	Abdomen	
	0	0	0	6	0	Skull	
	0	0	0	6	0	IVP	
	10	1	12	6	12	Others	
107	2	1	30	6	6	Chest	66.65
	5	1	40	6	20	Abdomen	
	3	2	40	6	24	Skull	
	0.17	9	50	6	7.65	IVP	
	3	1	30	6	9	Others	
108	10	1	30	6	30	Chest	130.5
	3	1	75	6	22.5	Abdomen	
	3	2	125	6	75	Skull	
	0	0	0	6	0	IVP	
	3	1	10	6	3	Others	

109	20	1	32	6	64	Chest	504
	5	2	40	6	40	Abdomen	
	0	0	0	6	0	Skull	
	0	0	0	6	0	IVP	
	10	20	20	6	400	Others	
110	1	1	30	6	3	Chest	78
	3	3	50	6	45	Abdomen	
	0	0	0	6	0	Skull	
	0	0	0	6	0	IVP	
	15	1	20	6	30	Others	
111	20	1	35	6	70	Chest	84
	2	1	40	6	8	Abdomen	
	0	0	0	6	0	Skull	
	0	0	0	6	0	IVP	
	2	1	30	6	6	Others	
112	0	0	0	0	0	Out of order	0
113	0	0	0	0	0	Out of order	0
114	0	0	0	0	0	No technician	0

115	0	0	0	0	0	Out of order	0
116	0	0	0	0	0	No technician	0
117	0	0	0	0	0	Not used	0
118	5	1	40	6	20	Chest	73.5
	1	1	125	6	12.5	Abdomen	
	1	2	125	6	25	Skull	
	0	0	0	6	0	IVP	
	10	1	16	6	16	Others	
119	0	0	0	0	0	Not used	0
120	0	0	0	0	0	Not used	0
121	0.5	1	30	6	1.5	Chest	3.9
	0	0	0	6	0	Abdomen	
	0.1	2	40	6	0.8	Skull	
	0	0	0	6	0	IVP	
	0.2	2	40	6	1.6	Others	
122	0	0	0	0	0	Out of order	0
123	0	0	0	0	0	Not used	0
124	0	0	0	0	0	Not used	0

125	10	1	30	6	30	Chest	72
	3	1	50	6	15	Abdomen	
	1	2	30	6	6	Skull	
	0	0	0	6	0	IVP	
	7	1	30	6	21	Others	
126	0	0	0	0	0	Not used	0
127	0	0	0	0	0	Not used	0
128	1	1	30	6	3	Dental X-ray	3
129	0.5	1	12	6	0.6	Chest	0.84
	0	0	0	6	0	Abdomen	
	0	0	0	6	0	Skull	
	0	0	0	6	0	IVP	
	0.4	1	6	6	0.24	Others	
130	5	1	25	6	12.5	Chest	26.5
	2	1	40	6	8	Abdomen	
	0	0	0	6	0	Skull	
	0	0	0	6	0	IVP	
	6	1	10	6	6	Others	

131	1	1	30	6	3	Chest	7
	0	0	0	6	0	Abdomen	
	0	0	0	6	0	Skull	
	0	0	0	6	0	IVP	
	2	1	20	6	4	Others	
132	0	0	0	6	0	Chest	11
	0.1	1	30	6	0.3	Abdomen	
	0.4	2	40	6	3.2	Skull	
	0	0	0	6	0	IVP	
	3	1	25	6	7.5	Others	
133	1	1	20	6	2	Others	2
134	10	1	80	6	80	Chest	192
	2	1	120	6	24	Abdomen	
	2	2	120	6	48	Skull	
	0	0	0	6	0	IVP	
	10	1	40	6	40	Others	
135	0	0	0	0	0	Not used	0
136	0	0	0	0	0	Not used	0

137	0	0	0	0	0	Not used	0
138	0	0	0	0	0	Out of order	0
139	0	0	0	0	0	Out of order	0
140	10	1	40	6	40	Chest	79.4
	5	1	50	6	25	Abdomen	
	2	2	30	6	12	Skull	
	0	0	0	0	0	IVP	
	8	1	3	6	2.4	Others	
141	4	1	20	6	8	Chest	39.4
	1	1	40	6	4	Abdomen	
	2	1	125	6	25	Skull	
	0	0	0	6	0	IVP	
	6	1	4	6	2.4	Others	
142	3	1	20	6	6	Chest	14
	0	0	0	6	0	Abdomen	
	0	0	0	6	0	Skull	
	0	0	0	6	0	IVP	
	8	1	10	6	8	Others	

143	7	1	30	6	21	Chest	53
	1	1	40	6	4	Abdomen	
	1	2	65	6	13	Skull	
	0	0	0	6	0	IVP	
	5	1	30	6	15	Others	
144	0	0	0	0	0	Out of order	0
145	0	0	0	0	0	Not used	0
146	3	1	12	6	3.6	Chest	18.4
	2	1	40	6	8	Abdomen	
	0.15	2	60	6	1.8	Skull	
	0	0	0	6	0	IVP	
	5	1	10	6	5	Others	
147	3	1	18	6	5.4	Chest	12.5
	0.2	3	40	6	2.4	Abdomen	
	0.1	1	50	6	0.5	Skull	
	0	0	0	6	0	IVP	
	3	1	14	6	4.2	Others	
148	1	2	50	6	10	Chest	134

	2	2	250	6	100	Abdomen	
	0	0	0	6	0	Skull	
	0	0	0	6	0	IVP	
	4	2	30	6	24	Others	
149	1	3	50	6	15	Chest	48
	0.2	3	50	6	3	Abdomen	
	0	0	0	6	0	Skull	
	0	0	0	6	0	IVP	
	2	3	50	6	30	Others	
150	1	1	50	6	5	Chest	16
	0.2	1	50	6	1	Abdomen	
	0	0	0	6	0	Skull	
	0	0	0	6	0	IVP	
	2	1	50	6	10	Others	
151	5	1	20	6	10	Chest	14
	0	0	0	6	0	Abdomen	
	0	0	0	6	0	Skull	
	0	0	0	6	0	IVP	

	2	1	20	6	4	Others	
152	0	0	0	0	0	Not used	0
153	0	0	0	0	0	Not used	0
154	2	1	15	6	3	Chest	6.175
	0.15	1	25	6	0.375	Abdomen	
	0.1	2	40	6	0.8	Skull	
	0	0	0	6	0	IVP	
	2	1	10	6	2	Others	
155	0.2	1	30	6	0.6	Chest	1
	0	0	0	6	0	Abdomen	
	0	0	0	6	0	Skull	
	0	0	0	6	0	IVP	
	0.2	1	20	6	0.4	Others	
156	0	0	0	0	0	Out of order	0
157	5	1	30	6	15	Chest	40
	0	0	0	6	0	Abdomen	
	0	0	0	6	0	Skull	
	0	0	0	6	0	IVP	

	10	1	25	6	25	Others	
158	8	1	20	6	16	Chest	36
	1	1	30	6	3	Abdomen	
	2	2	35	6	14	Skull	
	0	0	0	6	0	IVP	
	3	1	10	6	3	Others	
159	0	0	0	0	0	Not used	0
160	0.1	1	18	6	0.18	Chest	0.38
	0	0	0	6	0	Abdomen	
	0	0	0	6	0	Skull	
	0	0	0	6	0	IVP	
	0.2	1	10	6	0.2	Others	
161	5	1	30	6	15	Chest	35.5
	2	1	40	6	8	Abdomen	
	1	2	50	6	10	Skull	
	0	0	0	6	0	IVP	
	2	1	12.5	6	2.5	Others	
162	0	0	0	0	0	Not installed	0

163	0	0	0	0	0	Not installed	0
164	10	1	15	6	15	Chest	25
	0	0	0	6	0	Abdomen	
	0	0	0	6	0	Skull	
	0	0	0	6	0	IVP	
	10	1	10	6	10	Others	
165	10	1	25	6	25	Chest	72
	5	1	30	6	15	Abdomen	
	2	2	45	6	18	Skull	
	0	0	0	6	0	IVP	
	7	1	20	6	14	Others	
166	5	1	40	6	20	Chest	57.5
	0.5	1	50	6	2.5	Abdomen	
	2	2	50	6	20	Skull	
	0	0	0	6	0	IVP	
	5	1	30	6	15	Others	
167	0	0	0	0	0	Not used	0
168	0	0	0	6	0	Chest	54

	3	1	50	6	15	Abdomen	
	2	2	60	6	24	Skull	
	0	0	0	6	0	IVP	
	5	1	30	6	15	Others	
169	6	1	20	6	12	Chest	12

*IVP-Intravenous pyelogram

REFERENCES

Adhikari K.P., Jha L.N., Galan M.P. (2012), Status of radiation protection at different hospitals in Nepal, *J. Med. Phys.* 37(**4**): 240−244. doi: 10.4103/0971-6203.103611

Ahmad M. A. (2015), Safety of analytical X-ray appliances, Master's Thesis, University of Helsinki, Finland. Retrieved from: https://helda.helsinki.fi/handle/10138/155063 (22 May 2016)

Al-Kinani A.T. and Mohsen Yassin (2014), Study of the Quality Assurance of Conventional X-ray units at Medical city in Baghdad, *Arab Jr. of Nucl. Sci. & Appl.* 47(**2**): 129−137.

American Association of Physicists in Medicine (1981), Publication Committee, '*Basic in Diagnostic Radiology'*, AAPM Report No **4**, American Inst. of Phys. New York.

American Association of Physics in Medicine (1988), Publication Committee, '*Protocols for the Radiation Safety Surveys of Diagnostic Radiological Equipment*', AAPM Report No **25**, American Inst. of Phys. New York.

Amin Y.M., Rifiat M.N., Razak A.F.A., Lawai A. (2012), Radiological Safety Survey of Diagnostic Medical X-ray Machines Use in Private and Public Medical Facilities in Malaysia, *Prog. in Nucl. Sci. & Tech.* **3**: 146–148. DOI: 10.15669/pnts.3.146

Ammann E. and Kutschera (1997), X-ray tubes continuous innovative technology, *Brit. J. Radiol.* **70**, S1–S9. https://doi.org/10.1259/bjr.1997.0002

Archer B.R. (1994), Attenuation properties of diagnostic x-ray shielding materials, *Med. Phys.* 21(**9**), 1499−1507. doi: 10.1118/1.597408

Archer B.R. (1995), History of the shielding of diagnostic X-ray facilities, *Health Phys.* 69 (**5**): 750–758. **DOI:** 10.1097/00004032-199511000-00009

Archer B.R. (2005), Recent history of the shielding of medical X-ray imaging facilities, *Health Phys.* **88**: 579−586.

Archer B.R. and Gray J.E. (2005), Important changes in medical x-ray imaging shielding design methodology, A brief summary of recommendations in NCRP Report No. **147**, *Med. Phys.* 32(**12**), 3599−3601. doi: 10.1118/1.2124587

Asadinezhad M., Bahreyni Toossi M.T., Ebrahiminia A., Giahi M. (2017), Quality Control Assessment of Conventional Radiology Devices in Iran, *Iran. J. Med. Phys.* Mar 1;14(**1**): 1–7.

Atomic Energy Organization of Iran (2012), *Quality Control Procedure in Diagnostic Medical Imaging Devices*, (INRA-RP-RE-121-00/25-0-Esf.1387):**103**.

Atomic Energy Regulatory Board (1983), Notification No. 25/2/83-ER, Constitution of AERB, The Gazette of India, Part-II, Section 3(**ii**).

Atomic Energy Regulatory Board (1986), Safety Code No. AERB/SC/MED-**2**, '*Safety Code for Medical Diagnostic X-ray Equipment and Installations*' Approved by the Board on December, 1986, Mumbai, India.

Atomic Energy Regulatory Board (2001), Safety Code No. AERB/SC/MED-2 (**Rev.1**), '*Safety Code for Medical Diagnostic X-ray Equipment and Installations*' Approved by the Board on October 5, 2001, Mumbai, India.

Atomic Energy Regulatory Board (2006), Notification No. 30.1.2002-ER, Appointment of Chairman, AERB as the 'Competent Authority' of radiation protection in India, The Gazette of India, Part-II, Section 3(**ii**).

Atomic Energy Regulatory Board, Radiological Safety Division, Anushaktinagar, Mumbai, India. Format for Quality Assurance test for diagnostic X-ray equipment. Retrieved from: https://www.aerb.gov.in/images/PDF/DiagnosticRadiology/1-FORMAT-FOR-QUALITY-ASSURANCE-TEST-FOR-DIAGNOSTIC-X-RAY-EQUIPMENT.pdf (2 February 2017)

Atomic Energy Regulatory Board, Government of India, e-licensing of radiations applications (eLORA) system, Mumbai; updated 17th March 2019; cited 18 March 2019. Retrieved from: https://elora.aerb.gov.in/ELORA/prePopulateGraphData.htm (18 March 2019)

Bennett B.G. (1991), Exposures from Medical Radiation World-Wide, *Radiat. Prot. Dosim.* 36(**2−4**): 237–242. https://doi.org/10.1093/oxfordjournals.rpd.a081004

Binks W. (1955), Some aspects of radiation hygiene, *Brit. J. Radiol.* **28**: 654–661. https://doi.org/10.1259/0007-1285-28-336-654

Bosnjak J., Ciraj-Bjelac O., Strbac B. (2008), Implementation of quality assurance in diagnostic radiology in Bosnia and Herzegovina (Republic of Srpska), *Radiat. Prot. Dosim.* Feb; 129(**1–3**): 249–252. DOI: 10.1093/rpd/ncn011.

Brodsky A. and Kathren R.L. (1989), Historical Development of Radiation Safety Practices in Radiology, *Radiographics* **9**: 1267−1275. https://doi.org/10.1148/radiographics.9.6.2685944

Bushong S.C. (2013), *Radiologic science for Technologists: Physics, Biology, and Protection*, **tenth edition**, Elsevier Mosby, 3251 Riverport Lane, St. Louis, Missouri, USA, pp. 578 – 579.

Canada Metal, What makes lead good for radiation shielding? 8271 Lafrenaie, Montreal, Quebec. Retrieved from: https://*www*.canadametal.com/lead-good-for-radiation-shielding (5 April 2019).

Carlsson Carl A. and Carlsson Gudrun A. (1996), *Basic physics of X-ray imaging*, **second edition**, Department of Radiation Physics, Faculty of Health Sciences, Linkoping university, Sweeden.

Chen M.Y.M., Swearingen F.L.V., Mitchell R., Ott D.J. (1996), Radiation exposure during ERCP: effect of a protective shield, *Gastrointest. Endosc.* 43(**1**):1–5. https://doi.org/10.1016/S0016-5107(96)70250-X

Cousins C. and Sharp C. (2004), Medical interventional procedures—reducing the radiation risks, *Clin. Radiol.* 59(**6**): 468–473.

Cunha P., Freire B., Drexler G. (1992), Occupational exposure in X-ray diagnosis in Brazil, *Radiat. Prot. Dosim.* 43(**1−4**): 55–58. https://doi.org/10.1093/rpd/43.1-4.55

Curry T.S. III, Dowdy J.E., Murry R.C. Jr. (1990), *Attenuation. In: Christensen's physics of diagnostic radiology*, **fourth edition**, Lea & Febiger, Philadelphia, 70−92.

Dixon R.L. (1994), On the primary barrier in diagnostic x-ray shielding. *Med. Phys.* **21**: 1785−1793. https://doi.org/10.1118/1.597217

Ebisawa M.L.N.I., Magon M.F.A., Mascarenhas Y.M. (2009), Evolution of X-ray machine quality control acceptance indices, *J. App. Clin. Med. Phys.* 10(**4**): 252–259.

Esmaeili S. (2006), Measurement of patient skin dose of common techniques in diagnostic radiology in 15 radiology centers and quality control of those units in Mashhad, in Medical Physics, Mashhad University of Medical Sciences.

Euratom Radiation Protection No 91, Criteria for acceptability of radiological and nuclear medicine installations, Euratom Treaty and the Council Directives; European commission. Retrieved from: https://ec.europa.eu/energy/sites/ener/files/documents/091_en.pdf (15 July 2017)

European Commission (1996), *European guidelines on quality criteria for diagnostic radiographic images*, Publication EUR 16260 EN, Brussels, Belgium.

Evans R.D. (1955), *The atomic nucleus*, Malabar, FL: Krieger; 1985, Reprint of original, McGraw-Hill, New York, USA.

Faraj K.A., Ali R.T., Saeed A.O. (2013), Quality Control and Radiation Dose Measurement from Diagnostic X-ray Examination at different places of Hospitals in Sulaimania, *Int. J. Rec. Res. App. Stud.* 16(**2**): 62−72.

Gholamhosseinian-Najjar H., Bahreyni-Toosi M.T., Zare M.H., Sadeghi H.R., Sadoughi H.R. (2014), Quality Control Status of Radiology Centers of Hospitals Associated with Mashhad University of Medical Sciences, *Iran. J. Med. Phys.* Apr 1; 11(**1**): 182–187 DOI: 10.22038/ijmp.2014.2625.

Gholami M., Nemati F., Karami V. (2015), The Evaluation of Conventional X-ray Exposure Parameters Including Tube Voltage and Exposure Time in Private and Governmental Hospitals of Lorestan Province, Iran, *Iran. J. Med. Phys.* 12 (**2**); 85–95.

González A.B. and Darby S. (2004), Risk of cancer from diagnostic X-rays: estimates for the UK and 14 other countries, *The Lancet* **363**: 345–351. DOI:10.1016/S0140-6736(04)15433-0

Gori C., Belli G., Calvagno S., Capaccioli L. (1995), Quality Control in the Radiological Departments of the Florence General Hospital, *Radiat. Prot. Dosim.* 57(**1−4**): 315–316. DOI: 10.1093/oxfordjournals.rpd.a082550

Gray J.E., Winkler N.T., Stears J., Frank E.D. (1983), *Quality Control in Diagnostic Imaging*, An Aspen Publication, Maryland, USA.

Gray J.E., Archer B.R., Butler P.F., Hobbs B.B., Mettler F.A., Pizzutiello R.J., Schueler B.A., Strauss K.J., Suleiman O.H., Yaffe M.J. (2005), Reference values for diagnostic radiology: application and impact, *Radiology* **235**: 354−358. https://doi.org/10.1148/radiol.2352020016

Grover S.B., Kumar J., Gupta A., Khanna L. (2002), Protection against hazards: Regulatory bodies, safety norms, dose limits and protection devices, *Indian J. Radiol. Imag.* **12**: 157–167.

Haghparast M., Afzali Pour R., Ahmadi S., Golverdi Yazdi MS., Dindarloo Inaloo K., Saanei M. (2015), Quality control of radiology devices in Health Centers Affiliated with Hormozgan University of Medical Sciences, *Hormozgan Med. J.* 19(**1**): 51–57.

Hamed A.A., Elshirbiny N., Nassef M.H. (1999), Study of Radiation Exposure Dependence on the Physical Parameters of Medical Diagnostic X-ray Machines, *Radiat. Prot. Dosim.* 82(**4**): 277−283. https://doi.org/10.1093/oxfordjournals.rpd.a032636

Hart D., Hillier M.C., Wall B.F. (2002), *Doses to patients from medical x-ray examinations in the UK: 2000 review*, National Radiological Protection Board NRPB-W **14**. Oxfordshire, United Kingdom.

Hashemi M., Bayani Sh., Shahedi F., Momennezhad M., Zare H., Gholamhosseinian H. (2019), Quality assessment of conventional X-ray diagnostic equipment by measuring X-ray exposure and tube output parameters in Great Khorasan Province, Iran, *Iran. J. Med. Phys.* Jan; 16(**1**): 34–40.

Hassan G.M., Rabie N., Mustafa K.A., Abdel-Khalik S.S. (2012), Study on the quality assurance of diagnostic X-ray machines and assessment of the absorbed dose to patients, *Radiat. Eff. Defects S.* Sep; 167(**9**): 704–711. DOI: 10.1080/10420150.2011.559238

Havukainen R. and Pirinen M. (1993), Patient dose and image quality in five standard x-ray examinations, *Med. Phys.* **20**: 813−817. https://doi.org/10.1118/1.596987

Health Canada (2008), Safety code 35: Safety procedures for the installation, use and control of x-ray equipment in large medical radiological facilities. Retrieved from: http://www.hc-sc.gc.ca (22 January 2017)

Herman Cember and Thomas E. Johnson (2009), *Introduction to Health Physics*, **fourth edition**, McGraw-Hill, USA.

Huda W. (2015), Radiation Risks: What Is to Be Done? American Roentgen Ray Society, 124–127. https://www.ajronline.org/doi/10.2214/AJR.14.12834

Institute of Physics and Engineering in Medicine (1998), *Recommended standards for the routine performance testing of diagnostic x-ray imaging systems*, IPEM Report No. **77**, York, England.

International Atomic Energy Agency (1996), Food and Agriculture Organization of the United Nations, International Atomic Energy Agency, International Labor Organization, OECD Nuclear Energy Agency, Pan American Health Organization, World Health Organization. *International basic safety* *standards for protection against ionizing radiation and for the safety of radiation sources: safety series no.* ***115***. Vienna, Austria.

International Atomic Energy Agency (2014), *Diagnostic radiology physics; a handbook for teachers and students*, Vienna International Centre, Vienna, Austria.

International Commission on Radiological Protection (1982), *Protection of the patient in diagnostic radiology*, ICRP publication **34**, Pergamon Press, Oxford, United Kingdom.

International Commission on Radiological Protection (1991), *1990 recommendations of the International Commission on Radiological Protection: annals of the ICRP, 21 (**1-3**), publication* ***60***, Pergamon Press, Oxford, United Kingdom.

International Commission on Radiological Protection (2001), *Avoidance of radiation injuries from medical interventional procedure*, Annals of ICRP, ICRP Publication **85**, 30(**2**).

International Commission on Radiological Protection ICRP **103**, *The 2007 Recommendations of the International Commission on Radiological Protection*, Ann. ICRP. 2007; 37(**2–4**).

Jankowski J., Staniszewska M.A. (2000), Methodology for the set-up of a quality control system for diagnostic X-ray units in Poland, *Radiat. Prot. Dosim.* 90(**1-2**): 259–262. https://doi.org/10.1093/oxfordjournals.rpd.a033133

Johns Harold E. and Cunningham John R. (1983), *The Physics of Radiology,* **fourth edition**, Charles C Thomas publisher, South First Street, Springfield, Illinois, USA. ISBN 0-398-04669-7

Johnston James N. and Fauber Terri L. (2012), *Essentials of radiographic physics and imaging*, Elsevier Mosby, 3251 Riverport Lane, St. Louis, Missouri, USA. ISBN: 978-0-323-06974-8

Jomehzadeh Z., Jomehzadeh A., Tavakoli M.B. (2016), Quality control Assessment of Radiology Devices in Kerman Province, Iran, *Iran. J. Med. Phys.* Mar 1; 13(**1**): 25–35. DOI: 10.22038/ijmp.2016.7142.

Kathren R.L. (1964), William H. Rollins (1852−1929): X-ray Protection Pioneer, *J. Hist. Med. Allied Sci.* 19(**3**), 287–295. https://doi.org/10.1093/jhmas/XIX.3.287

Kharita M.H., Khedr M.S., Wannus K.M. (2008), A comparative study of quality control in diagnostic radiology, *Radiat. Prot. Dosim.* Jul 1; 130(**4**): 447–451. DOI: 10.1093/rpd/ncn096.

Kharita M.H., Wannus K.M., Khedr M.S. (2017), Evaluation of the Quality Control Program for Diagnostic Radiography and Fluoroscopy Devices in Syria during 2005−2013, *Iran. J. Med. Phys.* 14(**2**): 92−97. 10.22038/ijmp.2017.19712.1186

Khoshbin Khosnazar A., Hejazi P., Mokhtarian M., Nooshi S. (2013), Quality Control of radiography equipments in Golestan Province of Iran, *Iran. J. Med. Phys.* Jan 1; 10(**1**): 37–44. DOI: 10.22038/ijmp.2013.917.

Klein O, Nishina Y. (1929), Uber die Streuung von Strahlung durch freie Elektronen nach der neuen relativistischen Quanten-dynamik von Dirac, *Zeit. Fur. Phys.* **52**: 853−868; (in German).

Lee J., Cha E.S., Jeong M., Lee W.J. (2015), A national survey of occupational radiation exposure among diagnostic radiologic technologists in South Korea, *Radiat. Prot. Dosim.* 167(**4**): 525−531. https://doi.org/10.1007/BF01366453

Maree G.J. (1995), *Determination of the genetically-significant dose from diagnostic radiology for the South African population 1990–1991*, Phd Thesis of the University of Cape Town, South Africa.

McKetty Marlene H. (1998), *The AAPM/RSNA Physics Tutorial for Residents-X-ray Attenuation*, Department of Radiology, Howard University Hospital, 2041 Georgia Ave, NW, Washington, DC 20060, *Radiographics* **18**:151−163. https://doi.org/10.1148/radiographics.18.1.9460114

Meredith W.J. and Massey J.B. (1992), *Fundamental Physics of Radiology,* **third edition**, Varghese Publishing House, Bombay, India.

Mettler F.A. (2001), *Radiological risks associated with the various uses of radiation in medicine within the context of their associated benefits,* Proceedings of international conference 26−30 March 2001, Malaga, Vienna, Austria: International Atomic Energy Agency, 119−127.

Muhogora W.E. and Nyanda A.M. (2001), The Potential for reduction of Radiation doses to patients undergoing some common X-ray examinations in Tanzania, *Radiat. Prot. Dosim.* 94(**4**): 381−384. doi:rpd;94/4/381

Muhogora W.E., Ahmed N.A., Almosabihi A., Alsuwaidi J.S., Beganovic A., Ciraj-Bjelac O., Kabuya F.K., Krisanachinda A., Milakovic M., Mukwada G., Ramanandraibe M.J., Rehani M.M., Rouzitalab J., Shandorf C. (2008), Patient Doses in Radiographic Examinations in 12 Countries in Asia, Africa, and Eastern Europe: Initial Results from IAEA Projects, *American Roentgen Ray Society*, **190**: 1453- 1461. DOI: 10.2214/AJR.07.3039

National Council on Radiation Protection and Measurements (1989), *Medical X-ray, Electron beam and Gamma-ray Protection for energies up to 50 MeV (Equipment Design, Performance and use)*, NCRP Report, **102**, Bethesda, Maryland, USA.

National Council on Radiation Protection and Measurements (1990), *Quality assurance for diagnostic imaging*, NCRP Report **99**, Bethesda, Maryland, USA.

National Council on Radiation Protection and Measurements (2004), *Structural shielding design for medical X-rays imaging facilitie*s, NCRP Report, **147,** Bethesda, Maryland, USA.

Neofotistou V., Molfetas M., Panagiotakis N. (1995), Quality Control in Conventional Diagnostic Radiology in Greece, *Radiat. Prot. Dosim.* Jan 1; 57(**1–4**): 293–296. DOI 10.1093/oxfordjournals.rpd.a082545.

Operator Manual (2005), 07-661-7662 Collimator/Beam Alignment Test Tool, Fluke Corporation, USA.

Operator Manual Victoreen 07-494 (2006), Manual No. 168001 Rev **4**, Fluke Biomedical, Radiation Management Services, 6045 Cochran Road, Cleveland, Ohio, USA.

Operator Manual 06-526 RAD-CHECK^{TM} PLUS (2006), P/N 136201, Rev. **6**, Fluke Corporation, USA.

Operator Manual 451P (2013), Ion Chamber Survey Meter, PN FBC-0059, Rev **1**, Fluke Corporation, USA. Retrieved from: flukebiomedical.com/biomedical/usen/radiation-safety/survey-meters/451p-radiation-detector-ion-chamber-survey-meter.htm?pid=54793 (9 August 2017).

Osborn S.B. (1955), Radiation doses received by the diagnostic X-ray workers, *Brit. J. Radiol.* **28**: 650–654. https://doi.org/10.1259/0007-1285-28-336-650

Paolicchi F., Miniati F., Bastiani L., Faggioni L., Ciaramella A., Creonti I., Sottocornola C., Dionisi C., Caramella D. (2016), Assessment of radiation protection awareness and knowledge about radiological examination doses among Italian radiographers, *Insight Imaging* 7 (**2**): 233–242. doi: 10.1007/s13244-015-0445-6

Papp J. (2011), *Quality management in the imaging sciences,* **fourth edition,** Elsevier Mosby, 3251 Riverport Lane, Missouri, USA.

Papp J. (2015), *Quality Management in the Imaging Sciences,* **fifth edition,** Elsevier Health Sciences, 3251 Riverport Lane, Missouri, USA.

Pernicka F. and McLean I.D. (2007), Dosimetry in diagnostic radiology: an international code of practice, International Atomic Energy Agency.

Rasuli B., Pashazadeh A.M., Tahmasebi Birgani M.J., Ghorbani M., Naserpour M., Fatahi-Asl J. (2015), Quality control of conventional radiology devices in selected hospitals of Khuzestan province, Iran, *Iran. J. Med. Phys.* 2015 Jul 1; 12(**2**): 101–108. DOI: 10.22038/ijmp.2015.4773.

Rasuli B., Pashazadeh A.M., Ghorbani M., Juybari R.T., Naserpour M., (2016), Patient dose measurement in common medical X-ray examinations in Iran, *J. App. Clin. Med. Phys.* 17 (**1**): 374 – 386. https://aapm.onlinelibrary.wiley.com/doi/pdf/10.1120/jacmp.v17i1.5860

Rehani M.M. (1995), *Diagnostic imaging: quality assurance*, **43** Jaypee Brothers Medical Publishers, New Delhi, India, pp. 14−23.

Rehani M.M., Kaul R., Kumar P., Berry M. (1995), Does bridging the gap between knowledge and practice help? Example of patient dose reduction in radiology*, Med. Phys.* **20**:18−22.

Rehani M.M., Arun Kumar L.S., Berry M. (1992), Quality assurance in diagnostic radiology, *Indian J. Radiol.* **2**: 259−263.

Saghatchi F., Salouti M., Bahreini M.T. (2006), The quality control of x-ray Machines in Hospitals of Zanjan, International Conference on Quality Assurance and New Techniques in Sciences, Radiation Medicine [QANTRM], Nov; 13–15, Vienna, Austria.

Schandorf C. and Tetteh G.K. (1998), Analysis of the status of X-ray diagnosis in Ghana, *Brit. J. Radiol. & Imag.* **71:** 1040–1048. https://doi.org/10.1259/bjr.71.850.10211064

Seeram E. and Travis E.C. (1997), *Radiation protection*, Lippincott, Philadelphia, New York, USA.

Seibert J.A. (2004), X-Ray Imaging Physics for Nuclear Medicine Technologists. Part 1: Basic Principles of X-Ray Production, *J. Nucl. Med. Tech.* 32(**3**): 139−147.

Shepard S.J., Lin P.J., Boone J.M. (2002), *Quality Control in Diagnostic Radiology,* AAPM Report No. **74**.

Shrimpton P.C., Wall B.F., Jones D.G., Fisher E.S., Hillier M.C., Kendal G.M., Harrison R.M. (1986), A national survey of doses in patients undergoing an election of routine x-ray examinations in English hospitals, NRPB-R200. Oxfordshire, United Kingdom: National Radiological Protection Board.

Simkin D.J. and Dixon R.L. (1998), Secondary Shielding Barriers for Diagnostic X-ray Facilities: Scatter and Leakage, *Health Phys.* **74**: 350−365.

Smith P.G. and Doll R. (1981), Mortality from Cancer and all Causes among British Radiologists, *Brit. J. Radiol.* **54**, 187–194. https://doi.org/10.1259/0007-1285-54-639-187

Sonawane A.U., Meghraj S., Sunil K.J.V.K., Kulkarni A., Shirva V.K., Pradhan A.S. (2010), Radiological safety status and quality assurance audit of medical X-ray diagnostic installations in India, *J. Med. Phys.* 35(**4**), 229–234. doi: 10.4103/0971-6203.71764

Spelic D.C., Kaczmarek R.V., Suleiman O.H. (2004), Nationwide Evaluation of X-ray Trends survey of abdomen and lumbosacral spine radiography, *Radiology* **232**: 115−125. https://doi.org/10.1148/radiol.2321020397

Sprawls, P. (2017), *Interaction of Radiation with Matter*. Retrieved from: https://www.sprawls.org/ppmi2/INTERACT (5 April 2019).

Stannard J.N. (1988), *Radioactivity and health. A history*, Springfield, VA: National Technical Information Service.

Storm L. and Israel H. I. (1970), Photon cross sections from 1 keV to 100 MeV for elements Z=1 to Z=100, *Sci. Dir*. 7**(6)**: 565−681. https://doi.org/10.1016/S0092-640X(70)80017-1

Sungita Y.Y., Mdoe S.L.C., Msaki Peter (2006), Diagnostic X-ray facilities as per quality control performances in Tanzania, *J. App. Clin. Med. Phys.* 7 (**4**): 66−73. https://doi.org/10.1120/jacmp.v7i4.2291

Sun Z., Inskip P.D., Wang J., Kwon D., Zhao Y., Zhang, L. (2016), Solid cancer incidence among Chinese medical diagnostic X-ray workers, 1950-1995: Estimation of radiation-related risks, *Int. J. Cancer* **138,** 2875−2883. doi: 10.1002/ijc.30036

Supe S.J., Iyer P.S., Sasane J.B., Sawant S.G. and Shirva V.K. (1992), Estimation and significance of patient dose from diagnostic X-ray practices in India, *Radiat. Prot. Dosim.* 43(**1/4**): 209–211. https://doi.org/10.1093/rpd/43.1-4.209

Taylor L.S. (1979), *Organization for Radiation Protection-The operations of the ICRP and NCRP 1928-1974,* Washington, DC: U.S. Department of energy.

Thompson E. (1896), *Boston Med. Surg. J.* **135**: 610−611.

Tsalafoutas I.A. (2006), Excessive leakage radiation measured on two mobile X-ray units due to the methodology used by the manufacturer to calculate and specify the required tube shielding, *Brit. J. Radiol.* **79**, 162–164. https://doi.org/10.1259/bjr/17920806

Turner James E. (2005), Interaction of Ionizing Radiation with Matter, *Health Phys.* 88(**6**): 520–544.

United States Nuclear Regulatory Commission (2014), Reactor Concepts Manual: Biological Effects of Radiation. Retrieved from: http://www.nrc.gov/reading-rm/basic-ref/teachers/09.pdf (15 November 2016).

United Nations Scientific Committee on the Effects of Atomic Radiation (2000), *Sources and effects of ionizing radiation: report to the General Assembly, annex D, medical radiation exposures*, New York, NY: United Nations.

Vlachos I., Tsantilas X., Kalyvas N., Delis H., Kandaraskis Ioannis, Panayiotakis G. (2015), Measuring scatter radiation in diagnostic X-rays for radiation protection purposes, *Radiat. Prot. Dosim.* 165(**1-4**), 382–385. doi: 10.1093/rpd/ncv093

Wagner L.K., Fontenla D.P., Kimme-Smith C., Rothenberg L.N., Shepard J., Boone J.M. (1992), Recommendations on performance characteristics of diagnostic exposure meters: Report of AAPM Diagnostic X-ray Imaging Task Group No. 6, *Med. Phys.* Jan 1; 19(**1**): 231–241.

Wang J.X., Zhang L.A., Li B.X., Zhao Y.C., Wang Z.Q., Zhang J.Y., Aoyama T. (2002), Cancer incidence and risk estimation among medical X-ray workers in China, 1950 –1995, *Health Phys. Society*, 82(**4**): 455−466.

World health organization (WHO 1982), *Quality Assurance in diagnostic Radiology*, A guide prepared following workshop held in Neuherberg, Geneva, Switzerland.

Younis S.N., Ali R.T., Rashid S.A. (2014), Radiation protection evaluation from diagnostic departments in Erbil hospitals, *Zanco J. Med. Sci.* 18(**1**): 625−631.

Zoetelief J. (1998), Quality Control in Diagnostic Radiology in the Netherlands, *Radiat. Prot. Dosim.* 77(**4**): 257–266. DOI: 10.1093/oxfordjournals.rpd.a032321.

Brief Bio-Data of the candidate

1. **Name** : Jonathan Lalrinmawia
2. **Father's Name** : R Lalbiakdika
3. **Mother's Name** : Lalramliani
4. **Address** : Chhingchhip-161, Serchhip District, Mizoram
5. **Designation** : Research Scholar (Mizoram University)
6. **Date of Birth** : 19th May, 1990
7. **Educational qualifications** :

Degree	**Year**	**University/Board**	**Division**
HSLC	2006	Mizoram Board of School Education	First
HSSLC (Science)	2008	Mizoram Board of School Education	Second
B.Sc. (Physics)	2011	Mizoram University	First
M.Sc. (Physics)	2013	Mizoram University	First
B. Ed.	2015	Mizoram University	First
Pre-Ph. D Course	2015	Mizoram University	Grade 'O'
M. A. (Education)	2018	IGNOU	First *UGC-NET

8. Two years research project experienced entitled **'*Study of Radiation Safety Measures of X-Ray Installations in Mizoram*'** funded by Atomic Energy Regulatory Board, Govt. of India (No. AERB/CSRP/Proj.No. 58/02/2014).

9. **Area of research interest** : Medical Physics (Dosimetry/exposure assessment, Radiation monitoring, control, and safety, Radiography)

10. **Life Member/Memberships**

- ✓ Ex-Officio-***Mizoram Radio-Imaging Technologist Association*** **(MRITA)**, Aizawl, Mizoram *'The Mizoram Chapter of Indian Society of Radiographer & Technologist (ISRT)'*.
- ✓ Life Member-***Association of Medical Physicist of India*** **(AMPI),** Life Membership No - LM 02464.
- ✓ Life Member-***Indian Association for Radiation Protection*** **(IARP)**, Life Membership No. LM - 1539
- ✓ Life Member-***Indian Association of Physics Teachers*** **(IAPT)**, Life Membership No-10908, L7060; Naveen Nagar, Kanpur – 208 025.
- ✓ Life Member-***Physics Academy of the North East*** **(PANE),** Life Membership No- LM 0285; Physics Dept. GU, Guwahati-781014.
- ✓ Member-***Mizo Academy of Sciences*** **(MAS)**, Aizawl, Mizoram.
- ✓ Member-***Science Teachers' Association, Mizoram*** **(STAM)**, Aizawl, Mizoram.

11. **Publication** : 8

12. **Paper presented** : 7

13. **Conferences and Workshops attended** : 18

Paper published in peer reviewed journal

1. **Lalrinmawia J.**, Pau K.S., Tiwari R.C. (2019), An enumeration survey of diagnostic X-ray generators and essential safety parameters, ***Iranian Journal of Medical Physics***, Article in Press. https://doi.org/10.22038/IJMP.2019.39307.1519 © Publisher : **Mashhad University of Medical Sciences**

2. **Lalrinmawia J.**, Pau K.S., Tiwari R.C. (2019), Evaluation of radiation doses at diagnostic X-ray control panels and outside patient entrance doors in Aizawl district, India, ***Radiological Physics and Technology***, 12(**3**), 312−324. https://doi.org/10.1007/s12194-019-00526-6 © Publisher : Japanese Society of Radiological Technology and Japan Society of Medical Physics (**Springer Nature)**

3. **Lalrinmawia J.**, Pau K.S., Tiwari R.C. (2018), Qualitative study of mechanical parameters of conventional diagnostic X-ray machines in Mizoram, ***Radiological Physics and Technology***, 11(**3**), 274−283. https://doi.org/10.1007/s12194-018-0464-3 © Publisher : Japanese Society of Radiological Technology and Japan Society of Medical Physics (**Springer Nature)**

4. **Lalrinmawia J.**, Pau K.S., Tiwari R.C. (2017), Quality Assurance Assessment of Conventional Diagnostic X-ray Installations in Mizoram, ***Journal of Medical Physics***, 42 (**suppl 1**), 208−209. ISSN: 0971-6203. http://www.jmp.org.in/text.asp?2017/42/5/110/217113 © Publisher : Association of Medical Physicists of India (**Wolters Kluwer)**
5. **Lalrinmawia J.**, Pau K.S., Tiwari R.C. (2019), Investigation of conventional diagnostic X-ray tube housing leakage radiation using ion chamber survey meter in Mizoram, India, ***Science Vision***, 19(**3**), 43−50. DOI: https://doi.org/10.33493/scivis.19.03.02 © Publisher : **Mizo Academy of Sciences**
6. **Lalrinmawia J.**, Pau K.S., Tiwari R.C. (2019), Study on the intensity of radiation attenuated by protective barriers in diagnostic X-ray installations, ***Science Vision***, 19(**2**), 43−50. DOI: https://doi.org/10.33493/scivis.19.02.08 © Publisher : **Mizo Academy of Sciences**

Paper published in conference proceedings

1. **Lalrinmawia J.**, Pau K.S., Tiwari R.C. (2017), *Investigations of public dose due to stray radiation in x-ray installations in Mizoram*, Science and Technology for Shaping the Future of Mizoram, during 13th–14th October 2016, Mizoram University, pp. 305−309. ISBN: 978-93-85926-49-5
2. **Lalrinmawia J.**, Pau K.S., Tiwari R.C. (2017), *Investigations of workers dose due to stray radiation in x-ray installations in Mizoram*, Recent advances in physics research and its relevance, during 10th–12th November 2016, St. Anthony's College, pp. 258−263. ISBN: 978-93-86256-85-0

International conference

1. **Presented paper** on Study Tube Housing Leakage of 111 conventional diagnostic X-ray Machines using ion chamber Survey meter in ***33rd IARP International Conference-2018*** (Development towards Improvement of Radiological Surveillance at Nuclear Facilities and Environment), 16th–20th January 2018, DAE Convention Center, Anushaktinagar, Mumbai-094.
2. **Presented paper** on Quality assurance assessment of conventional diagnostic X-ray installations in Mizoram in ***17th Asia Oceania Congress of Medical Physics & 38th Annual Conference of Association of Medical Physicists of India***, 4th–7th November, 2017, Department of Radiological Physics, SMS Medical College, Jaipur.

National conference

1. **Presented paper** on Study of radiation attenuated by protective barrier in diagnostic X-ray installations in the ***Mizoram Science Congress-2018***, 4th–5th October, 2018, Pachhunga University College, Aizawl, Mizoram.
2. **Presented paper** on X-ray attenuation, interaction mechanism of shielding materials in ***4th National Conference of Indian Society of Radiographers and Technologists***, 7th–9th September, 2017, at Regional Institute of Paramedical and Nursing Sciences (RIPANS), Aizawl, Mizoram.
3. **Presented paper** on Investigations of workers dose due to stray radiation in X-ray installations in Mizoram in ***Xth Biennial National Conference of Physics***

Academy of North East, 10th–12th November, 2016, at St. Anthony’s College, Shillong, Meghalaya.

4. **Presented paper** on Investigations of public dose due to stray radiation in X-ray installations in Mizoram in **MSC (*Mizoram Science Congress*)**-16 National Conference, 13th–14th October, 2016, at Mizoram University, Tanhril, Aizawl.
5. **Presented paper** on Study on the mechanical attributes of diagnostic X-ray installation in Mizoram, India in the ***CMDAYS-2016 National Conference***, 29th–31st August, 2016, at the Department of Physics, Mizoram University, Tanhril, Aizawl.

Others

1. Interview on the topic of ‘***Mizoram a diagnostic X-ray khawl zir chianna leh X-ray zungzam hlauhawmna te***’ Radiation Safety Awareness recorded on 3rd February 2018 AIR, Aizawl; broadcast/telecast on 15th February, 2018, 8:35 am.
2. Presentation on the topic of Radiation Safety on training on ‘***Hospital Safety & Emergency Medical Services***’ under Administrative Training Institute, Mizoram, Aizawl, during 15th–17th November, 2016.
3. Presentation on the topic of X-ray Quality Assurance in ***One Day Radiation Safety Training*** under Radiation Safety Agency Directorate of Hospital & Medical Education, Aizawl on 31st May, 2016.

Conferences, workshops and seminar attended

1. 19th Orientation Course (UGC sponsored) held on 16th February – 15th March, 2016 at Mizoram University, Aizawl, Mizoram.

2. Short Term Course on applied Statistics (UGC sponsored) held on 7th–12th September, 2015 at Mizoram University, Aizawl, Mizoram.
3. National workshop on Microwave measurement with Devices and Testing Instruments, organized by Department of Electronics & Communication Engineering, NIT, Mizoram held during 22nd–26th September, 2015 at National Institute of Technology, Aizawl, Mizoram.
4. International workshop on Cancer Epidemiology, organized by Department of Biotechnology, sponsored by State Biotech-Hub Facility, held on 29th–30th November, 2016 at Department of Biotechnology, MZU, Aizawl, Mizoram.
5. State Consultation on Draft National Education Policy, 2019 at SCERT auditorium on 29th July, 2019.
6. National Consultation Meeting on Implementation of Vocational Education in Schools under Samagra Shiksha held on 21st–22nd February, 2019 at CIET-NCERT, DELHI organized by PSSIVE-BHOPAL, India.
7. Mizoram Science Congress-2018, held at Pachhunga University College, during 4th–5th October, 2018.
8. Seminar on Science and Technology for Sustainable Future, organized by National Council for Science & Technology Communication, Department of Science and Technology, New Delhi held on 30th April, 2018 at Seminar Hall, PUC, Aizawl, Mizoram.
9. 33rd IARP International Conference-2018 (Development towards Improvement of Radiological Surveillance at Nuclear Facilities and Environment) held at

DAE Convention Center, Anushaktinagar, Mumbai-094 during 16th–20th January, 2018.

10. 17th Asia Oceania Congress of Medical Physics & 38th Annual Conference of Association of Medical Physicists of India held at Department of Radiological Physics, SMS Medical College, Jaipur during 4th–7th November, 2017
11. 4th National Conference of Indian Society of Radiographers and Technologists, held at Regional Institute of Paramedical and Nursing Sciences (RIPANS-Aizawl), during 7th–9th September, 2017.
12. Seminar on National Science Day 2017, organized by Research and seminar committee GZRSC & MISTIC catalysed and supported by NCSTE DST, New Delhi held on 28 February, 2017 at GZRSC, Aizawl, Mizoram.
13. Xth Biennial National Conference of Physics Academy of North East, held at St. Anthony’s College, during 10th–12th November, 2016.
14. Seminar on Make in India: Science & Technology Driven Innovations, organized by National Council for Science & Technology Communication, Department of Science and Technology, New Delhi held on 4th November, 2016 at Pi Zaii Hall, Synod Conference Center, Aizawl, Mizoram.
15. MSC (Mizoram Science Congress)-16 National Conference, held at Mizoram University, during 13th–14th October, 2016.
16. CMDAYS-2016 National Conference, held at the Department of Physics, Mizoram University, during 29th–31st August, 2016.

17. Orientation on Micro Teaching for Capacity development of College Teachers at Institute of Advanced Study in Education, Aizawl on 14th–16th September, 2016.
18. Seminar on Science for Nation Building, organized by National Council for Science & Technology Communication, Department of Science and Technology, New Delhi held on 1st October, 2015 at Pi Zaii Hall, Synod Conference Center, Aizawl, Mizoram.

The information provided above is true to the best of my knowledge and belief.

(Signature)

PARTICULARS OF THE CANDIDATE

NAME OF CANDIDATE : Jonathan Lalrinmawia

DEGREE : M. Sc. Physics

DEPARTMENT : Physics

TITLE OF THESIS : Study of radiation and mechanical attributes of diagnostic X-ray installations in Mizoram

DATE OF ADMISSION : 13th Aug. 2015

APPROVAL OF RESEARCH PROPOSAL:

1. BOS : 7th April, 2016
2. SCHOOL BOARD : 21st April, 2016

REGISTRATION DATE : MZU/Ph.D/917 of 21.04.2016

EXTENSION (IF ANY) : Nil

Head

Department of Physics

An enumeration survey of diagnostic X-ray generators and essential safety parameters

Document Type: Original Paper

Authors

Ramesh Chandra Tiwari [1]; Jonathan Lalrinmawia [2]; Kham Suan Pau [3]

[1] Department of Physics, School of Physical Sciences, Mizoram University (A Central University), Tanhril campus, Aizawl

[2] Department of Physics, Mizoram University

[3] Mizoram State Cancer Institute, Zemabawk, Aizawl-796017, Mizoram, India

10.22038/IJMP.2019.39307.1519

Abstract

Introduction

Best radiography practice involves operational optimal machine performance, delivering cost effective healthcare services under appropriate safety conditions for workers and the public. This study aimed to investigate the safety status of conventional diagnostic X-ray installations in Mizoram, India.

Materials and Methods

Linearity of time (sec), linearity of current (mA), output reproducibility, table dose (µGy/mAs), peak voltage (kVp) accuracy and 16 essential safety parameters of 135 X-ray machines were considered. To measure output radiation and the effective peak potential of X-ray tube, battery-operated portable dosimeter and a portable wide-range digital kVp meter made by Fluke were used. Data were analyzed by using SPSS version 17.0 (SPSS, Inc., Chicago, IL, USA).

Results

Among different electronic parameters, 59.2% linearity of time; 82.6% linearity of current; 89.7% kVp accuracy; 35.1% output reproducibility; 92.8% table dose were beyond acceptable limit. It was observed from 16 essential safety parameters that 98.7% X-ray machines did not receive proper quality assurance (QA) test as per Atomic Energy Regulatory Board, India guidelines, 1.9% installations employed lead-line patient entrance door, 46.8% machines were operated without any protective barrier, 83.1% units operated without personnel monitoring service, 92.2% of the facilities recorded repeated examination due to over/under exposures, spoilt films and patient movement.

Conclusion

It appears that the present study had more problems regarding X-ray generators than previous studies in different parts of the world. The reasons may be improper QA tests, old machine used without proper maintenance, power supply problems. Such problem causes repeated exposure which increases the population dose, cost of imaging, and duration of imaging. The authors recommend that proper quality control (QC) must be implemented immediately by monitoring each and every diagnostic X-ray installation frequently throughout every year. As proper QC program were not implemented in the past years, many installations were not following standard installation guidelines.

Keywords

Quality assurance ; diagnostic X-ray ; radiation safety ; electronics parameter

Main Subjects

Medical Physics

ISSN:1735-160X

Iranian Journal of

Medical Physics

Vol.5, No.2, Serial Number 20-21, Autumn& Winter 2009

Contents

http://www.mums.ac.ir/physic_journal/fa/index

Articles in Press, Accepted Manuscript
Available Online from 29 September 2019

Files

XML

History

Share

How to cite

Statistics

Article View: *307*

Qualitative study of mechanical parameters of conventional diagnostic X-ray machines in Mizoram

Jonathan Lalrinmawia, Kham Suan Pau & Ramesh Chandra Tiwari

Radiological Physics and Technology

ISSN 1865-0333
Volume 11
Number 3

Radiol Phys Technol (2018) 11:274-283
DOI 10.1007/s12194-018-0464-3

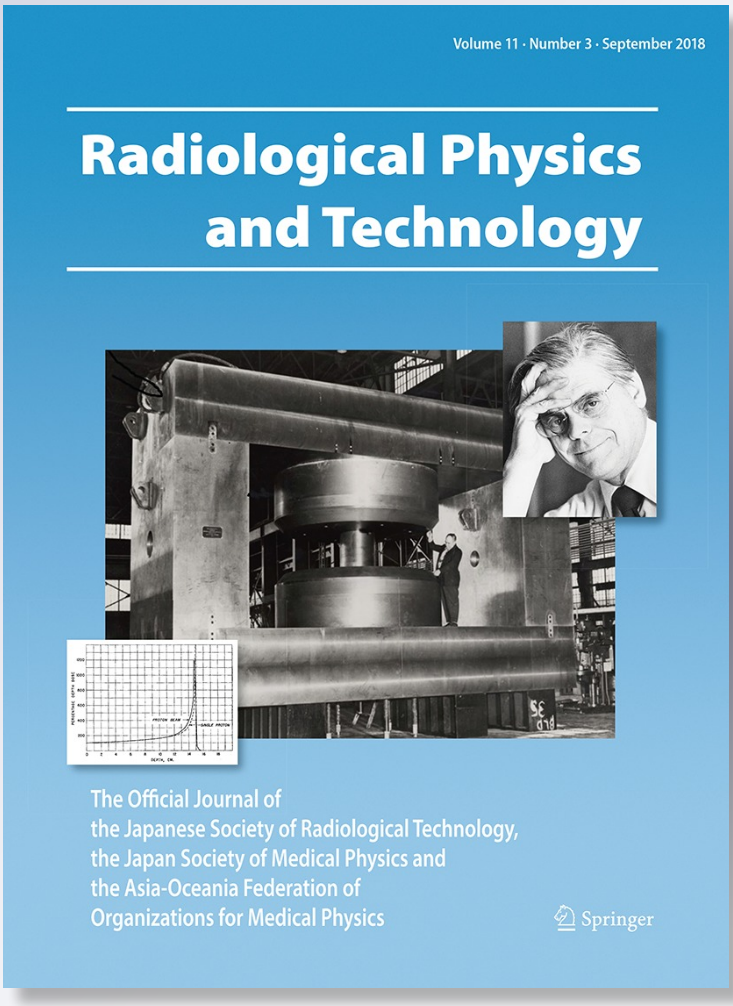
Volume 11 · Number 3 · September 2018
Radiological Physics and Technology
The Official Journal of the Japanese Society of Radiological Technology, the Japan Society of Medical Physics and the Asia-Oceania Federation of Organizations for Medical Physics
Springer

Springer

Your article is protected by copyright and all rights are held exclusively by Japanese Society of Radiological Technology and Japan Society of Medical Physics. This e-offprint is for personal use only and shall not be self-archived in electronic repositories. If you wish to self-archive your article, please use the accepted manuscript version for posting on your own website. You may further deposit the accepted manuscript version in any repository, provided it is only made publicly available 12 months after official publication or later and provided acknowledgement is given to the original source of publication and a link is inserted to the published article on Springer's website. The link must be accompanied by the following text: "The final publication is available at link.springer.com”.

Springer

Author's personal copy

Radiological Physics and Technology (2018) 11:274–283
https://doi.org/10.1007/s12194-018-0464-3

Qualitative study of mechanical parameters of conventional diagnostic X-ray machines in Mizoram

Jonathan Lalrinmawia[1] · **Kham Suan Pau**[2] · **Ramesh Chandra Tiwari**[1]

Received: 26 September 2017 / Revised: 7 May 2018 / Accepted: 10 May 2018 / Published online: 18 May 2018
© Japanese Society of Radiological Technology and Japan Society of Medical Physics 2018

Abstract

The present study examined the mechanical attributes of 135 conventional diagnostic X-ray machines in Mizoram, India. The purpose of studying the X-ray mechanical parameters, such as congruency, perpendicularity of the central beam, and half-value layer, was to improve the quality of the diagnostic image and reduce the patient dose. A battery-operated portable dosimeter was used to measure output radiation of the X-ray machine. The half-value layer was measured at a constant accelerating potential of 70 kVp and tube load. To measure the congruency and beam alignment perpendicularity, a congruence and alignment tool was used. The survey data were collected between June 2015 and June 2016. The authors followed international standard test procedures, and the results were compared to national and international standards. SPSS Statistics for Windows, Version 17 was used to calculate the mean, range, and standard deviation. The half-value layer ranged from 0.45 to 3.00 mm; the mean half-value layer was 1.60 ± 0.51 SD mm. In comparison with national and international standards, only 27.83% (national) and 15.64% (international) of the machines' filtration were found to be within acceptable limits. The congruence misalignment of the *x*-axis varied between 0.50% and 15.30% of the source-to-image distance; for the *y*-axis, it ranged from 0.50 to 10.90%. When the congruence between the radiation beam and optical field was tested, 80.85% of diagnostic X-ray machines did not meet the prescribed acceptance parameters. When the perpendicularity between the central beam and the image receptor was tested, 69.81% did not meet safety standards.

Keywords Central beam perpendicularity · Congruence between radiation and optical field · Half-value layer · Conventional diagnostic X-ray · Radiation safety

1 Introduction

Medical diagnostic X-rays have been reported to be the major contributor of public exposure to man-made ionizing radiation [1]. Approximately 51.00% of the population dose was estimated to be caused by diagnostic X-ray examinations [2]. To minimize and control unreasonable exposure, the International Commission on Radiological Protection (ICRP) detailed important guidelines, suggesting that all medical exposures should adhere to the safety principles of optimization and justification [3]. In India, the Atomic Energy Regulatory Board (AERB) is the national regulatory body [4]. The AERB sets the national standards and safety codes that specify the safe use of radiation sources, including diagnostic X-ray machines [5]. It was reported by Supe et al. that "most of the rural areas have very old X-ray machines for which quality assurance (QA) tests have never been undertaken" [6]. It seems equally true that no proper QA tests have been performed for the units that we studied in Mizoram [7].

Among the mechanical characteristics of X-rays, the half-value layer (HVL) is one of the most important parameters that affect both the quantity and quality of the X-ray output [8]. HVL is the amount of aluminum (Al) required to reduce the intensity of radiation to one-half of its original value, at a fixed peak accelerating potential (kVp) and tube loading (mA) [9]. HVL thickness is measured to guarantee that the permanently installed filter on the X-ray tube is maintained to minimize patient exposure [8]. This is the best way to determine if adequate filtration exists, as it is otherwise difficult to measure. At the same time, the addition of a filter for a fixed input

---

✉ Ramesh Chandra Tiwari
ramesh_mzu@rediffmail.com

[1] Department of Physics, Mizoram University, Aizawl, Mizoram 796004, India

[2] Mizoram State Cancer Institute, Zemabawk, Aizawl, Mizoram 796017, India

Author's personal copy

parameter has a very small effect on high-energy X-rays, but removes soft X-rays from the beam. The softer X-ray components are almost completely removed by heavy filtration, and the radiation transmitted approaches monochromy [10]. Most of the softer X-rays are not transmitted through the patient to form an image, but are absorbed by the patient. Increasing the HVL decreases the patient dose [9]. However, the extra filtration eliminates suitable beams and a higher tube load is necessary to reach the desired output; this increases the stray radiation rate [11].

When an X-ray beam passes through a filter, its intensity is reduced, because the beam is attenuated; some energy is absorbed, and remaining energy is simply deflected out of the beam. As observed in radioactive decay, in photon attenuation, there is a constant fractional change in photon number, which results in an equal change in another factor as follows:

$$I = I_{\mathrm{o}} e^{-\mu x} \tag{1}$$

where I_{o} is the intensity values when there is no filter between the source and measuring instrument; I is the intensity when a thickness x (in mm) is interposed; and μ is the linear attenuation coefficient of the material (Fig. 1). One consequence of the exponential attenuation is that "it is impossible to reduce an X-ray beam to zero no matter how thick the material inserted." However, we can significantly reduce X-ray radiation by half [12]. HVL is inversely proportional to the attenuation coefficient, and is related as follows:

$$\frac{I}{I_{\mathrm{o}}} = e^{-\mu x}$$

According to the definition of HVL

$$D_{1/2} = \frac{0.6931}{\mu} \tag{2}$$

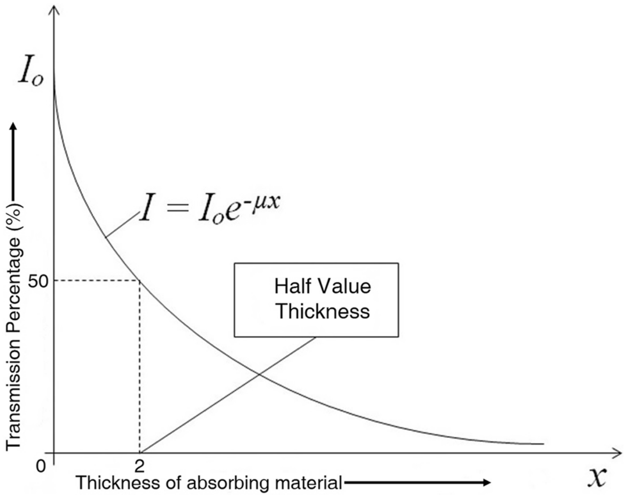

Fig. 1 Attenuation curve showing the half-value thickness

where $D_{1/2}$ is the HVL thickness [10, 13].

The linear attenuation coefficient μ is the sum of the attenuation coefficients of three types of interactions: photoelectric absorption, Compton scattering, and pair production.

Thus, the purpose of this study of X-ray mechanical parameters, such as congruency between the X-ray beam and the optical/light field, was to ensure that the light field and X-ray field were properly aligned [8]. In a clinical environment, it is important to ensure reproducibility from image to image and for the facility to collimate ionizing radiation as much as possible, per the As Low as Reasonably Achievable (ALARA) principle. The radiation produced by diagnostic X-ray machines is invisible to the human eye. Therefore, a collimator-visible light is the only indicator that allows the radiation technician to visualize the location and size of the X-ray field. Visualization of the X-ray field is achieved by a mirror reflecting the light from a light bulb. The bulb position is adjusted, so that the reflected light appears to have the same origin as the focal spot of the tube [14]. It is important to assess the congruency between them, as the beam must be aligned to the Bucky tray to avoid anatomy and grid cutoffs.

Assessment of the perpendicularity between the central X-ray beam and the image receptor should be emphasized, as perpendicularity minimizes image distortion, which improves the representation of the anatomy in question. Optical field and X-ray radiation field misalignment may be caused by shifts in the relative positions of the light bulb filament and anode focal spot. Such shifts are caused by differences between light bulbs, changes in the mirror position, or shifts in the collimator position on the tube head [15].

There are 195 machines at 118 different locations across the state of Mizoram. However, in the present study, we only considered 135 conventional diagnostic X-ray units that were significant to our objectives, as shown in Fig. 2. Conventional X-rays contributed 5172.16 mA-min per week, i.e., 90.94% of the workload of all X-ray facilities; the remaining 9.06% was from dental, mammographic, computed tomographic, and fluoroscopic examinations (Table 1). This workload was calculated using the formula published previously by the NCRP [16–18]:

$$W = \frac{\text{patients}}{\text{day}} \times \frac{\text{films}}{\text{patient}} \times \frac{\text{mAs}}{\text{film}} \times \frac{\text{days}}{\text{week}} \times \frac{1\,\text{min}}{60\,\text{s}}. \tag{3}$$

The general diagnostic X-ray examinations are of the skull, chest, abdomen, extremities and pelvic. Except chest X-ray, all other examinations were done in vertical projection and all institutions worked 6 days a week. Let us take equipment number one (Table 1), for example, where chest, abdomen, skull, and other extremities were examined. For chest X-ray, we have

$$\begin{aligned} W &= \frac{2 \times 1 \times 20 \times 6}{60} \text{ mA min per week} \\ &= 4 \text{ mA min per week for chest X-ray.} \end{aligned}$$

Author's personal copy

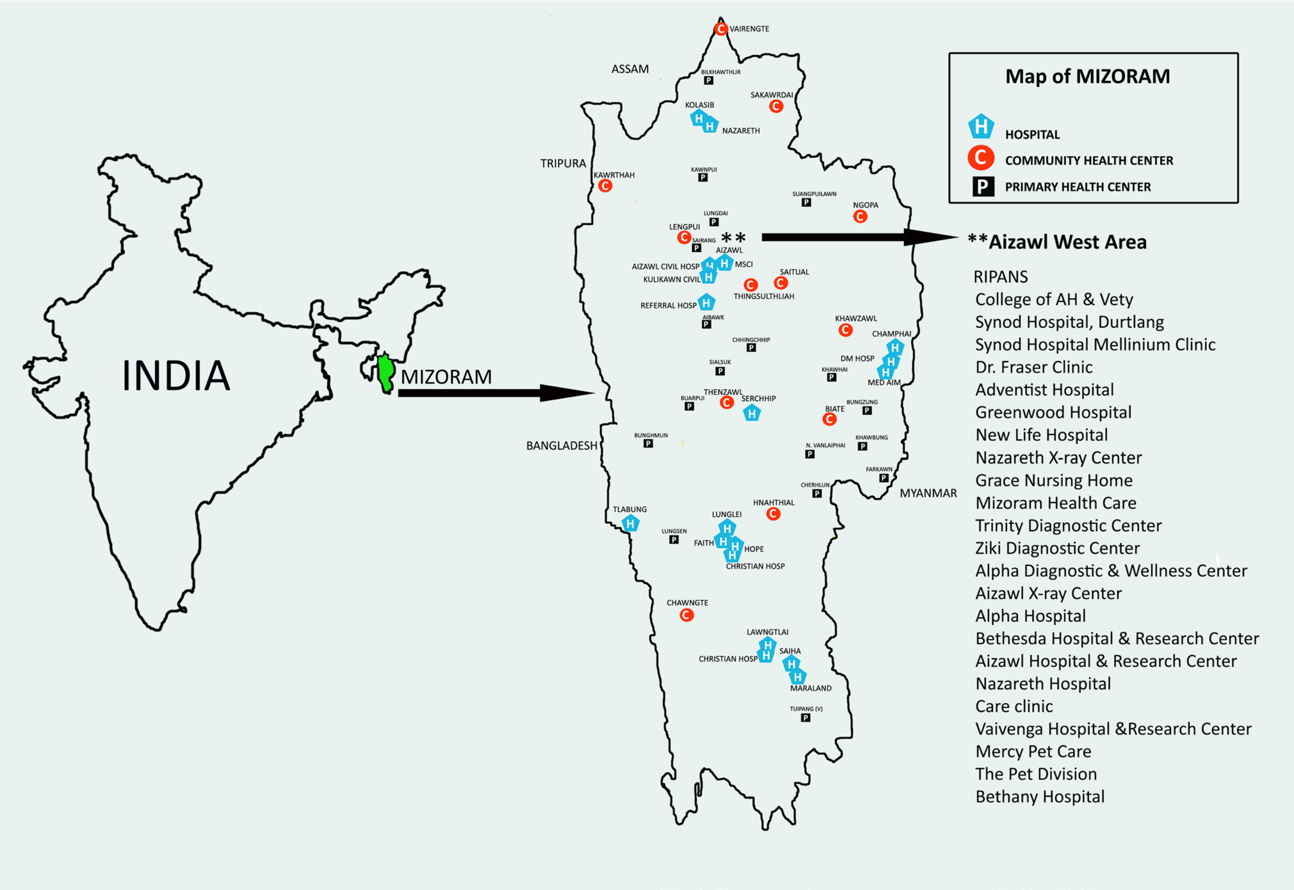
INDIA
MIZORAM
ASSAM
TRIPURA
BANGLADESH
MYANMAR
VAIRENGTE
BILKHAWTHLIR
SAKAWRDAI
KOLASIB
NAZARETH
KAWRTHAH
KAWNPUI
SUANGPUILAWN
NGOPA
LUNGDAI
LENGPUI
SAIRANG
**
AIZAWL
AIZAWL CIVIL HOSP
MSCI
KULIKAWN CIVIL
SAITUAL
THINGSULTHLIAH
REFERRAL HOSP
AIBAWK
KHAWZAWL
CHAMPHAI
CHHINGCHHIP
SIALSUK
DM HOSP
KHAWHAI
MED AIM
THENZAWL
BUARPUI
SERCHHIP
BIATE
BUNGZUNG
BUNGHMUN
N. VANLAIPHAI
KHAWBUNG
FARKAWN
CHERHLUN
HNAHTHIAL
TLABUNG
LUNGLEI
LUNGSEN
FAITH
HOPE
CHRISTIAN HOSP
CHAWNGTE
LAWNGTLAI
SAIHA
CHRISTIAN HOSP
MARALAND
TUIPANG (V)
Map of MIZORAM
H HOSPITAL
C COMMUNITY HEALTH CENTER
P PRIMARY HEALTH CENTER
**Aizawl West Area
RIPANS
College of AH & Vety
Synod Hospital, Durtlang
Synod Hospital Mellinium Clinic
Dr. Fraser Clinic
Adventist Hospital
Greenwood Hospital
New Life Hospital
Nazareth X-ray Center
Grace Nursing Home
Mizoram Health Care
Trinity Diagnostic Center
Ziki Diagnostic Center
Alpha Diagnostic & Wellness Center
Aizawl X-ray Center
Alpha Hospital
Bethesda Hospital & Research Center
Aizawl Hospital & Research Center
Nazareth Hospital
Care clinic
Vaivenga Hospital &Research Center
Mercy Pet Care
The Pet Division
Bethany Hospital

Fig. 2 Locations of the diagnostic X-ray machines included in this study

Table 1 Workload of diagnostic X-ray facilities in Mizoram (data taken between June 2015 and June 2016)

Unit	Patient per day	Film per patient	Tube loading (mAs)	Days per week	Workload (mA min/week)	Total workload (mA min/week)
1	2	1	20	6	4	21.175
	0.15	1	65	6	0.975	
	0.4	1	30	6	1.2	
	0	0	0	0	0	
	3	1	50	6	15	
2[a]	2	1	20	6	4	15
	0.2	1	30	6	0.6	
	0.4	2	30	6	2.4	
	0	0	0	0	0	
	4	1	20	6	8	

[a] Workload was considered for 169 machines like unit 1 and unit 2. Conventional X-ray – 5172.16 mA-min/week; dental X-ray – 140.06 mA-min/week; fluoroscopy, mammography, and CT scan – 374.99 mA-Amin/week

Likewise, other diagnostic examinations were calculated and summed up to get the workload for that particular installation.

In this study, the authors considered the mechanical characteristics of conventional diagnostic X-rays: HVL, congruency between the radiation beam and the optical field, and perpendicularity of the central beam [19]. The aim was to enhance awareness among radiation workers, improve the quality of radiographic images, and directly reduce the patient dose.

Author's personal copy

2 Materials and methods

2.1 Half-value layer

A battery-operated portable dosimeter (RAD-CHECK™ PLUS model 06-526, Fluke Biomedical-Cleveland, Ohio, USA) was used to measure primary beam from a conventional X-ray machine. The calibration measurements were traceable to the National Institute of Standards and Technology (NIST, Gaithersburg, MD, USA). X-ray dosages were measured in roentgens (R) with a scale having minimum and maximum value of 0.001 R and 1.999 R, respectively [20]. Al sheets with different thicknesses (two sheets 0.5 mm thick; three sheets 1.0 mm thick) were used to filter the ionizing radiation using a measuring stand [21]. The HVL could be measured for 97 of 135 conventional X-ray units (71.85%), because 14 units were out of order and 24 had been condemned (Table 2).

To measure the HVL, we set the source at a table-top distance of 100 cm and centered the X-ray field by adjusting the dosimeter position through the collimator, so the entire chamber would be included in the X-ray field. The HVL was measured at a constant tube voltage setting; 70 kVp was used for conventional X-ray equipment. Keeping the tube voltage and tube loading at a constant, we made an exposure without the Al filter. This was followed by exposures with 0.5, 1.0, 1.5, 2.0, 2.5, and 3.0 mm of aluminum placed in the X-ray beam on top of the test stand. The test stand was placed in relation with the X-ray beam, such that the filter lay at the center between the X-ray source and detector. Throughout this experiment, we kept the input parameter constant, and the test stand, X-ray tube, and dosimeter were maintained at fixed positions. The transmission percentage was calculated from each data point, and a graph was plotted for transmission percentage versus Al thickness. We drew a horizontal line from the point corresponding to one-half of the original exposure and noted the half-value thickness in millimeters (mm) [8]. However, the value of a suitable HVL may not be acquired, because this measurement of arrangement was not a narrow beam. According to the AERB safety code for 70–100 kV, the minimum filtration of a useful beam for a maximum rated operating tube potential should be 2.0 mm of Al [22]. However, according to international standards, the total filtration in the useful beam should be equivalent to not less than 2.5 mm of Al [14, 23, 24].

We also measured kVp accuracy and tube output consistency for improved clarification. A wide-range digital kVp meter (model 07-494, Fluke Biomedical, Cleveland, Ohio, USA) was used to measure the output kVp. To evaluate output consistency, a battery-operated RAD-CHECK™ PLUS portable dosimeter (model 06-526, Fluke Biomedical-Cleveland, Ohio, USA) was used. The tube output coefficient of variation was calculated for each unit.

2.2 Radiation beam and optical field congruency

To test the congruency of the radiation beam and the optical field, a congruency tool (manual no. 07-661-7662, Fluke Biomedical, Cleveland, Ohio, USA) was used. The congruency test tool is a flat copper plate with a rectangular outline and markings etched on the surface [25]. The congruencies of the diagnostic X-ray units with adjustable collimators and working collimator bulbs were studied. For several reasons, the congruency between the radiation and the light field could only be measured in 47 (34.81%) units (Table 2). To measure the congruency, we leveled the table and adjusted the X-ray tube, so that the beam was perpendicular to the table. The tube was centered on the table, and there was a distance of 100 cm from the focal spot to the tabletop. The collimator shutters were adjusted, so that the edges of the light field coincided with the rectangular outline of the collimator tool [25]. The collimator tool was oriented, such that the dot in the lower left corner corresponded to the position of a supine patient's right shoulder. This allowed the direction of the collimator fault to be determined at a later time. Cassettes of 8 × 10 inches (20 × 25 cm) were placed on the center top of the table, and they were aligned to the X-ray tube and exposed at 60 ± 10 kVp and 10 ± 3 mAs.

The maximum allowed misalignment in congruency between the radiation beam and the optical field is 2% of the source-to-image distance (SID) [9, 24]. If the X-ray was just within the image of the rectangular frame of the optical field, it indicated good congruency between the light and the X-ray field. However, if an edge of the X-ray field was on

Table 2 X-ray machines with a defect that made determination of a given parameter impossible

Details of defects	No. of X-ray units	Parameters could not study
Circular collimators in mobile X-ray	32	Congruency, perpendicularity
Optical field not working	4	Congruency, perpendicularity
Non-adjustable collimator	6	Congruency
Darkroom not functioning	8	Congruency, perpendicularity
X-ray out of order	14	Congruency, perpendicularity, HVL
X-ray condemn	24	Congruency, perpendicularity, HVL

Author's personal copy

the first spot of the rectangular frame, ± 1 cm to either side of the line, then the edges of the X-ray and light fields were misaligned by 1% of the distance between the X-ray source and the table top. Similarly, the edge of the X-ray falling on to the second spot, by ± 2 cm, indicated an error of 2% at 40 inches (100 cm) [25].

2.3 Perpendicularity between the central beam and image receptor

Similarly, an alignment tool (manual no. 07-661-7662, Fluke Biomedical, Cleveland, Ohio, USA) was used to test central beam alignment perpendicularity. The beam alignment test tool is a plastic cylinder, 6 inches tall with a 1/16-inch-diameter steel ball at each end [25]. The perpendicularity of the diagnostic beam of 53 (39.25%) working diagnostic X-ray units was studied (Table 2). The test used the same experimental setup as the congruency test; we placed the beam alignment test tool in the center of the collimator tool and evaluated them simultaneously [25].

According to the specifications of the National Center for Devices and Radiological Health (NCDRH), the X-ray beam should be perpendicular to the plane of the image receptor. The following principle was applied for a source-to-table distance of 40 inches. If the images of the two steel balls overlapped, the central beam was perpendicular to the image receptor, within 0.5°. If the image of the top ball intercepted the first circle, then the beam was approximately 1.5° from perpendicular. If the image of the top ball intercepted the second circle, the misalignment was approximately 3° [25]. As per specifications, the angle between the central beam of X-ray and the plane of the image receptor should not differ by more than 1.5° from the perpendicular [24, 26].

The measured data were presented as the mean, range, and standard deviation (SD), which were analyzed using SPSS Statistics for Windows, Version 17.0 (SPSS, Inc., Chicago, IL, USA).

3 Results and discussion

3.1 Half-value layer

A graph between the transmission percentage of the X-rays and the thickness of the added Al filter was plotted for each unit (Fig. 3). The curves were found to be non-linear, as the X-ray beam originating from the diagnostic X-ray unit was not mono-energetic. Each layer of the attenuator (Al) acts as a successive filter and gradually changes the quality and the quantity of the beam. However, under heavy filtration, the softer component of the X-ray beam was almost completely removed due to absorption and scattering by the Al atoms. The transmitted X-rays were nearly monochromatic and the attenuation curve tended to approach a straight line [10]. Most of the attenuation curves displayed exponential behavior, and there is a finite chance that some incident photons pass through a filter of any thickness with no interaction [27]. We observed some irregular exponential curves (Fig. 3); there were several reasons for the sharp corners. The primary reason was the output inconsistency of different X-ray machines, as shown in Fig. 4, and 35.05% units showed an output coefficient of variation > 0.05. 20.62%

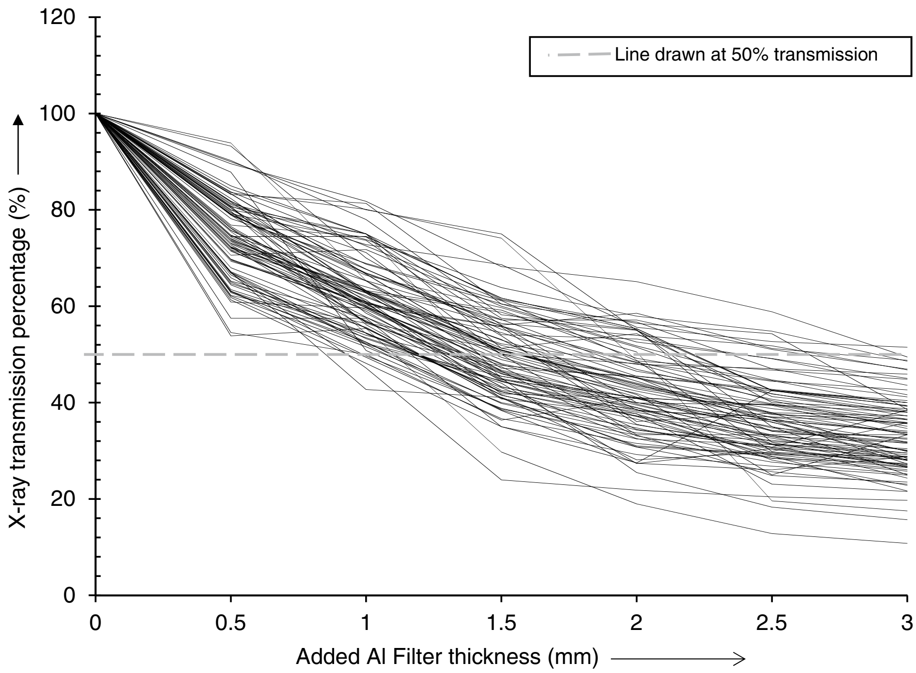

Fig. 3 Attenuation curves of 97 X-ray machines using an Al filter at 70 kV

Author's personal copy

units had an output coefficient of variation higher than 0.1 and it was as high as 0.72 (Table 3). As shown in Table 3, the mean of coefficient of variation for output was 0.08 ± 0.12 SD. Moreover, a few institutions installed X-ray facilities in small rooms, where scattered radiation could not be avoided by any experimental setup and may affect the HVL measurement [10].

The HVL thickness at 70 kV was recorded from each curve. The measured value was supposed to be larger than the actual value, as already mentioned, the arrangement was not a narrow beam. From these HVL values, the total filtration for each equipment was derived using a conversion table [28]. The maximum value of the total filtration was 3.5 mm and the minimum was 0.5 mm (Table 4). These filters significantly minimized the patient dose by filtering soft X-rays that increase the patient dose but do not contribute to image formation [9, 10]. The filter not only reduced the primary radiation dose, but also scattered the dose considerably [29]. Of 97 conventional X-ray units, 27.83% passed and 72.17% failed the test, as per the AERB safety code (Fig. 5) [22]. However, according to international standards, only 15.46% of the equipment did not require filter correction (Fig. 5) [14, 23, 24]. The calculated mean for the total filtration at the different installations was only 1.43 ± 0.80 SD mm, as shown in Table 4. It appears that most units had insufficient filter (Table 4), although the mean X-ray tube age was 8.38 ± 7.72 SD years. However, an absence of proper, frequent QA testing seems to be the primary reason for the insufficiency. Furthermore, in a study of the accuracy of output kVp, the authors found that only 23.71% were within ± 10 kV, while others were out of ± 10 kV, as detailed in Fig. 6. We measured kVp accuracy before studying HVL, but we did not adjust or modify it. As the quality of the X-rays fully depends on the accelerating potential, it can directly affect the HVL thickness [30].

3.2 Congruency between light and radiation

Among 135 conventional X-ray machines, 32 mobile X-ray machines had circular fixed collimators; the optical light field of 4 X-rays did not work; and 6 types of equipment had non-adjustable collimators. This is because the collimators were being maintained in a permanently fixed position. The authors also found that 8 units were not maintained in a darkroom, 14 units were out of order, and 24 units were condemned (Table 2). Due to these constraints, only 47 units were in a ready-to-study condition.

The congruency misalignment of the *x*-axis varied between 0.50 and 15.30% of the SID; the congruency of the *y*-axis varied between 0.50 and 10.90% of SID (Table 5). When compared with the safety standards, the x-axis of 32 units was found to be beyond the acceptable

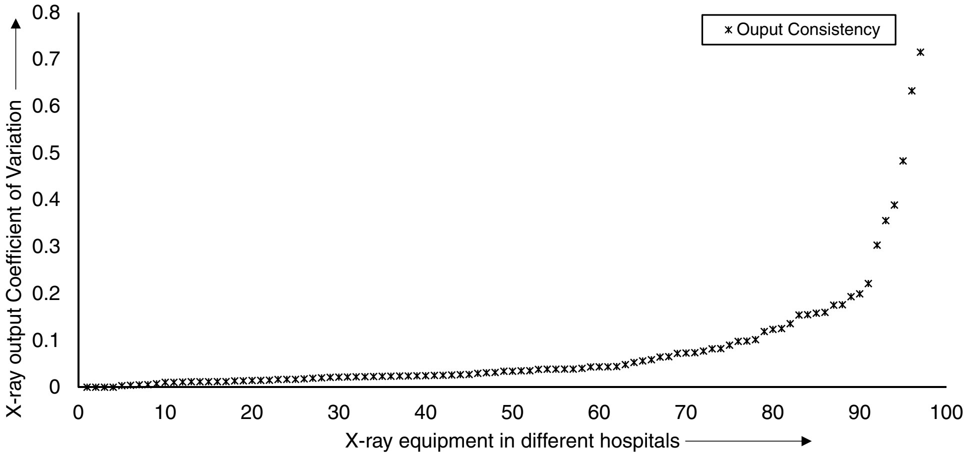

Fig. 4 X-ray output consistency of 97 X-ray machines

Table 3 Output consistency (coefficient of variation) of 97 X-ray units

Parameter	*N*	Range	Minimum	Maximum	Mean	SD
Output consistency	97	0.72	0.00	0.72	0.08	0.12

Table 4 Total filtration of 97 X-ray units

Parameters	*N*	Range	Minimum	Maximum	Mean	SD
HVL	97	3 mm Al	0.5 mm Al	3.5 mm Al	1.43 mm Al	0.80 mm Al
Age	97	44 years	< 1 year	44 years	8.38 years	7.72 years

Author's personal copy

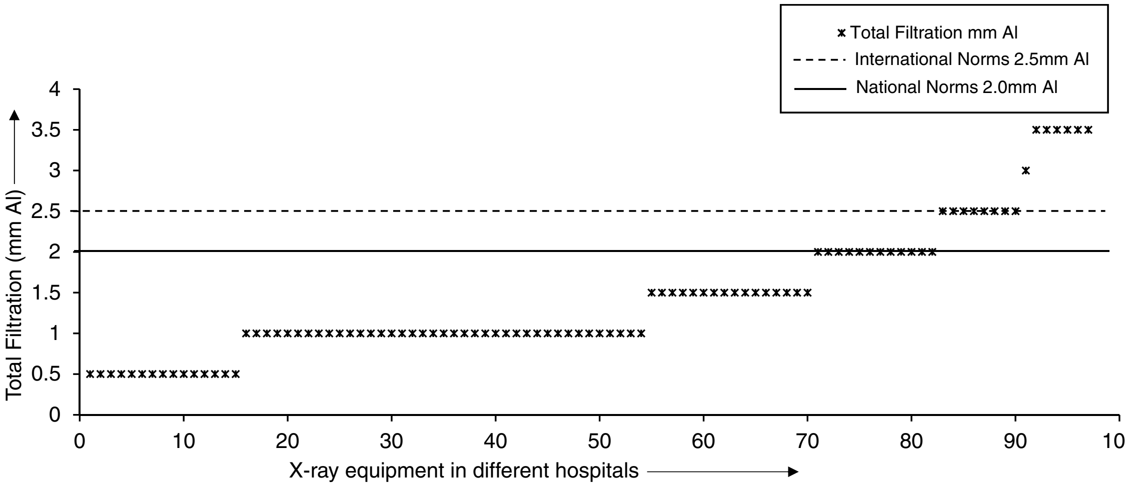

Fig. 5 Total filtration measured at 70 kV in 97 X-ray machines

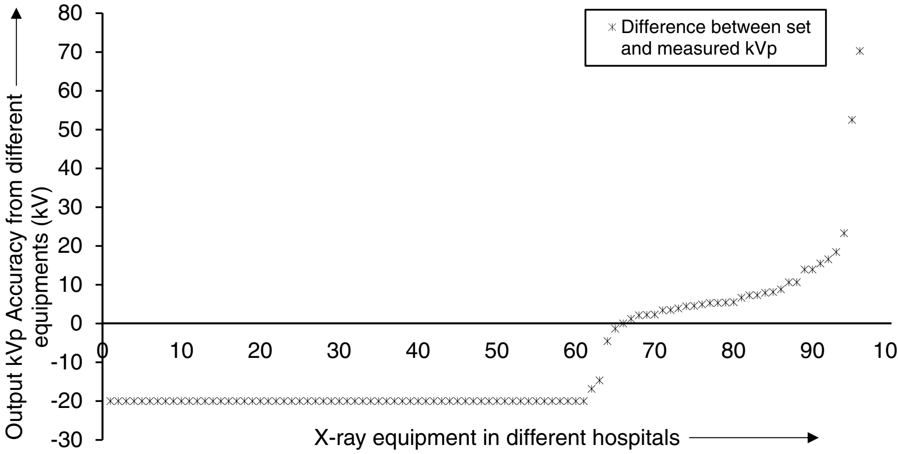

Fig. 6 Accelerating potential reproducibility of different X-ray machines

Table 5 Congruency between the radiation beam and the optical field of 47 X-ray machines

Congruency	*N*	Range (% of SID)	Minimum (% of SID)	Maximum (% of SID)	Mean (% of SID)	SD (% of SID)
$x+x'$[a]	47	14.80	0.50	15.30	3.78	2.54
$y+y'$[b]	47	10.40	0.50	10.90	3.69	2.25
$x+x'+y+y'$[c]	47	17.90	1.50	19.40	7.47	3.56

[a] Total misalignment of both x- and x'-axes

[b] Total misalignment of both y- and y'-axes

[c] Total misalignment of all the four axes

limit, whereas only 15 were within the acceptable limit. For y-axis, only 11 of 47 units were within the safety limit [8, 9, 24] (Fig. 7). The calculated means for the x- and y-axes were 3.78 ± 2.54 SD% and 3.69 ± 2.25 SD% of SID (Table 5). When considering a whole axis (x and y), 38 of 47 (80.85%) units were outside the acceptable limit. Due to this problem of congruency, radiation workers cannot escape radiation when opening the collimator fully, as previously mentioned. The amount of unwanted primary and secondary radiation increases enormously when opening the collimator fully, and the patient and radiation worker dose increases rapidly. In some diagnostic centers with severe misaligned units, technicians fully opened the collimator and did not use optical light; they focused the beam based on mental imagery. Moreover, if

Author's personal copy

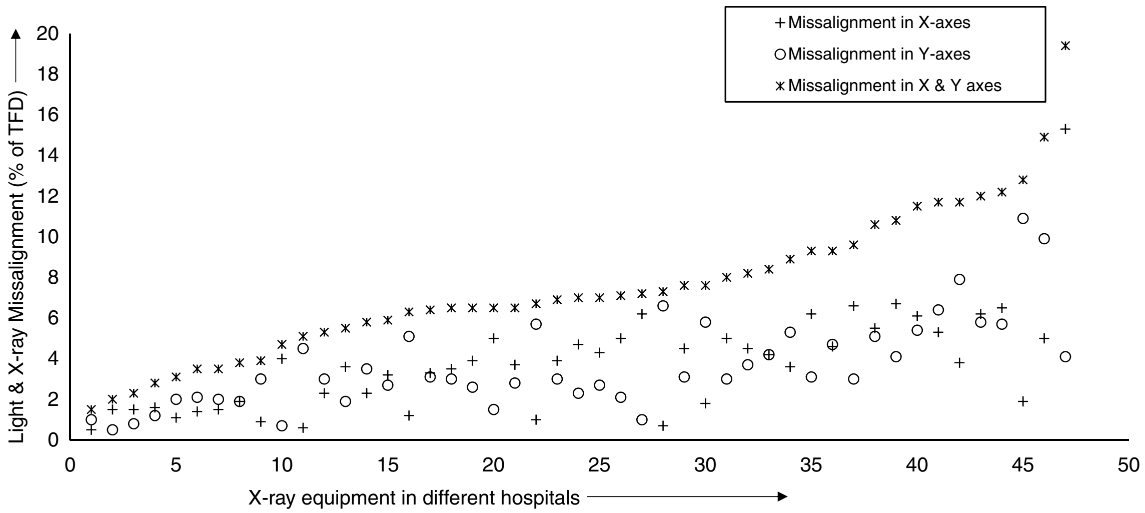

Fig. 7 Misalignment between the optical light and the X-ray beam of 47 X-ray units

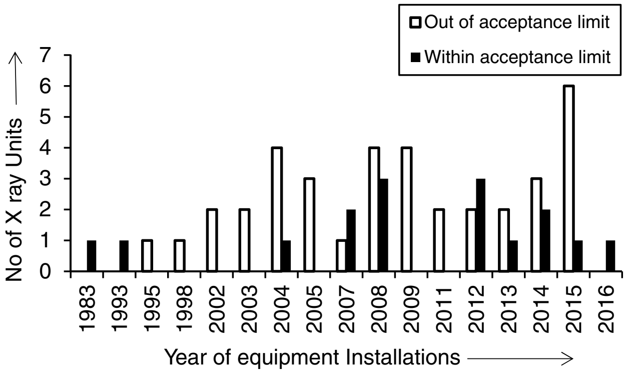

Fig. 8 Relationship between the year of installation and congruency misalignment

the technicians are not mindful of protection issues, the practice may result in an unreasonable increase in the patient dose [31].

Six X-ray units included in the present study were installed in 2015, of which 5 were outside the acceptable limit. This showed that newly installed units also have congruency problems, and according to certain bodies, these units require proper, frequent quality checks and maintenance by a service engineer [4] (Fig. 8). Of the 9 units that did not meet the safety standard, 8 were AERB approved. However, of the 38 acceptable units, 28 (73.68%) were AERB approved units and 10 (26.32%) had an unknown approval status due to the lack of information about old machines. Sungita et al. studied 196 X-ray units; the accuracy of beam alignment and collimation of 80 units were tested. In their study, 60% of the units passed the tests [25]. In 2010, Sonawane et al. reported that 77% of 118 medical diagnostic X-ray machines were within the safety limits [32]. In comparison with those findings, the current situation of the present study area was far behind.

Table 6 Angle between the central X-ray beam and image receptor of 53 X-ray units

Fault in perpendicularity	0.5°	0.5°–1.5°	1.5°–3°	3° above
No. of X-ray units	5	11	17	20

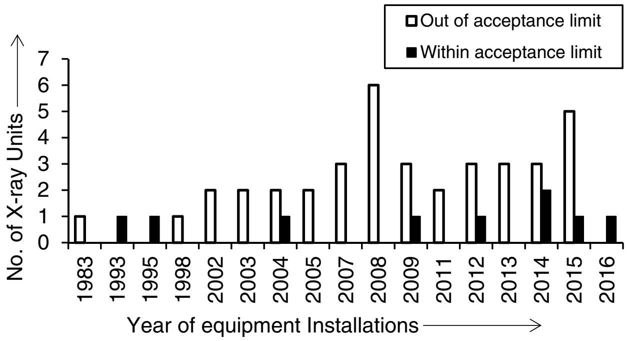

Fig. 9 Relationship between the year of installation and the perpendicularity of the central beam

3.3 Perpendicularity of the central beam and image receptor

The authors performed perpendicularity measurements on 53 X-ray units; 6 types of equipment with non-adjustable collimators were studied (Table 2). Of the X-ray units with misalignment of less than 1.5°, 30.19% were within the acceptable limit. There were 37 units with misalignment > 1.5°. According to the safety code, 69.81% were

Author's personal copy

Table 7 Status of the congruency and perpendicularity of different manufacturers of diagnostic X-ray units

Manufacturer	Congruency			Perpendicularity		
	Within tolerance (%)	Out of tolerance (%)	Total	Within tolerance (%)	Out of tolerance (%)	Total
M.E. X-ray(India) Pvt. Ltd.	12.50	87.50	16	38.09	61.90	21
M/s. Siemens Ltd.	16.67	83.33	6	33.33	66.67	6
M/s. Squarem Systems Pvt. Ltd.	20.00	80.00	5	40.00	60.00	5
M/s. Philips Electronics India Ltd.	0.00	100.00	5	0.00	100.00	5
M/s. Wipro GE Healthcare Pvt. Ltd.	75.00	25.00	4	25.00	75.00	4
Allengers Medi Sys	66.67	33.33	3	75.00	25.00	4
Others	0.00	100.00	8	0.00	100.00	8
Total	19.15	80.85	47	30.19	69.81	53

outside the acceptable limit [24, 26] (Table 6). Even for new X-ray units (Fig. 9), the authors found problems pertaining to congruency between light and radiation, and perpendicularity between the central beam and the image receptor. Of the 7 X-ray units installed in 2015, 6 had problems with beam alignment perpendicularity. Of the 16 units that were within tolerance, 14 were AERB-approved units and 2 were unknown. Of the 37 acceptable units, 27 (72.97%) were AERB approved and 10 (27.03%) were unknown. Owing to problems in perpendicularity, the radiographer often repeats imaging which doubles the dose received. Once again, to minimize the associated radiation risk and maximize the benefit of medical examination, unnecessary radiation exposure should be eliminated [33].

Table 7 shows different X-ray manufacturers and their congruency and perpendicularity statuses. Among the different manufacturers, ME X-ray Pvt., Ltd. contributes 34.04% in congruency study and 39.62% in the perpendicularity study. At the same time, 87.50 and 61.90% of ME X-rays were outside the acceptable limits of congruency and perpendicularity, respectively.

4 Conclusion

The total filtration of units ($n = 97$) at different institutions was compared with national and international standards; 27.83% met the national standard; and only 15.46% met the international standard. It appears that most of the equipment in the present study had poor filters. In the congruency study, from the 47 units which we could study, 80.85% were found to be beyond the acceptable limit. At the same time, the optical lights of 4 X-ray units did not work; 6 units had fixed their collimators to full, and more than 10 units had misalignments above 10% of the SID. When testing the central beam and image receptor perpendicularity of 53 units, 69.81% of X-ray units were more than 1.5° off perpendicularity and did not pass the test. These faults result in significantly increased patient and radiation worker doses. In the present study, both new and old machines had similar problems. The authors recommend that the equipment be properly checked by a service engineer periodically, followed by re-measurement of all parameters for verification and certification.

Acknowledgements The authors express their sincere thanks to the Committee for Safety Research Programme (CSRP), the Atomic Energy Regulatory Board (AERB, Mumbai), Government of India, for financial assistance through Major Research Project No.AERB/CSRP/58/02/2014 awarded in September 30, 2014.

Funding This study was funded by the Committee for Safety Research Programme (CSRP) and the Atomic Energy Regulatory Board (AERB), project number AERB/CSRP/58/02/2014; September 30, 2014.

Compliance with ethical standards

Conflicts of interest The authors declare that they have no conflicts of interest.

Ethical approval This article does not contain any human and animal studies.

References

1. Bennett BG. Exposures from medical radiation world-wide. Radiat Prot Dosimetry. 1991;36:237–42.
2. Bushong SC. Radiologic science for technologists: physics, biology, and protection, tenth edition, 3251 Riverport Lane, St. Louis, Missouri 63043. Amsterdam: Elsevier Mosby; 2013. pp. 578–9.
3. International Commission on Radiological Protection. Recommendations of the Commission on Radiological Protection. ICRP Publication 60. Ann of the ICRP 21 Oxford: Pergamon; 1990.
4. Atomic Energy Regulatory Board. Notification No. 30.1.2002-ER, Appointment of Chairman, AERB as the 'Competent Authority' of radiation protection in India, The Gazette of India, Part-II, Sect. 3(ii), 2006.
5. Atomic Energy Regulatory Board. Notification No. 25/2/83-ER, Constitution of AERB, The Gazette of India, Part-II, Sect. 3(ii); 1983.

Author's personal copy

6. Supe SJ, Iyer PS, Sasane JB, Sawant SG, Shirva VK. Estimation and significance of patient dose from diagnostic X-ray practices in India. Radiat Prot Dosimetry. 1992;43(1/4):209–11.
7. Lalrinmawia J, Pau KS, Tiwari RC. Quality assurance assessment of conventional diagnostic X-ray installations in Mizoram. J Med Phys. 2017;42 Suppl S1:208–9. http://www.jmp.org.in/text.asp?2017/42/5/110/217113. (ISSN: 0971–6203).
8. Gray JE, Winkler NT, Stears J, Frank ED. Quality control in diagnostic imaging. Maryland USA. Germantown: An Aspen Publication; 1983.
9. Papp J. Quality management in the imaging sciences 5th ed. 3251 Riverport Lane. Missouri: Elsevier Health Sciences; 2015.
10. Johns HE, Cunningham JR. The physics of radiology, 4th ed. Springfield, Illinois 62717, USA: Thomas CC; 1983.
11. Asadinezhad M, Toosi MTB, Ebrahiminia A, Giahi M. Quality control assessment of conventional radiology devices in Iran. Iran J Med Phys. 2017;14(1):1–7.
12. Meredith WJ, Massey JB. Fundamental Physics of Radiology, 3rd ed. Bombay: Varghese Publishing House; 1992.
13. Ahmad MA. Safety of analytical X-ray appliances, Master's Thesis, University of Helsinki, Finland, 2015.
14. IAEA. Diagnostic radiology physics; A handbook for teachers and students. 1400 Vienna, Austria, 2014.
15. American Association of Physicists in Medicine. Publication Committee, Basic in Diagnostic Radiology, AAPM Report No 4; American Institute of Physics, New York, 1981.
16. Lalrinmawia J, Pau KS, Tiwari RC. Investigations of workers dose due to stray radiation in X-ray installations in Mizoram. Recent advances in physics research and its relevance. New Delhi: Excel India publishers; 2017. pp. 258–63. (ISBN: ISBN: 978-93-86256-85-0$4).
17. Lalrinmawia J, Pau KS, Tiwari RC. Investigations of public dose due to stray radiation in X-ray installations in Mizoram. Science and technology for shaping the future of Mizoram. New Delhi: Allied publishers Pvt. Ltd.; 2017, pp. 305–9. (ISBN: 978-93-85926-49-5).
18. National Council on Radiation Protection and Measurements. Structural shielding design for medical X-rays imaging facilities. Bethesda, MD: NCRP; NCRP Report; 2004. p. 147.
19. Ebisawa MLNI., Magon MFA, Mascarenhas YM. Evolution of X-ray machine quality control acceptance indices. J Appl Clin Med Phys. 2009;10(4):252–9.
20. Operator Manual 06-526 RAD-CHECK™ PLUS. P/N 136201, Rev. 6, Fluke Corporation, USA, 2006.
21. Rasuli B, Pashazadeh AM, Ghorbani M, Juybari RT, Naserpour M. Patient dose measurement in common medical X-ray examinations in Iran. J Appl Clin Med Phys. 2016;17(1):374–86.
22. Atomic Energy Regulatory Board. Safety Code No. AERB/SC/MED-2 (Rev. 1), 'Safety Code for Medical Diagnostic X-ray equipment and Installations' AERB, Mumbai, 2001.
23. Health Canada. Safety code 35: Safety procedures for the installation, use and control of X-ray equipment in large medical radiological facilities. Retrieved January 22 2017 from http://www.hc-sc.gc.ca (2008).
24. Radiation Protection No 91. Criteria for acceptability of radiological and nuclear medicine installations. Euratom Treaty and the Council Directives; European commission. https://ec.europa.eu/energy/sites/ener/files/documents/091_en.pdf, p. 6.
25. Operator Manual. 07-661-7662 Collimator/Beam Alignment Test Tool. Fluke Corporation, USA; 2005.
26. Sungita YY, Mdoe SLC. Msaki Peter. Diagnostic X-ray facilities as per quality control performances in Tanzania. J Appl Clin Med Phys 2006;7 (4):66–73.
27. Turner JE. Interaction of Ionizing Radiation with Matter. Health Phys. 2005;88(6):;520 – 544.
28. National Council on Radiation Protection and Measurements. Medical X-ray, Electron beam and Gamma-ray Protection for energies up to 50 MeV (Equipment Design, Performance and use). Bethesda: NCRP; NCRP Report, 102; 1989.
29. Vlachos I, Tsantilas X, Kalyvas N, Delis H, Kandaraskis I, Panayiotakis G. Measuring scatter radiation in diagnostic X-rays for radiation protection purposes. Radiat Prot Dosimetry. 2015;165(1–4):382–5.
30. American Association of Physics in Medicine. Publication Committee 'Protocols for the Radiation Safety Surveys of Diagnostic Radiological Equipment' AAPM Report No 25 American Institute of Physics, New York; 1988.
31. Paolicchi F, Miniati F, Bastiani L, Faggioni L, Ciaramella A, Creonti I, et al. Assessment of radiation protection awareness and knowledge about radiological examination doses among Italian radiographers. Insight Imaging. 2016;7(2):233–42.
32. Sonawane AU, Meghraj S, Sunil KJVK, Kulkarni ASVK Pradhan AS. Radiological safety status and quality assurance audit of medical X-ray diagnostic installations in India. J Med Phys. 2010;35:229–34.
33. Hude W. Radiation risks: what is to be done? American Roentgen Ray Society. 2015;204:124–7.

Radiological Physics and Technology
https://doi.org/10.1007/s12194-019-00526-6

Evaluation of radiation doses at diagnostic X-ray control panels and outside patient entrance doors in Aizawl district, India

Jonathan Lalrinmawia[1,2] · **Kham Suan Pau**[2] · **Ramesh Chandra Tiwari**[1]

Received: 11 February 2019 / Revised: 20 July 2019 / Accepted: 20 July 2019
© Japanese Society of Radiological Technology and Japan Society of Medical Physics 2019

Abstract

The purpose of this research was to measure the radiation level and estimate the dosage at the control panel (CP) and outside the patient entrance door (PED) of diagnostic X-ray installations. This is important for ensuring the safety of workers and the public, particularly in the study area, where there is no proper radiation monitoring service. A water phantom, 10-L fresh water in a plastic container, was used as the source of scattered radiation. Using an ion-chamber survey meter, the stray radiation rate was measured at the CP and outside the PED for both chest and couch missions. The CPs were fully covered by a protective barrier, providing a negligible exposure rate (i.e., 0.07–4.2 mR/h for chest and 0.21–3.8 mR/h for couch). By contrast, installations that did not properly cover the CP showed relatively high exposures (from 18 to 205 mR/h for chest and 2.4–270 mR/h for couch). The radiation rates outside the PED in installations having lead-lined doors were negligibly low; whereas, in installations having no lead-lining, exposure rates reached as high as 95 and 110 mR/h for chest and couch missions, respectively. The occupational doses were well below the Atomic Energy Regulatory Board dose limit (i.e., 40 mR/week). However, excessive doses were observed in public spaces outside the PED, compared with the dose limit for the public (i.e., 2 mR/week).

Keywords Conventional diagnostic X-ray · Occupational dose · Public dose · Protective barrier · Patient entrance door · Radiation safety

1 Introduction

Shortly after the discovery of X-rays by Wilhelm Conrad Roentgen in 1895, the harmful effects of radiation exacerbated by inadequate protection were widely known [1]. However, until the 1950s, scientific reports concerning late radiation effects caused by low-level exposure did not appear [2]. The recent study of solid cancer incidence among Chinese medical diagnostic X-ray workers by Sun et al. showed that the risk for solid cancers increased significantly as cumulative radiation exposure increased [3]. In developed countries, the contribution of diagnostic X-rays to cancer ranged from 0.6 to 1.8% of the cumulative risk of cancer to age 75 years [4]. Because of the potential health effects of ionizing radiation, recommendations and protection guidelines were made by experts and national/international bodies to reduce the health effects of X-rays for workers and members of the public [1, 5, 6]. The main objective of radiation protection is to ensure that the doses received by workers and members of the public are kept below permissible levels [7]. The International Commission for Radiation Protection is the pertinent international regulatory body, and in India, the Atomic Energy Regulatory Board (AERB) is the national counterpart. These bodies recommend norms for permissible dose limits for the public and for workers [8].

Among man-made ionizing radiation sources, a major contributor to public and occupational exposure is medical diagnostic X-rays [9, 10]. Diagnostic X-ray examinations account for approximately 51% of the population doses [11]. Radiation workers and the general public are mainly exposed to radiation from primary and scattered varieties. However, they receive very small amounts of primary radiation, so that most of the doses result from scattered radiation [12]. When primary radiation interacts with matter, it is either absorbed or changed via energy level and/or direction of

---

✉ Ramesh Chandra Tiwari
ramesh_mzu@rediffmail.com

[1] Department of Physics, Mizoram University, Aizawl, Mizoram 796004, India

[2] Mizoram State Cancer Institute, Zemabawk, Aizawl, Mizoram 796017, India

Published online: 06 August 2019

motion, after which it becomes scattered radiation [13]. Photon interactions involve three important mechanisms: photoelectric, coherent–incoherent scattering, and pair production [14]. However, in medical diagnostic radiology, only the photoelectric effect and coherent–incoherent scattering are important, because the energy employed ranges up to 150 keV [15].

The use of protective shields can significantly reduce radiation exposure of X-ray operators and the general public [16]. Protection can be ensured, and risks can be controlled by suitable design and commissioning of equipment [17]. It is well known that the essential requirement in the practical approach to radiation protection is measurement of the hazard [18]. Using a survey meter, the authors measured stray radiation from X-ray tubes as leakage radiation and scattered radiation from the water phantom, ceiling, wall, etc., at the control panel (CP) and outside the patient entrance door (PED). The primary radiation transmitted through the patient to the couch and floor in couch missions, or through the patient to the chest stand and wall in chest missions, was negligible [19]. Using calculated workload (*W*) (mA-min/week) and exposure rates, doses were calculated in units of mR/week and compared to safety standards. Possible reasons for excessive doses were also discussed. In a study of occupational exposure in Brazil by Cunha et al. and a national survey of occupational exposure among diagnostic technologists in South Korea by Lee et al., radiation workers were monitored [10, 20]. However, in this study, none of the workers or the public were properly monitored using personal monitoring devices, which is the reason the authors followed the method described.

2 Materials and methods

The number of fixed and mobile-fixed X-ray machines in the present study area was 37, which were installed at 31 different institutions (Fig. 1). Mobile X-rays were used as fixed in this study. Workloads of 3022.45 mA-min/week (58.4% of all workload across the state (i.e., Mizoram) were performed using this equipment. Among these, 83.8% were AERB-type approved units, and 16.2% machines had unknown approval statuses because of missing information. Some of the machines were very old. Among these institutions, some of the CPs were properly covered by protective barriers, whereas others were partly covered by a barrier or had no barrier at all. Only a few PEDs had lead-lined doors, whereas others employed typical wooden doors, plywood lined doors, or aluminum plane sheet-lined doors. The nature, type, and thickness of CP barriers and PEDs were measured and recorded. The authors also examined product manuals for accurate information. The protective barriers used by the X-ray users were lead lined, 6-feet high, 2.5–3-feet wide, with a lead thickness equivalent to 1.5–1.7 mm. The lead-lined doors were 1.5-mm lead thickness equivalent.

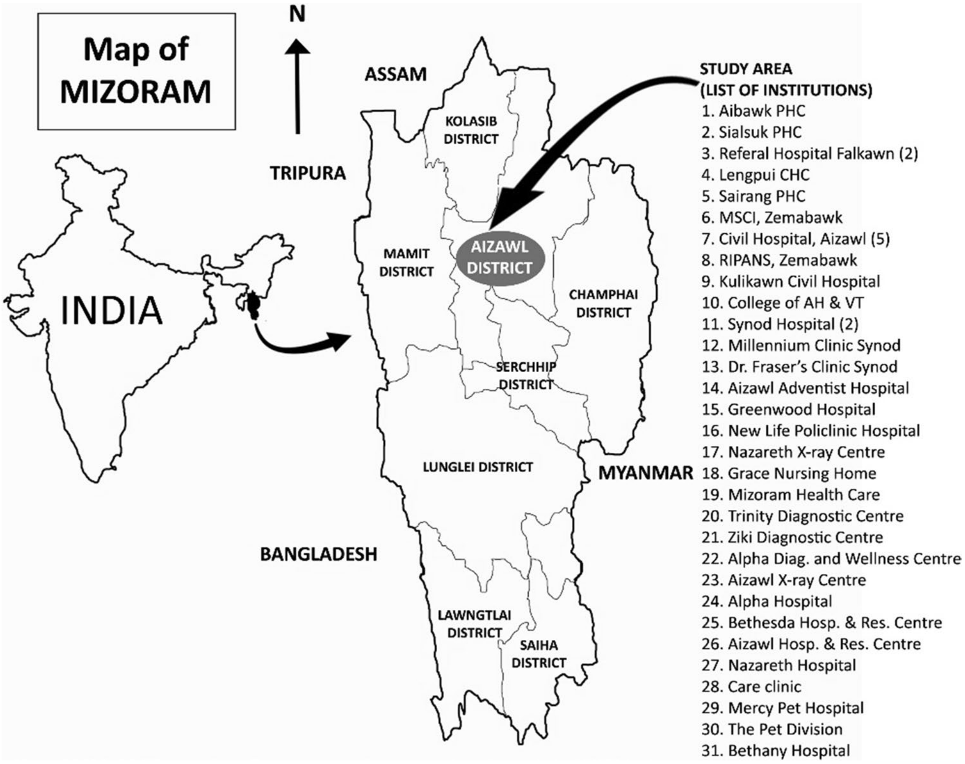
Map of MIZORAM
N
ASSAM
TRIPURA
INDIA
KOLASIB DISTRICT
MAMIT DISTRICT
AIZAWL DISTRICT
CHAMPHAI DISTRICT
SERCHHIP DISTRICT
LUNGLEI DISTRICT
MYANMAR
BANGLADESH
LAWNGTLAI DISTRICT
SAIHA DISTRICT
STUDY AREA
(LIST OF INSTITUTIONS)
1. Aibawk PHC
2. Sialsuk PHC
3. Referal Hospital Falkawn (2)
4. Lengpui CHC
5. Sairang PHC
6. MSCI, Zemabawk
7. Civil Hospital, Aizawl (5)
8. RIPANS, Zemabawk
9. Kulikawn Civil Hospital
10. College of AH & VT
11. Synod Hospital (2)
12. Millennium Clinic Synod
13. Dr. Fraser's Clinic Synod
14. Aizawl Adventist Hospital
15. Greenwood Hospital
16. New Life Policlinic Hospital
17. Nazareth X-ray Centre
18. Grace Nursing Home
19. Mizoram Health Care
20. Trinity Diagnostic Centre
21. Ziki Diagnostic Centre
22. Alpha Diag. and Wellness Centre
23. Aizawl X-ray Centre
24. Alpha Hospital
25. Bethesda Hosp. & Res. Centre
26. Aizawl Hosp. & Res. Centre
27. Nazareth Hospital
28. Care clinic
29. Mercy Pet Hospital
30. The Pet Division
31. Bethany Hospital

Fig. 1 Location of the present study area (37 machines installed in 31 different institutions)

Sketches were made for all X-ray installations indicating X-ray source, couch, chest stand, protective barrier, CP, PED, etc. Distances from the CP to the couch and chest stand and from the couch and chest stand to the PED were measured and recorded (Fig. 2). A water phantom, 10-L fresh water in a plastic container, was used as a source of scattered radiation. The plastic container was a perfect cube structure where all the sides (i.e., length, width, and height) were equivalent (i.e., 31 cm each). The thickness of this container was 1 cm, and it was uniform throughout the body (Fig. 3). It was positioned on the couch for vertical exposure (couch mission) and at a chest stand for horizontal exposure (chest mission). Field sizes were adjusted to the maximum and focused on the water phantom. Exposure rates were measured at the CP and outside the PED separately for both chest and couch missions. For measuring exposure rates, a pressurized ion-chamber survey meter (Model 451 P, Fluke Biomedical, Everett, WA, USA) was used. It had a 230-cc active volume air ionization chamber pressurized to eight atmospheres. The calibration measurements are traceable to the National Institute of Standards and Technology (NIST, Gaithersburg, MD, USA) [21]. All measurements were performed in freeze mode.

The stray radiation levels at the CP and outside the PED were measured using the maximum accelerating potential setting (i.e., 85–120 kVp) and minimum input-tube current (i.e., 25–50 mA) with fixed exposure time of 1 s [22]. The survey meter was placed at a height in relation to the water phantom base with its measuring surface towards the water phantom [23]. In this configuration, the survey meter could measure stray radiation scattered from the phantom, the walls, the floor, and the ceiling, including leakage from the X-ray tube [24]. The workload for each piece of equipment was calculated in mA-min/week using Eq. (1) [25, 26]. Patients per day were calculated based on patient records kept by the institutions. The total number of patient exams throughout a year was divided by the total number of working days during that period.

$$W=\frac{\text{patients}}{\text{day}}\times\frac{\text{films}}{\text{patient}}\times\frac{\text{mAs}}{\text{film}}\times\frac{\text{days}}{\text{week}}\times\frac{1\text{ min}}{60\text{ s}}. \tag{1}$$

Then, the radiation dose in units of mR/week was calculated from the workload and stray radiation rates using Eq. (2) [27, 28]:

$$\begin{aligned}\text{Dose}\left(\frac{\text{mR}}{\text{week}}\right) =&\text{workload}\left(\frac{\text{mA}-\text{min}}{\text{week}}\right)\\ &\times\text{Exposure Rate}\left(\frac{\text{mR}}{\text{h}}\right)\\ &\times\left(\frac{1}{60}\right)\times\left(\frac{1}{\text{mA used}}\right),\end{aligned} \tag{2}$$

where mA is the input-tube current from the survey. The authors measured tube voltage for each machine to improve clarification using a wide-range digital kVp meter (model 07-494, Fluke Biomedical, Cleveland, Ohio, USA). For evaluating kVp accuracy, the authors considered the tube

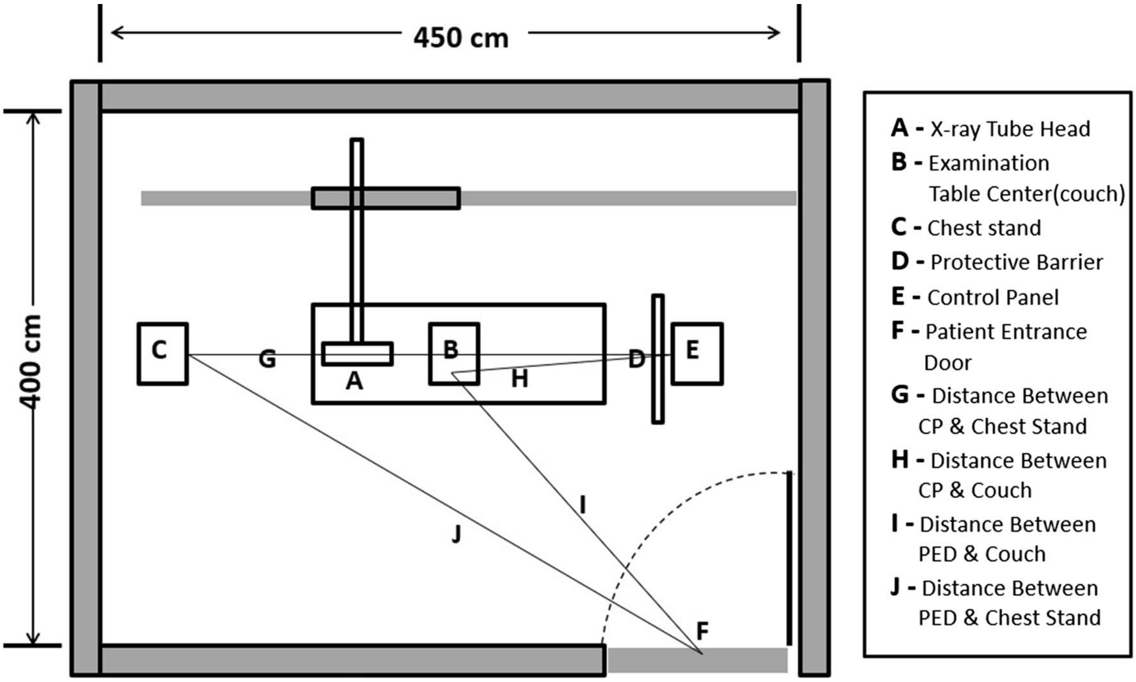
450 cm
400 cm
A
B
C
D
E
F
G
H
I
J
A - X-ray Tube Head
B - Examination Table Center(couch)
C - Chest stand
D - Protective Barrier
E - Control Panel
F - Patient Entrance Door
G - Distance Between CP & Chest Stand
H - Distance Between CP & Couch
I - Distance Between PED & Couch
J - Distance Between PED & Chest Stand

Fig. 2 Layout of the X-ray installation room

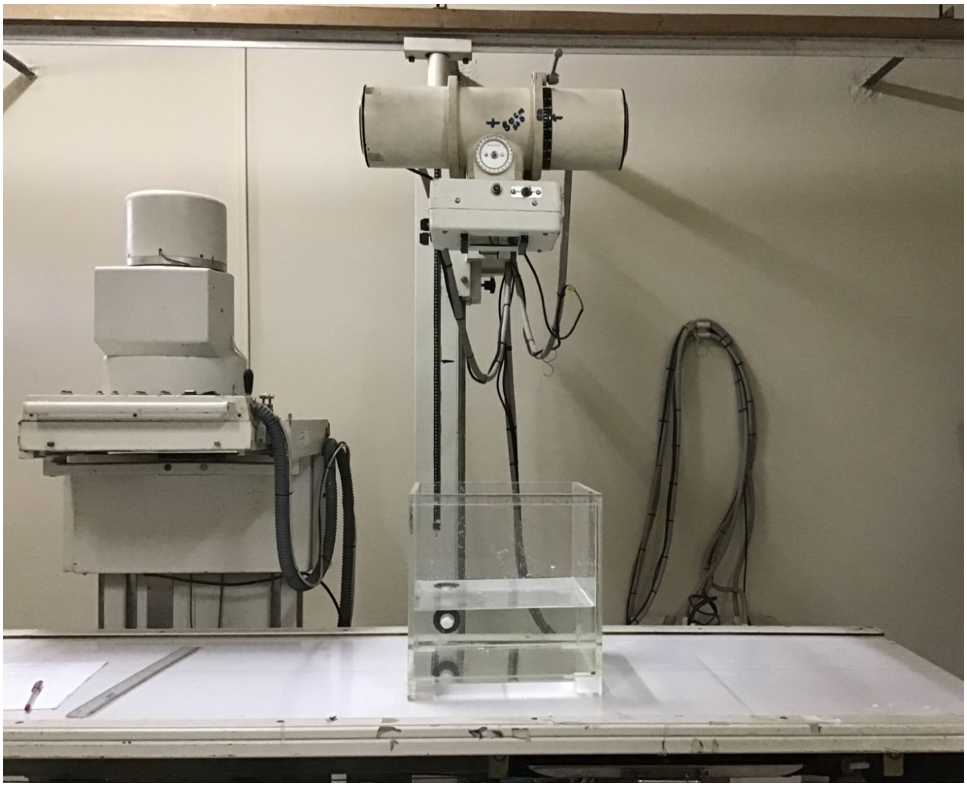

Fig. 3 A water phantom setting to measure stray radiation for vertical exposure (couch mission)

voltage between 50 and 150 kVp with 5 kVp steps, and the tube loading and focus-to-detector distance (FDD) were set as per the Fluke manual [29, 30]. To calculate mean, range, and standard deviation (SD), SPSS Statistics for Windows, v.17.0 was used (SPSS, Inc., Chicago, IL, USA).

3 Results and discussion

3.1 Exposures rate at CP for both chest and couch missions

The CPs were located at different distances from the couch and chest stand. 94.4% of CPs were within 300 cm for couch missions and 62.5% were so for chest missions. This is in contrast to the recommended distance, which should be more than 300 cm [6]. The stray radiation measured at the CPs was mostly scattered and originated from two main sources: the phantom on the couch and the one on the chest stand. Exposure rates at the CPs in different installations varied from 0.07 to 360 mR/h (Fig. 4). For chest missions, 16 CPs were properly protected by barriers from stray radiation, whereas seven were partly covered by barriers, and nine had no barriers at all. For couch missions, 16 CPs were properly protected by barriers, whereas seven were partly covered by barriers and 13 had none. For the chest and couch missions where CPs were properly covered by barriers, significantly lower exposure rates were found for different units. By contrast, installations with partial or absent barriers showed very high exposure rates: 50 times more than cases with CPs properly covered with barriers (Table 1).

3.2 Comparison between different utilization of CP barriers

The exposure rates for chest missions in installations with CPs properly covered by a protective barrier, CPs with insufficient covers, and those with no barriers at all are shown in Fig. 5. The CPs that were fully covered by protective barriers had relatively negligible exposure rates (i.e., 0.07–4.2 mR/h with mean ± SD of 0.68 ± 1.03 mR/h). Contrastingly, installations in which the CPs were not properly covered had relatively high exposure (18–205 mR/h with mean ± SD of 74.29 ± 68.40 mR/h). Furthermore, it was found that the exposure rates at CPs where barriers were absent ranged from 1.1 to 235 mR/h with mean ± SD of 50.36 ± 86.86 mR/h (Table 1). There were institutions that showed low exposure rates, but they had no barriers installed. These types of equipment were mobile-fixed devices with low electronic input parameters and were lower-efficiency units (Fig. 5). By comparing the exposure rates at institutions without barriers and with inadequate barriers covering the CPs for chest missions, barriers that did not properly cover CPs had relatively high exposure rates (Table 1). The reason was that, for barriers not covering CPs properly or improperly installed barriers, the operators considered only stray radiation from the couch.

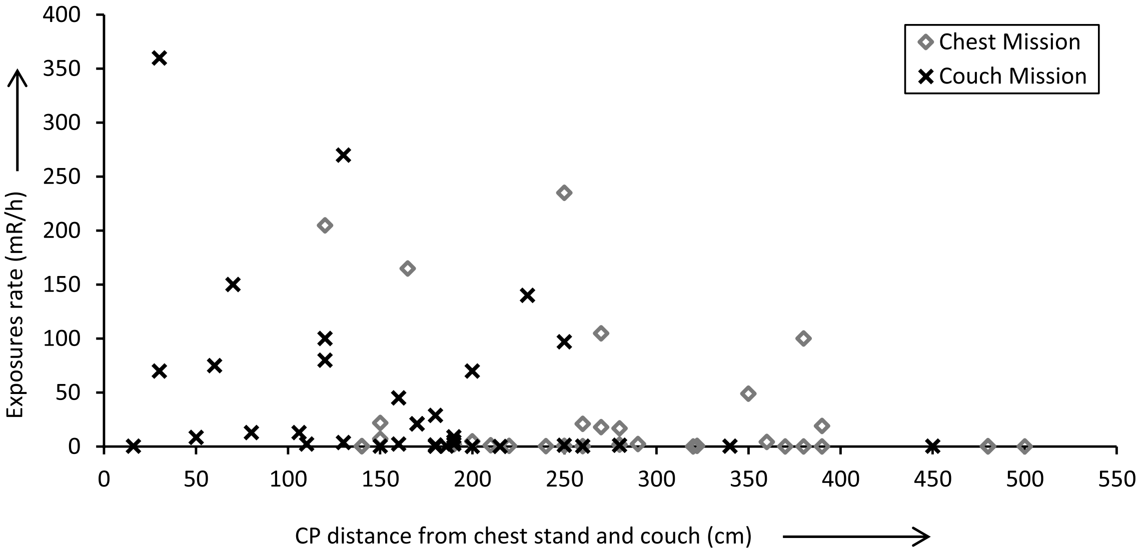

Fig. 4 Exposure rates measured at CPs for both chest and couch missions

Table 1 Exposures rates measured at CPs behind different arrangements of protective barriers at different installations

Barrier	No. of machines	Minimum exposure rate (mR/h)	Maximum exposure rate (mR/h)	Range (mR/h)	Mean (mR/h)	SD (mR/h)
Chest mission						
Barrier covering CP properly	16 (50%)	0.07	4.2	4.13	0.68	1.03
Barrier not covering CP properly	7 (21.9%)	18	205	187	74.29	68.4
Barrier not available	9 (28.1%)	1.1	235	233.9	50.36	86.86
Couch mission						
Barrier covering CP properly	16 (44.4445%)	0.21	3.8	3.59	1	1.04
Barrier not covering CP properly	7 (19.4444%)	2.4	270	267.6	73.86	99.8
Barrier not available	13 (36.1111%)	8.5	360	351.5	81.65	93.75

For that, they adjusted the barrier. As such, the CPs were fully opened for chest-scattering radiation. In some installations, there were chest stands located adjacent to the CPs. Moreover, for other parameters, such as variation in distance between the chest stand and CP, the generator type may have affected exposure rates.

Exposure rates for couch missions in installations covering CPs properly with protective barriers with inadequate CP covers and with no barriers at all are shown in Fig. 6. For couch missions, the exposure rate for barriers covering the CPs properly varied 0.21–3.8 mR/h with mean ± SD of 1.00 ± 1.04 mR/h. Similar to the chest-mission exposure rates measured at fully covered CPs, these were significantly low. There was not much difference between the exposure rates at CPs with no barriers and those with partial barriers. The former had 8.5–360 mR/h with mean ± SD of 81.65 ± 93.75 mR/h, whereas the latter ranged from 2.4 to 270 mR/h with mean ± SD of 73.86 ± 99.8 mR/h (Table 1). In the present study, the significant effects of distance on the exposure rates were not recognized, even though each piece of equipment was operating with nearly equal parameters. One of the main reasons is that none of the X-ray equipment followed the same installation geometry and even the same models at different institutions showed different efficiencies, such as with kVp reproducibility (Fig. 7) [26, 30].

3.3 Exposure rates outside the PED for both chest and couch missions

For evaluating public doses, exposure rates outside the PED were measured, where exposure was mainly caused by stray radiation scattered from the phantoms. These were located at different distances from the PED (Fig. 8). For chest and couch missions, only two and three installations, respectively, were equipped with lead-lined doors. A large number (> 90%) of installations used solid

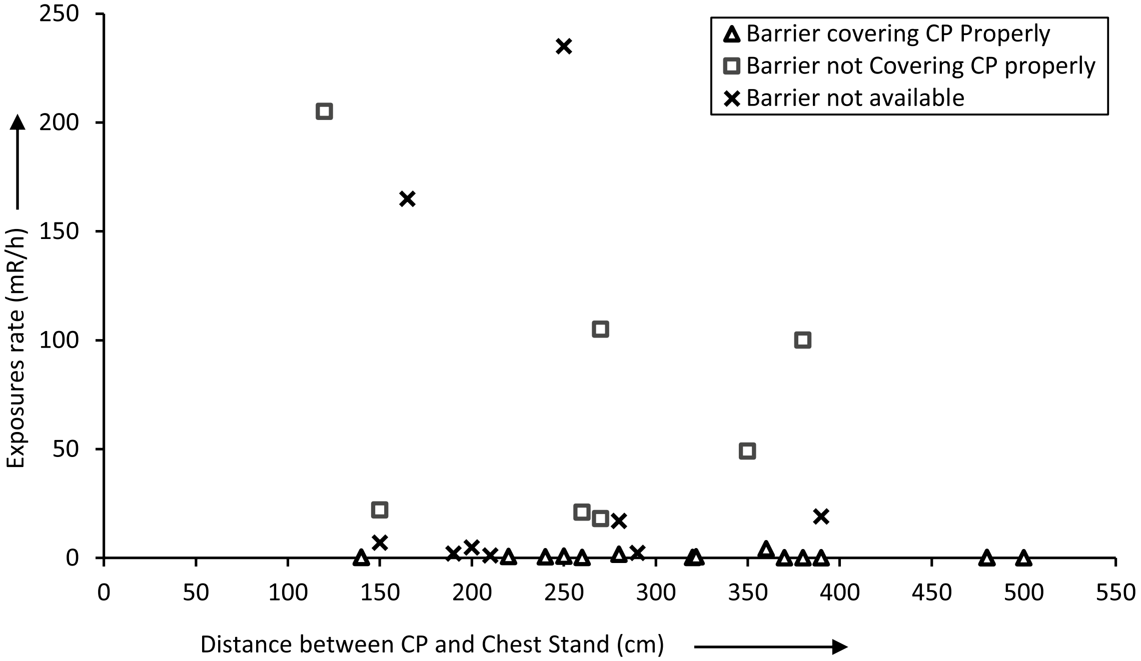

Fig. 5 Exposure rates measured at CPs for chest missions (comparing different barrier utilizations)

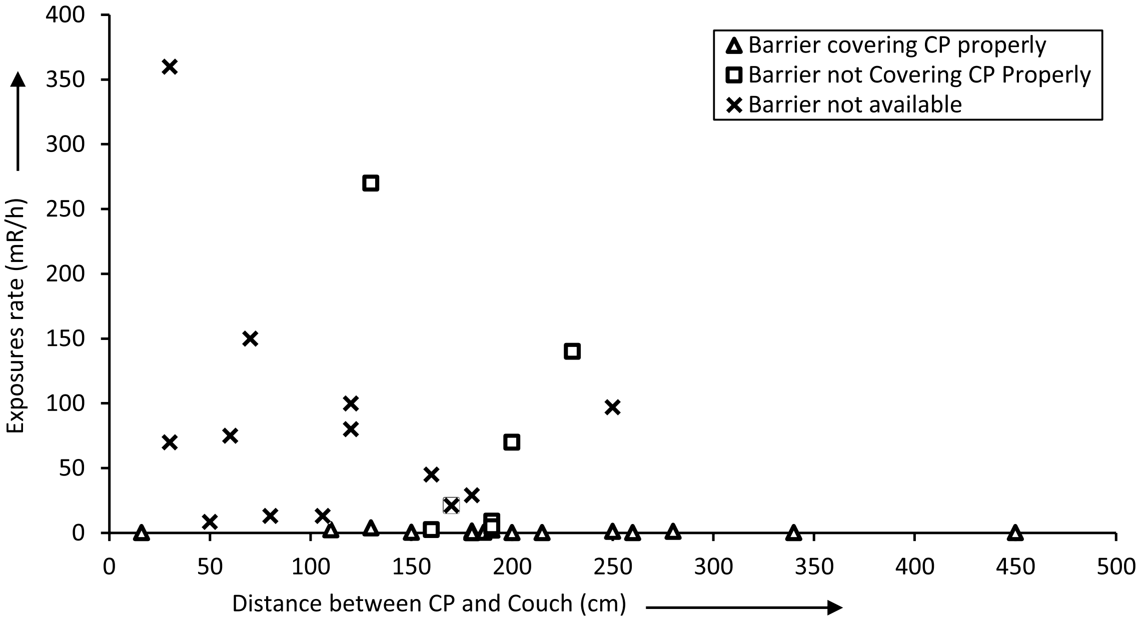

Fig. 6 Exposure rates measured at CPs for couch missions (comparing different barrier utilizations)

wooden doors, plywood doors, aluminum plane sheet doors, etc. (Table 2). It was found that all institutions had at least a simple traditional PED. The mean of the exposure rate outside lead-lined PEDs was mean ± SD of 0.05 ± 0.04 mR/h and mean ± SD of 1.78 ± 2.79 mR/h for chest and couch missions, respectively. Those institutions that did not employ lead-lined doors had a mean exposure rate of mean ± SD of 18.03 ± 22.22 mR/h and mean ± SD of 30.83 ± 30.46 mR/h for chest and couch missions, respectively. These figures show that lead-lined doors had significantly greater effect on attenuation of

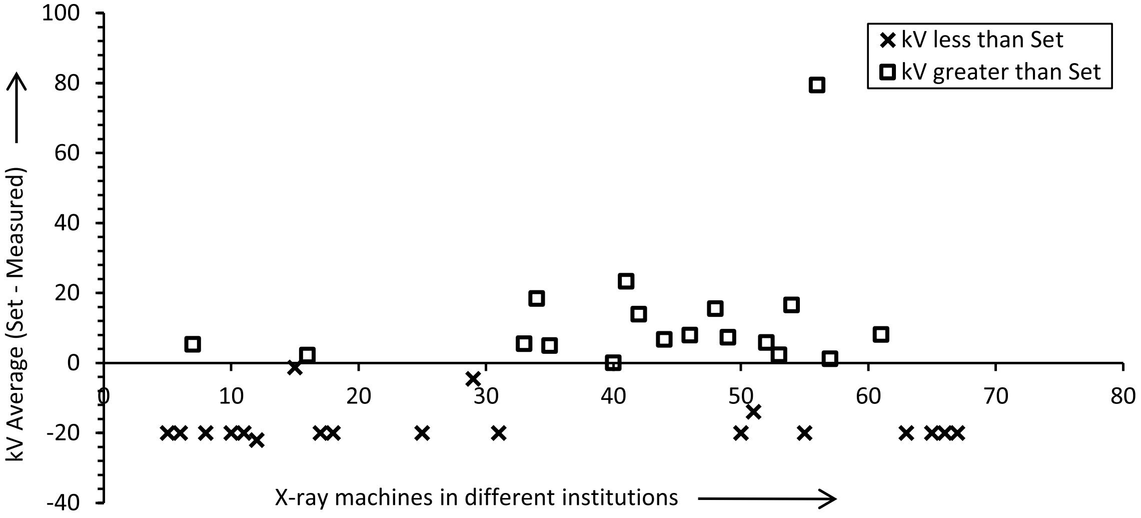

Fig. 7 Accelerating potential reproducibility of different X-ray machines

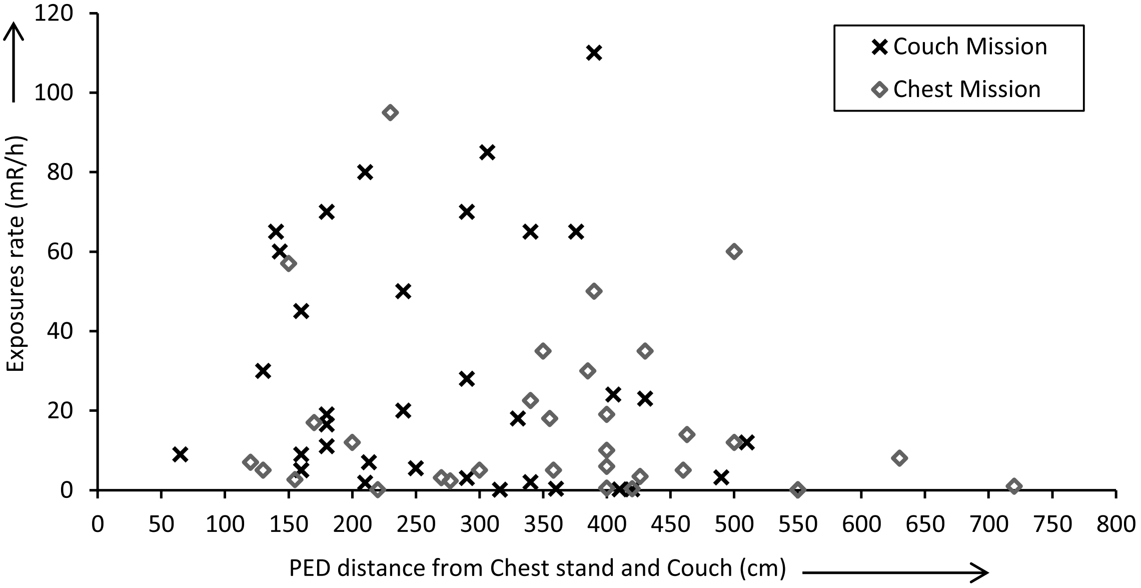

Fig. 8 Exposure rates measured at the PEDs for both chest and couch missions

Table 2 Exposure rates measured behind different types of PEDs in different installations

Type of door	No. of units	Minimum exposure rate (mR/h)	Maximum exposure rate (mR/h)	Range (mR/h)	Mean (mR/h)	SD (mR/h)
Chest mission						
Lead-lined door	2 (6.25%)	0.03	0.08	0.05	0.05	0.04
No lead-lining	30 (93.75%)	0.1	95	94.9	18.03	22.22
Couch mission						
Lead-lined door	3 (8.33%)	0.16	5	4.84	1.78	2.79
No lead-lining	33 (91.67%)	0.13	110	109.87	30.83	30.46

the exposure rate compared to the alternatives observed in this study (Table 2).

3.4 Comparison between lead-line PEDs and other typical PEDs

The radiation exposure rates outside PED in installations having lead-lined doors or typical doors for both chest and couch missions are shown in Figs. 9 and 10. The rates outside the PED for chest missions with lead-lined doors installed were negligibly low (0.08 and 0.03 mR/h). Similarly, for couch missions where lead-lined doors were installed, the rates outside the PEDs ranged from 0.16 to 5 mR/h (Table 2). These exposure rates show that lead-lined doors are very good shielding materials, which are recommended by a variety of different bodies [6, 25]. However, in installations without lead-lining, exposure rates ranged up to 95 mR/h for chest missions to 110 mR/h for couch missions (Table 2). The high exposure rates in these installations show that alternatives, such as wooden doors, plywood

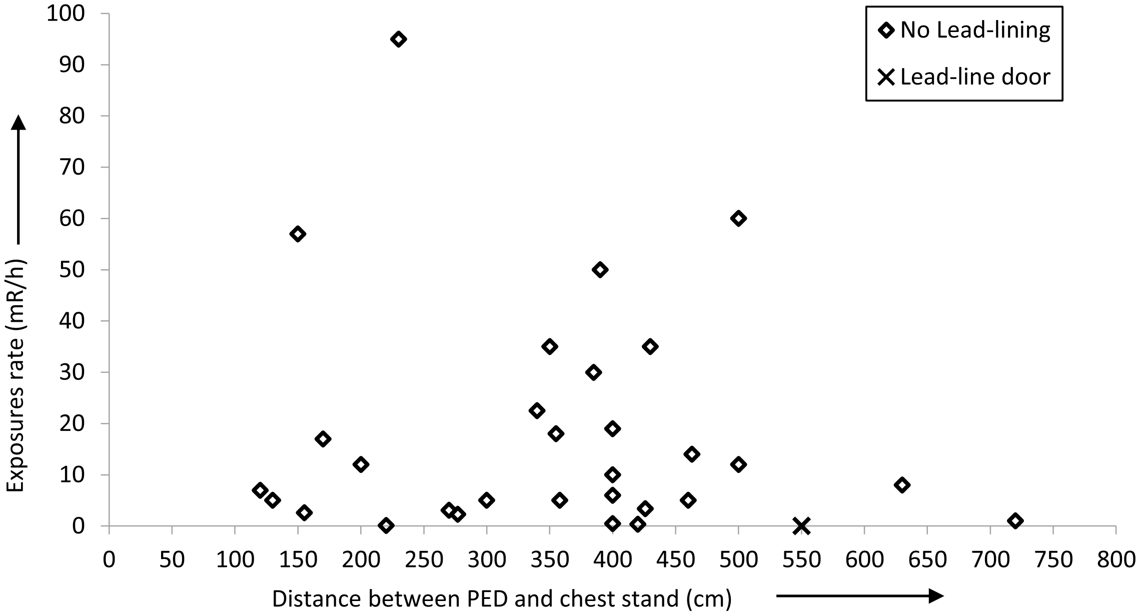

Fig. 9 Exposure rates measured at the PEDs for chest missions (comparing different barrier utilizations)

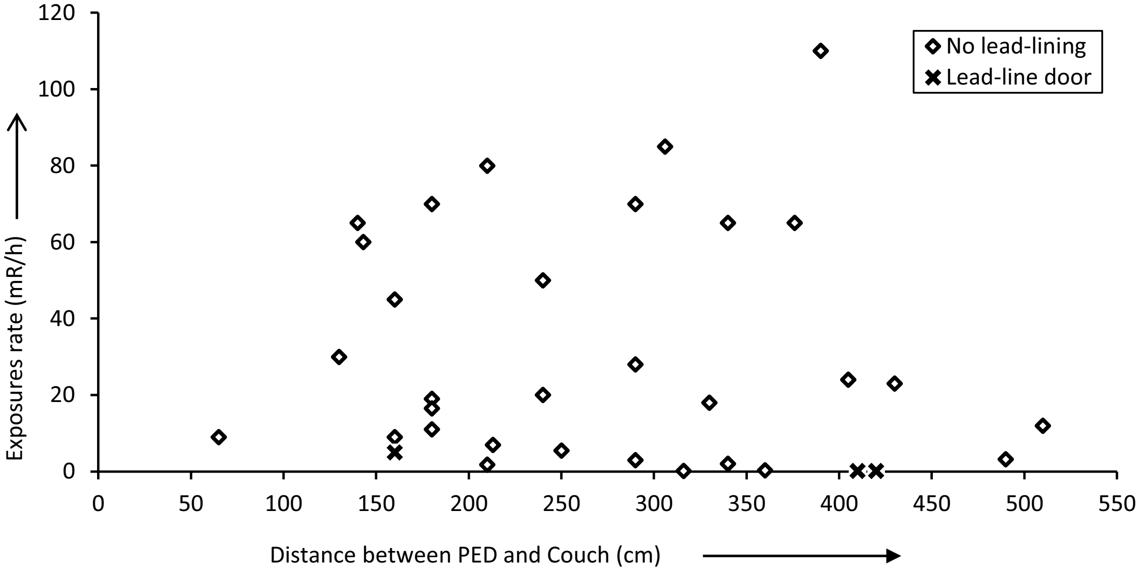

Fig. 10 Exposure rates measured at the PEDs for couch missions (comparing different barrier utilizations)

doors, and aluminum plane sheets, are not nearly as effective as lead. This was similar to the results for measuring the CP exposure rates. Lower exposure rates were found in few installations where lead-lined doors were not installed. The reason was the same for CP exposure.

3.5 Workloads for chest and couch examinations

General diagnostic X-ray examinations are classified as chest, skull, abdomen, pelvic, intravenous pyelogram, and extremities. At all institutions, X-ray teams work 6 days per week. The number of patients examined per day varies amongst institutions. With intravenous pyelograms, 5–6 X-ray films are used; whereas, all other examinations use 1 or 2 X-ray film(s). For chest X-ray, the range of 6–50 mAs tube loading is applied, whereas other examinations use 20–120 mAs, such as when considering Table 3 unit 6, where chest, abdomen, skull, and other extremities are examined. For chest X-ray, workload is calculated using Eq. (1) as follows:

$$W = \frac{1 \times 1 \times 25 \times 6}{60}\ \text{mA-min/week}$$
$$= 2.5\ \text{mA-min/week for chest X-ray.}$$

Similarly, other examinations are calculated and summed to get the total workload for a particular installation. The calculated workload shows that the couch workload is greater than that of chest work in almost every institution, because examinations using the chest stands require horizontal projection of the X-ray, whereas all other examinations use vertical projection (Fig. 11).

3.6 Public and occupational dose levels

Radiation doses calculated as milliroentgen per week at the CPs and outside the PEDs are considered occupational and public doses, respectively. As indicated in Eq. (2), these doses not only depend on the exposure rates but also on the workload [27]. This is why most of the high doses result from high exposure rates and high workloads. However, at a few installations, these two parameters compensated each other (Table 4). It can be seen from Table 4 that those installations having high doses had parameters higher than the mean value. Interestingly, some high exposure rates did not always result from high radiation doses. As shown in Figs. 2, 3, and 7, high exposure rates arising from improper barriers, non-protected, or unlined doors did not lead to high doses because of low workloads. Some of these were only used for couch missions, whereas others were not used (i.e., there was no workload). Moreover, X-ray units 29, 46, and 52 showed high workloads, but had significantly lower exposure rates because of proper CP covering and lead shielding of the PED. This is why these doses were negligibly low (Table 5).

The occupational doses (which varied from ~ 0.01 to 24.18 mR/week) were compared with dose limits for radiation workers prescribed in the AERB Safety Code: 40 mR/week [6, 27]. All these institutions were well below this dose limit, as indicated in a previous study in rural areas [31] (Fig. 12).The highest dose found was 24.18 mR/week, which is 60.45% of the dose limit. These doses are still relatively high compared to the others, and the reason may be as follows. First, the control panel was at a distance of 200 cm from the chest stand and only 70 cm from the couch, which contradicts the recommended distance of 300 cm [6]. Second, despite the short distance, the machine was operated without any barrier[s]. Third, the workload of

Table 3 Workload of diagnostic X-ray facilities in the present study area

Unit	Patient per day	Film per patient	Tube loading (mAs)	Days per week	Workload (mA-min/week)	Total workload (mA-min/week)	Examinations conducted
5[a]	1	1	80	6	8	20	Chest
	3	1	40	6	12		Others
6[a]	1	1	25	6	2.5	20	Chest
	0.2	2	50	6	2		Abdomen
	0.1	1	50	6	0.5		Skull
	3	2	25	6	15		Others
7[a]	10	1	40	6	40	250	Chest
	5	2	60	6	60		Abdomen
	5	2	45	6	45		Skull
	2	5	60	6	60		IVP
	15	1	30	6	45		Others

[a] Workload for each piece of equipment was calculated as with units 5, 6, and 7. It can be seen that some diagnostic units examined chest, abdomen, skull, intravenous pyelogram, and other extremities, whereas others examined only one, two, or more

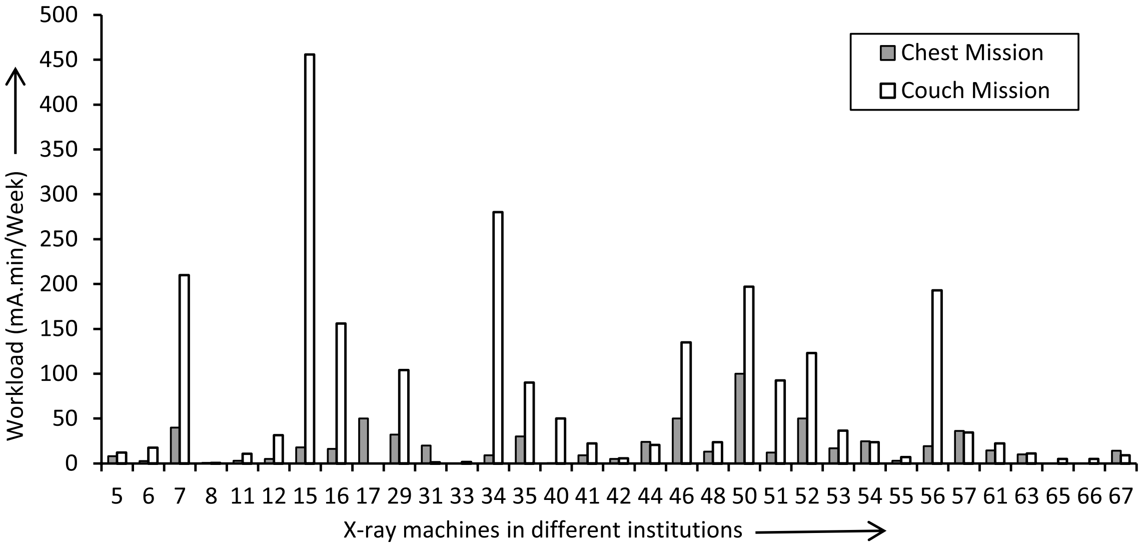

Fig. 11 Workload of different institutions for both chest and couch examinations

Table 4 Exposure rates and workload for the three highest public and occupational doses

High public dose						High occupational dose					
Dose (mR/week)		Exposure rates (mR/h)		Workload (mA-min/week)		Dose (mR/week)		Exposure rates (mR/h)		Workload (mA-min/week)	
Unit[a]	Dose[b]	Chest[c]	Couch[d]	Chest	Couch	Unit	Dose[e]	Chest	Couch	Chest	Couch
15	3.72	12	24	18	456	34	8.35	100	140	9	280
34	1.64	6	28	9	280	56	24.18	4.8	150	19.2	192.84
50	7.11	95	60	100	197	57	4.356	105	270	36	34.4
Mean	0.71	14.62	27.65	19.2	72.3	Mean	1.34	26.6	43.1	19.2	72.3

Mean value was calculated from each and every unit

[a] A particular X-ray unit/machine

[b] Calculated dose outside PED

[c] Chest mission/horizontal exposure

[d] Couch mission/vertical exposure

[e] Calculated dose at CP

Table 5 Exposure rates and workload for low occupational and public doses

Public dose						Occupational dose					
Dose (mR/week)		Exposure rates (mR/h)		Workload (mA-min/week)		Dose (mR/week)		Exposure rates (mR/h)		Workload (mA-min/week)	
Unit	Dose	Chest	Couch	Chest	Couch	Unit	Dose	Chest	Couch	Chest	Couch
10	0	50	80	0	0	11	0.62	0	100	3	10.6
18	0	0	70	0	0	25	0	0	360	0	0
25	0	0	50	0	0	40	1.53	235	0	0.2	50
33	0.02	0	65	0	1.6	49	0	165	0	0	0
63	0.7	57	0	10	11.2	53	1.26	205	0	16.8	36.48
29	0.1	3.1	2	32	104	29	0.02	0.49	0.35	32	104
46	0.52	14	18	50	135	46	0.01	0.34	0.3	50	135
52	0.15	1	3.2	50	123	52	0.02	0.15	0.38	50	123

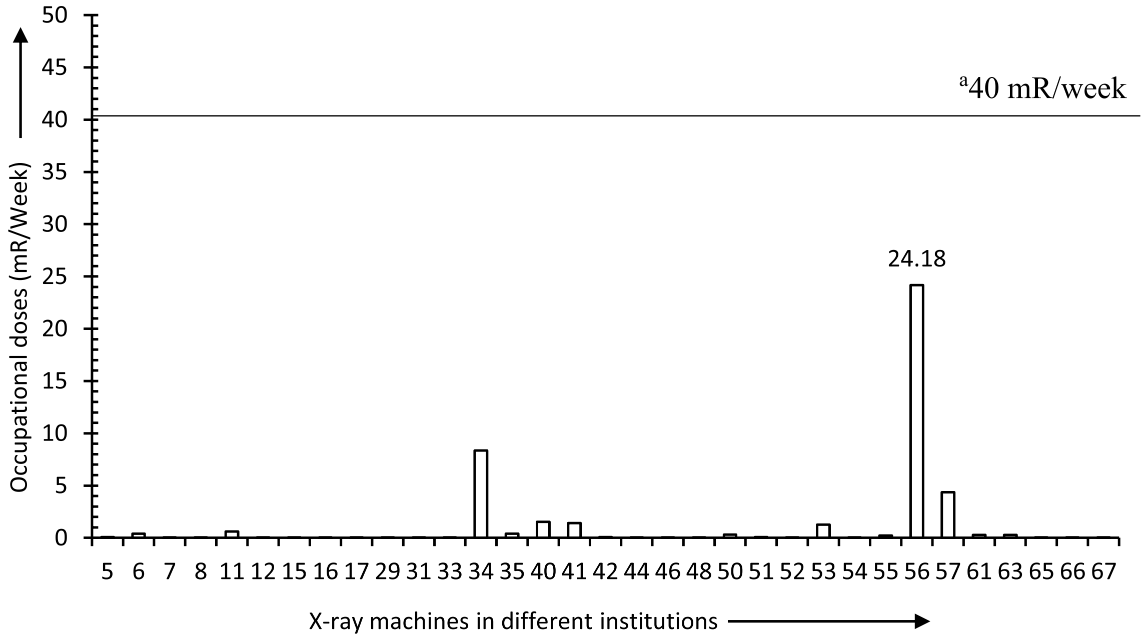

Fig. 12 Doses at the CPs (occupational dose) caused by stray radiation ([a]AERB dose limit for radiation workers)

192.84 mA-min/week was high, compared with the mean workload of 72.3 mA-min/week (Table 4). Thus, the authors measured high exposure rates at the CP, all of which automatically generated relatively high doses compared with others. Further, the use of properly installed lead protective barriers (1.5–1.7 mmPb) was found to provide adequate protection from stray radiation at CPs. However, less than 50% of the institutions covered their CPs properly.

Some marginal doses or overdoses were observed in public spaces outside the PED (Fig. 13), relative to the dose limit for the public: 2 mR/week [6]. The highest dose found was 7.11 mR/week, which is 3.55 times the public dose limit. High workload is the main reason for such high doses

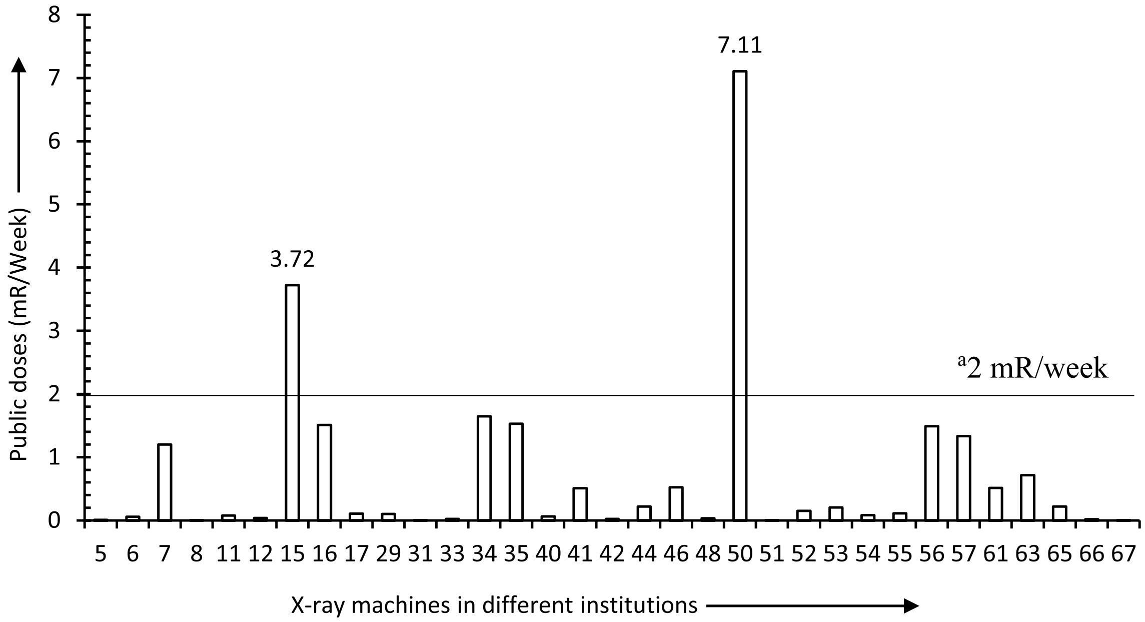

Fig. 13 Doses at the PEDs (public dose) owing to stray radiation ([a]AERB dose limit for members of the public)

at unit 15 (Fig. 13), where the workload of 456 mA-min/week was 6.31 times the mean value. Although the PED was non-lead lined, the distance of the PED from the chest stand (i.e., 500 cm) and from the couch (i.e., 405 cm) results in average exposure rates (Table 4). Regarding unit 50, there was inadequate space between the PED and the chest stand (i.e., 230 cm) and the couch (i.e., 143 cm). These high exposure rates were measured outside a plywood PED having a thickness of 0.33 cm. High workloads, i.e., 2.72 times the mean value for couch mission and 5.21 times the mean value for chest mission were found (Table 4). These doses could be significantly reduced by following the standard installation layout and by employing lead-lined doors as recommended by the regulatory bodies [6, 25].

In the present study, radiation doses were found to depend on the input electrical parameters and installation layout. This is why quality assurance tests are mandatory for diagnosing and rectifying machine performance. Because repeated exposures were not included in this study, the doses reported appear underestimated. However, the study used maximum field sizes and longer exposure times than normal X-ray examinations. There was also high kV. Thus, the dose underestimation may have been compensated, falling on the safer side.

4 Conclusions

The authors did not find any excessive doses at the CP, as per the safety code. However, the absence of barriers and barriers not effectively covering CPs with respect to couch and chest missions should be rectified to decrease ancillary doses. The highest dose contributed by stray radiation from the couch and chest missions to the CP was 24.18 mR/week, which is 60.45% of the dose limit.

There were two installations where the dose outside the PED, a public space, exceeded the safety recommendations of 2 mR/week. The highest dose was found to be 7.11 mR/week, about 3.55 times the dose limit. The most often used materials (i.e., solid wood, plywood lined, and plane sheet lined) in the entrance doors attenuated radiation relatively less than did the lead-lined doors. The lead-lined doors appreciably reduced the radiation rate outside the PEDs. However, more than 90% of the institutions used traditional doors.

Acknowledgements The authors express their sincere thanks to the Committee for Safety Research Program (CSRP), the Atomic Energy Regulatory Board (AERB, Mumbai), and the Government of India, for financial assistance through Major Research Project Grant no. AERB/CSRP/58/02/2014 awarded in September 30, 2014.

Funding This study was funded by the Committee for Safety Research Program (CSRP) and the Atomic Energy Regulatory Board (AERB): project number AERB/CSRP/58/02/2014; September 30, 2014.

Compliance with ethical standards

Conflict of interest The authors declare that they have no conflicts of interest.

Ethical approval This article does not contain any human studies. This article does not contain any animal studies.

References

1. Archer BR. History of the shielding of diagnostic X-ray facilities. Health Phys. 1995;69:750–8.
2. Bushong SC. Radiation protection. In: Ballinger PW, editor. Merrill's atlas of radiographic positions and radiologic procedures, vol. 1. 7th ed. St. Louis: Mosby Year Book; 1991. p. 17–33.
3. Sun Z, Inskip PD, Wang J, Kwon D, Zhao Y, Zhang L, et al. Solid cancer incidence among Chinese medical diagnostic X-ray workers, 1950–1995: estimation of radiation-related risks. Int J Cancer. 2016;138:2875–83.
4. González AB, Darby S. Risk of cancer from diagnostic X-rays: estimates for the UK and 14 other countries. Lancet. 2004;363:345–51.
5. Archer BR. Recent history of the shielding of medical X-ray imaging facilities. Health Phys. 2005;88:579–86.
6. Atomic Energy Regulatory Board. Safety Code No. AERB/SC/MED-2 (Rev. 1), 'Safety code for medical diagnostic X-ray equipment and installations' AERB, Mumbai, 2001.
7. Binks W. Some aspects of radiation hygiene. Br J Radiol. 1955;28:654–61.
8. Grover SB, Kumar J, Gupta A, Khanna L. Protection against hazards: regulatory bodies, safety norms, dose limits and protection devices. Indian J Radiol Imaging. 2002;12:157–67.
9. Bennett BG. Exposures from medical radiation world-wide. Radiat Prot Dosimetry. 1991;36:237–42.
10. Cunha P, Freire B, Drexler G. Occupational exposure in X-ray diagnosis in Brazil. Radiat Prot Dosimetry. 1992;43:55–8.
11. Bushong SC. Radiologic science for technologists: physics, biology, and protection. 10th ed. St. Louis: Elsevier Mosby; 2013. p. 578–9.
12. Osborn SB. Radiation doses received by the diagnostic X-ray workers. Br J Radiol. 1955;28:650–4.
13. Carlsson CA, Carlsson GA. Basic physics of X-ray imaging. 2nd ed. Sweden: Linkoping University; 1996.
14. Johns HE, Cunningham JR. The physics of radiology. 4th ed. Springfield: Thomas CC, Publisher; 1983. p. 133–64.
15. IAEA. Diagnostic radiology physics; a handbook for teachers and students. Austria: IAEA; 2014.
16. Chen MYM, Swearingen FL, Mitchell R, Ott DJ. Radiation exposure during ERCP: effect of a protective shield. Gastrointest Endosc. 1996;43:1–5.
17. Cousins C, Sharp C. Medical interventional procedures—reducing the radiation risks. Clin Radiol. 2004;59:468–73.
18. Simkin DJ, Dixon RL. Secondary shielding barriers for diagnostic X-ray facilities: scatter and leakage. Health Phys. 1998;74:350–65.
19. Dixon RL. On the primary barrier in diagnostic X-ray shielding. Med Phys. 1994;21:1785–93.

20. Lee J, Cha ES, Jeong M, Lee WJ. A national survey of occupational radiation exposure among diagnostic radiologic technologists in South Korea. Radiat Prot Dosimetry. 2015;167(4):525–31.
21. Operator Manual 451P Ion Chamber Survey Meter. PN FBC-0059, Rev 1, Fluke Corporation, USA; 2013.
22. Sonawane AU, Singh M, Kumar SJVK, Kulkarni A, Shirva VK, Pradhan AS. Radiological safety status and quality assurance audit of medical X-ray diagnostic installations in India. J Med Phys. 2010;35:229–34.
23. Vlachos I, Tsantilas X, Kalyvas N, Delis H, Kandaraskis I, Panayiotakis G. Measuring scatter radiation in diagnostic X-rays for radiation protection purposes. Radiat Prot Dosimetry. 2015;165:382–5.
24. Tsalafoutas IA. Excessive leakage radiation measured on two mobile X-ray units due to the methodology used by the manufacturer to calculate and specify the required tube shielding. Br J Radiol. 2006;79:162–4.
25. NCRP. Report No. 147. Structural shielding design for medical X-ray imaging facilities; 2004.
26. Lalrinmawia J, Pau KS, Tiwari RC. Qualitative study of mechanical parameters of conventional diagnostic X-ray machines in Mizoram. Radiol Phys Technol. 2018;11:274–83.
27. Format for Quality Assurance test for diagnostic X-ray equipment. https://www.aerb.gov.in/images/PDF/DiagnosticRadiology/1-FORMAT-FOR-QUALITY-ASSURANCE-TEST-FOR-DIAGNOSTIC-X-RAY-EQUIPMENT.pdf. Accessed 5 Feb 2019.
28. Lalrinmawia J, Pau KS, Tiwari RC. Investigations of public dose due to stray radiation in X-ray installations in Mizoram. Science and technology for shaping the future of Mizoram. New Delhi: Allied publishers Pvt. Ltd.; 2017. p. 305–9. ISBN 978-93-85926-49-5.
29. Operator Manual Victoreen 07-494. Manual No. 168001 Rev 4, Fluke Biomedical, Radiation Management Services, 6045 Cochran Road, Cleveland, Ohio 44139, USA; 2006.
30. Lalrinmawia J, Pau KS, Tiwari RC. Quality assurance assessment of conventional diagnostic X-ray installations in Mizoram. J Med Phys. 2017;42(Suppl S1):208–9 **(ISSN: 0971-6203)**.
31. Lalrinmawia J, Pau KS, Tiwari RC. Investigations of workers dose due to stray radiation in X-ray installations in Mizoram. Recent advances in physics research and its relevance. New Delhi: Excel India Publishers; 2017. p. 258–63. ISBN 978-93-86256-85-0.

Publisher's Note Springer Nature remains neutral with regard to jurisdictional claims in published maps and institutional affiliations.

Abstract

The huge potential for medical applications of X-rays was evident from the first investigations. As experience was gained in the early days, it became more and more evident that ionizing radiation can harm biological systems. Ionizing radiation originated form medical diagnostic X-ray machines have been reported to be the major contributor of public exposure to man-made ionizing radiation. Approximately 51% of the population dose was estimated to be caused by diagnostic X-ray examinations. The population exposure due to medical radiation is likely to be increasing worldwide, particularly in the countries where medical services are in the earlier stages of development. Twenty seven years ago, Supe *et al*. (1992) reported that “most of the rural areas have very old X-ray machines for which quality assurance tests have never been undertaken”. Till today, it seems equally true that no such study as per Atomic Energy Regulatory Board (AERB) guidelines have been performed for the X-ray machines in Mizoram. Information on image quality and patient dose is better known in some developed countries, however, it is grossly lacking in the majority of the developing countries and in the present study area as well. Accordingly, the present study entitled “**Study of Radiation and Mechanical attributes of diagnostic X-ray installations in Mizoram**” was designed with the following objectives:

- To investigate mechanical properties of X-ray units; such as optical and radiation field congruence, central radiation beam alignment perpendicularity.
- To investigate input/output characteristics of X-ray units; such as accelerating potential, tube current, exposure time, output consistency, radiation filter.

- To investigate radiation characteristics of X-ray installations; such as leakage and scattered radiations from diagnostic X-ray units.
- Comparison of the data generated with National and International standard and recommendations for improvement.

In total, there were 195 X-ray facilities at 118 different institutions across the state of Mizoram. Out of which 26 X-ray machines were condemned because these machines were beyond repair. Among these, 64.5% were AERB-type approved units and 35.5% machines had unknown approval statuses because of missing information. Among different X-ray facilities, 69.2% were conventional diagnostic X-ray machines and 90.9% of the total workload (5687.21 mA-min/week) had been performed in this type of machines.

For measuring the output radiation of diagnostic X-ray equipment a battery operated portable dosimeter (RAD-CHECK PLUS model 06-526, Fluke Biomedical-Cleveland, Ohio, USA) was used. The wide-range digital kVp meter (model 07-494, Fluke Biomedical, Cleveland, Ohio, USA) non-invasively measures the effective peak potential applied to tungsten target of diagnostic X-ray tube. The ion chamber survey meter (model 451P, Fluke Biomedical, Everett, WA, USA) was used to measure X-ray above 25 keV. The calibration measurements are traceable to the National Institute of Standards and Technology (NIST, Gaithersburg, MD, USA). The beam alignment test tool, when used with the collimator test tool, provides a simple test for congruency and beam alignment perpendicularity. The investigator used thermo-luminescent dosimeter badge to know whether he is working within the safe dose limits prescribed by AERB.

The investigators took several data from 16 important safety parameters such as frequency of quality assurance, X-ray room layout, availability of personnel monitoring service (PMS), lead apron, gonad shielding, repeated exposure and repetition reason, qualified personnel, collimator bulb, field size knob, patient entrance door (PED), protective barrier, waiting area, chest stand, warning light, dark rooms were checked and recorded. This information was collected from radiation workers and/or the heads of institutions through observation and interviews.

Data presented as mean, range, coefficient of variation, standard deviation, standard error mean and correlation were analyzed by using SPSS statistics for windows version 17.0. (SPSS, Inc., Chicago, IL, USA). T-test was also conducted to check the existence of significant difference between the amount of leakage radiation measured at different position with respect to the X-ray tube as well as to check the significant difference between radiation level measured with and without control panel (CP) barriers as well as PEDs in chest and couch missions.

In radiography, radiation dose and image quality are greatly depend on X-ray generator parameters. Among different X-ray generators parameters studied in the present study, 59.2% linearity of time (sec); 82.6% linearity of current (mA); 89.7% peak kilo-voltage (kVp) accuracy; 35.1% output reproducibility; 92.8% table dose (μGy/mAs) were beyond acceptable limits. The reasons for such poor performance were improper quality assurance tests, old machine used without proper maintenance, power supply problems. Therefore, implementation of quality control program on a regular basis is necessary to reduce X-ray machine malfunctioning, to produce high quality diagnostic images with the lowest radiation dose to the patient.

It was observed from 16 essential safety parameters that none of the X-ray machines undergone a regular quality assurance test as per the AERB guidelines, only 1.9% equipment employed lead-lined PED, 46.8% machines were operated without any protective barrier, 83.1% units operated without PMS, lead apron were not available in 38.3% machines, 92.2% of the facilities recorded repeated examination due to over/under exposures, spoiled films and patient movement. Due to the absence of proper quality control program in the past, many installations were not following standard installation guidelines which were laid down by several regulatory bodies.

Half value layer is measured to guarantee that the permanently installed filter on the X-ray tube is maintained to minimize patient exposure. The calculated total filtrations of conventional X-ray machines at different institutions were compared with national and international standards; 27.83% met the national standard and only 15.46% met the international standard. It appears that most of the equipment in the present study had poor filters. In congruency between radiation and optical field study, from the 47 units which we could study, 80.85% were found to be beyond the acceptable limit. At the same time, the optical lights of 4 X-ray units did not work; 6 units had fixed their collimators to full, and more than 10 units had misalignments above 10% of the source to image distance. When testing the central beam and image receptor perpendicularity of 53 units, 69.81% of X-ray units were more than 1.5

degrees off perpendicularity and did not pass the test. These faults will result significant increase in patient and radiation worker doses through primary and secondary radiation. In these particular parameters, both new and old X-ray machines had similar problems.

The authors did not find any excessive doses at the CP, per the safety code. The highest dose contributed by stray radiation from the couch and chest missions to the CP was 24.18 mR/week, which is 60.45% of the dose limit. There were three installations where the dose outside the PED, a public space, exceeded the safety recommendations of 2 mR/week. The highest dose was found to be 7.11 mR/week, about 3.55 times the dose limit. The most often used materials (i.e., solid wood, plywood-lined, and plane sheet-lined) in the entrance doors attenuated radiation relatively less than did the lead-lined doors. The lead-lined doors appreciably reduced the radiation rate outside the PEDs. Unfortunately, more than 90% of the institutions used traditional doors.

It was noticeable from the present study that each type of PED attenuated radiation but in different quantity where lead-lined door attenuated relatively large amount (>90% in chest and couch missions). Installing plywood and plywood-plane sheet-lined door is healthier than no door at all because it attenuated considerable amount of radiation. On the other hand, patient entrance door which can reduce any kinds of stray radiations below a level of 1 mSv y^{-1} is recommended by various regulatory bodies. Again, CP protective barriers attenuated significant amount of incident radiation. Among them, lead and concrete barriers attenuated more than

90% of incident radiation while plywood plane sheet-lined barrier attenuated relatively lesser quantity. In comparison to national and international safety standard, tube housing leakage of all the X-ray machines were well below the safety limit. Regarding fixed and mobile X-ray machines, there was no significant difference in leakage radiation between them even though fixed X-ray can operate at higher input parameter.

The information obtained from the present investigation will be very useful for establishment of effective quality assurance programs as this kind of information is lacking in the present study area. Regular quality control of conventional X-ray equipment and fixing their defects can play an important role in increasing the machine longevity, reducing absorbed dose of patients, and improving the quality of radiographic images. The participation of medical physicists, radiographers and radiologists in the implementation of quality control programs at various stages of development will enhance equipment performance improvement in the present study area.